Investigation of the Efficacy of a Novel CsA Formulation Alone or in Combination with Cell Therapy in a Humanised Mouse Model of GvHD

By

Jennifer M. Corbett

B.Sc. M.Sc.

A thesis submitted to Maynooth University for the degree of

Doctor of Philosophy

Department of Biology

Institute of Immunology

Maynooth University

February 2016

Research Supervisor: Dr. Karen English

Enterprise Mentor: Dr. Ivan Coulter

TABLE OF CONTENTS:

CHAPTER 3 : CsA ENHANCES MSCγ POTENCY THROUGH SOCS1

CHAPTER 4 : SMPILL® PROVIDES ENHANCED CSA EFFICACY IN A HUMANISED MOUSE MODEL OF AGVHD IN A TARGETED MANNER

DECLARATION OF AUTHORSHIP

I certify that the work presented herein is, to the best of my knowledge, original, resulting from research performed by me, except where acknowledged otherwise. This work has not been submitted in whole, or in part, for a degree at this or any other university.

_____   _____

Jennifer M. Corbett B.Sc. M.Sc**.**   Date

ABSTRACT

The immunomodulatory ability of mesenchymal stromal cells (MSC) make them an ideal cellular therapy for inflammatory diseases such as acute Graft versus Host Disease (aGvHD). Cyclosporine (CsA) is an immunosuppressive drug commonly used as prophylaxis and treatment of aGvHD. However, oral bioavailability of CsA is suboptimal. The elucidation of MSC and CsA interactions will be beneficial as aGvHD patients in clinics would have undergone prophylaxis involving CsA immunosuppression and MSC may be administered alongside CsA therapy. The key goals of this thesis were to (1) investigate the direct interactions of MSC and CsA and elucidate the mechanisms by which these interactions occur *in vitro* and *in vivo*, and (2) establish the efficacy of a novel and more clinically applicable CsA treatment, by means of optimal targeted delivery, in a humanised model of aGvHD.

This study has defined the direct interactions of MSC and CsA, identifying MSC activation and timing of CsA as being crucial for beneficial immunosuppressive functions. We proposed a mechanism by which CsA regulated IFNγ signalling in MSC through suppressor of cytokine signaling 1 (SOCS1) inhibition resulting in the enhancement of MSCγ suppression of $CD3^+$ T cells and increased indoleamine 2,3-deoxygenase (IDO).

For the first time, we have shown that a novel CsA formulation, SmPill® provided safe and superior efficacy in comparison to routinely used CsA drugs, Neoral® and Sandimmune® IV in a humanised model of aGvHD. We have shown this enhanced efficacy using pre-clinical survival studies, histopathology and cytokine analysis and hypothesise that this enhancement over these conventional CsA drugs is mediated through targeted delivery to systemic and GI tissues. Therefore, making it a highly attractive candidate for routine clinical use for aGvHD treatment.

Moreover, we have investigated the interactions of MSC with SmPill® and Sandimmune® IV in a humanised model of aGvHD. We have shown that 1) CsA therapies did not impair MSC efficacy in aGvHD 2) Sandimmune® IV can be efficacious with both resting and licensed MSC therapy and 3) MSC but not MSCγ hamper SmPill® efficacy.

Overall, this thesis has furthered our knowledge of MSC interactions with CsA *in vitro* and *in vivo* and presented translational pre-clinical results demonstrating the efficacy of a novel CsA formulation alone and in combination with MSC therapy for aGvHD.

PUBLICATIONS

Published Manuscripts

McClean S, Healy M, Collins C, Carberry S, O'Shaughnessy L, Dennehy R, Adams A, Kennelly H, **Corbett J**, Carty F, Cahill L, Callaghan M, English K, Mahon B, Doyle S, and Shinoy M. (2016). Linocin and OmpW are involved in attachment of the cystic fibrosis associated pathogen *Burkholderia cepacia* complex to lung epithelial cells and protect mice against infection. *Infection and Immunity*, 84(5):1424-37.

Manuscripts in Preparation

Corbett J, Coulter I.S, and English K. MSC activation and timing of CsA are crucial for beneficial immunosuppressive effects of combined therapy in a humanised model of acute graft versus host disease.

Corbett J, Coulter I.S., and English K. Differential characteristics of oral, systemic and targeted release formulations of Cyclosporine A in a humanised mouse model of acute graft versus host disease.

Abstracts for Conference Proceedings

Cyclosporine Antagonises the immunosuppressive ability of Human Mesenchymal Stromal Cells.

Corbett J, Coulter I & English K

Irish Society of Immunology Annual Meeting. 2013. Crowne Plaza Hotel, Santry, Dublin

Cyclosporine and IFNγ Enhance Human Mesenchymal Stromal Cells Immunosuppressive ability.

Corbett J, Coulter I & English K

Irish Society of Immunology Annual Meeting. 2014. Crowne Plaza Hotel, Santry, Dublin

Cyclosporine A and IFNγ Enhance Human Mesenchymal Stromal Cells Immunosuppressive ability.

Corbett J, Coulter I & English K

European Congress of Immunology 4th Meeting. 2015. Vienna, Austria

ABBREVIATIONS

APC	Antigen Presenting Cell
ATG	Anti-Thymocyte globulin
BMT	Bone marrow transplant
BSA	Bovine Serum Albumin
CB	Cord blood
CBU	Cord blood unit
CCL	Chemokine (C-C motif) ligand
CD	Cluster of differentiation
cDNA	Complementary Deoxyribonucleic acid
CFSE	Carboxyfluorescein succinimidyl ester
CMV	Cytomegalovirus
CsA	Cyclosporine A
CTL	Cytotoxic T lymphocyte
CXCL	Chemokine (CXC motif) ligand
DAMPs	Damage associated molecular patterns
DC	Dendritic cell
dH2O	Distilled water
DMEM	Dulbecco's modified eagle's medium
DMSO	Dimethyl sulfoxide
DNA	Deoxyribonucleic acid
EAE	Experimental autoimmune encephalomyelitis
EBAO	Ethidium bromide acridine orange
EBV	Epstein-Barr virus
EDTA	Ethylenediaminetetraacetic acid
ELISA	Enzyme linked immunosorbent assay
FACS	Fluorescence-activated cell sorting
FBS	Fetal bovine serum
Fix/Perm	Fixation/Permeabilisation
FSC	Forward scatter
GAPDH	Glyceraldehyde 3-phosphate dehydrogenase
GI	Gastrointestinal tract

GvHD	Graft versus host disease
GvL	Graft versus leukaemia
GVT	Graft versus tumour
Gy	Gray
H & E	Haematoxylin and Eosin
HBV	Hepatitis B virus
HCV	Hepatitis C virus
HGF	Hepatocyte growth factor
HLA	Human leukocyte antigen
HRP	Horseradish peroxidase
HSCT	Haematopoietic stem cell transplantation
ICAM-1	Intracellular adhesion molecule-1
IDO	Indoleamine 2,3-dioxygenase
IFN	Interferon
IL	Interleukin
ISCT	International Society for Cellular Therapy
IV	Intravenous
kDa	Kilodalton
kg	kilogram
LPS	Lipopolysaccharide
MAC	Membrane attack complex
MFI	Mean fluorescent intensity
MHC	Major histocompatibility complex
miHA	Minor histocompatibility antigen
moAB	Monoclonal antibody
MP	Methylprednisolone
MSC	Mesenchymal stromal cell
MSCγ	Mesenchymal stromal cell stimulated with IFNγ
MTX	Methotrexate
NFAT	Nuclear Factor of activated T cells
NK	Natural Killer cell
NSG	NOD-scid IL-2 receptor gamma knockout mouse
PAMPs	Pathogen associated molecular patterns

PB	Peripheral blood
PBMC	Peripheral blood mononuclear cell
PBS	Phosphate buffered saline
PCR	Polymerase chain reaction
Pen/Strep	Penicillin/Streptomycin
PGE2	Prostaglandin E2
PHA	Phytohaemagglutinin
RBC	Red blood cell
RNA	Ribonucleic acid
mRNA	Messenger Ribonucleic acid
RPM	Revolutions per minute
RPMI	Roswell Park Memorial Institute
RT	Room temperature
SDS-PAGE	Sodium dodecyl sulphate polyacrylamide gel electrophoresis
SOCS1	Suppressor of cytokine signalling 1
SSC	Side scatter
STAT1	Signal transducer and activator of transcription 1
TGFβ	Transforming growth factor β
TLR	Toll like receptor
TNF	Tumour necrosis factor
TSG6	Tumour necrosis factor stimulated gene 6
Treg	Regulatory T cell
VCAM-1	Vascular cell adhesion molecule-1
VEGF	Vascular endothelial growth factor

ACKNOWLEDGEMENTS

Firstly, I would like to express my sincere gratitude to my supervisor Karen for the opportunity to pursue my PhD in the Cellular Immunology Lab. Your unwavering support and encouragement guided me every step of the way. I will be forever grateful for all your help and advice. I have learned so much from you and will look forward to working together in the future.

I wish to offer a sincere thank you to Ivan Coulter, my collaborator at Sigmoid Pharma Ltd. Thank you for your advice and support throughout my PhD. I would also like to thank everyone at Sigmoid Pharma Ltd. who helped me along the way. I enjoyed this collaboration and would welcome the opportunity again in the future. In addition, I would like to acknowledge the Irish Research Council for giving me the opportunity to take part in this collaboration through the Enterprise Partnership Scheme.

To all past and present members of the Cellular Immunology Lab who I had the pleasure of working with, Emer, Marc, Helen, Fiona, Laura, Aine & Josh, I want to thank all of you for your help, especially on my big harvest days! I wish you all the best of luck in future endeavours.

A special thank you to Helen, Fiona, Therese, Susan & Siobhan. Your friendship made this PhD enjoyable every day. I will never forget the laughs, tea breaks, cycling and most of all your support during the tough days. I wish each of you the best of luck in your future careers.

To my mother and father, how can I thank you enough? You motivated me and encouraged me to keep going every day. I appreciate everything you have taught me in life. To my sisters and brothers Shirley, Ger, Emily, Stephanie, and Jason, thank you all for your love and support in everything I do. I am so proud to have you as my family. My student life has come to an end now, I promise!

A special thank you to Kevin, Jack, Alice and all my grandparents. Thank you for believing in me and for all the prayers!

Last but certainly not least, my boyfriend James. Your love and friendship means everything to me and I couldn't have finished this PhD without it. Thank you for your patience and for supporting me all the way. I could not have gotten through my late night harvests without you. I owe you big time! Thank you.

CHAPTER 1

INTRODUCTION

1.1. MESENCHYMAL STROMAL CELLS

The field of mesenchymal stromal cell (MSC) research emerged from the findings of Friedenstein in the 1960s, who first chronicled a rare, non-haematopoietic cell population in the bone marrow that formed plastic adherent colonies *in vitro* (Friedenstein *et al*. 1966; Friedenstein *et al*. 1968; Friedenstein *et al*. 1974). Based on these findings, Owen and co-workers first suggested the self-renewal and multi-lineage differentiation capacity of these cells after a series of studies demonstrating this potential *in vitro* (Ashton *et al.* 1980; Owen & Friedenstein 1988). In the years following this, Caplan coined the term "mesenchymal stem cells" to describe these cell's stem-like nature and identified them as potential agents for regenerative medicine owing to their involvement in bone and cartilage turnover (Caplan 1991). Building on all of this work, Pittenger and colleagues demonstrated that individual clonally derived human MSC were capable of differentiating into adipocytes, osteocytes and chondrocytes *in vitro* (Pittenger *et al.* 1999). MSC are present in most, if not all, tissues and can be derived from many sources in adults (bone marrow, adipose tissue, peripheral blood) or neonatal tissues (particular parts of the placenta and umbilical cord) or from many species including human, rat, mouse, monkey and pig (Hass *et al*. 2011; Fraser *et al*. 2006; Cao *et al*. 2005; Rozemuller *et al.* 2010).

The potential for MSC therapy in regenerative medicine has been appraised over the last decade following extensive *in vitro* and *in vivo* investigation. In particular, pre-clinical and clinical studies have illustrated their therapeutic value in cardiovascular (Orlic *et al*. 2001; Saito *et al*. 2002; Stamm *et al*. 2003) and orthopaedic applications (Quarto *et al*. 2001; Murphy *et al*. 2002). However, with growing evidence of the tissue reparative and cytoprotective mechanisms displayed by MSC, mediated through secretion of trophic factors, the primary focus of using MSC in regenerative medicine shifted towards delineating MSC interaction with the host immune response (Di Nicola

et al. 2002; Bartholomew *et al.* 2002; Krampera *et al.* 2003; Barry *et al.* 2005; Caplan & Dennis 2006). Findings from these studies implicated MSC as being responsive to a milieu of damage and inflammation and promoted MSC as being key regulators of local tissue inflammation. MSC are thought to play a role in promoting tissue homeostasis through the regulation of damaging immune responses and promoting repair. (Dazzi *et al.* 2012; Shi *et al.* 2012; Bernardo & Fibbe 2013). Accordingly, these dynamic features of MSC make them an attractive candidate for cellular therapy.

In 2005, the International Society for Cellular Therapy (ISCT) addressed the inconsistency between nomenclature and biological functions of MSC, suggesting that the term "mesenchymal stromal cell" is a more fitting reflection of MSC biologic attributes (Horwitz *et al.* 2005).   Additionally, with growing discrepancies in the field with regard to isolation/expansion techniques and differing methods of characterising these cells, the ISCT issued a set of guidelines for defining MSC *in vitro* (Dominici *et al.* 2006). This set of guidelines proposed that MSC must be plastic adherent, should express CD73, CD90 and CD105 but not CD11b, CD14, CD19, CD34, CD45, CD79α or HLA-DR surface molecules and additionally, must be capable of differentiating into adipocytes, chondrocytes and osteocytes *in vitro* (Dominici *et al.* 2006). More recently, guidelines surrounding the experimental approach in assessing MSC potency for clinical use were put forward by the ISCT with the aim of standardizing such methods to achieve comparable results within the field of MSC research (Krampera *et al.* 2013; Galipeau *et al.* 2016).

1.2. MSC AND IMMUNE REGULATION

The immunomodulatory abilities of MSC *in vitro* were initially reported with the use of T cell proliferation assays, employing various T cell stimuli, whereby the ability of MSC to suppress T cell proliferation in these settings was determined (Bartholomew *et al.* 2002; Le Blanc *et al.* 2003). This feature paved the way for the application of MSC as a potential immunomodulatory therapy in allogeneic transplantation. In 2004, allogeneic MSC therapy was successfully used to treat a paediatric patient suffering from grade IV steroid resistant GvHD, providing an early glimpse of the therapeutic potential of these cells (Le Blanc *et al.* 2004). Since then, there have been major advances in understanding the mechanisms by which MSC modulate specific immune cells. In particular, the mechanisms by which MSC suppress T cell proliferation (English *et al.* 2007; Tobin *et al*. 2013), monocyte differentiation (Ramasamy *et al*. 2007), dendritic cell (DC) maturation, antigen presentation (English *et al*. 2008; Spaggiari *et al*. 2009; Liu *et al.* 2014), and natural killer (NK) cell function (Spaggiari *et al*. 2008; Noone *et al*. 2013; Lu *et al.* 2015) have now been extensively characterised *in vitro*. In addition, the exposure of MSC to proinflammatory cytokines, such as interferon gamma (IFNγ) and tumor necrosis factor alpha (TNFα), has been shown to "license" or activate these cells to become more potent suppressors of inflammation (Krampera *et al.* 2006; Ryan *et al.* 2007; English *et al*. 2007; Polchert *et al*. 2008). Accordingly, all of these findings suggest that MSC modulatory potential cannot be pinned down to a single component or mechanism but is reliant on a myriad of factors.

MSC were originally suggested to be invisible to allogeneic immune cells which commercialised them as an "off the shelf" therapy permitting the use of a universal donor (Vaes *et al*. 2012). However, multiple observations in pre-clinical and clinical studies have now questioned the immune-privileged status of MSC (Ankrum, Ong, *et al*. 2014). For example *in vivo* studies have shown that MSC are undetectable 48 h after infusion

(Toma *et al*. 2009), stimulate innate responses (Grinnemo *et al*. 2004), elicit cellular and humoral responses (Badillo *et al*. 2007) and can induce immune memory (Nauta *et al*. 2006). These findings suggest that MSC are not immune-privileged but in fact are immune evasive. As the exact mechanisms involved in MSC immune modulation *in vivo* remain unclear, the establishment of such interactions will be fundamental in the broad scale implementation of this promising cell therapy for inflammatory disorders like GvHD. Therefore, the interactions of MSC and the immune system requires more in-depth investigation to facilitate a more conclusive understanding of how these cells mediate their therapeutic effects.

1.3. MSC AND THE INNATE IMMUNE SYSTEM

1.3.1. MSC AND THE COMPLEMENT SYSTEM

The innate immune system provides a non-specific and fast acting response which triggers a cascade of chemokines and cytokines following the recognition of pathogen associated molecular patterns (PAMPs). A central component of innate immunity is the complement system which has been implicated in the rejection of transplanted allografts (Hughes & Cohney 2011). The complement system is made up of a large number of distinct plasma proteins that react with one another to opsonize pathogens and induce a series of inflammatory responses to modify immune responses (Janeway *et al*. 2001). Complement can integrate the interactions between innate and adaptive immune responses and it has been suggested to be a key mediator of the broad immune modulation mediated by MSC (Moll *et al*. 2011).

Recently, MSC were shown to activate the complement system where all 3 complement activation pathways were involved in generating the membrane attack complex

(MAC) to directly injure MSC and lead to the subsequent clearance of MSC after infusion (Li & Lin 2012). However, MSC have also been shown to be able to protect themselves from lytic activity of complement components through the expression of cell surface complement inhibitors CD46, CD55 and CD59 (Moll *et al*. 2011; Li & Lin 2012) and through the secretion of factor H (Tu *et al.* 2010). MSC themselves can trigger the complement cascade through the upregulation of complement activation products on their cell surface and through secretion of soluble anaphylatoxins which was shown to correlate with their *in vitro* suppressive ability of peripheral blood mononuclear cells (PBMC) (Moll *et al*. 2011). These findings provide evidence of the complement system being integrally involved in governing the immunomodulatory activity of MSC and demonstrates how complement activation mediates the interaction of MSC with other immune cells. Hence, it comes as no surprise that adoptive MSC transfer will also encounter cells of the innate immune system.

1.3.2. MSC AND DENDRITIC CELLS

Dendritic cells (DC) are distinctive antigen presenting cells (APC) that play a pivotal role in the induction of adaptive peripheral tolerance. They are located in the skin, airways, lymphoid tissues, other organs and blood. This distribution of DC strategically places these cells for their primary role in detection of specific antigen for presentation to CD4^{+} T cells. MSC interact with DC and the elucidation of these mechanisms will aid in defining how MSC mediate their immunomodulatory effects.

MSC were shown to block the differentiation of DCs from their monocyte precursors by interfering with the cell cycle (Ramasamy *et al*. 2007). Furthermore, MSC have been shown to interrupt three key features of DC transition from an immature to a mature

phenotype (Figure 1.1.). Firstly, the lipopolysaccharide (LPS) induced upregulation of co-stimulatory molecules CD40, CD80, CD86 and MHC Class II by DC is restricted by MSC (English *et al.* 2008; Jung *et al.* 2007; Djouad *et al.* 2007). Second, antigen presentation by DC is impaired by MSC (Beyth *et al.* 2005; English *et al.* 2008) and finally, DC migration to lymph node derived chemotactic signals was hampered by MSC through maintenance of tissue anchoring E-cadherin on the surface of DC while C-C chemokine receptor type 7 (CCR7) was downregulated (English *et al.* 2008). MSC therapy was shown to inhibit T cell priming as the migratory capacity of LPS activated DC was significantly hampered (Chiesa *et al.* 2011). Thus, *in vitro* and *in vivo* findings can be linked and suggest the impairment of T cell priming by DC, as a result of modulation by MSC, prevents an efficient antigen-specific immune response in secondary lymphoid organs.

The disruption of DC maturation by MSC is achieved by soluble factors and cell contact signals. MSC were shown to secrete high levels of IL6 which induced a semi-mature phenotype in DC and resulted in the partial inhibition of bone marrow progenitor differentiation into DC (Djouad *et al.* 2007). Blocking PGE2 synthesis in MSC was shown to revert most of the inhibitory effects MSC exerted on DC function and differentiation, implicating a key role for PGE2 in these processes (Chen *et al.* 2007).

In terms of cell contact signals utilised by MSC for DC modulation, the Notch signalling pathway has been proposed as a candidate for facilitating MSC mediated effects on DC (Cheng *et al*. 2003; Li *et al*. 2008). MSC were shown to promote DC into a regulatory phenotype (dependent on Jagged-2 (a Notch ligand)) (Zhang *et al*. 2009) while Notch dependent signalling facilitated MSC expansion of functional tolerogenic DC (Cahill *et al*. 2015). These MSC educated tolerogenic DC produced anti-inflammatory cytokines to provide a state of tolerance (Zhang *et al.* 2009; Liu *et al*. 2012) whereby their regulatory function was shown to suppress alloresponses *in vivo* and prolong allograft survival (Ge *et*

al. 2009; Huang *et al.* 2010). More recently, Liu *et al.,* showed how Notch signalling was required for MSC to generate regulatory DC from a HSC population and subsequent infusion of these regulatory DC were shown to alleviate colitis in mice (Liu *et al.* 2015). The requirement for MSC cell contact mechanisms was demonstrated further by Aldinucci *et al*. where MSC required cell contact with human monocyte derived DC for the inhibition of DC function. DC co-cultured with MSC were unable to form active immune synapses, maintained their endocytic activity and continued to possess podosome-like structure, however the exact mechanism of inhibition in this case remains unclear (Aldinucci *et al*. 2010).

MSC modulation of DC function and the induction of tolerogenic DC are key features of MSC immune modulation which are relevant in transplantation, however, significant gaps in our understanding of the exact mechanisms employed by MSC in this context remain unclear.

1.3.3. MSC AND NATURAL KILLER CELLS

Natural Killer (NK) cells are cytotoxic lymphocytes of the innate immune system capable of recognising and destroying virally infected, allogeneic or abnormal host cells (Biron 1997; Ruggeri *et al*. 1999). Importantly, NK cells provide a first line of defence targeting cells that escape cytotoxic T cell (CTL) recognition or display inadequate expression of self-major histocompatibility complex (MHC) class I molecules (Ljunggren & Karre 1990). Their functions are tightly regulated by a series of receptors which transduce activation or inhibitory signals (Lanier 1998). The immunomodulatory functions of NK cells are mediated in response to and through secretion of cytokines, IFNγ in particular, and chemokines (Gidlund *et al*. 1978; Wang *et al*. 2012). Importantly, NK cell mediated lysis is

inversely correlated with expression levels of MHC class I which render allogeneic MSC potential targets for NK cells. Therefore, understanding the interactions and crosstalk between NK cells and MSC will aid in the advancement of this cellular therapy (Noone *et al*. 2013).

Over the last decade, there have been major developments in identifying mechanisms used by MSC to evade clearance by NK cells. Initially it was suggested that MSC alter NK cell phenotype to suppress proliferation and cytokine production using the soluble factors transforming growth factor-beta (TGFβ) 1, indoleamine 2,3-dioxygenase (IDO) and PGE2 (Sotiropoulou *et al*. 2006; Spaggiari *et al*. 2008). However, it has been reported that NK cells, activated by IL2 or IL15, are capable of lysing autologous and allogeneic MSC (Spaggiari *et al*. 2006; Gotherstrom *et al*. 2011). Interestingly, NK mediated lysis was inhibited when MSC were licensed with IFNγ due to MHC class I molecule upregulation on the surface of licensed MSC (Spaggiari *et al*. 2006). These findings were supported by Noone *et al.* and implicated IDO production by human MSC as a key mediator providing MSC protection from NK cell lysis through the suppression of NK activation and increased expression of HLA-ABC (Noone *et al.* 2013). These findings suggest that the outcomes of NK cell and MSC interactions *in vitro* are dependent upon the activation status of both NK cells and MSC and the cytokines present in the milieu.

In animal models, MSC were shown to illicit a heightened immune response which was influenced by the degree of MHC I and II mismatch and resulted in an expansion of NK cells in the periphery (Eliopoulos *et al*. 2005; Isakova *et al*. 2014). This suggests that MSC are targeted and lysed by NK cells *in vivo*. However, hypoxic MSC displayed an increased ability to engraft in allogeneic recipients by reducing NK cytotoxicity and decreased the number of infiltrating NK cells in ischemic hind limbs (Huang *et al.* 2014). Interestingly, in an inflammatory model of biomaterial incorporation, NK cells were shown to recruit MSC

for enhanced tissue repair via the incorporation of inflammatory signals in the biomaterials (Almeida *et al*. 2012). Despite their MHC I expression, MSC are recognised and killed by cytokine activated NK cells, even if they can also strongly inhibit NK cell cytotoxicity (Spaggiari *et al*. 2006; Spaggiari *et al*. 2008; Poggi *et al*. 2005). However, it's important to note that IFNγ pre-licensed MSC are less susceptible to NK killing (Noone *et al*. 2013). This suggests that there are complex interactions between NK cells and MSC that are not fully understood. In particular, these findings suggest that MSC are not immune-privileged which may impact on the use of a universal donor for MSC therapy. However, a large body of evidence suggests that allogeneic MSC can mediate protective effects even though they seem to disappear within 72-96 hours post administration (Eggenhofer *et al* 2012; Parekkadan *et al* 2010). Further understanding of how to enhance/prolong MSC engraftment/survival and therefore strengthen MSC therapeutic efficacy will undoubtedly aid in the successful implementation of MSC as a mainstay cellular therapy.

1.4. MSC AND THE ADAPTIVE IMMUNE SYSTEM

1.4.1. MSC AND T CELLS

One of the defining characteristics of MSC is the capacity for T cell modulation and this is the basis for MSC therapeutic intervention in T cell mediated diseases. The modulation of innate immune cells by MSC, as described above, can have indirect suppressive effects on adaptive immunity (Figure 1.1). However, MSC can directly inhibit T cell function through a combination of chemokines, direct cell contact and through the release of soluble factors (Di Nicola *et al*. 2002; English *et al*. 2007; Ren *et al*. 2008). MSC can attract T cells into close proximity via the secretion of Chemokine (C-C motif) ligand

(CCL) 2, Chemokine (CXC motif) ligand (CXCL) 9 and CXCL10 (Ren *et al*. 2008) before anchoring the T cell via intracellular adhesion molecule-1 (ICAM-1) and (vascular cell adhesion molecule-1) VCAM-1 on the surface of MSC (Ren *et al*. 2010) to more potently exert its immunosuppressive effects. The proliferation and cytotoxic function of activated T cells is suppressed by MSC through the secretion of a wide range of soluble factors including, TGFβ, hepatocyte growth factor (HGF) (Di Nicola *et al*. 2002), IDO (Meisel *et al*. 2004), PGE2 (Németh *et al*. 2009), IL10 (Yang *et al*. 2009), IL6 (Najar *et al.* 2009), Galectin-9 (Gieseke *et al*. 2013) and TNF-stimulated gene 6 (TSG6) (Lee *et al*. 2009). However, the proinflammatory cytokines IFNγ and TNFα have been shown to be essential for the induction of IDO and PGE2 by MSC (Meisel *et al*. 2004; Krampera *et al.* 2006; Ryan *et al*. 2007; English *et al.* 2007). The requirement for proinflammatory cytokines in MSC activation and subsequent production of soluble factors capable of modulating T cell mediated inflammation suggests a dynamic cross-talk between MSC and T cells.

Interestingly, the suppressive ability of MSC is not MHC-restricted (Le Blanc *et al.* 2003; Ryan *et al*. 2007) nor is it restricted to naive T cell activation and proliferation, as MSC have also been shown to inhibit the response of antigen specific memory T cells to their cognate antigens (Krampera *et al*. 2003). The proposed mechanisms by which MSC modulate T cell function have included the induction of apoptosis (Plumas *et al*. 2005). Akiyama et al., demonstrated that MSC utilise CCL2 mediated chemo-attraction to induce T cell apoptosis through Fas/FasL signalling *in vivo* (Akiyama *et al*. 2012). However, Xu et al., have shown that MSC can provide survival signals by mediating an anti-apoptotic effect on T cells *in vitro* through the secretion of IL6 (Xu *et al.* 2007).

Alternatively, studies have shown that MSC can modulate T cell function by inducing T cell anergy due to the lack of co-stimulatory molecule (CD80 and CD86) expression. Importantly, evidence suggests that MSC-induced T cell unresponsiveness is transient and

can be restored following removal of MSC (Di Nicola *et al*. 2002; Krampera *et al*. 2003). While the Krampera *et al*., study was the first to demonstrate the inhibitory effect of MSC on T cell response to cognate peptide, it didn't explore MSC antiproliferative effect on T cells. In another study, MSC were shown to inhibit T cell proliferation by rendering T cells anergic through cell cycle arrest at the G0/G1 phase even after MSC removal and with subsequent addition of exogenous IL2 (Glennie *et al.* 2004). Apart from the various culture conditions, the diverse stimuli used in these different study designs may partially account for the variations observed. In particular, Glennie *et al*., re-stimulated T cells from the bulk cultures but in the Di Nicola *et al*., study, re-stimulation was performed after the selection of viable cells, which may have been spared by the initial inhibition (Glennie *et al*. 2004; Di Nicola *et al.* 2002). However, this potent suppression obtained *in vitro* was not achieved *in vivo* where administration of MSC to a model of autoimmune encephalomyelitis (EAE) transiently promoted tolerance by inducing T cell anergy but T cell responsiveness was restored following IL2 administration *in vivo* (Zappia et al. 2005). This suggests that the inhibitory proliferative effect on T cells is dependent on MSC/T cell ratio, where there is a much higher number of T cells *in vivo* than an *in vitro* setting.

Other mechanisms of MSC modulation of T cells include shifting the T helper lymphocyte balance and the induction/expansion of regulatory T (Treg) cells. In an EAE disease model, the administration of MSC favorably altered the balance between a proinflammatory environment predominately of IFNγ producing Th1 and IL17 producing Th17 cells to a more anti-inflammatory environment composed of IL4 producing Th2 cells (Bai *et al.* 2009). Similarly, Batten *et al*., who described using human MSC for tissue engineering of a heart valve, resulted in a skew from a Th1 response to a Th2 response achieving a new balance (Batten *et al.* 2006). Using a model of allergic airway inflammation, Kavanagh and Mahon reported that allogeneic MSC therapy suppressed allergen-driven pathology through a Treg dependent mechanism. The increased CD4^{+} FoxP3^{+} T cells

present in the lung and spleen along with elevated IL10 production, suggested the expansion of Treg *in vivo* (Kavanagh & Mahon 2011). MSC support of Treg *in vitro* has been shown to involve a sequential process dependent on cell contact, PGE2 and TGFβ1 for the expansion of fully functional Treg capable of allosuppression (English *et al.* 2009). However, MSC were also shown to indirectly expand Treg generation by differentiating monocytes toward an anti-inflammatory macrophage phenotype where the subsequent CCL18 secretion resulted in Treg expansion (Melief *et al.* 2013). The promotion of Treg generation following MSC administration *in vivo* has been observed in a wide range of disease models. There have been numerous reports of increased Treg cell numbers following MSC therapy in animal models of allergic airway inflammation (Cahill *et al.* 2015), diabetes (Zhao *et al*. 2008), EAE (Luz-Crawford *et al*. 2013), colitis-associated colorectal cancer (Tang *et al.* 2015) and heart transplant model (Casiraghi *et al*. 2008). The therapeutic benefit of MSC expanded Treg was evident when Tregs were depleted in a kidney allograft transplantation model (Ge *et al*. 2010) and in a model of airway inflammation (Cahill *et al*. 2015). The increase in Tregs has been established as a primary mechanism employed by MSC to regulate immune response. One hypothesis is that MSC directly induce the differentiation of Treg cells from naive CD4^{+} T cells (Del Papa *et al.* 2013). However, this study did not provide evidence for the capacity of MSC to induce a population of Treg from Foxp3^{−} T cells. Cahill *et al.,* have shown that MSC expand rather than induce a population of Treg and that Jagged-1 expression by MSC facilitates MSC expansion of Treg *in vitro* (Cahill *et al.* 2015).

More recently, the microRNA, miR-21, was shown to negatively regulate the immunoregulatory cytokine TGFβ1 in MSC and miR-21(-/-) MSC reduced colonic inflammation in a mouse model of colitis in a TGF-β1-dependent manner (Wu *et al.* 2015). The studies illustrate the dynamic interactions MSC have on T cells via cell contact or with secreted soluble factors and given specific environment cues, MSC can suppress T cell

proliferation or expand T reg. Thus far data on MSC induction of Treg has been less convincing.

1.4.2. MSC AND B CELLS

While the effects of MSC on T cell biology has attracted most of the attention in clinical applications of MSC, as described above, the interactions of MSC on B cell functions is poorly understood. Additionally, data pertaining to the interactions of MSC and B cells is scarce and presents inconsistent results (Corcione *et al*. 2006; Rasmusson *et al.* 2007; Traggiai *et al*. 2008; Tabera *et al*. 2008; Franquesa *et al.* 2012).

B cells are a major cell type involved in adaptive immunity and are specialised in antigen presentation and antibody production. While most studies on MSC interaction with B cells suggest that MSC inhibit B cell function (Corcione *et al*. 2006; Tabera *et al.* 2008; Franquesa *et al*. 2012; Asari *et al.* 2009), other studies have demonstrated a supportive role for MSC in B cell expansion and differentiation (Rasmusson *et al.* 2007; Traggiai *et al.* 2008; Ji *et al*. 2012). Mechanisms proposing that MSC provide a supportive role for B cells have demonstrated the requirement for cell contact (Rasmusson *et al*. 2007; Traggiai *et al.* 2008) and that the soluble factor VEGF, produced by MSC, mediated anti-apoptotic effects through the inhibition of the pro-apoptotic caspase 3 cascade (Healy *et al.* 2015). In line with this study, Luz-Crawford *et al* demonstrated the capacity for MSC to enhance B cell survival with a partial role for IL1RA. Moreover this group showed that MSC inhibited plasmablast differentiation (*in vitro* and *in vivo*) possibly through the generation of IL10 producing Breg, although the *in vivo* evidence is less convincing (Luz-Crawford *et al*. 2016; Franquesa *et al*. 2015). Recently, MSC were shown to inhibit marginal zone B cells through inhibition of caspase-3 which suggest that MSC inhibit B cell commitment (Chen *et al*. 2016). While

resting MSC enhanced B cell production of IL10 in LPS activated mouse B cells, IFNγ stimulated MSC inhibited IL10 production by activated B cells via a mechanism requiring cell contact and involving the Cox-2 pathway (Hermankova *et al*. 2016).

However, in a clinical study where chronic GvHD patients were treated with MSC, MSC were shown to promote the survival and proliferation of CD5^{+} regulatory B cells with an increase in IL10 (Peng *et al* 2015) . The differences in these studies are likely to do with variability in experimental protocols and varied B cell populations. Particularly when starting B cell populations consist of whole PBMC populations (Traggiai *et al* 2008) and purified B cells (Corcione *et al* 2006; Rasmusson *et al*. 2007). Therefore, the presence of T cells within the culture can influence MSC interaction with B cells (Rosado *et al* 2014) and the presence of pro-inflammatory cytokines like IFNγ may influence the effect of MSC on B cell survival and functions. Overall, this highlights how small differences in experimental design and set-up can seemingly produce substantially different outcomes. However, careful dissection of the published findings and use of rational design to develop meaningful experiments are powerful tools that may allow the decoding of such complex findings as evidential in the recent publications from a number of groups explaining these inconsistent results (Healy *et al*. 2015; Franquesa *et al*. 2015; Luz-Crawford *et al*. 2016).
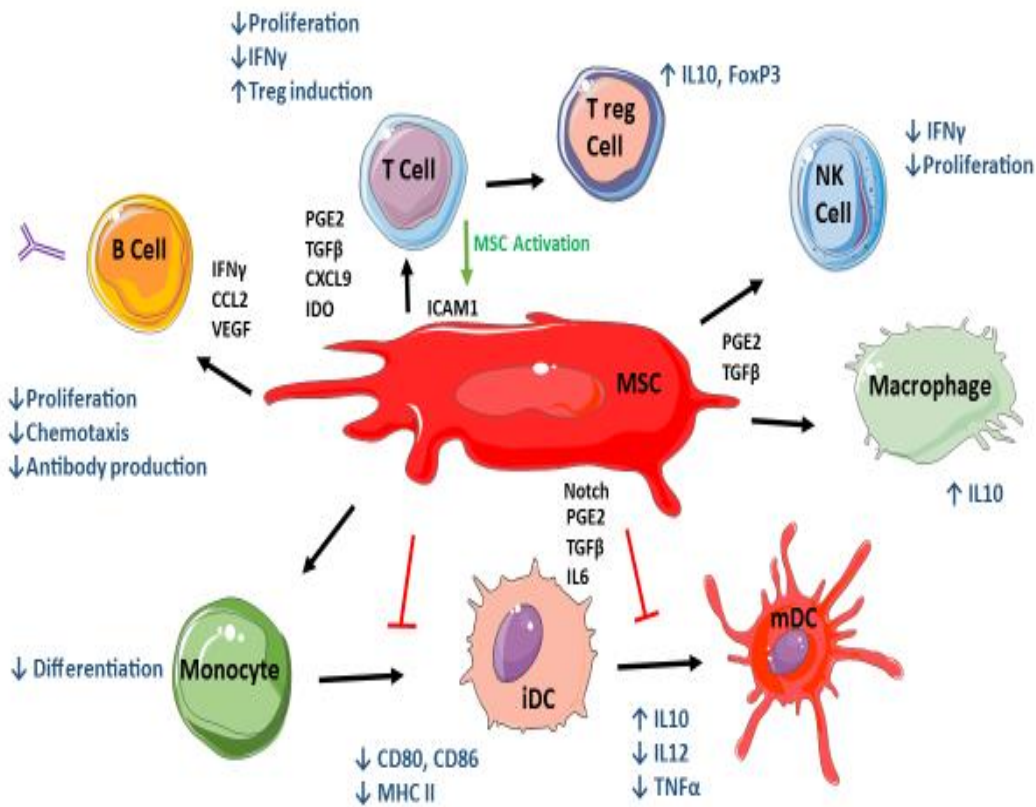
Figure 1.1. MSC modulation of the immune system. Schematic representation illustrating the range of immunomodulatory effects mediated by MSC. MSC regulate critical roles of innate and adaptive immune cells by suppressing their development or effector functions through the release of soluble factors and contact dependent signals. Different mechanisms target various facets of immune cell functioning. In many cases, bi-directional cross-talk influences these outcomes. IFNγ secreted by T cells in particular are key for MSC activation. MSC, in turn, inhibit T cell proliferation, cytokine production and expand the number of Treg. MSC inhibit B cell proliferation, differentiation into antibody secreting plasma cells and impair B cell chemotaxis. Monocyte differentiation is inhibited by MSC. The maturation and activation of DC are inhibited by MSC. MSC derived PGE2 and TGFβ reprogramme macrophages to secrete IL10. Black arrows and text pertain to responses driven by MSC and the effects of such on immune cells are indicated by blue arrows and text.

1.5. MAJOR HISTOCOMPATIBILITY COMPLEX MOLECULES; BARRIERS IN TRANSPLANTATION

The major histocompatibility complex (MHC), human leukocyte antigen (HLA) in humans, is an intrinsic part of the immune system and contains important polymorphic genes encoding proteins that present antigen to self-restricted T cells (Snell 1948; Dausset 1958). MHC molecules are essential in immune regulation (Billingham *et al.* 1953) by supporting the discrimination of self from non-self (Doherty & Zinkernagel 1975). The exact pattern of MHC gene expression or haplotype is almost unique to each individual, therefore cells that do not recognise recipient MHC molecules become activated (Snell 1948). In essence, immune cells recognise non-self MHC as foreign and endeavour to clear these cells from the body.

In transplantation, MHC can potentiate a substantial barrier to the success of both solid organ and bone marrow transplantation (BMT). Donor tissue or cells that express different MHC molecules to that of the recipient are subject to recognition and result in the rejection of tissue or clearance of cells by the recipient's immune system. This was a key finding discovered through a body of work carried out by Gorer, Snell and Dausset and others in the early 20th Century which has been fundamental to the advancements made in understanding the immune system and its manipulation during transplantation. Gorer made the discovery that sera from humans possessed natural antibodies that could distinguish between red blood cells isolated from three different strains of mice (Gorer 1936). Concurrently, Snell identified tumor transplantation resistant genes or histocompatibility genes (H genes). In collaboration with Gorer, Snell discovered the H-2 locus, encoding for major histocompatibility which resulted in rapid transplant rejection (Gorer *et al.* 1948; Snell & Higgins 1951).

The above studies focused MHC molecules at the forefront of investigations in transplantation tolerance. The discovery of the first HLA antigen, by Dausset in 1958, was made following the screening of patients who had received multiple blood transfusions (Dausset 1958). This study revealed that sera from some donors resulted in clumping of leukocytes and that anti-sera was capable of detecting alloantigen present on human leukocytes, which Dausset named MAC but is now referred to as HLA-A2 (Dausset 1958; Degos 2009). From these early findings, Dausset hypothesised that this human antigen and any further antigens yet to be discovered at this time would play very important roles in transplantation, particularly in human BMT between MHC mismatched donors.

The discovery of HLA genes and their role in transplantation rejection supported the concept of immunological tolerance and tissue transplantation developed by Billingham, Medawar and Brent (Billingham *et al*. 1953). Together these discoveries contributed significant knowledge to the field of transplantation and with the subsequent discoveries of powerful immunosuppressive drugs, such as Cyclosporine A or tacrolimus, the field was revolutionised as transplantation between MHC mismatched patients was permitted (Balduzzi *et al.* 1995).

While fully matching donor and recipient MHC type improves outcomes, alloreactivity can occur through the recognition of host-derived antigens bound to host MHC molecules by donor T cells (Janeway *et al.* 2001). These antigens are called minor histocompatibility molecules (miHA) and provide distinct HLA-binding peptides derived from polymorphic proteins (Janeway *et al* 2001). In an allogeneic haematopoietic stem cell transplantation setting where donor/recipient are fully MHC matched, disparaties between donor and recipient miHA can lead to a graft versus leukaemia effect, which will be discussed further in section 1.6, or graft versus host disease (section 1.7).

1.6. HAEMATOPOIETIC STEM CELL TRANSPLANTATION

Haematopoietic stem cell transplantation (HSCT) is an important therapeutic option for patients suffering with life-threatening haematological malignancies and inherited blood disorders (Ferrara & Deeg 1991). It involves the intravenous (IV) infusion of autologous or allogeneic stem cells to re-establish haematopoietic function in patients whose bone marrow or immune system is damaged, as a result of a bone marrow infiltrative process such as leukaemia, or in cases where the immune system is defective. Additionally, this treatment allows patients with cancer to receive higher doses of chemotherapy than bone marrow can usually tolerate and bone marrow function is then salvaged by replacing the marrow with previously harvested stem cells (Verburg *et al.* 2001). The number of HSCT carried out is ever increasing with 25,000 procedures performed globally in 2009 (Ferrara *et al*. 2009) and a surge of up to 40,000 procedures were reported in Europe alone in 2013 (Passweg *et al.* 2015) providing evidence that HSCT has become common practice. In a long term survival study of 854 patients who had received autologous HSCT for haematologic malignancy, it was projected from this cohort that the probability of surviving 5 years was 80% and surviving 10 years was 69% (Bhatia *et al.* 2005). With increased survival rates and improved outcomes being reported for patients following HSCT, the use of this treatment has expanded towards the use in cases of severe autoimmune diseases where patients are refractory to conventional therapy (Farge *et al.* 2010).

Patients receiving HSCT will firstly undergo a pre-conditioning regimen consisting of chemotherapy, radiotherapy and/or T cell depletion (Ruutu *et al*. 2014). These pre-conditioning regimens are classed as myeloablative or non-myeloablative. Myeloablative conditioning is the administration of total body irradiation and/or alkylating agents at doses which will not allow autologous hematologic recovery thus, stem cell support is required to rescue marrow function (Bacigalupo *et al*. 2009). Non-myeloablative conditioning is a

regimen which will cause minimal cytopenia and does not require stem cell support (Bacigalupo *et al*. 2009). These pre-conditioning regimens are designed to eliminate the patient's diseased haematological cells, leaving them highly immunocompromised and equipped for the engraftment of donor bone marrow. The engrafted haematopoietic compartment which contain donor T and B cells present in the graft not only reconstitute adaptive immune capacity in the recipient but can benefit the recipient further as activated donor T cells can have an effect on the remaining leukaemia (Graft versus Leukaemia or GvL) or tumor cells (Graft versus Tumor or GvT) (Horowitz *et al.* 1990; Eibl *et al.* 1996).

HSCT has evolved over the years in terms of harvesting methods as HSC were originally harvested from bone marrow (BM) and subsequently detected in other sites such as cord blood (CB) and peripheral blood (PB) (Lu *et al*. 1993; McCredie *et al.* 1971). As the number of HSC infused during the transplantation is predictive of a better outcome for HSCT patients, the method of harvest must contain enough autologous or allogeneic HSC (Hequet 2015). HSC from CB display high clonogenic potential and is transplantable across HLA barriers however, their use for allogeneic HSCT can be complicated due to limited cell recovery from low CB volume collection and require more than one CB unit (CBU) for successful use in adults (Barker *et al*. 2005). PB and not BM HSC are preferentially harvested when the main aim is to obtain a GvL effect however, HSC are not present in PB under normal conditions making it is necessary to mobilise HSC from the BM to the PB for harvest (Hequet 2015).

A completely matched sibling donor is generally considered an ideal donor however, in the case of unrelated donors, a complete match or a single mismatch is considered acceptable for most transplantation and in certain circumstances a greater mismatch is tolerated. As discussed in section 1.5, the degree of HLA disparity has significant consequences in transplantation and closely matched HLA loci (HLA-A, -B, -C and -DRB1)

is detrimental to the success of HSCT and lower incidences of mortality (Flomenberg *et al.* 2004). However, many patients who may benefit from this treatment lack a suitably matched unrelated adult donor which has led to increasing need for unrelated CBU as an alternative graft (Eapen *et al.* 2011).

With the use of HLA mismatched, unrelated and cord blood donors as sources for HSC, HSCT patients are at risk of infectious complications, including *Pneumocystis* pneumonia, invasive fungal infections and viral infections, remain a major cause of transplant related morbidity and mortality (Park *et al.* 2006; Lin & Liu 2013). Additionally, active donor T cells can cause pathology in the form of graft versus host disease (GvHD) as a result of donor/host HLA mismatch at both HLA and miHA level (Korngold & Sprent 1978). It is important to highlight that the antigenic targets of GvHD are mainly miHA because donor and recipients are MHC fully matched (Schroeder *et al* 2011). Whereas the MHC molecules are only the the antigenic targets in cases where donor/recipient are not MHC matched (Schroeder *et al* 2011).

GvHD has been described as a mirror image of solid organ transplantation rejection in that it is the donor allogeneic T cells that recognise the recipient MHC antigen on host cells as foreign (Gale & Reisner 1986). It is a multi-system inflammatory disease which mainly targets the skin, GI tract and liver. There are two presentations of GvHD, acute (aGvHD) and chronic (cGvHD). By definition, the acute form occurs within the first 100 days post transplantation, the chronic disease occurs after 100 days. However, there have been presentations of GvHD where symptoms of both acute and chronic have manifested in patients, suggesting that this classification is not satisfactory (Filipovich *et al.* 2005). Clinical presentations of GvHD are discussed further in section 1.7.2.

1.7. ACUTE GRAFT VERSUS HOST DISEASE

1.7.1. ACUTE GvHD IMMUNOPATHOLOGY

Graft versus host disease (GvHD) is a major complication following HSCT resulting in target tissue damage and apoptosis, as illustrated in figure 1.2. The prerequisites for GvHD development are dependent on a host unable to mount a reaction against the graft (i.e immunodeficient) and the immunocompetent donor cells recognising tissue antigens (HLA) belonging to the recipient (Billingham 1966). With improvements in donor and recipient selection, preconditioning regimens, GvHD prophylaxis and treatment, and monitoring of infectious complications transplant-related mortality is mostly associated with relapse of the primary malignancy (Markey *et al*. 2014). Even though advancements have been made, GvHD remains a major cause of HSCT treatment failure. The overall incidence of GvHD is between 35-45% in recipients of full matched sibling donor grafts to 60-80% in recipients of one-antigen HLA mismatched unrelated donor grafts, leading to high rates of mortality (Ferrara *et al.* 2009).

The development of aGvHD has been characterised as having three phases involved in disease initiation (Figure 1.2). The three phases are broken down as follows; (1) the pre-conditioning regimen prior to transplantation and associated inflammation, (2) priming of donor T cells and differentiation and (3) the effector phase of tissue damage mediated by inflammatory cytokines and effector cells (Ferrara & Reddy 2006).

In phase 1, the pre-conditioning regimen patients undergo prior to transplantation is necessary to facilitate engraftment of donor immune cells but can cause tissue/organ damage, especially in the gastrointestinal (GI) tract. The permeability in the gut is affected following pre-conditioning and results in the leakage of lipopolysaccharide (LPS) into the periphery and subsequent inflammatory response (Ferrara *et al*. 2009). The pathophysiology of GvHD in phase 1 can be considered a "cytokine storm" as dysregulated cytokines form a network

of cells directly responsible for mediating tissue damage (Ferrara & Deeg 1991). The release of inflammatory cytokines such as TNFα have directly been associated with GvHD pathology as elevated TNFα serum levels were detected in patients with severe GvHD (Holler *et al.* 1990). Murine studies have been useful in proposing mechanisms by which phase 1 events such as priming of macrophages in GvHD mice and LPS triggered release of TNFα, lead to GvHD progression (Nestel *et al.* 1992). Furthermore, murine studies provided more evidence of the role of TNFα in early GvHD pathogenesis as TNFα neutralisation or blockade resulted in diminished inflammation (Via *et al*. 2001; Korngold *et al*. 2003).

Another key study showed how the activation of the LPS-Toll-Like Receptor (TLR) 4 pathway with subsequent IL1β release played a crucial role in murine GvHD pathology (Liang *et al*. 2014). Furthermore, PAMPs and damage associated molecular patterns (DAMPs) generated following pre-conditioning tissue damage can activate the Nlrp3 inflammasome during the early phase 1 and induce acute GvHD (Jankovic *et al.* 2013). Multiple intestinal cell subsets were shown to express pro-IL1β after allo-HCT, which underline its broad function as a key proinflammatory cytokine (Jankovic *et al.* 2013). It was suggested that the tissue damage associated with pre-conditioning, delivered the first signal needed for pro-IL1β synthesis in the form of enteric bacteria–derived PAMPs (Jankovic *et al*. 2013). The second signal was provided by the DAMP uric acid, which was released from damaged cells leading to inflammasome activation and subsequent secretion of bio-active IL1β (Jankovic *et al*. 2013). This highlights the importance of IL1β in the early stage of GvHD and identifies it as a therapeutic target.

Neutralisation of IFNγ had protective effects in the GI of murine GvHD (Mowat 1989) however, IFNγ facilitates GvL effects which suggests that IFNγ blockade is likely deleterious in patients after allogeneic HSCT and not beneficial as previously suggested (Yang *et al*. 2005). However, blockade of IL6 was shown to increase Treg reconstitution

and reduce severity in aGvHD as it displayed critical involvement in altering the balance between the effector and regulatory arms of the immune system (Chen *et al*. 2009; Tawara *et al*. 2011).

The pre-conditioning regimen also induces the upregulation of chemokines and adhesion molecules in GvHD target organs. CXCL10 was markedly increased in the GI of GvHD mice (Mapara *et al.* 2006) while CCL3 was shown to be instrumental in T cell recruitment to the lung, liver and spleen of GvHD mice (Panoskaltsis-Mortari *et al.* 2000; Serody *et al*. 2000). Sophisticated *in vivo* imaging studies have provided invaluable evidence of donor T cell migration and homing to target tissues (phase 2) in the early days following transplantation supporting the role for chemokines in GvHD progression (Panoskaltsis-Mortari *et al*. 2004; Anthony & Hadley 2012).

Inflammation in phase 1 has been shown to have two potential effects. (1) It activates recipient antigen presenting cells (APC), enhancing the ability of professional APCs to prime donor T cells and (2) these cytokines can provide costimulatory signals to donor T cells (TNFα, IL6). Ultimately these effects can lead to the generation of inflammation which permits the migration of donor T cells into target tissues (Ferrara *et al.* 2009).

The hallmark of phase 2 involves the priming and differentiation of effector donor T cells during GvHD progression (Figure 1.2). Donor T cells within the graft become activated by the inflammatory environment created by the pre-conditioning regimen. The proinflammatory cytokines and chemokines, mentioned above, activate endothelium to promote tissue inflammation, host APC upregulate MHC class II and costimulatory molecules and donor T cells are trafficked into target organs (Ferrara & Reddy 2006). It is generally perceived that donor CD8$^+$ T cells are predominantly activated by recipient haematopoietic APCs whereas donor CD4$^+$ T cells can also be activated by recipient non-haematopoietic APC within the GI tract (Markey *et al.* 2014). Donor APC can further

contribute to GvHD, once donor T cells have been primed by recipient APC (Matte *et al.* 2004). Once primed, donor T cells undergo proliferation and differentiation where further cytokine production ensues and, in some cases, cytolytic function is gained (Figure 1.2). Murine studies have demonstrated that the priming and differentiation of naive (as opposed to memory) T cells result in GvHD development (Anderson *et al.* 2003; Dutt *et al.* 2011). This suggests that depletion of naive T cells may prevent GvHD while permitting the transfer of donor memory T cells and subsequent pathogen-specific immunity. Investigation into the role of individual APC subsets in GvHD development, with ablation of individual APC subsets, has shown that no single recipient APC subset is mandatory for GvHD development (Shlomchik *et al.* 1999; Li *et al.* 2012). However, Koyama *et al.*, have shown that non-haematopoietic recipient APC within target organs induced GvHD by the promotion of alloreactive donor T cell expansion within the GI tract (Koyama *et al.* 2012). Other studies in murine GvHD models have demonstrated the role of co-stimulatory molecules in GvHD and have shown that protection from GvHD is achieved following blockade of CD80 and CD86, however further treatment was required for complete GvHD prevention (Blazar *et al.* 1996; Saito *et al.* 1996). Over the last number of years, the investigations described here have explored the effectiveness in suppressing different facets of donor T cell expansion and activation. This suggests that a principal determinant of GvHD development is due to T cell priming and differentiation. While many therapeutic approaches, as described in more detail in 1.8, potently inhibit donor T cell expansion and differentiation, GvHD still develops in up to 35-50 % of HSCT cases (Jacobsohn & Vogelsang 2007). This suggests that the standard therapeutic approach is inadequate.

Phase 3 is the effector phase of GvHD where the culmination of pre-conditioning associated inflammation, subsequent alloantigen presentation and T cell priming and differentiation lead to a multi-system immune response in which inflammatory cytokines, CTL and NK cells mediate apoptosis of target tissues (Figure 1.2) (Ferrara *et al.* 2009).

While chemokines and adhesion molecules facilitate T cell migration into target tissues, inflammatory cytokines produced mainly by monocytes/macrophages and T cells, such as TNFα, IL1β and IL12, drive GvHD pathology by inducing apoptosis of target tissue without direct interaction (Antin & Ferrara 1992; Hill & Ferrara 2000). However, CD8^{+} T cell mediated damage is dependent on the cognate interaction between CD8^{+} T cells and tissue (Matte-Martone *et al*. 2008). Cytolytic damage by T cells is carried out via perforin and granzyme molecules, TNF signalling and the Fas/FasL pathway (Graubert *et al*. 1997; Hattori *et al*. 1998).

Throughout the years, murine models of GvHD have played an instrumental role in defining the mechanisms involved in the key phases of GvHD pathogenesis. Each of these phases have identified key players in disease initiation and maintenance therefore classifying different areas for intervention where GvHD management could be achieved. It is important to note however, that donor T cells are required to target remaining leukaemia (GvL) through the induction of target tissue apoptosis which means that any therapeutic interventions must mediate a balance between GvHD and GvL (Figure 1.2).

As GvHD and GvL reactions target the same antigens, it makes it difficult to separate and balance these immune reactions. Approaches to distinguish between GvHD and GvL include the identification of leukaemia associated antigens or miHA that are preferentially expressed on haematopoietic tissues and exploiting them as immunotherapeutic targets (Welniak et al. 2007). Existing potential avenues include adoptive transfer of miHA specific T cells or vaccination of miHA peptide, protein, mRNA or DNA (Riddell *et al*. 2007). However, the number of patients that could be treated in this manner at present remains quite low because of the phenotypic frequencies of the miHA and their cognate HLA restriction molecules (Feng *et al.* 2008).
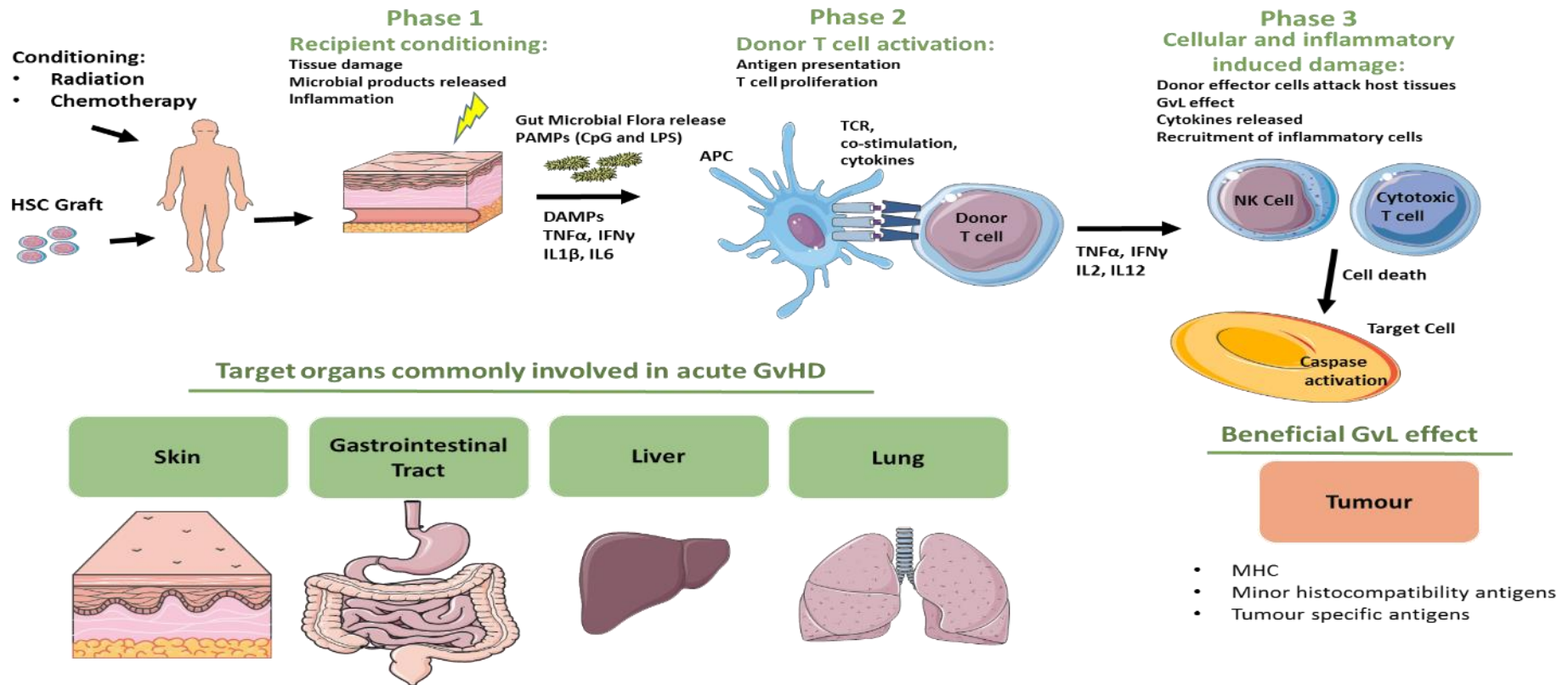
Figure 1.2. The pathophysiology of acute GvHD occurs in 3 phases and affects multiple organs. Schematic representation illustrating the key phases involved in aGvHD progression. In phase1, the initial damage to host tissue is a result of preconditioning treatment which perpetuates an inflammatory cascade involving the secretion of proinflammatory cytokines, DAMPs and PAMPs. Damage to intestinal mucosa in particular releases lipopolysaccharide (LPS) into the periphery. These factors contribute to the activation of host/donor antigen presenting cell (APC). Phase 2 involves the activation of donor T cells, where they proliferate, differentiate into effector T cells and migrate into target tissues. In phase 3, effector T cells release inflammatory cytokines which recruit inflammatory cells and apoptosis of target tissues ensues.

1.7.2. CLINICAL FEATURES OF aGvHD

GvHD is a systemic condition characterised by the targeted apoptosis of the skin, GI tract and the liver. Clinical symptoms of GvHD are primarily presented in the skin (81%) followed by the GI tract (54%) and liver (50%) (Martin *et al.* 1990). In the skin, the characteristic maculopapular rash can spread throughout the body causing ulceration and blisters from apoptosis inducing lymphocytes (Ferrara *et al.* 2009). Involvement of the GI tract in GvHD, includes apoptosis of the epithelial cells lining the GI tract resulting in diarrhoea and severe abdominal pain (Martin *et al.* 1990). The clinical manifestations of GI GvHD are often non-specific requiring the need for histological examinations, which reveal ulcerations, apoptotic bodies and crypt abscess formation in the small intestine and colon (Weisdorf *et al.* 1990). Similarly, liver GvHD can be difficult to distinguish from other causes of liver dysfunction (drug toxicity or secondary effects of pre-conditioning regimen), however clinical jaundice and hyperbilirubinaemia (elevated bilirubin levels in the blood) are typical manifestations of GvHD damage in the liver (Fujii *et al.* 2001). Manifestation of idiopathetic pneumonia syndrome is commonly associated with GvHD progression in lung and apoptosis in lung biopsies have been reported (Markey *et al.* 2014; Xu *et al.* 2013).

The severity of aGvHD is characterised by the extent of involvement of these organs and a grading system is used to index patient prognosis. There are four grades of GvHD development; I (mild), II (moderate), III (severe), and IV (very severe). The average long term survival rate for grade III GvHD is very poor (25%) and grade IV survival rate is just 5% which suggest that a reduction in GvHD pathology could lead to improved survival rates (Cahn *et al.* 2005).

1.7.3. CLINICAL FOCUS ON GI GvHD

As mentioned above, the GI tract plays a key role in the initiation of systemic GvHD through the propagation of a "cytokine storm" as a result of bacterial translocation from the disruption of the physical barrier in the GI (Figure 1.2). Therefore, the primacy of the GI tract as a target organ in GvHD has focused experimental approaches aiming to reduce GI damage by fortification of the GI mucosal barrier using novel "cytokine shields" such as IL11 or keratinocyte growth factor (Hill & Ferrara 2000). However, in a phase I/II double-blind clinical trial of recombinant IL11 in the prevention of acute GvHD, patients who received IL11 experienced severe fluid retention and early mortality made it difficult to determine whether IL11 reduced the rate of acute GvHD (Antin *et al.* 2002).

In recent times, microbiome studies have shown that gut microflora can impact the severity of aGvHD. Jenq *et al.*, observed that the elimination of Lactobacillales from the flora of mice before BMT aggravated GvHD, whereas reintroducing the predominant species of Lactobacillus mediated significant protection against GvHD (Jenq *et al.* 2012). Microbiome analysis revealed that aGvHD mice had a dramatic loss of bacterial diversity and a distinct microbiota composition compared with mice that did not develop aGvHD (Jenq *et al.* 2012). Similarly in humans, diversity of intestinal microbiota at engraftment was an independent predictor of mortality in allo-HSCT recipients as patients with lower intestinal diversity had poor outcomes (Taur *et al.* 2014). This suggests that microbiota diversity is important for immune regulation and manipulation of the intestinal microbiota holds potential for improvement of aGvHD therapies.

As mentioned in section 1.7.2, clinical manifestations of GI aGvHD are non-specific which pose a barrier to GI aGvHD treatment as diagnosis and prognosis rely on the presence of clinical symptoms. Currently there are no laboratory tests validated to make predictions of aGvHD development risk, patient responsiveness to treatment or survival. However,

some research groups have focused on biomarker discovery to diagnose GI GvHD (regenerating islet-derived 3-alpha) and predictive biomarkers for therapeutic response, (fecal calprotectin and alpha-1 antitrypsin) (Ferrara *et al.* 2011; Rodriguez-Otero *et al.* 2012). These biomarkers could improve GI aGvHD diagnostics and provide personalised treatment plans for high risk and low risk patients; thus optimal immunosuppression can be achieved without unwanted side effects.

1.8. THERAPEUTIC INTERVENTION FOR AGvHD

1.8.1. PRIMARY PROPHYLAXIS FOR AGvHD PREVENTION

Despite the advances and the level of research dedicated to controlling the development of aGvHD, the progress made in terms of eradicating the disease has been modest. The European Group for Blood and Marrow Transplantation (EBMT) and European Leukemia Net (ELN) working group published guidelines for prophylaxis of GvHD. The general consensus was that a prophylaxis regimen of Cyclosporine A (CsA) (3mg/kg/day from day -1) given intravenously in combination with a short course of methotrexate (MTX) (15mg/m^2 on day 1, 3, 6, 11) was the most widely used approach in Europe (Ruutu *et al.* 2014). The dose of CsA was adapted according to toxicity and/or drug levels particularly when switching to oral administration. There is evidence supporting the improved quality of life and reduction of GvHD with the inclusion of antithymocyte globulin (ATG) for unrelated donor transplantations and a reduced risk of tumor relapse (Finke *et al.* 2009; Kroger *et al.* 2002). However, it has been recommended that in cases where minimally intensive conditioning are required, ATG should be avoided as it may increase the risk of rejection or relapse and may interfere with GvL effect (Cragg *et al.* 2000; Ruutu *et al.* 2014). In a randomised trial comparing prednisone with ATG/prednisone combination as initial aGvHD therapy, the combination therapy resulted in too much immunosuppression where it

failed to control aGvHD and patients experienced more infectious complications than the single therapy (Cragg *et al.* 2000). Therefore, the ideal prophylactic regimen would reduce the organ damage associated with GvHD but not impair haematopoietic engraftment or the GvL/GvT effect.

1.8.2. FIRST LINE TREATMENTS FOR aGvHD

Once established, GvHD can prove difficult to treat. Currently in Europe, the standard first line therapy for aGvHD is glucocorticosteroids such as methylprednisolone (MP) (Ruutu *et al.* 2014). A typical steroid regimen for aGvHD therapy consists of methylprednisolone administered at 2 mg/kg per day for 7 to 14 days, followed by a gradual reduction in dose depending on patient response rates (Van Lint *et al.* 1998). For GI GvHD, non-absorbable oral steroid treatment in the form of budesonide (9mg/day) is recommended along with a systemic therapy, while topical steroids are recommended for skin GvHD (Ruutu *et al.* 2014). The administration of MP and other steroids has resulted in significant increases in survival and provided huge improvements to the standard of living for GvHD patients (Van Lint *et al.* 2006; MacMillan *et al.* 2002). However, there are major limitations to steroid therapy which include the increased risk of infection, hyperglycaemia, osteoporosis and growth defects which may be life threatening (Deeg 2007; Arora 2008). It is important to note that steroid therapies have proved beneficial for very many patients to date (Van Lint *et al.* 1998; Van Lint *et al.* 2006; Ruutu *et al.* 2014). Depending on the patient and the severity of aGvHD, the systemic exposure to steroid therapy can be tapered and the duration of therapy reduced (Cragg *et al.* 2000). However, the biggest problem with this treatment is the development of steroid resistant GvHD. In these cases where patients no longer respond to treatment, a second line of therapy is required.

1.8.3. SECOND LINE TREATMENTS FOR aGvHD

Salvage therapy or a second line of treatment is required when a patient has progressive GvHD pathology in any organ over 3 days, if there have been no improvement in condition over 7 days, worsening grade III aGvHD, or if there is incomplete response to treatment over 14 days (Deeg 2007). In Europe, a failure of response to steroid treatment (2mg/kg/day) in patients after 7 days was considered corticosteroid resistance, however clear signs of aGvHD on day 5 after steroid treatment also qualified as resistance (Ruutu *et al.* 2014). There is no standard second line treatment for aGvHD, instead widely used components include monoclonal antibodies, ATG, CsA or mesenchymal stem cells (Ruutu *et al.* 2014). Therefore, the choice of secondary therapy should be guided by the outcomes of the first line treatment and prophylaxis therapy.

Monoclonal antibodies (moAb) have a unique capacity for specific antigens which can be used to target and enable direct interference with the cellular mechanisms that are involved in GvHD pathophysiology. Visilizumab is an anti-CD3 monoclonal antibody used as a second line treatment to induce apoptosis of activated T cells (Carpenter *et al.* 2005). While results from clinical trials were promising, there were complications associated with Visilizumab including increased risk of Epstein Barr Virus (EBV) and subsequent lymphoproliferative disease (Carpenter *et al*. 2005). The moAb Alemtuzumab binds to CD52 and induces apoptosis of lymphocytes, monocytes and DC. Findings from clinical trials revealed that Alemtuzumab decreased the incidence of both acute and chronic GvHD development (Gómez-Almaguer *et al.* 2008; Gutiérrez-Aguirre *et al.* 2012). However, there are complications associated with this moAb which include neutropenia, infection with cytomegalovirus and increased relapse rates (Gómez-Almaguer *et al.* 2008; Gutiérrez-Aguirre *et al.* 2012). One of the most successful moAbs

used to date have targeted the production of TNFα during aGvHD. Two moAbs capable of such include Etanercept, which binds trimeric and membrane bound TNFα and Infliximab, designed to bind monomeric, trimeric soluble and membrane bound TNFα (Horiuchi *et al.* 2010). Clinical studies of Etanercept in combination with MP resulted in the complete resolution of symptoms in 77% of patients compared with 50% of patients treated with steroids alone (Levine *et al.* 2008). In another study, Etanercept alone was effective in 80%, 17% and 57% of grade II-IV patients respectively, however no patient achieved complete remission (Park *et al*. 2014). High grade aGvHD was shown to have limited response to infliximab in a clinical trial where, out of 71% of patients with grade III-IV aGvHD, only 15% achieved complete remission with the use of infliximab alone as a second line treatment for steroid refractory aGvHD (Pidala *et al*. 2009).

Over the last three decades, the potent immunosuppressant ATG has been successful in reducing the frequency of aGvHD without increasing the risk of tumor relapse (Kroger *et al*. 2002). However, strategies for intensive patient monitoring and prophylaxis for opportunistic infections must be implemented when possible (Martin *et al.* 2012). As T cell depletion increases the risk of viral infections in GvHD patients, viral loads should be monitored during administration of second line therapy until the number of T cells in the blood has recovered (Martin *et al.* 2012; Uhlin *et al*. 2014).

The incomplete efficacy of these second line treatments for steroid refractory aGvHD suggests that a more efficacious therapy or treatment plan needs to be designed. Recent advances involving CsA therapy for aGvHD will be detailed further in section 1.9 while the approaches using mesenchymal stem cell therapy for aGvHD will be discussed further in section 1.10.

1.9. CYCLOSPORINE THERAPY FOR AGvHD

1.9.1. MECHANISMS OF CYCLOSPORINE IMMUNE MODULATION

Since the late 1970's, cyclosporine (CsA) has played an important role in the advancement of transplant medicine. CsA was initially discovered while searching for novel antifungal agents but it was found to have many immunologic properties which made it an attractive agent for immunosuppression (Borel 1976). It was this work led by Borel that exhibited the cell-mediated specificity of CsA suppression *in vitro* and *in vivo* (Borel 1976; Hess & Tutschka 1980). Following this discovery, a large scale clinical trial demonstrated one year graft survival of 72% and 52% in recipients of cadaveric renal transplants who received either cyclosporine or azathioprine and steroids, respectively, for immunosuppressive therapy (European Multicentre Trial Group 1983). These encouraging results helped lead to the approval of CsA for use in the clinics in the early 1980s. With improved rates of acute rejection and graft survival rates at 1 (82%), 5 (69%) and 10 (54%) years, cyclosporine has become a mainstay for modern immunosuppression for solid organ transplants and HSCT (Marcen *et al*. 2009; Ruutu *et al*. 2014).

The mechanism of action of CsA involves the inhibition of calcineurin (Figure 1.3). Calcineurin is a calcium/calmodulin-dependent serine threonine protein phosphatase (Ke & Huai 2003). In the absence of CsA, calcineurin is active and can dephosphorylate regulatory sites on several transcription factors, most notably nuclear factor of activated T-lymphocytes (NFAT) (Flanagan *et al*. 1991). CsA inhibition of calcineurin occurs through the binding of CsA to the immunophilin, cyclophilin (Liu *et al*. 1991). This complex prevents the dephosphorylation and translocation of NFAT from the cytoplasm to the nucleus where inhibition at this level prevents transcription of genes required for T-cell activation (such as IL2) and subsequent immune response (Flanagan *et al.* 1991).

While the mechanism of CsA action is widely known to affect T cell function, CsA has also been shown to reduce antigen presentation by APC however, the mode of action on DC remains unclear (Varey *et al.* 1986). However, Muller *et al.*, showed that antigen presentation was not directly influenced by CsA and that it was carry over of CsA from APC to T cell that mimicked a drug effect on antigen presentation (Muller *et al.* 1988). More recently, CsA has been described as having an inhibitory effect on MHC-restricted antigen presentation *in vivo* (Lee *et al.* 2007), a decreased allostimulatory capacity through upregulation of B7-DC (Geng *et al.* 2008) and an anti-tolerogenic effect on DC where Treg proliferation was reduced from 72 to 47% (Pino-Lagos *et al.* 2010). Each of these effects reported pose implications in terms of immunosuppression in clinical transplantation.

Recently, CsA has also shown great promise as an antiviral therapy through its inhibition of proteins other than cyclophilin (Liu *et al.* 2011; Shen *et al.* 2013; Watashi *et al.* 2014). As discussed in section 1.8, viral infections are one of the leading causes of graft failure as a result of immunosuppressive therapy. In the liver, viruses such as hepatitis C virus (HCV) and hepatitis B virus (HBV) suppress interferon signalling for favourable viral infection/replication which subsequently inhibits host cell immunity (Rehermann & Nascimbeni 2005). Liu *et al.*, have shown *in vitro* that treatment of CsA restored intracellular IFNα expression and signalling, which was downregulated by HCV infection, through the suppression of negative regulators of IFN signalling (SOCS1 and PIAS-x) (Liu *et al.* 2011). Similarly, CsA was shown to inhibit HBV infection *in vitro* by targeting a membrane transporter which was essential for viral entry (Watashi *et al.* 2014). These findings are supported by clinical studies where liver transplant patients that received CsA for immunosuppression experienced a sustained virological response of 43% in comparison to 14% when tacrolimus was used instead (Cescon *et al.* 2009). These findings suggest mechanisms by which CsA can be used to reconstitute intracellular innate responses through viral infection inhibition and this can be applicable in HSCT patients.

While CsA has proved to be a powerful immunosuppressant in transplantation medicine, there is a growing body of research suggesting that CsA plays a modulatory role. CsA treatment was shown to enhance the migratory capacity of trophoblasts and decidual stromal cells through the upregulation of the chemokine CXCL12 via activation of mitogen-activated protein kinase/extracellular signal-regulated kinase (MAPK/ERK) signalling (Du *et al.* 2012; Zhao *et al.* 2012; Wang *et al*. 2013; Meng *et al.* 2012). This has implicated a role for CsA, distinct from its role in T cell immunosuppression, as a potential immune modulator through the enhancement of chemokines.

The specific T cell inhibitory activity of CsA, as described above, make it an ideal therapy for a T cell driven disease like GvHD. For prophylaxis of aGvHD, CsA is administered for up to six months after allogeneic HSCT (Ruutu *et al.* 2014). Over the years, CsA has also been reported to be an effective second line treatment of established GvHD and is currently recommended throughout Europe (Deeg *et al.* 1985; Parquet *et al*. 2000; Finke *et al*. 2009; Ruutu *et al.* 2014). However, the metabolism of CsA in the GI tract has been shown to significantly affect it's bioavailability as its absorption is slow, variable and incomplete (Webber *et al.* 1992). The added complications of damaged GI mucosa as a result of the conditioning regimen undergone by allogeneic HSCT patients could further influence CsA pharmacokinetics with reduced intestinal absorption (Kimura *et al*. 2010). Therefore, novel approaches to enhance CsA absorption could improve the efficacy of CsA in GvHD prevention.
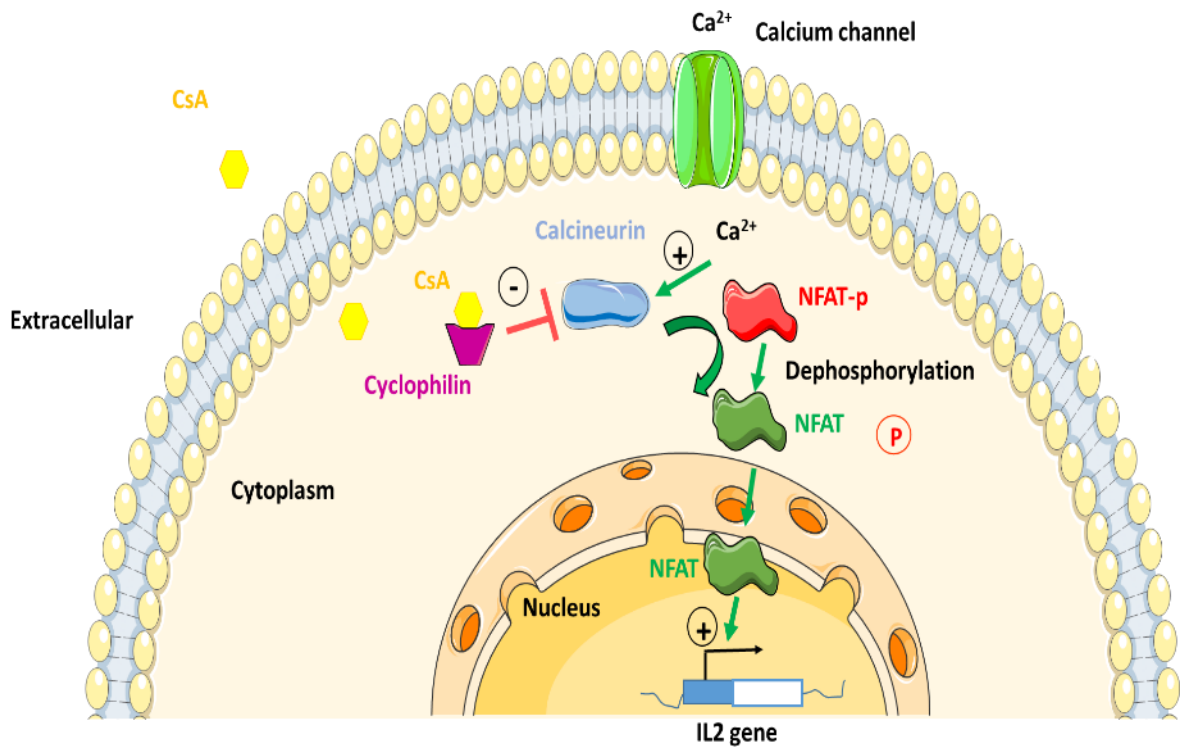
Figure 1.3. The mechanism of action of Cyclosporine. Cyclosporine (CsA) enters the cell via passive diffusion. Once in the cytoplasm, CsA binds to the immunophilin, cyclophilin, where a cyclophilin-CsA complex is formed. This complex binds to and inhibits the function of the enzyme calcineurin, which has serine/threonine phosphatase activity. As a result, calcineurin fails to dephosphorylate the nuclear factor of activated T cells (NFAT) in the cytoplasm which stops the translocation of NFAT into the nucleus. In the absence of CsA, NFAT binds to the promoter of the IL2 gene and initiates IL2 production. As a consequence of CsA presence, T cells do not produce IL2 which is necessary for full activation.

1.9.2. CYCLOSPORINE BIOAVAILABILITY ENHANCEMENT

CsA has proved to be an efficacious prophylaxis and treatment for established aGvHD. However, once patients are well enough to tolerate oral therapy they are moved from intravenous administration to oral administration where variability in bioavailability can occur (Ruutu *et al.* 2014). With intravenous administration there is 100% bioavailability however, with oral administration the CsA absorption in the GI is affected by food intake, fat content and GI movements which can reduce the bioavailability to 30% (Beauchesne *et al.* 2007). Over the years, much focus has been on efforts to enhance oral CsA bioavailability. Sandimmune® and the more advanced Neoral® are oral formulations of CsA which were designed for this purpose. Neoral® in particular has been shown to enhance oral bioavailability of CsA more efficiently than Sandimmune® and reduce the variability in pharmacokinetic parameters within and between patients receiving CsA therapy (Parquet *et al.* 2000; Yocum *et al.* 2000). As Sandimmune® is an oil-in-water emulsion, CsA absorption is affected by food intake and fat content, GI movements and bile secretion, however the microemulsion Neoral® formulation achieves a fast release of CsA at the site of absorption which improves the disolution of CsA in the GI tract, independent of food or bile secretion (Yocum *et al.* 2000; van Mourik *et al.* 1999). However, CsA nephrotoxicity still presents as a side effect in the clinic which suggests that there is still interindividual variability in pharmacokinetics of CsA. Therefore, an optimal delivery of CsA needs to be achieved in order to balance therapeutic effects and unwanted side effects.

Our collaborators, Sigmoid Pharma Ltd., have developed a sophisticated drug delivery technology called SmPill® which encapsulates CsA into a multi-bead format where the outer coating controls the release of CsA. The beads are designed to release CsA via two formulations, immediate release beads and colonic release beads. These formulations deliver CsA systemically (immediate release) but also specifically target the GI tract (colonic

release). As aGvHD is a multi organ inflammatory disease with the GI tract having a primary role in initiation, this dynamic CsA therapy, SmPill®, holds great promise to be an efficacious CsA therapy for aGvHD.

1.10. MSC THERAPY FOR aGvHD

The first use of MSC therapy for GvHD was performed by Le Blanc *et al*. and demonstrated striking immunosuppressive effects in patients with steroid resistant grade IV GvHD (Le Blanc *et al.* 2004). Most notably, a 9 year old patient who had received a MHC-matched HSC transplant from a non-related donor to treat leukaemia was diagnosed with severe steroid resistant aGvHD of the gut and liver. Haplo-identical MSC were generated and administered as a therapy over 2 doses. While the MSC therapy achieved remarkable immunosuppressive effects, the exact mechanism by which MSC mediated this effect was unknown (Le Blanc *et al.* 2004). However, this study established the safety of MSC therapy and importantly did not inhibit the engraftment of the transplanted graft where complete chimerism was achieved (Le Blanc *et al.* 2004). Later, this and other research groups demonstrated that autologous or allogeneic MSC can treat GvHD equivocally (Le Blanc *et al*. 2008; Fang *et al.* 2007; Muller *et al* 2008; von Bonin *et al* 2009). Following these academic led trials, Osiris Therapeutics produced MSC-like cells called Prochymal™ which proved to be very safe and beneficial following their infusion into patients with aGvHD in a Phase II trial (Kebriaei *et al*. 2009). This report represented the first prospective trial of third party, unmatched MSC for the treatment of aGvHD providing evidence that MSC can effectively induce a response in a high percentage (77%) when used in combination with existing therapy (Kebriaei *et al*. 2009).

However, aspirations of routine MSC application for the treatment of aGvHD suffered a setback following the results of a large scale phase III clinical trial by Osiris Therapeutics. In the Phase III clinical trial, Prochymal™ was beneficial for the treatment of aGvHD in the gut and liver but not the skin of steroid refractory aGvHD patients (Martin *et al*. 2010). However, overall the treatment was deemed unsuccessful and failed to reach its primary endpoint (Martin *et al.* 2010). In this trial, Prochymal™ was infused at 2 million cells/kg twice weekly for 4 weeks but the trial failed to meet its primary clinical endpoint of achieving an overall complete response rate compared with placebo control (Martin *et al.* 2010). Therefore, this pivotal phase III study does not support the use of MSC in this clinical situation. It has been suggested that distinct culture conditions may have some impact on MSC product performance (Galipeau 2013). In the negative phase III study reported by Osiris Therapeutics for treatment of steroid-resistant GvHD, MSC manufacturing consisted of large lots of 10,000 doses from each volunteer donor in contrast, to phase II studies where MSC underwent substantially less proliferative pressure (Martin *et al*. 2010; Galipeau 2013). The differences between the functionality of industrial MSC and MSC manufactured by academic centres may provide rationale for the different outcomes seen in these conflicting trial outcomes. Clinical data from the Karolinska Institute supports this by suggesting that late passage random donor MSC are less effective than comparable early passage MSC in regard to survival outcomes in patients with GvHD (von Bahr *et al.* 2012).

Galipeau has pointed out that MSC have a huge inter-donor variability in terms of their immunoregulatory function (Galipeau 2013)**.** In particular**,** IFNγ responsiveness is mandatory for MSC immunosuppressive function *in vivo* (Krampera *et al*. 2006). As, the phase III Osiris trial used MSC derived from one donor, it is possible that this MSC donor may have had low responsiveness to IFNγ. The ISCT have suggested potency assays be used to assess MSC donor responsiveness to IFNγ to overcome this discrepancy (Krampera *et al*. 2013; Galipeau *et al*. 2016).

Another important variable in relation to differences between industrially expanded MSC and MSC used in an academic setting is cryopreservation. Human clinical trials administer cryopreserved products that are thawed within hours of transfusion as opposed to pre-clinical studies where MSC are not cryopreserved before administration (Galipeau 2013; Moll *et al.* 2014). It was assumed that thawed MSC possess the same biochemical, homing and immune modulatory features as their non-cryopreserved counterparts but this is an area that warrants further investigation to elucidate any differences.

There have been many clinical studies of MSC therapy for aGvHD conducted thus far and overall these studies have shown that MSC infusion appears to be a safe treatment option for aGvHD, however the interpatient variability is evident by the selection of academic and industrial trials in table 1.1. However, as discussed above, there are many unresolved issues in using MSC therapy for the treatment of aGvHD which include the source of MSC, the total number of cells per dose, the number of doses required, immunogenicity of MSC, potency of MSC, cryopreservation and the expansion/culture methods of MSC. Overall, these studies highlight the potential of MSC for steroid resistant GvHD. However, the elucidation of MSC mechanisms of action coupled with an understanding of the interactions of MSC with immunosuppressive drugs are essential for the successful implementation of MSC therapy for aGvHD.

Table 1.1 Select number of clinical studies of MSC for treatment of aGvHD

Reference	Study type	MSC Source	MSC dose/kg	Response
(Le Blanc et al. 2004)	Case report	Bone marrow; related donor	1×10^6	Complete response. Patient still alive 1 year post transplant
(Ringden et al. 2006)	Phase I	Bone marrow; HLA-identical, haploidentical, and unrelated	1×10^6	5 patients survived 2 months to 3 years after infusion
(Fang et al. 2007)	Efficacy	Adipose tissue; Haploidentical and unrelated donors	1×10^6	aGvHD resolved in 5 patients; of these, 4 remained alive after a median 40-month follow-up
(Muller et al. 2008)	Safety & Feasibility	Bone marrow; HSC donor and third-party related donors	$0.4 \times 10^6 - 3 \times 10^6$	2 patients with severe aGvHD did not progress to cGvHD; one experienced complete remission
(Le Blanc et al. 2008)	Phase II	Bone marrow; HLA-identical; HLA-haploidentical; third party.	1.4×10^6	CR[1] in 63 % of children and 43 % of adults; PR[2] in 16 % of children and 17 % of adults; 3 relapses; 2-year survival: 53 %
(von Bonin et al. 2009)	Cohort	Bone marrow; Third party HLA-mismatched	0.9×10^6	2 patients (15 %) responded and required no further IS[3] therapy. 11 patients received IS concomitantly with MSC; after 28 days, 5 of these (45 %) had responded. 4 patients (31 %) remained alive at 257-day follow-up
(Kebriaei et al. 2009)	Phase II	Osiris therapeutics; unrelated donors	2 or 8×10^6 combined with steroids	CR in 77 %, PR in 16 % of patients
(Lucchini et al. 2010)	Multicentre	Bone marrow; unrelated HLA-mismatched donors	1.2×10^6	OR[4] (71.4 %), CR (23.8 %) No patients presented GvHD progression after MSC infusion, but 4 patients presented GvHD recurrence 2–5 months post-infusion. 2 patients developed limited cGvHD

---

[1] Denotes complete response
[2] Denotes partial response
[3] Denotes immunosuppressant
[4] Denotes overall response

1.11. MSC AND INTERACTIONS WITH IMMUNOSUPPRESSIVE DRUGS

Immunosuppressive (IS) drugs have revolutionised transplant medicine over the last 30 years. However, with the failure of prophylaxis or first line treatments and continued development of steroid resistance in aGvHD, as detailed in section 1.8, a more efficacious therapy or treatment plan needs to be designed. MSC show immunomodulatory properties, as explored in section 1.2 - 1.4, and have demonstrated their potential as a potential successful treatment for steroid refractory aGvHD (Le Blanc *et al*. 2004), however, their interactions with IS drugs remain unclear due to conflicting data presented in the literature.

Buron *et al*., briefly assessed the interactions of MSC with IS drugs *in vitro* using proliferation assays and it was revealed that mycophenolate acid (MPA) was the most suited candidate for co-treatment while the combination of MSC with either CsA or rapamycin antagonised the suppression of PBMC proliferation (Buron *et al.* 2009). This study showed that while drugs have inhibitory effects on MSC mediated suppression, MSC can also interupt IS drug mediated suppression resulting in the enhancement of PBMC proliferation, particularly in the case of rapamycin. Alternatively, MSC were reported to support the immunosuppressive action of CsA on T cells through Jagged-1 mediated inhibition of NF-κB signalling (Shi *et al*. 2011).

Findings from transplant models supported the negative effects reported of co-treatment of MSC with CsA and even demonstrated the acceleration of allograft rejection when the combined treatment was administered (Inoue *et al*. 2006; Eggenhofer *et al.* 2011). However, Jia *et al*., reported that a high dose of CsA in combination of MSC could prolong survival of allogeneic corneal graft in rats (Jia *et al*. 2012). This suggests that the dose of CsA can have differential effects on MSC effectiveness as an immunomodulator. As discussed in section 1.2, exposure of MSC to proinflammatory cytokines, such as IFNγ and TNFα, has been shown to promote the activation or licensing of these cells into becoming

43

more potent suppressors of inflammation (Krampera *et al.* 2006; Ryan *et al*. 2007; English *et al*. 2007; Polchert *et al.* 2008). Therefore the effect that IS drugs have on the activation status of MSC and the mechanisms employed to facilitate such effect has yet to be defined.

More recently, IS drugs, rapamycin in particular, were suggested to be able to enhance the potency of MSC immunosuppression *in vitro* and *in vivo* (Girdlestone *et al.* 2015)*.* In this case the enhancement of MSC was mediated by the pre-treated uptake of the drug within the cell as opposed to co-addition of MSC with rapamycin. In a similar manner, the steroid budesonide was shown to enhance the potency of MSC through the enhancement of IDO production using microparticles to facilitate steroid uptake within the cell (Ankrum *et al.* 2014). These novel approaches could lower the costs associated with MSC therapy as less but more potent cells could be engineered.

Another benefit of a combining MSC with IS drugs lies in the capacity for MSC to promote repair balancing the potential damage caused by IS drug side effects. In a model of ischaemia reperfusion injury, MSC were shown to alleviate kidney fibrosis in CsA immunosuppressed rats (Alfarano *et al.* 2012). However, Chung *et al*., report that MSC aggravated chronic CsA nephrotoxicity by inducing oxidative stress (Chung *et al*. 2013). This particular model was a CsA-induced renal injury model with daily administration of CsA. It is likely that the high concentrations of CsA in these tissues, as a result of chronic dosing, inhibited the tissue-repairing functions of MSC. These studies highlight that the dose of CsA and activation status of MSC are integrally connected and co-administration requires careful consideration to achieve beneficial effects.

Possible explanations for the variability observed between these studies are the different experimental conditions used in each study, in particular the ratio of MSC to T cell *in vitro*, the activation status of MSC and the timing, dose and type of IS drug used. Some of the key challenges, presented here, in defining optimal conditions for co-administration

of MSC and IS drugs require a thorough exploration on the effect of IS drugs on MSC activation, a definition of the effect of MSC on IS drug efficacy and to conclude whether or not MSC can reduce unwanted side effects from IS drugs.

1.12. ANIMAL MODELS OF aGvHD

The use of animal models in research provide a platform to rigorously investige the efficacy and mechanism of action of therapies for human diseases. They also provide important insights into the pathophysiology of diseases. Although non-human primates are currently used as disease models, this costly method is subject to a much more vigorous ethical restraint. Therefore, the use of mouse models is a more feasible approach for hypothesis driven experimentation. Most of the mouse aGvHD models that are available involve the transplantation of mouse allogeneic donor lymphocytes into irradiated hosts. GvHD development within these models is dependent on the dose of pre-conditioning, the amount and type of transplanted lymphocytes; thus severity of disease can be controlled (Schroeder & DiPersio 2011).

The most commonly used and straightforward mouse models of GvHD involve transplantation of MHC mismatched lymphocytes into a mouse host. Differences in MHC antigens are responsible for immune-mediated rejection, a factor that is exploited by the development of these models. MHC mismatch models can also contain mismatches at the miHA loci. The severity of aGvHD is dependent on $CD4^+$ and $CD8^+$ T cell involvement in terms of "cytokine storm" inititiation and direct tissue damage, respectively. The most common murine MHC mismatch model for aGvHD study involves transplantation of C57BL/6 ($H2^b$) purified donor T cells into a sub-lethally irradiated BALB/c ($H2^d$) recipient

where the number of donor splenic T cells administered is important in determining the level of aGvHD that develops (Schroeder & DiPersio 2011).

miHA-mismatched models exhibit less morbidity than MHC-mismatched models and therefore require significantly more splenocytes (25-30 x 10^6) to trigger severe aGvHD, which generally occurs within 21 – 30 days (Blazar *et al.* 1991). Examples of which are the B10.D2 → BALB/c (H-2^d), where the disease manifests primarily in the skin whereas B10 → BALB.B (H-2^b) mice failed to develop any skin GvHD and instead manifested systemic disease (Kaplan *et al.* 2004). This shows that the genes in the MHC locus can determine the nature of GvHD.

Recently, humanised aGvHD models have been developed to permit the engraftment of human haematopoietic cells using severely immunodeficient mice. These models hold advantage over murine models of aGvHD as they generate a system whereby human T cell mediated aGvHD can be studied and manipulated *in vivo*. Initially, non-obese diabetic severe combined immunodeficiency (NOD/SCID) mice were used to xenotransplant human cells into mice, however engraftment of cells was low (1–20%) (Mosier *et al.* 1988; Hoffmann-Fezer *et al*. 1993; Christianson *et al.* 1997). The low engraftment was due to the fact that NOD/SCID mice lack functional T and B cells but retain NK cell function and can therefore respond to foreign antigens (Shultz *et al.* 1995). The main drawbacks of using this particular model was due to low levels of engraftment and frequent development of lethal thymic lymphomas which impaired the life-span of these mice to ~ 8 months (Shultz *et al*. 1995). Subsequently, to improve the engraftment levels of xenotransplanted cells, a targeted mutation in the IL2rγ in the RAG-2$^{-/-}$ strain of mouse was introduced to facilitate significantly higher human lymphocyte development in this model. The use of RAG2-deficient and IL-2-receptor-γ-deficient mice (BALB/cA-RAG2$^{-/-}$ IL2rγ$^{-/-}$), which lack functional T, B and NK cells, were shown to achieve a high human T-cell chimerism of more

than 20% (up to 98%) in more than 90% of mice, with consistent development of GvHD within 14 to 28 days and a total mortality rate of 85% shorter than 2 months (van Rijn *et al.* 2003).

The most permissive mouse model for human T cell engraftment to date is derived by introducing a deletion of the common γ-chain of the IL2 receptor to a NOD/SCID background, subsequently known as NOD/SCID IL2rγ^{null} (NSG) mice. Pearson *et al.*, were the first to demonstrate a humanised model using NSG mice that were deficient for T and B cells, demonstrated reduced NK cell activity and a 6 fold higher level of human lymphocyte engraftment than that observed in the NOD-SCID mouse model (Pearson *et al.* 2008). In addition to enhanced engraftment levels, the lifespan of the NSG humanised mouse model was considerably longer than the NOD/SCID mouse model, making it ideal for long term studies (Shultz *et al.* 2005). The development of this model has paved the way for other GvHD studies (Hippen *et al.* 2012; Tobin *et al.* 2013) and it has been deemed one of the most suitable humanised mouse models for studying GvHD as it mimics sufficient similarities of clinical GvHD (Ali *et al.* 2012).

The development of such clinically relevant models demonstrates the advances made in immunological research over the last few decades. For the purpose of this thesis the NOD/SCID IL2rγ^{null} humanised mouse model was used to investigate the efficacy of a novel delivery formulation of CsA, SmPill®, alone and in combination with mesenchymal stem cell therapy for the treatment of aGvHD.

1.13. AIMS AND OBJECTIVES

This chapter has highlighted the current understanding of how MSC interact with and modulate cells of the immune system, the obstacles associated with CsA in treatment of aGvHD and explored the potential interactions of MSC with CsA for aGvHD therapy. This thesis aims to investigate two distinct areas in aGvHD therapy which remain to be addressed:

(1) The direct interactions of MSC and CsA and elucidate the mechanisms by which these interactions occur *in vitro* and *in vivo*.

(2) Establish the efficacy of a novel and more clinically applicable CsA treatment, by means of optimal targeted delivery, in a humanised model of aGvHD.

Despite the advances made in our understanding of how MSC modulate the immune system, the direct interactions of MSC with CsA remain unclear. The elucidation of these interactions will be beneficial as aGvHD patients in trials would have undergone prophylaxis involving CsA immunosuppression and MSC may be administered alongside CsA therapy. The goal of Chapter 3 is to determine how CsA modulates the activation and function of MSC and to elucidate the mechanism by which such effect is mediated.

Chapter 4 of this thesis will establish the efficacy of a novel CsA formulation, SmPill®, in a humanised model of aGvHD compared to conventional CsA formulations, Neoral® and Sandimmune®. This novel CsA formulation will subsequently be used in Chapter 5 to examine a number of hypotheses focused on how CsA interacts with MSC therapy during GvHD. These hypotheses include:

(1) GI targeted delivery of CsA can have systemic therapeutic effects in aGvHD

(2) Oral and intravenous CsA exert differential effects on MSC efficacy in aGvHD

(3) MSC pre-stimulated with IFNγ ameliorates negative effects as a result of co-administration with CsA in aGvHD.

Overall this study is designed to further the current knowledge of immune modulation by MSC in combination with CsA and provide important information regarding targeted and systemic delivery of CsA for aGvHD therapy. This study will contribute to the clinical application of MSC as interactions with the immunosuppressive drug, CsA currently used for the prevention and management of aGvHD are elucidated. Therefore, this thesis will advance our understanding of how a novel CsA formulation alone and in combination with MSC mediate their effects *in vivo* and will benefit the development of future clinical trials using these novel therapeutic approaches in aGvHD.

CHAPTER 2
MATERIALS AND METHODS

2.1. METHODS

2.1.1. REGULATORY ISSUES

2.1.2. ETHICAL APPROVAL AND HPRA COMPLIANCE

All procedures involving the use of animals or human materials were carried out by licensed personnel. Ethical approval for all work was granted by the ethics committee of Maynooth University (BRESC-2013-13). Project Authorisation was received from the HPRA (AE19124/P002) whereby the terms of the animal experiments within this project were outlined and adhered to.

2.1.3. COMPLIANCE WITH GMO AND SAFETY GUIDELINES

All GMO/GMM work was performed according to approved standard operation procedures and recording protocols approved by the Environmental Protection Agency (Ireland). Safe working practices were employed throughout this study as documented in the Biology Department, Maynooth University Safety manual.

2.1.4. ANIMAL STRAINS

The following mouse strain was used: NOD.Cg-Prkdc^{scid}IL2^{tmlWjl}/Szj (Jackson Labs, Bar Harbour, Maine, USA). All mice were housed according to Dept. of Health (Ireland) guidelines and used with ethical approval under the terms of AE19124/P002 project authorisation from HPRA. Sample sizes for animal experiments were determined by statistical power calculation using SISA. SISA software is online at http://home.clara.net/sisa/power.htm

2.2. CELL CULTURE

2.2.1. CULTURE OF HUMAN MESENCHYMAL STROMAL CELLS (MSC)

Bone marrow stromal cells were generated by collaborators at NUI Galway. Briefly, bone marrow aspirates were taken from the iliac crest of donor patients according to an approved clinical protocol (Murphy *et al.* 2002). Isolated human MSC were resuspended in complete DMEM (Sigma-Aldrich, Wicklow, Ireland) supplemented with 10 % (v/v) fetal bovine serum (FBS) (Labtech, Uckfield, UK), 50 U/ml penicillin (Sigma-Aldrich) and 50 μg/ml streptomycin (Sigma-Aldrich) (Table 2.1) and seeded at 1×10^6 cells in a T175 flask (Sarstedt, Sinnottstown, Ireland). cDMEM was replaced every 3-4 days. Once cells reached 70-90 % confluence, human MSC were trypsinised as normal with 0.25 % trypsin / 1mM EDTA (Invitrogen-Gibco (Bio-Sciences), Dublin, Ireland) and seeded or cryopreserved (section 2.2.4).

2.2.2. HUMAN PERIPHERAL BLOOD MONONUCLEAR CELL (PBMC) ISOLATION

Whole blood buffy coat packs, which contained red blood cells, white blood cells and platelets, were supplied by the Irish Blood Transfusion Service (IBTS) at St. James's Hospital, Dublin. PBMC were isolated from whole blood by density gradient centrifugation. The contents of buffy coat packs were diluted 1 in 2 with phosphate buffered saline (PBS) (Oxoid Ltd., Basingstoke, Hampshire, England). 25 ml diluted blood was carefully layered on top of 15 ml lymphoprep (Axis-Shield PoC AS, Oslo, Norway) in a 50 ml centrifugation tube (Sarstedt). The samples were centrifuged at 2400 rpm for 25 min at room temperature with no brake and low acceleration. After centrifugation, the white buffy coat layer

containing PBMC was removed into a sterile 50 ml tube, leaving red blood cells and remaining plasma behind. PBMC were centrifuged at 1800 rpm for 10 min at 4 ºC with the brake at normal settings. Supernatant was removed and the PBMC pellet was washed in 20 ml of PBS and centrifuged at 1500 rpm for 5 min at 4 ºC for a total of two times. Remaining red blood cells were lysed using 5ml 1x red blood cell lysis buffer (Biolegend, London, UK) for 5 min. 25 ml of complete RPMI (cRPMI) (RPMI 1640 (Sigma-Aldrich) supplemented with 10 % (v/v) heat inactivated FBS, 50 U/ml penicillin (Sigma-Aldrich), 50 μg/ml streptomycin (Sigma-Aldrich), 2mM L-glutamine (Sigma-Aldich) and 0.1% (v/v) 2-mercaptoethanol (Gibco)) (Table 2.1) was added to quench lysis. PBMC were centrifuged at 1000 rpm for 10 min at 4 ºC to remove platelets. The PBMC pellet was resuspended in 25 ml of cRPMI and counted.

2.2.3. MEASUREMENT OF CELL VIABILITY

Cells were resuspended in their specific growth media and diluted 1/2 in 2 % (w/v) ethidium bromide/acridine orange (EB/AO) (Sigma-Aldrich). 10 μl was pipetted on to a haemocytometer; live cells (green) and dead cells (orange) were counted using a fluorescent light microscope.

2.2.4. CRYOPRESERVATION AND RECOVERY OF CELLS FROM LIQUID NITROGEN

For long term storage, MSC were resuspended at 2×10^6/ml (MSC) in 500 μl freezing medium (DMEM containing 10% (v/v) FBS supplemented with 10 % (v/v) Dimethyl Sulfoxide (DMSO) (Sigma-Aldrich)). For PBMC cryopreservation, cells were resuspended at 5×10^7/ml in heat inactivated FBS. 50 μl of DMSO was added to a 1.5 ml cryo-tube

(Thermo Fisher Scientific, Massachusetts, USA) before the resuspended PBMC were added to the cryo-tube. Cells were gradually cooled at 1°C per minute overnight and then transferred to liquid nitrogen for storage. To recover cells, vials were quickly thawed at 37 °C. Just as the vial contents thawed, cells were transferred to a 15 ml tube (Sarstedt) where 5 ml of warmed medium was added (drop by drop) before cells were centrifuged at 300 g for 5 min. The pellet was resuspended in 1 ml of complete cell specific culture media, counted and used for experiments as required.

2.3. CHARACTERISATION OF MSC

2.3.1. GENERAL FLOW CYTOMETRY AND CHARACTERISATION OF MSC

For analysis by flow cytometry, cells (MSC or PBMC) were harvested, washed in sterile PBS and resuspended in FACS Buffer (PBS supplemented with 2 % heat inactivated FBS) to yield approximately 1×10^5 cells/FACS tube (4 ml polypropylene tubes) (Falcon, BD Biosciences, Oxford, UK) or 1×10^5 cells/well in 96 well V bottom Plate (Lennox, Dublin, Ireland). Fluorochrome conjugated antibodies (Table 2.3) or isotype controls were incubated with cells for 15 min at 4 °C. After 15 min, cells were washed in 2 ml of FACS Buffer, vortexed and centrifuged at 300 g for 5 min. The supernatant was removed and cells resuspended in 50 µl counting beads (3×10^5/ml) (Calibrite™ Beads, BD Biosciences) or 100 µl of cell fixative (PBS supplemented with 2 % (v/v) formaldehyde solution (Sigma-Aldrich)). Cells were then analysed by flow cytometry (Accuri C6 flow cytometer, BD Biosciences) using CFlowPlus software (BD Biosciences).

2.3.2. DIFFERENTIATION OF MSC

MSC were seeded at a density of 5 x 10^4 cells/well in a 6 well tissue culture plate in 2 ml cDMEM for osteogenic and adipogenic differentiation, or 2 x 10^5 cells were centrifuged in a 15 ml falcon tube at 200 g for 8 min to form a cell pellet for chondrogenic differentiation. Once 70 % confluence was reached (typically 2-3 days), cells were incubated in osteogenic, adipogenic or chondrogenic differentiation medium (Table 2.1), cDMEM media was added to control wells.

Fresh medium was added every 3-4 days for 21 days. At day 21, the medium was removed from the osteogenic and adipogenic cultures and the cells were washed in PBS and then fixed in 10 % (v/v) neutral buffered formalin for 20 min at room temperature. Formalin was removed and cells were washed in 2 ml of PBS. 1 ml of 1 % Alizarin Red, or 0.5 % Oil Red O (Sigma-Aldrich) was added to the fixed osteocytes or adipocytes and allowed to incubate for 20 min at RT. Excess stain was removed and the cells were washed with dH_2O. Finally, 1 ml of dH_2O was added to each well and cells were examined under the microscope. The chondrocyte cell pellets were harvested by aspirating off all the media and washing pellets twice with PBS. Pellets were placed in 1 ml of trizol and stored at -20°C. Chondrocyte pellets were analysed for the expression of collagen II, collagen x and aggrecan by RT-PCR (Table 2.6). Briefly, RNA was isolated from the pellets (section 2.6.1), reversed transcribed into cDNA (section 2.6.3) and the expression of chondrocyte markers were analysed by RT-PCR (section 2.6.4).

2.3.3. LABELLING OF PBMC AND MEASUREMENT OF MSC SUPPRESSION *IN VITRO*

Human PBMC were resuspended at 5×10^7/ml in warm PBS. PBMC (5×10^7) were labelled with 10 μM carboxyfluorescein succinimidyl ester (CFSE) or 10μM cell proliferation dye eFluor® 670. Cells were incubated for 10 min at room temperature in the dark. After 10 min, 2 ml of cold PBS was added and PBMC were centrifuged at 600 g for 5 min then washed twice in PBS. Labelled PBMC were then used to determine the effect of MSC or CsA on PBMC proliferation. Labelled PBMC (5×10^4/well) were seeded into a 96 well round bottom tissue culture plate (Fisher, Ballycoolin, Ireland) already containing 1×10^4/well MSC (1:5) or 1.25×10^3/well MSC (1:40), which were seeded a day before. CD3/CD28 Dynabeads® beads (Gibco) were added (1×10^4/well) to activate PBMC proliferation. After 4 days, PBMC were harvested and the level of proliferation by CD3^{+} cells was analysed by flow cytometry (section 2.3.1) and enumerated using counting beads (3×10^5/ml) (Calibrite™ Beads, BD Biosciences).

2.4. STIMULATION OF HUMAN MSC WITH PRO-INFLAMMATORY CYTOKINES

Human MSC at 3×10^5/well of a 6 well tissue culture plate were allowed to adhere overnight. MSC were stimulated with IFNγ (Peprotech, London, UK) or TNFα (Peprotech) at 50 ng/ml or 20ng/ml respectively for 24 or 48 h. The expression of immunomodulatory mediators (IDO & COX2) and adhesion molecules (ICAM1) and chemokines (CCL2, CXCL9) were analysed by qPCR (Section 2.6.6 and Table 2.6).

2.5. BIOCHEMICAL METHODS

2.5.1. PROTEIN EXTRACTION

Intracellular protein was extracted from adherent MSC. 6 well plates were placed on ice and media removed. Cells were washed with 3 ml of ice cold PBS. Cells were scraped in 1 ml ice cold PBS and added to a 1.5 ml tube. Samples were centrifuged at 15,000 rpm for 5 min and PBS was removed. The pellets were then resuspended in 90 µl cell lysis buffer (Table 2.2) and left on ice for 10 min. Samples were resuspended by gentle pipetting to aid the lysis process and left on ice for a further 10 min. Protein lysates were then subjected to centrifugation at 12,000 g for 10 min at 4 ℃. 90 µl of the supernatant which constitutes the intracellular protein was added to a new 1.5ml tube and stored at -20 °C. Prior to loading protein lysates, samples were mixed with 4X sample buffer (Table 2.2) and boiled for 5 min.

2.5.2. SDS-POLYACRYLAMIDE GEL ELECTROPHORESIS (SDS – PAGE)

SDS-PAGE was carried out in accordance with the Laemmli method as modified by Studier (Laemmli 1970; Studier 1973). Samples and appropriate prestained (10-180 kDa) protein markers were loaded into separate 0.75 mm wells. Electrophoresis was performed at 60 V through a 5% polyacrylamide stacking gel and then through a 8-15% polyacrylamide resolving gel at 80 V for up to 2 hours. The percentage of the gel that was chosen was based on the size of the proteins being electrophoresed. Proteins under 30 kDa in size were electrophoresed on a 15% acrylamide gel, proteins between 30 kDa- 80 kDa were analysed on a 10% acrylamide gel and proteins greater than 80 kDa were electrophoresed on an 8% gel.

2.5.3. IMMUNOBLOTTING

Following separation by electrophoresis, the proteins were transferred electrophoretically to nitrocellulose membranes (GE Healthcare, Buckinghamshire, England) in a Hoefer TE 70 Semiphor semi-dry transfer unit (GE Healthcare) at 100mA for between 40 and 80 mins depending on protein size. 3 layers of Whatmann blotting paper (Sigma-Aldrich) were placed on the bottom surface of the transfer unit followed by one layer of nitrocellulose membrane. The resolving gel was then placed on top with care to avoid any air bubbles. Finally 3 more layers of Whatmann blotting paper were added and the unit closed. Following transfer, non-specific binding of antibody was blocked by incubating the nitrocellulose membranes at room temperature for 1 h with blocking buffer (tris buffered saline (TBS)), 0.1% (v/v) Tween-20 with 5% (w/v) non-fat dry milk) (Table 2.2) under gentle agitation. The membranes were then incubated under agitation at 4°C overnight with the primary antibodies diluted in TBS containing 0.1% (v/v) Tween-20 (TBST) with 5% (w/v) skimmed milk powder or BSA as indicated in Table 2.4. The membranes were subsequently subjected to 3 x 5 min washes in TBST (Table 2.2). Membranes were then incubated in a secondary antibody (Table 2.5) specific for the primary antibody in TBST containing 5% (w/v) skimmed milk powder for 1 h in the dark at room temperature. The membranes were then washed a further 3 times for 5 min each in TBST in the dark. The immunoreactive bands were detected using Odyssey infrared imaging system (Licor, Biosciences, Dublin, Ireland) or using enhanced chemiluminescence development (WesternBright ECL HRP Substrate, Advansta, Labtech).

2.5.4. ENZYME LINKED IMMUNOSORBENT ASSAY (ELISA)

All ELISAs were carried out according to manufacturer's instructions (R & D Systems, Abingdon, UK or eBioscience, Paisley, Scotland). Specific capture antibodies (human IFNγ, TNFα, IL1β, IL2, IL6, IL17, or IL23) in PBS were added to 96 well Nunc-Immuno™ plates (Thermo Fisher Scientific) and incubated overnight at room temperature. Plates were then washed 3 times in wash buffer (PBS supplemented with 0.05 % v/v Tween 20) and then incubated in blocking solution (PBS supplemented with 1 % w/v BSA) for a minimum of 1 h. Plates were then washed and incubated with 100 μl/well of sample supernatant or corresponding cytokine standard for 2 h at room temperature. After washing, plates were incubated with specific detection antibodies for a further 2 h at room temperature. Plates were washed again and incubated with 100 μl/well of streptavidin horseradish peroxidase (HRP) (R & D Systems) conjugate diluted 1/40 in specific reagent diluent (Tris buffered solution (TBS) (Sigma-Aldrich) supplemented with BSA) for 20 min. After washing, plates were incubated with 100 μl/well of tetramethylbenzidine (TMB) substrate (Sigma-Aldrich) for 20 min at room temperature out of direct light. The reaction was stopped after 20 min by adding 50 μl/well of 1 M H_2SO_4. The absorbance (optical density (O.D)) of the samples and standards were measured at 450 nm for all ELISA using a miroplateplate reader (BioTek EL800, Swindon, UK) with Gen5 Data Analysis Software. The cytokine concentration of each sample was determined by comparison to the standard curve of known cytokine concentrations using GraphPad Prism5 software.

2.5.5. BRADFORD ASSAY

The concentration of protein harvested from cell lysates or tissue homogenates were determined by Bradford assay. Bovine Serum Albumin (BSA) standards of known protein

concentration and samples were diluted in water (20 µl) and mixed with 180 µl of Bradford assay reagent (Bio-Rad, California, USA) and protein concentration determined by the level of colorimetric change. The OD was measured for each well at 590nm using a BioTek ELx800 microplate reader with Gen5 Data Analysis Software (BioTek). The concentrations of protein in each sample were extrapolated from a standard curve that related the OD of each standard amount to the known concentration. Standards were assayed in duplicate to generate the standard curve. All samples were also assayed in duplicate. Data analysis was performed using GraphPad Prism5 software.

2.6. MOLECULAR TECHNIQUES

2.6.1. RNA ISOLATION

Total RNA was extracted using trizol® reagent (Invitrogen-Ambion) according to the manufacturer's instructions. Briefly, 1×10^6 cells were lysed in 1 ml trizol at room temperature for 5 min. 100 µl of RNA-grade 1-Bromo-3-chloropropane (Sigma-Aldrich) was added to the cells, mixed vigorously and incubated at room temperature for 5 min. Samples were centrifuged at 12,000 g for 15 min at 4 °C. Two distinct layers resulted with RNA remaining in the clear, aqueous upper layer. 350-400 µl of RNA was carefully removed, ensuring the lower white DNA layer was not disturbed, and precipitated with 500 µl isopropanol (Sigma-Aldrich). The samples were incubated at room temperature for 10 min and followed by centrifugation for 10 min at 4 °C. The resulting RNA pellet was washed with 1 ml 75 % (v/v) ethanol and centrifuged at 7,500 g for 5 min at 4 ºC. The ethanol was aspirated and the RNA pellet was allowed to briefly air dry prior to resuspension in 30 µl RNase-free water (Promega, Southhampton, UK). The purity and concentration of RNA was determined using a spectrophotometer (Nanodrop 2000, ThermoScientific, Wilmington,

DE, USA) which calculated the ratio of absorbance at 260/280 nm. A ratio between 1.8 and 2.0 indicated sufficient purity of the RNA. Samples outside this range were discarded.

2.6.2. DNASE TREATMENT OF RNA

Genomic DNA was removed from RNA samples by treatment with DNase I (Invitrogen, Paisley, UK). 1 µl of DNase (amplification grade) was added to 1 µg of RNA and incubated for 15 min at room temperature. 1 µl of 25 mM EDTA (Invitrogen) was added to the mixture and incubated at 65 ºC for 10 min to inactivate the enzyme.

2.6.3. CDNA SYNTHESIS

Following DNase treatment, total RNA was reverse transcribed using 5X All-In-One Mastermix (ABM-NBS Biologicals, Cambridgeshire, UK). This ready to use mastermix formulation, containing EasyScript™ Reverse Transcriptase, RNaseOFF ribonuclease inhibitor, dNTP mix, Oligo (dT)s and random primers, was diluted to a 1X concentration in nuclease-free water (ABM-NBS Biologicals). The conditions for cDNA synthesis were as follows: 42 ºC for 50 min, 85 ºC for 5 min and 4 ºC for 10 min. Quantification of cDNA was performed by measuring the absorbance value of the sample 260 nm. Samples were stored -20 ºC until required.

2.6.4. REVERSE TRANSCRIPTION-POLYMERASE CHAIN REACTION (RT-PCR)

PCR was used to determine the presence of specific DNA sequences (or mRNA following reverse transcription) using primers summarised in Table 2.6. Expression of the housekeeping gene, Glyceraldehyde 3-phosphate dehydrogenase (GAPDH) was used as a positive control. PCR reactions contained 2.5 mM $MgCl_2$ (Promega), 25 mM dNTP (Promega), 1 x GoTaq reaction buffer (Promega), 40 U/ml Taq polymerase (Promega) and 0.4 pM of the appropriate primer pairs (Sigma-Aldrich). The reaction mastermix was adjusted to a final volume of 24 μl with nuclease-free water. The PCR conditions were as follows: denaturation at 95 °C for 45 sec (2 min for first cycle), annealing for 45 sec (optimal annealing temperatures are summarised in Table 2.6) and extension for 45 sec at 72 °C. DNA products were resolved on a 1.3 % w/v agarose gel and detected by binding of gel red (Biotium, Hayward, CA).

2.6.5. AGAROSE GEL ELECTROPHORESIS

Agarose gels were prepared by adding 1.3% (w/v) agarose in TAE and heating until completely dissolved. The solution was then cooled before 5 μl GelRed nucleic acid stain (Biotium) was added and the solution was poured into a gel tray. Following solidification, agarose gels were submerged in TAE buffer and subjected to electrophoresis at 110 V. Samples were run simultaneously with a 1 Kb molecular weight ladder. Nucleic acid products were visualised under ultraviolet (UV) light (254 nm) and images acquired using a Gel Logic 212 Pro gel documentation system (Carestream Health, Connecticut, USA).

2.6.6. REAL TIME POLYMERASE CHAIN REACTION (qPCR)

cDNA was analysed for the quantification of mRNA expression. Briefly, cDNA (1μg) was amplified in the presence of SYBR® Green JumpStart™ Taq ReadyMix (Sigma-Aldrich).

Accumulation of gene-specific products was measured continuously by means of fluorescence detection over 40 cycles. Each cycle consisted of: denaturation at 95 °C for 15 sec, annealing at optimum temperature (Table 2.6) for 30 sec, and extension at 72 ℃ for 45 sec followed by a melt curve cycle of 95 °C for 15 sec, 55 °C for 15 sec and 95 °C for a final 15 sec. Quantification of target gene expression was obtained using an Eco Real-Time PCR System (Illumina, Inc. San Diego, CA USA). Expression was quantified in relation to the housekeeper GAPDH using the ΔCT method. The ΔCT method was determined by subtracting the GAPDH value from the target CT value for each sample. The fold change in relative gene expression was determined by calculating the $2^{-\Delta CT}$ values (Schmittgen & Livak 2008).

2.7. HUMANISED MOUSE MODEL OF AGVHD

2.7.1. ACUTE GRAFT VERSUS HOST DISEASE HUMANISED MOUSE MODEL

A humanised mouse model of acute graft versus host disease (aGvHD) was developed and optimised from a protocol described by Pearson et al. (Pearson *et al.* 2008). NOD.Cg-Prkdc^{scid}IL2^{tmlWjl}/Szj (NOD-Scid IL-2γnull) (NSG) were exposed to a conditioning dose of 2.4 Gray (Gy) of whole body gamma irradiation. Freshly isolated human PBMC were administered by intravenous injection to the tail vein using a 27 gauge

needle and a 1 ml syringe between 4 h but no longer than 24 h following irradiation. Before infusion, PBMC were washed three times with sterile PBS. From previous studies (Tobin *et al*. 2013), the optimum dose for PBMC for aGvHD development was found to be 8.0 x 10^5 gram^{-1} and this dose was used for all aGvHD studies. aGvHD development was determined by examining features including weight loss exceeding 15 % total body weight, ruffled fur, hunched posture. Animals were returned to their cages where they were monitored closely for the first hour and at regular intervals thereafter for any signs of distress or ill health. Animals were weighed daily and weight loss was documented accordingly. Any animals which displayed greater than 15 % total body weight loss were sacrificed humanely. In addition, an animal welfare score sheet was utilized throughout the study.

2.7.2. PATHOLOGICAL SCORING SYSTEM FOR AGVHD

The development of aGvHD was assessed using a series of pathological features. Mice with weight loss greater than 15 % total body weight were considered to have aGvHD and were sacrificed. Other pathological features taken into consideration were; posture (hunching), activity, fur texture and diarrhoea. Any animals scoring a cumulative score of 8 for the pathological features were considered to have aGvHD and were sacrificed humanely. The scoring system used were; posture: 0; normal, no hunching; 0.5; slight hunching that straightens when walking; 1.0; animal stays hunched when walking; 1.5; animal does not straighten out; 2.0; animal tends to stand on rear toes. Activity: 0; normal, very mobile and hard to catch; 0.5; slower than normal and little easier to catch; 1.0; no activity, but will move when touched; 1.5; no activity, very little movement when touched; 2.0; no activity at all, not even when touched. Fur: 0; normal, no fur pathology; 0.5; ridging on the side of belly and neck; 1.0; ridging across and side of belly and neck; 1.5; fur is matted and ruffled;

2.0; badly matted on belly and top. Diarrhoea: 0; normal; 0.5 mild change in bowel movement; 1.0; moderate change in bowel movement; 1.5; severe change in bowel movement; 2.0; extensive diarrhoea.

2.7.3. INTRAVENOUS ADMINISTRATION OF HUMAN MSC OR PBMC

Before infusion, human PBMC or MSC were washed three times with sterile PBS. PBMC were administered to mice at $8.0 \times 10^5 \, g^{-1}$ and MSC were administered at $6.4 \times 10^4 \, g^{-1}$. These doses were determined as being optimal from previous work in this laboratory (Tobin *et al.* 2013; Healy thesis 2015) PBMC or MSC were delivered to the tail vein using a 27 gauge needle and a 1 ml syringe. Each mouse received a total of 0.3 ml. PBMC were given on day 0 while MSC were given on day 6. Following i.v injection, animals were returned to their cages where they were monitored as above.

2.7.4. PREPARATION AND ADMINISTRATION OF CYCLOSPORINE FORMULATIONS

SmPill® formulated cyclosporine (Sigmoid Pharma, Invent Centre DCU, Dublin) consisted of 2 types of cyclosporine (CsA) loaded beads (diameter in the range of 1 – 1.4 mm). The immediate release beads had a 10.87% loading of CsA (109 µg/mg). For each of these beads the average weight was in the range of 2-3mg and the resultant active pharmacological ingredient (API) was 220 – 330 µ/mg per bead. The beads for the colonic release of CsA had a 10% loading of CsA (100µg/mg) with an API of between 250-350 µg per bead. Each bead was weighed prior to administration to ensure correct dosage

(25mg/kg). Administration was carried out by oral gavage. Briefly, each bead was loaded at the end of a feeding needle (Vet Tech, Cheshire, UK) with a syringe containing 200µl PBS connected to it. Mice were carefully scruffed and the feeding needle was inserted into the mouth of the mouse. The feeding needle was carefully guided down the oesaphagus, where the beads were released with the aid of 200µl PBS in a syringe. The Neoral® formulation of CsA (provided by Sigmoid Pharma) was in the form of a 100mg tablet. The CsA solution was removed from the inside of the tablet by needle (18G) and 5ml syringe and collected into a 50ml tube. Prior to administration the Neoral® was diluted in PBS to yield a 25 mg/kg dose and 300µl was delivered by oral gavage as described above. The Sandimmune® formulation of CsA (provided by Sigmoid Pharma) was in the form of a 50mg/ml injectable solution. The CsA solution was diluted in PBS to yield a 25 mg/kg dose prior to administration. Sandimmune® was delivered to the tail vein using a 27 gauge needle and a 1 ml syringe. Each mouse received a total of 0.3 ml. Following each procedure, animals were returned to their cages where they were monitored as above.

2.8. CELLULAR AND CYTOKINE ANALYSIS FROM GVHD MICE
2.8.1. ISOLATION OF HUMAN SPLENOCYTES FROM GVHD MICE

Spleens were removed aseptically from mice into a 50ml tube containing cRPMI supplemented with 10% (v/v) heat inactivated FBS, 50 U/ml penicillium, 50 µg/ml streptomycin and 2 mM L-glutamine (Table 2.1). Spleens were homogenised through a 70 µm filter into a 50ml tube using a sterile plunger and the isolated splenocytes were then suspended in 10 ml cRPMI containing 0.1 % v/v 2-mercaptoethanol (Invitrogen-Gibco). This homogenate was centrifuged at 300 g for 5 min and resuspended in 1 ml of red blood cell lysis buffer solution (BioLegend, San Diego, USA) for 10 min at room temperature. 2

ml of medium was added to the suspension to neutralise the lysis solution which was then centrifuged at 600 g for 5 min. Supernatant was removed and the cells were then resuspended in fresh cRPMI and counted. The cells were resuspended for FACS analysis (Section 2.9.1 or Section 2.9.2).

2.8.2. CYTOKINE ANALYSIS FROM SPLENIC CELL CULTURES

Spleens were removed from mice as described above and single cell suspensions were prepared. Cells were seeded at 2×10^5 per well in a 96 well round bottom plate and cultured in cRPMI. Cells were unstimulated or stimulated with 100 ng/ml Phorbal 12-myrisate 13-acetate (Sigma-Aldrich) and 1 µg/ml ionomycin (Sigma-Aldrich). Supernatants were harvested after 72 h for detection of IL1β, IL2, IL6, IL17, IL23 and IFNγ. Cytokines in supernatants were detected by ELISA as described in Section 2.5.4.

2.8.3. ISOLATION OF HUMAN CELLS FROM THE LIVER OR LUNGS OF GVHD MICE

Livers and lungs were removed aseptically from mice into a 50 ml tube containing cRPMI (Table 2.1). Tissues were homogenised through a 70 µm filter into a fresh 50 ml tube using a sterile plunger and the isolated cells were then suspended in 25 ml cRPMI . This homogenate was layered over 15 ml lymphoprep density gradient (Axis-Shield) and centrifuged at 2400 rpm for 25 min with no brake and low acceleration. The interface was collected by aspiration into a fresh labelled 50 ml tube. The interface was washed twice with

25 ml PBS and centrifuged at 300 g for 5 min. Supernatant was removed and the cells were resuspended for FACS analysis (Section 2.9.1 or Section 2.9.2).

2.8.4. ISOLATION OF HUMAN CELLS FROM THE GI TRACT OF GVHD MICE

Small intestines and colons were removed aseptically from mice into a 15 ml tube containing cRPMI (Table 2.1). The tissue samples were placed in 10 ml digestion solution (20 U/ml DNase I (Roche Diagnostics, Germany), 300 U/ml collagenase from *Clostridium histolyticum* (Sigma-Aldrich) and PBS) at 37 ºC under constant horizontal shaking at 300 rpm. After 1 hour of digestion, the homogenates were passed through a 70 μm filter into a fresh 50 ml tube using a sterile plunger and the isolated cells were then suspended in 25 ml cRPMI and centrifuged at 1500 rpm for 10 min. The cells were resuspended in 8 mls of 40% Percoll (Sigma-Alrdich), overlayed onto 4 mls of 80% Percoll (Sigma-Aldrich) and centrifuged at 2200 rpm for 20 min with no brake and low acceleration. The interface was removed by aspiration and transfered to a new tube. 15ml of PBS was added and the interface was centrifuged at 1400 rpm for 8 min at 4 ºC. The supernatant was removed and the cells were resuspended for FACS analysis (Section 2.9.1 or Section 2.9.2).

2.8.5. CYTOKINE ANALYSIS FROM THE TISSUES OF GVHD MICE

The lungs, liver, small intestine and colon were removed from mice as described above where a section was immediately snap frozen and stored at - 80 ºC. Tissues were thawed and gut contents were removed. The tissues were chopped finely and homogenised using an Ultra-Turrax homogeniser (IKA, Staufen, Germany) in 1 ml of chilled homogenisation

buffer (PBS: 2% heat inactivated FBS supplemented with protease inhibitor cocktail (Roche, Dublin, Ireland)). The homogenate was microcentrifuged at 13,000 rpm for 15 min at 4 ºC. The supernatant was removed and stored at - 20 ºC. The protein concentration of tissue extracts were determined by Bradford assay (Section 2.5.5). Protein extracts were analysed for IL1β, IL2, IL6, IL17, IL23 and IFNγ. Cytokines in supernatants were detected by ELISA as described in Section 2.5.4.

2.9. ANALYSIS OF HUMAN PBMC *IN VITRO* AND *IN VIVO* BY FLOW CYTOMETRY

2.9.1. DETECTION OF CYTOKINE PRODUCTION BY HUMAN CELLS

TNFα, IFNγ and IL2 were analsyed intracellularly by flow cytometry. Briefly, PBMC recovered from coculture assays or *in vivo* studies following stimulation with 100 ng/ml PMA, 1 µg/ml ionomycin and 1X Brefeldin A for 4 h, were washed in 150 µl FACS buffer and centrifuged at 950 rpm for 5 min in 96 well v bottomed plates. PBMC were labelled with CD45 PercP, CD4 APC and CD8 FITC or corresponding isotype control antibodies for 15 min at 4 °C. The cells were washed twice in 150 µl FACS buffer, centrifuged at 950 rpm for 5 min and fixed with 100 µl fix/permeabilisation buffer (eBioscience) for 1 h or overnight. The cells were then permeabilised with 200 µl permeabilisation buffer (eBioscience), washed with 150 µl FACS buffer and blocked using 3 µl 2 % rat serum for 15 min. The cells were labelled with TNFα PE, IFNγ PE, IL2 PE or isotype control antibodies and left at 4 ºC for 1 h. Samples were washed twice with 150 µl FACS buffer, resuspended in counting beads (3 x 10^5/ml) and analysed by flow cytometry (Accuri C6 flow cytometer, BD Biosciences) using CFlowPlus software (BD Biosciences).

2.9.2. INTRACELLULAR STAINING OF CELLS TO DETECT FOXP3 AND NFAT EXPRESSION

FoxP3 and NFAT expression was analysed intracellularly using a FoxP3 staining kit (eBioscience). Briefly, PBMC recovered from coculture assays or *in vivo* studies, were washed in 150 µl FACS buffer and centrifuged at 950 rpm for 5 min. For FoxP3 assays, PBMC were labelled with CD4 FITC and CD25 APC or corresponding isotype control antibodies for 15 min at 4 °C. For NFAT assays, PBMC were labelled with CD3 FITC or corresponding isotype control antibodies for 15 min at 4 °C. The cells were washed twice in 150 µl FACS buffer, centrifuged at 950 rpm for 5 min and fixed with 100 µl fix/permeabilisation buffer (eBioscience) for 1 h. The cells were then permeabilised with 200 µl permeabilisation buffer (eBioscience), washed with 150 µl FACS buffer and blocked using 3 µl 2% rat serum for 15 min. The cells were labelled with FoxP3 PE, NFAT PE or isotype control antibodies and left at 4 ℃ for 1 h or overnight. Samples were washed twice with 150 µl FACS buffer, resuspended in counting beads (3×10^5/ml) and analysed by flow cytometry (Accuri C6 flow cytometer, BD Biosciences) using CFlowPlus software (BD Biosciences).

2.10. HISTOLOGY

2.10.1. TISSUE PREPARATION

The lungs, liver, spleen, small intestine and colon were harvested from experimental mice at day 13 and fixed in 10% (v/v) neutral buffered formalin for at least 24 h. Samples were transferred to 70% ethanol for a further 24 h. Samples were processed for histology using an automated processor (Shandon Pathcentre, Runcorn, UK) which immersed the

tissues in fixatives and sequential dehydration solutions including ethanol (70%, 80%, 95% x 2, 100% x 3) and xylene (x 2) (Sigma-Aldrich). After processing, tissues were embedded in paraffin wax (Sigma-Aldrich) using a Shandon Histocentre 2 (Shandon) and left to set at 4°C overnight. A Shandon Finesse 325 microtome (Thermo-Shandon, Waltham, MA, USA) was used to cut 5 µm sections of each tissue. Sections were placed in cold water before being transferred to a hot water bath (42°C) to remove any folding of the sections. Tissue sections were placed onto microscope slides (VWR, Ballycoolin, Ireland) and left to air dry overnight. Samples were then stained with H&E (Section 2.10.2) and blindly scored using the system outlined in section 2.10.4.

2.10.2. HAEMATOXYLIN/EOSIN STAINING

Before commencing with H&E staining, slides were heated to 56 °C for a minimum of 1 h to aid wax clearance. Slides were then transferred to xylene (Sigma-Aldrich) for 10 min. This was repeated with fresh xylene for a further 10 min. Samples were then re-hydrated following immersion in 3 decreasing concentrations of ethanol (100 % x 2, 90 % and 80 %) for 5 min each. Samples were then transferred to dH_2O for 5 min before being immersed in Haemotoxylin (Sigma-Aldrich) for 3 min. Samples were then washed under H_2O for 2 min before being placed in 1% acid alcohol for no longer than 20 sec. Samples were washed again under H_2O before being immersed in Eosin Y (Sigma-Aldrich) for 3 min and back to washing under H_2O again. Slides were dehydrated through immersion in a series of increasing ethanol concentrations (80 %, 90 %, 100 %) for 5 min each. Samples were air dried, mounted with DPX mounting media (BDH) and examined under a light microscope.

2.10.3. DETECTION OF APOPTOSIS USING TERMINAL DEOXYNUCLEOTIDYL TRANSFERASE MEDIATED dUTP NICK END LABELING (TUNEL) ASSAY

TUNEL assay was carried out using a commercially available kit (In Situ Cell Death Detection Kit, Roche). Formalin fixed paraffin embedded slides were heated to 56°C for a minimum of 1 h to aid wax clearance. Slides were then transferred to xylene (Sigma-Aldrich) for 10 min. This was repeated with fresh xylene for a further 10 min. Samples were then re-hydrated following immersion in 3 decreasing concentrations of ethanol (100% x 2, 90% and 80%) for 5 min each. Samples were then transferred to dH_2O for 2 min before being immersed in boiling antigen unmasking solution (Vector, Peterborough, UK) for 6 min. Samples were then washed in PBS for 2 min. Tissue sections were circumscribed with ImmEdge™ wax pen (Vector). Once wax was dry, 10 µl of enzyme-label solution (Roche) was added directly onto the tissue. Samples were incubated for 1 h in a humidified chamber at 37 ºC. Samples were washed in PBS before 100 ng/ml of DAPI nuclear stain (Sigma-Aldrich) was added to each tissue sample. Slides were incubated at room temperature and protected from light. Samples were air dried, mounted with VectaMount™ aqueous mounting media (Vector) and examined under a fluorescent microscope.

2.10.4. HISTOLOGICAL SCORING

Following H&E staining, slides were coded without reference to prior treatment and examined in a blind manner. A semi-quantitative scoring chart was used to assess disease progression in the lungs, liver and GI tract (Tobin *et al*. 2013). Pathological scoring was carried out as follows:

Score	Lung	Liver	GI Tract
0	Normal	Normal	Normal
1	Rare scattered areas of mononuclear cells	Isolated collections of mononuclear cells in the parenchyma	Mild necrotic cells with minor mononuclear cell infiltration
2	Mild and more focused areas of mononuclear cell infiltration	Endothelialitis present in at least one vessel and distinct increase in mononuclear cell infiltration	Dispersed but mild villous blunting, necrosis and increased cell infiltration
3	Moderate levels of cellular infiltration and damage to lung architecture	Endothelialitis present in more than one vessel with a further increase in mononuclear cell infiltration	Dispersed and moderate villous blunting, necrosis with further increased cell infiltration and colonic crypt ulceration
4	Pervasive mononuclear cell infiltration with pervasive damage to lung architecture	Endothelialitis present in virtually all vessels with extensive levels of mononuclear cell infiltration	Dispersed and severe villous blunting, necrotic cells with pervasive mononuclear cell infiltration and colonic crypt ulceration

2.11. STATISTICAL METHODS

The students paired t test was used when statistical analysis was required between two experimental groups. One way ANOVA was used to test for statistical significance of differences when multiple experimental groups were compared. Mantel-Cox test (log rank test) were used to compare survival between treatment groups. The ratio for median survival was computed using GraphPad Prism. Power analysis was carried out to determine the number of animals that would yield a significant difference in the *in vivo* studies. Statistical methods (Power analysis (SISA)) were used to determine the minimum number of animals

per treatment group to obtain a power in the study.   SISA software is online at

http://home.clara.net/sisa/power.htm

Table 2.1 Media for Cultured Cells

Media	Composition	Supplier
Complete Dulbecco's Modified Eagle's Media (cDMEM) for MSC Culture	Dulbecco's Modified Eagle's Media (DMEM) 10% (v/v) FBS 50 U/ml penicillin 50 µg/ml streptomycin	Sigma-Aldrich Labtech Sigma-Aldrich Sigma-Aldrich
Adipocyte Media	Complete Dulbecco's Modified Eagle's Media (cDMEM) (4.5mg/ml glucose) 5µg/ml insulin in 0.1N acetic acid 50µM indomethacin 1µM dexamethasone 0.5µM IBMx in EtOH	Sigma-Aldrich Sigma-Aldrich Sigma-Aldrich Sigma-Aldrich Sigma-Aldrich
Osteocyte Media	Complete Dulbecco's Modified Eagle's Media (cDMEM) 1mM dexamethasone 20mM β-glycerolphosphate 50µM L-ascorbic acid-2-phosphate 50ng/ml L-thyroxine sodium pentahydrate	Sigma-Aldrich Sigma-Aldrich Sigma-Aldrich Sigma-Aldrich Sigma-Aldrich
Chondrocyte Media	Complete Dulbecco's Modified Eagle's Media (cDMEM) (4.5mg/ml glucose) 100nM dexamethasone 50µg/ml ascorbic acid 2 phosphate 40µg/ml L-proline 1 % v/v ITS + supplement 10µg/ml TGF-β3	Sigma-Aldrich Sigma-Aldrich Sigma-Aldrich Sigma-Aldrich BD Biosciences BD Biosciences
Complete media for Human PBMC culture	RPMI 1640 10% (v/v) heat inactivated FBS 50 U/ml penicillin 50 µg/ml streptomycin 2mM L-glutamine 0.1% (v/v) 2-mercaptoethanol	Sigma-Aldrich Labtech Sigma-Aldrich Sigma-Aldrich Sigma-Aldrich Gibco

Table 2.2 Buffers

Buffer	Composition
Blocking Buffer for Immunoblotting	TBS, 0.1% (v/v) Tween-20 (TBST) with 5 % (w/v) non-fat dry Milk
Laemmli sample buffer	62.5 mM Tris-HCl, pH 6.8, 10% (w/v) glycerol, 2% (w/v) SDS, 0.7 M β-mercaptoethanol and 0.001% (w/v) bromophenol blue
Phosphate Buffered Saline (PBS)	2.7 mM KCl, 1.5mM KH_2PO_4, 137 mM NaCl and 8 mM Na_2HPO_4, pH 7.4
RIPA Lysis Buffer	50 mM Tris-HCl pH 7.4, 1% (v/v) Igepal, 150 mM NaCl, 0.5% (w/v) Sodium Deoxycholate, 1 mM EDTA, 0.1% (w/v) SDS 1 mM Na_3VO_4, 1 mM PMSF and protease inhibitor cocktail
SDS running Buffer	25 mM Tris, 192 mM glycine, 0.1% SDS.
TAE (Tris-acetate-EDTA) Buffer	40 mM Tris base, 0.1% (v/v) glacial acetic acid, 1 mM EDTA
TBS (Tris buffered saline)	25 mM Tris, pH7.4, containing 0.14M NaCl.
TBST (Tris buffered saline with Tween)	25 mM Tris, pH7.4, containing 0.14M NaCl 0.1% (v/v) Tween-20
Transfer Buffer	25 mM Tris, 192 mM glycine, 20% (v/v) methanol

Table 2.3 Antibodies for Flow Cytometry

Antibody	Fluorochrome	Clone	Isotype	Supplier
CD3	APC/FITC	UCHT1	Mouse IgG1 k	eBioscience
CD4	APC/FITC	SK3	Mouse IgG1 k	eBioscience
CD8	FITC	RPA-T8	Mouse IgG1 k	eBioscience
CD25	PE/APC	BC96	Mouse IgG1 k	eBioscience
CD29	FITC	TS2/16	Mouse IgG1 k	eBioscience
CD34	PE	4H11	Mouse IgG1 k	eBioscience
CD44	FITC	IM7	Rat IgG2b k	eBioscience
CD45	PercP	2D1	Mouse IgG1 k	eBioscience
CD73	APC	AD2	Mouse IgG1 k	eBioscience
CD90	FITC	eBIO5E10	Mouse IgG1 k	eBioscience
CD105	APC	SN6	Mouse IgG1 k	eBioscience
CD106	PE	STA	Mouse IgG1 k	eBioscience
CD117	PE	YB5.B8	Mouse IgG1 k	eBioscience
CD119	PE	GIR-208	Mouse IgG1 k	eBioscience
CD161	APC	HP-3G10	Mouse IgG1 k	eBioscience
FoxP3	FITC/PE	236A/E7	Mouse IgG1 k	eBioscience
HLA-ABC	FITC	W6/32	Mouse IgG2a k	eBioscience
HLA-DR	PE	L243	Mouse IgG2a k	eBioscience
ICAM 1	PE	HA58	Mouse IgG1 k	eBioscience
IDO	PE	eyedio	Mouse IgG1 k	eBioscience
IFNγ	FITC/PE	4S.B3	Mouse IgG1 k	eBioscience
IL2	FITC/PE	MQ1-17H12	Rat IgG2a k	eBioscience
NFAT	Alexa Fluor® 488	7A6	Mouse IgG1 k	Biolegend
TNFα	FITC/PE	MAB11	Mouse IgG1 k	eBioscience

Table 2.4 Primary Antibodies for Immunoblotting

Primary Antibodies For Immunoblotting	Dilution Factor	Diluent	Supplier
IDO	1:1000	5% BSA TBST	Cell Signalling
Phospho –STAT1	1:1000	5% BSA TBST	Cell Signalling
SOCS1	1:500	5% BSA TBST	Cell Signalling
Total STAT	1:1000	5% BSA TBST	Cell Signalling
β-actin	1:5000	5% Milk TBST	Cell Signalling

Table 2.5 Secondary Antibodies for Immunoblotting

Secondary Licor Antibodies	Dilution Factor	Diluent	Supplier
IRDye 680 Goat Anti-Mouse	1:5000	5% Milk TBST	Licor Biosciences
IRDye 800CW Goat Anti-Rabbit	1:5000	5% Milk TBST	Licor Biosciences
Secondary ECL Antibodies	**Dilution Factor**	**Diluent**	**Supplier**
Anti-Mouse HRP	1:1000	5% Milk TBST	Cell Signalling
Anti-Rabbit HRP	1:1500	5% Milk TBST	Cell Signalling

Table 2.6 Primers Sequences

Primer	Forward 5' – 3'	Reverse 3' – 5'	Product size (bp)	Anneal temp (ºC)
GAPDH	ACAGTTGCCATGTAGACC	TTTTTGGTTGAGCACAGG	540	58
CCL2	AGACTAACCCAGAAACATCC	ATTGATTGCATCTGGCTG	143	52.1
CXCL9	AGGTCAGCCAAAAGAAAAAG	TGAAGTGGTCTCTTATGTAGTC	116	54.9
COX2	AAGCAGGCTAATACTGATAGG	TGTTGAAAAGTAGTTCTGGG	113	54.8
Collagen 2a	GCCCAAGAGGTGCCCCTGGAATA	CCTGAGAAAGAGGAGTGGACATA	703	57
Collagen x	GCCCAAGAGGTGCCCCTGGAATAC	CCTGAGAAAGAGGAGTGGACATAC	703	73
Aggrecan	TGAGGAGGGCTGGAACAA GTACC	GGAGGTGGTAATTGCAGGGAAC	350	55
ICAM1	ACCATCTACAGCTTTCCG	TCACACTTCACTGTCACC	83	52.8
IDO	TTGTTCTCATTTCGTGATGG	TACTTTGATTGCAGAAGCAG	90	56.1
SOCS1	AGCTTAACTGTATCTGGAGC	AAAAATAAAGCCAGAGACCC	118	52.6

CHAPTER 3

CsA ENHANCES MSCγ POTENCY THROUGH SOCS1 INHIBITION

3.1. INTRODUCTION

Mesenchymal stromal cells (MSC) are a heterogenous population of multipotent, nonhematopoietic cells that reside in the bone marrow. Due to their aptitude for plastic adherence, they can be easily isolated from the bone marrow, and other tissues such as adipose tissue, to facilitate research on their functionalities. To avoid disparities within the field, the International Society for Cellular Therapy (ISCT) have assigned a minimal set of criteria whereby MSC can be defined and characterised. Initially, the ISCT described MSC as being plastic adherent, possessing or lacking expression of a panel of surface markers (shown in Table 3.1) and hold the capability of differentiating into osteocytes, adipocytes and chondrocytes *in vitro* (Dominici *et al.* 2006). Perhaps the most interesting characteristic of MSC is their capacity for regulating immune responses. The ISCT have now defined and set out guidelines for assessing these immune-modulatory characteristics (Krampera *et al.* 2013). Some of these guidelines include the standardisation of functional assays using interferon (IFN)-γ and tumor necrosis factor (TNF)-α as model priming agents for MSC, together with the indoleamine- 2,3-deoxygenase (IDO) response being a central investigative element for MSC immune regulation assays *in vitro* (Krampera *et al.* 2013).

The immunomodulatory effects mediated by MSC make them an attractive tool as a cellular therapy in alloimmunity and inflammatory disorders such as acute Graft versus Host Disease (aGvHD). Importantly "licensing" or activation greatly enhances their immunosuppressive effect (Krampera *et al.* 2006). In particular, IFNγ or TNFα have been revealed as being key stimuli for the activation of MSC to modulate immune responses by upregulating anti-inflammatory mediators such as IDO and prostaglandin E2 (PGE2) respectively (English *et al.* 2007; Polchert *et al.* 2008; Chinnadurai *et al.* 2014). Activated MSC also upregulate T cell chemoattractants such as CXCL9, CXCL10 and CCL2 and

utilise the adhesion molecules ICAM-1 and VCAM-1 to enhance attachment between MSC and T cells (Ren *et al*. 2010; Ren *et al.* 2008).

The immunosuppressive drug cyclosporine (CsA) is commonly used to prevent rejection of transplanted organs, to treat autoimmune disorders and for prophylaxis or treatment of GvHD (Trull *et al*. 1995; Vogelsang *et al.* 1999; Gan *et al*. 2003). In these settings, T cells are the central mediators associated with initiating and maintaining these unwanted inflammatory responses. CsA targets T cells by preventing the transcription of cytokine genes fundamental for T cell proliferation, namely IL2, by hindering calcium-dependent signal transduction pathways (Liu *et al.* 1991; Flanagan *et al.* 1991). While T cells have been identified as the primary target for CsA to exert it's inhibitory activity, CsA has been shown to have effects on other cells such as dendritic cells (DC). In particular, CsA was shown to impair DC maturation, migration and function (Duperrier *et al*. 2002; Chen *et al*. 2004).

However, little is known about CsA interactions with MSC immunosuppressive capacity. While there are numerous *in vitro* and *in vivo* studies reporting beneficial effects of CsA in combination with MSC (Le Blanc *et al.* 2004; Maccario *et al.* 2005; Zhang *et al.* 2007; Pischiutta *et al.* 2014; Girdlestone *et al*. 2015), there are equal numbers of studies showing CsA as having a negative impact on MSC immunosuppressive ability (Inoue *et al*. 2006; Buron *et al*. 2009; Eggenhofer *et al*. 2011; Jia *et al.* 2012). This suggests that the interaction of CsA on MSC immunosuppressive activity is multifactorial and that there are no key mechanisms defined as of yet. Therefore, the aim of this chapter was to firstly characterise the interactions of CsA on MSC immunomodulatory functions and secondly to investigate how these interactions can regulate the suppressive activity of MSC by defining the specific processes involved. Therefore the objectives of this chapter are;

- To examine the influence of CsA on MSC surface marker expression and trilineage differentiation ability *in vitro.*

- To assess the impact that clinically relevant concentrations of CsA have on the immunosuppressive ability of MSC *in vitro*.

- To investigate the immunosuppressive effect of CsA on the pre-activation of MSC with IFNγ *in vitro.*

- To determine the effect CsA has on gene expression and protein production of the key immunomodulatory mediators utilised by MSC *in vitro.*

- To identify a mechanism by which CsA can influence key signal transduction events involved in MSC immunosuppression.

3.2. HUMAN MSC SURFACE PHENOTYPE AND DIFFERENTIATION CAPACITY IS UNCHANGED IN THE PRESENCE OF CsA

Human bone marrow derived MSC were isolated and expanded to passage 2 by collaborators in NUI Galway, as described in section 2.2.1. As there is no single surface antigen that specifically identifies MSC, a range of markers were used to characterise these cells. According to the ISCT, MSC must express CD73, CD90 and CD105 and lack the expression of CD34, CD45 and HLA-DR (Dominici *et al.* 2006). MSC also express the surface markers CD29, CD44, CD106 (VCAM-1) with low levels of HLA-ABC.

For this study, human bone marrow derived MSC were cultured in the presence or absence of CsA (100 ng/ml, 500 ng/ml, 1 µg/ml) for 24 and 48 h to determine if CsA had an effect on the surface marker expression which is characteristic of MSC. These concentrations of CsA were selected as they are close to residual blood levels of transplant patients making them clinically relevant (García Cadenas *et al.* 2014). The cells were labelled with antibodies specific for each surface antigen and analysed by flow cytometry for the expression of a range of cell surface antigens (Table 3.1). Flow cytometric analysis demonstrated that the MSC population lacked detectable expression of the major histocompatibility antigen HLA-DR but expressed HLA-ABC. MSC expressed the adhesion molecules CD29, CD44, CD73, CD90, CD105 & CD106 while they lacked expression of the hematopoietic markers CD34 and CD45. These findings are expected and consistent with the minimal criteria outlined by the ISCT (Dominici *et al*. 2006). The addition of CsA (100 ng/ml, 500 ng/ml & 1 µg/ml) for 24 and 48 h had no impact on MSC surface marker phenotype.

Table 3.1 Table of surface marker expression of human mesenchymal stromal cells

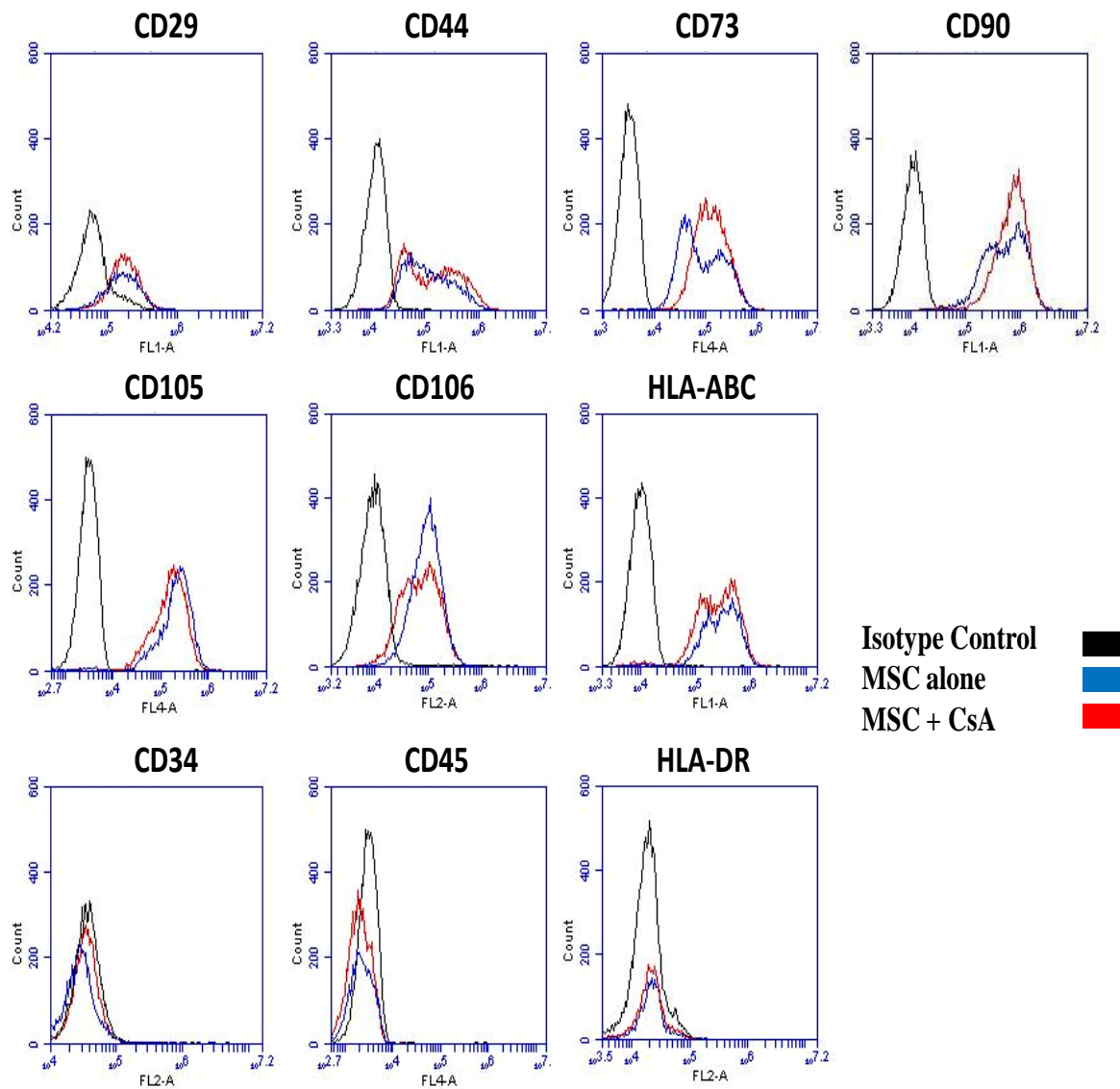| Surface Antigen	Positive (+) / Negative (-) Expression
CD29	+
CD34	-
CD44	+
CD45	-
CD73	+
CD90	+
CD105	+
CD106	+
HLA-ABC	+
HLA-DR	-

Figure 3.1. CsA did not alter the surface phenotype of MSC. MSC were cultured alone or in the presence of CsA (100 ng/ml, 500 ng/ml, 1 µg/ml) for 24 and 48 h. The fluorescent intensity of CD markers and HLA antigens (CD29, CD34, CD44, CD45, CD73, CD90, CD105, CD106, HLA-ABC, HLA-DR) on human MSC were examined by flow cytometry. Isotype controls are represented by a black open histogram while cell specific markers were represented by a blue open histogram (- CsA) or a red open histogram (+ CsA). The addition of CsA had no effect on hMSC surface antigen expression. This data is representative of surface marker expression of hMSC +/- CsA using five hMSC donors at passage 5 & 6 and three doses of CsA (100 ng/ml, 500 ng/ml, 1 µg/ml) at two timepoints (24 and 48 h). 1 µg/ml CsA was used for the data shown above.

3.3. CsA DOES NOT HAMPER hMSC CAPACITY FOR TRILINEAGE DIFFERENTIATION

MSC have the ability to differentiate into oseteocytes, adipocytes and chondrocytes under differentiating conditions *in vitro*. Human MSC were cultured in differentiation media in the presence or absence of CsA (100 ng/ml, 500 ng/ml and 1 µg/ml) over a period of twenty-one days without passage (Figure 3.2). In addition, MSC were cultured in media without differentiation components, but in the presence or absence of CsA (100 ng/ml, 500ng/ml and 1 µg/ml), for the same period of time to assess spontaneous differentiation. Bone differentiation and mineralisation was visualised using Alizarin Red S which stains the calcium deposits within the cell. Oil Red O stained the lipid vacuoles that accumulated in the cytoplasm indicating the differentiation of MSC into adipocytes. In each case, CsA had no visible effect on the differential capacity of MSC into osteocytes or adipocytes (Figure. 3.2). In addition, MSC cultured without conditioning components but in the presence or absence of CsA did not display spontaneous differentiation into osteocytes or adipocytes. Chondrocyte differentiation was determined through the expression of Collagen 2a, Collagen x and Aggrecan by semi-quantitative RT-PCR (Figure 3.3). In addition to differentiation media, CsA increased the expression of Collagen 2a and Aggrecan while the expression of Collagen x remained unaltered. This data confirms that MSC are plastic adherent cells that can undergo trilineage differentiation and shows that CsA had no hampering effect on these differentiation processes *in vitro.*
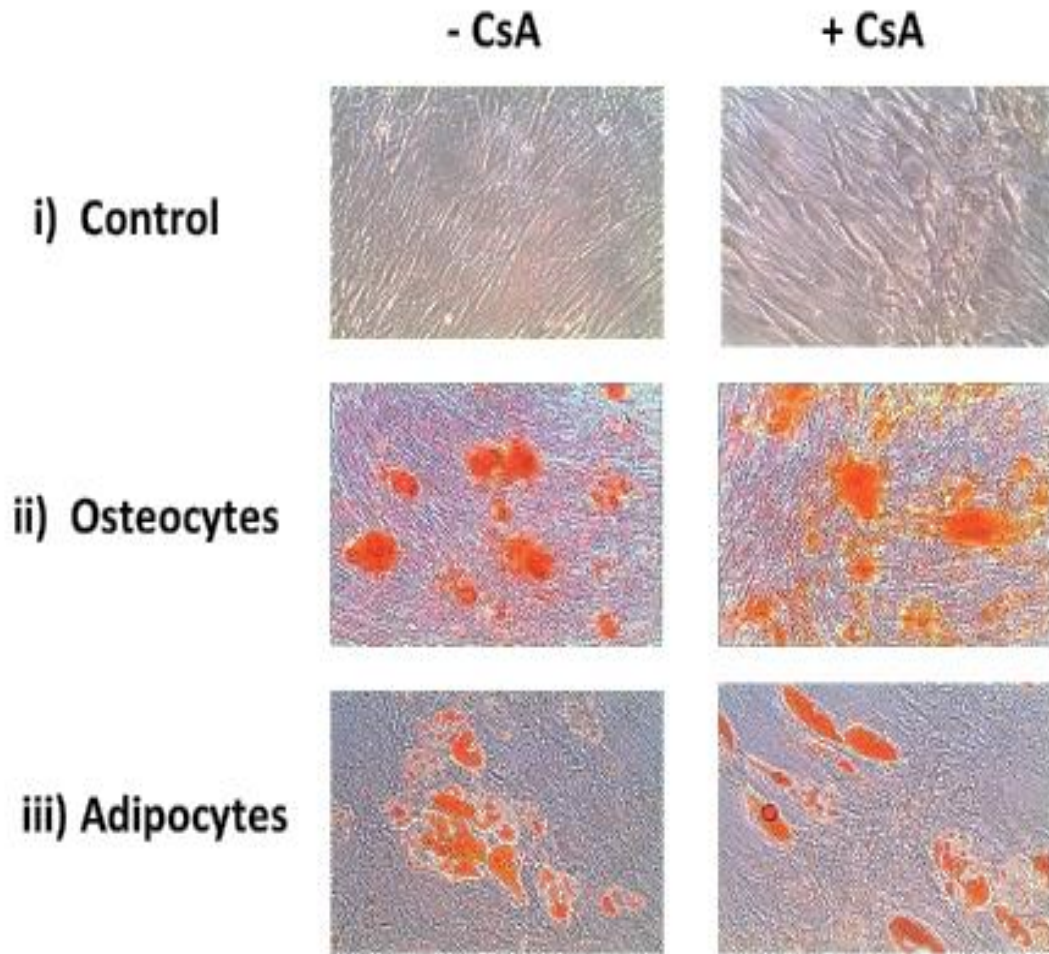
Figure 3.2. MSC differentiated into osteocytes and adipocytes following treatment with differentiation media in the presence (+) or absence (-) of CsA. MSC were seeded at 5 x 10^4 in 6 well plates and cultured in specific differentiation media in the presence or absence of CsA (100 ng/ml, 500 ng/ml and 1 µg/ml repeatedly following media change) over a period of twenty-one days without passage. **i)** MSC cultured in the absence of differentiation components (control) were plastic adherent and spindle-shaped and did not positively stain for alizarin red or oil red O (x100). **ii)** MSC differentiated into osteocytes (x100). Alizarin red S staining of calcium deposits indicated osteogenic differentiation. In **iii),** MSC differentiated into adipocytes (x100). Oil Red-O stained the lipid vacuoles that accumulated in the cytoplasm. CsA had no altering effect on either differentiation process. The above images are representative of MSC cultures from four donors from passage 4- 6 and three concentrations of CsA, (100 ng/ml, 500 ng/ml and 1 µg/ml). 1 µg/ml CsA was used for the data shown above.
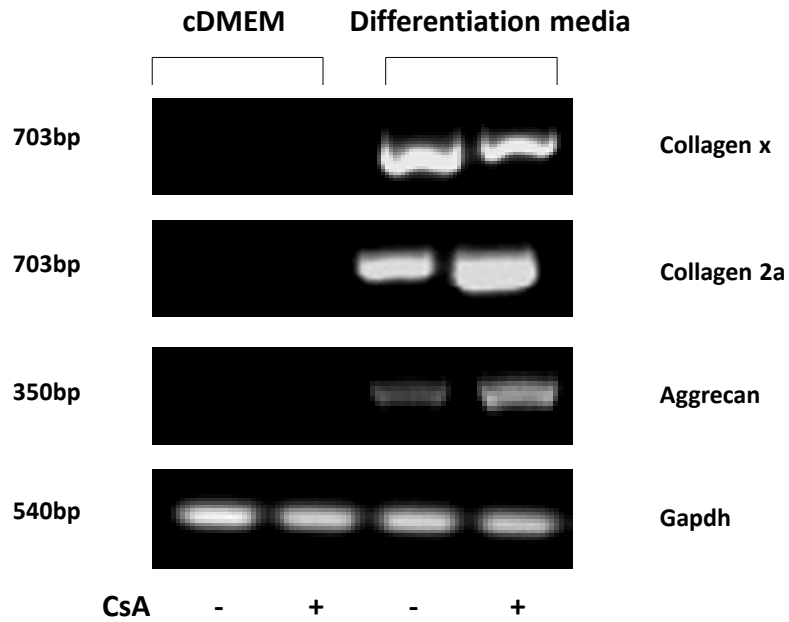
Figure 3.3. MSC undergo chondrocyte differentiation following treatment with differentiation media in the presence (+) or absence (-) of CsA. MSC were seeded at 2 x 10^5 in 15 ml tubes (pellet culture) and cultured in specific differentiation media in the presence or absence of CsA (100 ng/ml, 500 ng/ml and 1 µg/ml repeatedly following media change) over a period of twenty-one days without passage. RT-PCR analysis of chondrocyte markers Collagen x, Collagen 2a and Aggrecan in pellet cultures was carried out after induction of chondrogenic differentiation. RNA from each sample was extracted, cDNA was synthesised and used as a template for RT-PCR. Expression of each chondrocyte marker was compared to the housekeeping gene GAPDH. CsA, in addition to differentiation media, increased expression of Collagen 2a and Aggrecan while the expression of Collagen x remained unaltered. Representative example of MSC cultures from four donors from passage 4-6 and three concentrations of CsA, (100 ng/ml, 500 ng/ml and 1 µg/ml). 1 µg/ml CsA was used for the data shown above.

3.4. CsA AND IFNγ ENHANCE THE IMMUNOSUPPRESSIVE ABILITY OF MSC IN A DOSE DEPENDENT MANNER

The immunosuppressive ability of MSC is a key characteristic in defining MSC (Dominici *et al*. 2006; Krampera *et al.* 2013). MSC require activation to exert their immunosuppressive potential (English *et al*. 2007; Ryan *et al.* 2007) however, in the absence of strong pro-inflammatory activation, evidence suggests that allogeneic MSC may stimulate immune responses and T cell cytokine production (Li *et al.* 2012; Cuerquis *et al*. 2014). IFNγ in particular plays an important role in MSC immunosuppression (Krampera *et al*. 2006). Elegant studies utilising IFNγ (-/-) T cells or neutralising antibodies have demonstrated the key role played by IFNγ in this context (Polchert *et al*. 2008; Sheng *et al*. 2008; Wang Lei *et al*.2013). The calcineurin inhibitor CsA has been established as an immunosuppressive agent which reduces T cell IL2 production in addition to other cytokines such as IFNγ (Kang *et al.* 2007; Tramsen *et al*. 2014). While there are numerous studies reporting beneficial (Ringden *et al*. 2006; Dan Shi *et al.* 2010) or abrogating effects (Hoogduijn *et al.* 2008; Eggenhofer *et al.* 2011) by CsA on MSC immunosuppressive function, there has been no specific mechanism validating either case.

It is hypothesised that CsA would therefore hamper the proinflammatory microenvironment provided by activated PBMC, particularly at low PBMC densities, resulting in impaired licensing of MSC. In addition, effects MSC have on CsA immunosuppression will be examined. Thus, MSC were licensed with IFNγ stimulation (50 ng/ml) before the addition of CsA (1 µg/ml) and their immunosuppressive ability was assessed using high (1:40 MSC:PBMC) and low (1:5 MSC:PBMC) PBMC densities in a proliferation co-culture assay.

In this study, the suppressive ability of MSC was assessed by measuring the proliferation of activated and labelled peripheral blood mononuclear cells (PBMC) in co-

culture *in vitro* assays, as detailed in section 2.3.3. Briefly, PBMC were labelled with a fluorescent proliferation dye, activated with CD3/CD28 beads and cultured with resting or licensed MSC for four days in the presence or absence of CsA. Cells were harvested on day four and stained with fluorescent antibody CD3 and fluorescent dye 7-Aminoactinomycin D (7AAD) to examine viability in CD3$^+$ proliferating T cells. PBMC proliferation (proliferation dye dilution) was analysed by flow cytometry.

In the presence of MSC, the proliferation of PBMC was significantly reduced (P < 0.001) (Figure 3.4). This shows that MSC are immunosuppressive of T cell proliferation and therefore comply with the guidelines as set out by the ISCT (Dominici *et al*. 2006; Krampera *et al*. 2013). However, MSC were significantly less suppressive (P < 0.05) in the presence of CsA at 1:5 ratio (Figure 3.4). MSC did not impair CsA immunosuppression of activated PBMC as there was no significant difference when compared to CsA alone.

IFNγ licensed MSC were shown to more potently suppress T cell proliferation than MSC alone at 1:5 (P < 0.05) and 1:40 (Figure 3.4) ratios. Interestingly, licensed MSC in the presence of CsA maintained suppressive ability at 1:5 and, at the 1:40 ratio were significantly more suppressive than licensed MSC alone (P < 0.001). This suggests that preactivation of MSC safeguarded MSC from reduced potency with CsA co-addition at 1:5 and further enhanced MSC suppression at 1:40 (Figure 3.4). Also, at 1:40 where PBMC density is high, MSC in the presence of CsA were significantly more suppressive than MSC alone (P < 0.05) or licensed MSC (P < 0.001). However the possibility that CsA present in these groups mediated the suppressive effect observed cannot be ruled out. This data suggests that MSC can have beneficial immunosuppressive capacity in combination with CsA and identified licensing of MSC as a key facilitator of this effect.
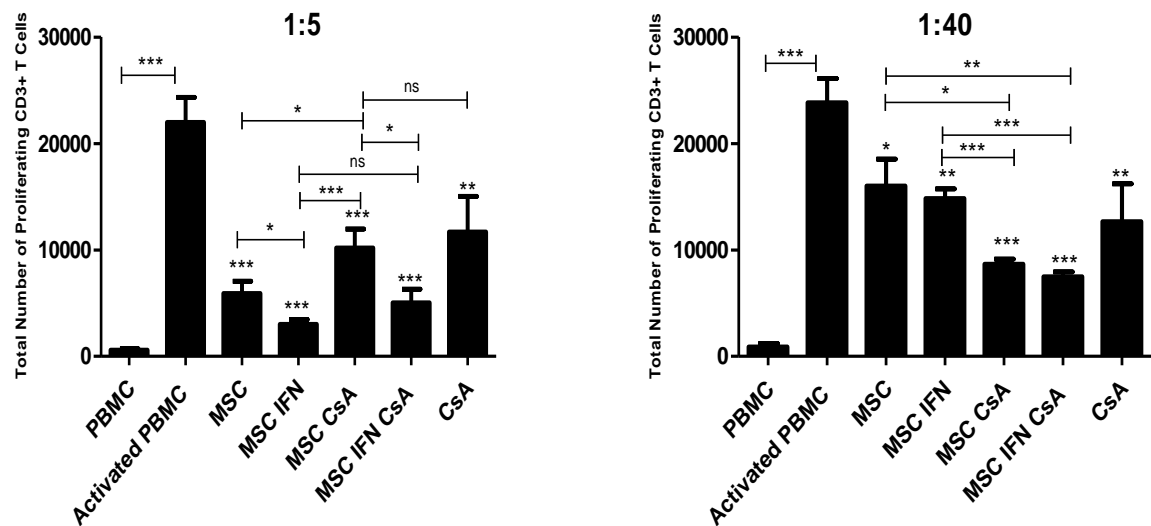
Figure 3.4. CsA maintains the immunosuppressive ability of licensed MSC. MSC were cultured alone or stimulated with IFNγ (50 ng/ml) for 24 h. After these stimulations, MSC were seeded (1 x 10^4 per well for 1:5 and 1.25 x 10^3 for 1:40 ratios) into a 96 well round bottom plate. The following day CD3/CD28 activated PBMC were labelled with a proliferation dye and added (5 x 10^4 per well). Some groups were cultured in the presence of CsA (1 μg/ml). On day four, cells were harvested and stained with fluorescent antibody CD3 and fluorescent 7AAD viability dye to analyse CD3$^+$ proliferation using flow cytometry. The assay was performed on four MSC donors and three PBMC donors (n=12). Statistical analysis was carried out using unpaired student *t*-test where * <0.05, ** <0.01 and *** <0.001. Stars with no bar are in comparison to the PBMC group.

3.5. IFNγ AND CsA ENHANCE MSC SUPPRESSION OF IFNγ, TNFα AND IL2 PRODUCING CD3^{+} T CELLS *IN VITRO* IN A DOSE DEPENDENT MANNER

IFNγ, TNFα and IL2 are key proinflammatory cytokines produced by immune cells to mediate inflammatory events during injury or pathological conditions such as GvHD (Ju *et al.* 2005; Korngold *et al.* 2003). MSC respond to inflammation and adopt immunoregulatory mechanisms accordingly, as shown in section 3.4. MSC and licensed MSC have been shown to specifically reduce levels of IFNγ, TNFα and IL2 in *in vitro* co-cultures with activated PBMC (Aggarwal & Pittenger 2005; Prasanna *et al.* 2010). CsA has also been shown to significantly reduce these cytokines and the number of immune cells producing them (Tramsen *et al*. 2014; Haider *et al*. 2008). It is known that the immunosuppressive abilities of MSC do possess certain caveats where under certain conditions, such as suboptimal activation or low T cell densities, they have been reported to enhance immune responses. (Li *et al*. 2012; Najar *et al*. 2009). Furthermore, there have been reports of double negative immunosuppressive effects of using MSC and CsA *in vitro* and *in vivo* (Buron *et al*. 2009; Eggenhofer *et al.* 2011). However, investigations into MSC and CsA interactions have been insufficient to date whereby little has been defined mechanistically. Therefore, this study will explore further the collaborative effects of CsA, MSC and, particularly, licensed MSC in terms of CD3^{+} T cell cytokine profiles. Therefore, CsA and MSC/licensed MSC were assessed in a co-culture assay at high and low PBMC densities, as described in section 3.4, in order to quantify how effectively the cytokines are reduced in supernatant, determined by ELISA, and the number of CD3^{+} T cells producing them, using flow cytometry.

In the supernatants, MSC and licensed MSC significantly suppressed the levels of TNFα but not IFNγ or IL2 (Figure 3.5). However, MSC and licensed MSC significantly suppressed the levels of IFNγ, TNFα and IL2 when combined with CsA. As CsA alone

significantly suppressed these cytokines, it could therefore be suggested that this anti-inflammatory effect was mediated by CsA without obstruction from MSC in doing so.

In terms of T cell cytokine production, at a ratio of 1:5, MSC and licensed MSC significantly redcuced the number of CD3$^+$ IFNγ$^+$ T cells in a PBMC co-culture assay (P <0.01 and P < 0.001 respectively). CsA had no significant effect on MSC suppression of CD3$^+$ IFNγ$^+$ T cells, however CsA significantly enhanced licensed MSC suppression of CD3$^+$ IFNγ$^+$ T cells in comparison to MSC alone (P < 0.05). At 1:40, the number of CD3$^+$ IFNγ$^+$ T cells were reduced by all groups but not significantly. While CsA alone significantly suppressed CD3$^+$ IFNγ$^+$ T cells, this capacity is significantly hampered when combined with MSC at high T cell densities (1:40) (Figure 3.6).

In a similar suppressor assay which measured TNFα producing T cells, MSC and licensed MSC significantly suppressed the number of CD3$^+$ TNFα$^+$ T cells alone and in combination with CsA at the 1:5 ratio (all P < 0.001). At 1:40, the number of CD3$^+$ TNFα$^+$ T cells were decreased by MSC, licensed MSC and both in combination with CsA at 1:40. However, CsA alone significantly reduced the number of TNFα producing CD3$^+$ T cells and this potency was significantly decreased when combined with MSC (P < 0.05). Notably, licensed MSC significantly suppressed CD3$^+$ TNFα$^+$ T cells in combination with CsA (P < 0.05) with no significant differences to the potency of CsA alone (Figure 3.7). This suggests that licensing of MSC can facilitate a beneficial affiliation with CsA in suppressing CD3$^+$ TNFα$^+$ T cells.

In the case of IL2, as expected, CsA significantly reduced the number of IL2 producing CD3$^+$ T cells (Figure 3.8). At 1:5, MSC or licensed MSC alone significantly reduced the number of CD3$^+$ IL2$^+$ T cells in a suppressor assay and the combination of CsA enhanced this significantly (Figure 3.8). At 1:40, MSC and licensed MSC exhibit impaired suppression of IL2 producing CD3$^+$ T cells. However, when combined with CsA, there is a

significant suppression of $CD3^+$ $IL2^+$ T cells for both MSC and licensed MSC at 1:40 (both

$P < 0.001$). This suggests that MSC have no hampering effect on CsA suppression of IL2

producing $CD3^+$ T cells.

In summation, at high T cell densities, MSC do not negatively impact CsA

suppression of IL2 producing $CD3^+$ T cells. However, the presence of MSC in these assays

hampered CsA suppression of TNFα and IFNγ producing $CD3^+$ T cells. Importantly, the

hampering effect of MSC on CsA suppression of TNFα $CD3^+$ T cells is mitigated by

licensing the MSC. This data suggests that CsA uses different mechanisms to regulate these

cytokines and, depending on inflammatory cues, MSC can hinder these processes.

(A) IFNγ

(B) TNFα

(C) IL2
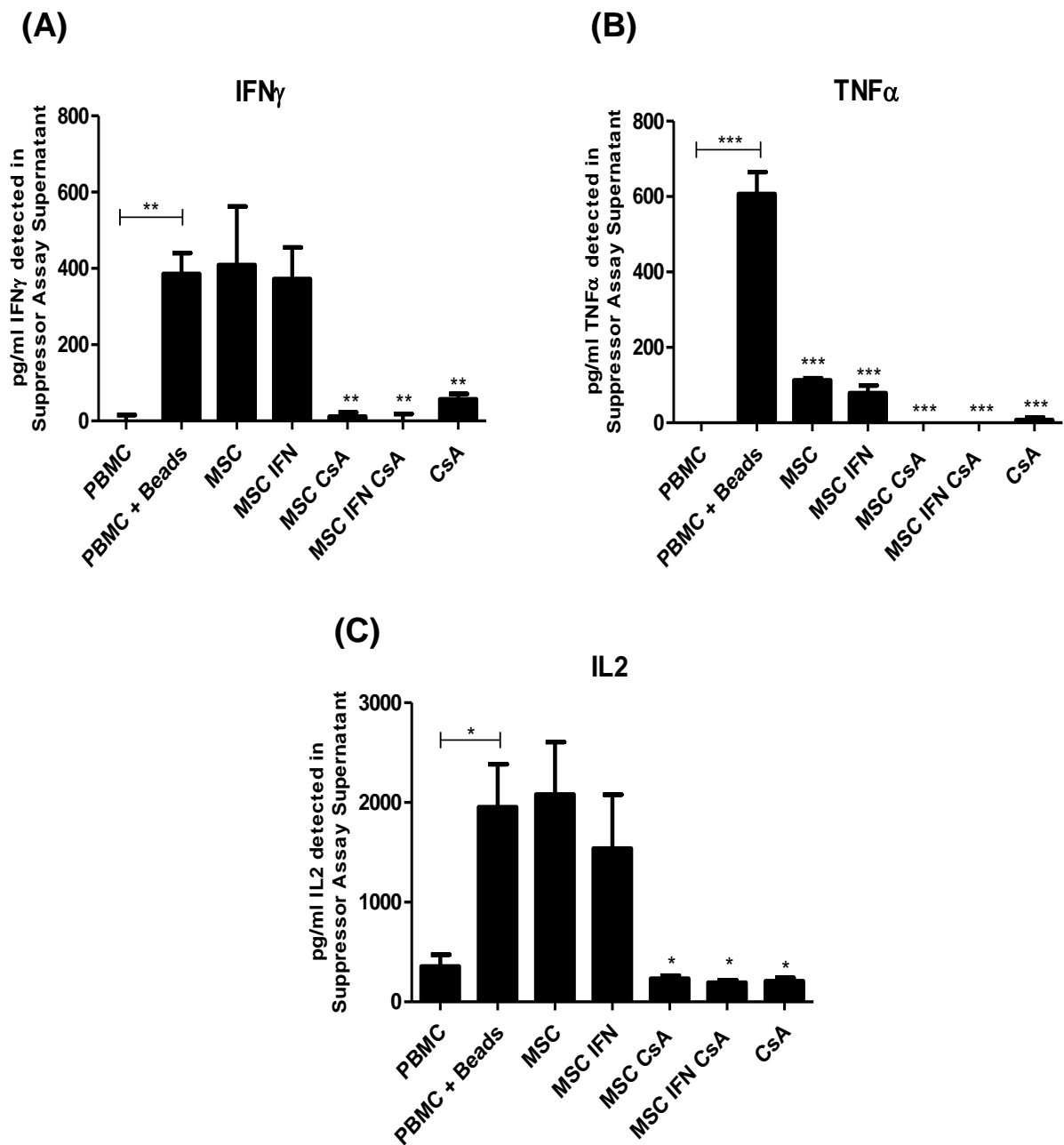
Figure 3.5. CsA suppressed the levels of IFNγ, TNFα and IL2 in a co-culture of MSC and PBMC. MSC were cultured alone or stimulated with IFNγ (50 ng/ml) for 24 h. After these stimulations, MSC were seeded (1 x 10^4 per well) into a 96 well round bottom plate. The following day CD3/CD28 activated PBMC were added (5 x 10^4 per well). The MSC:PBMC ratio was 1:5. Some groups were cultured with CsA (1 μg/ml). On day four, supernatant was collected and analysed by ELISA for the detection of IFNγ (A), TNFα (B) and IL2 (C). The assay was performed on three MSC donors from passages 5-7 against three different PBMC donors (n=3). Statistical analysis was carried out using unpaired student *t*-test where * <0.05, ** <0.01 and *** <0.001. Stars with no bar are in comparison to the PBMC group.
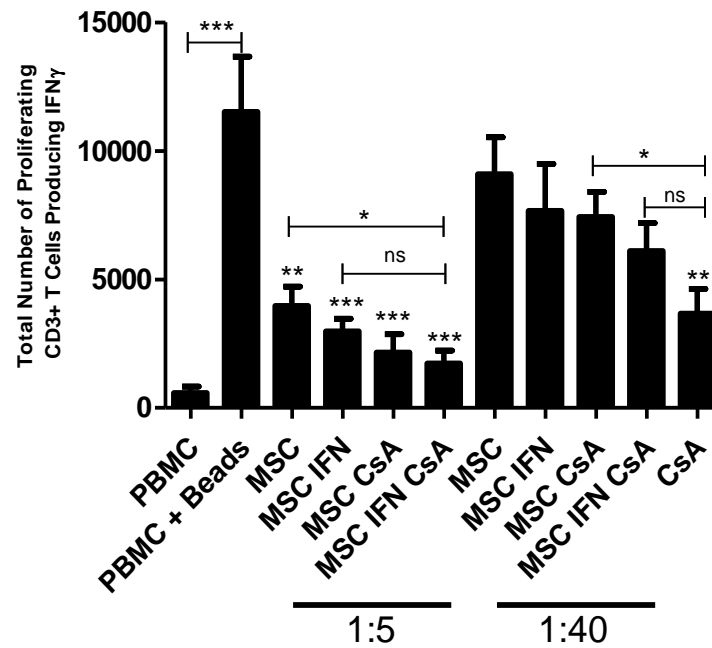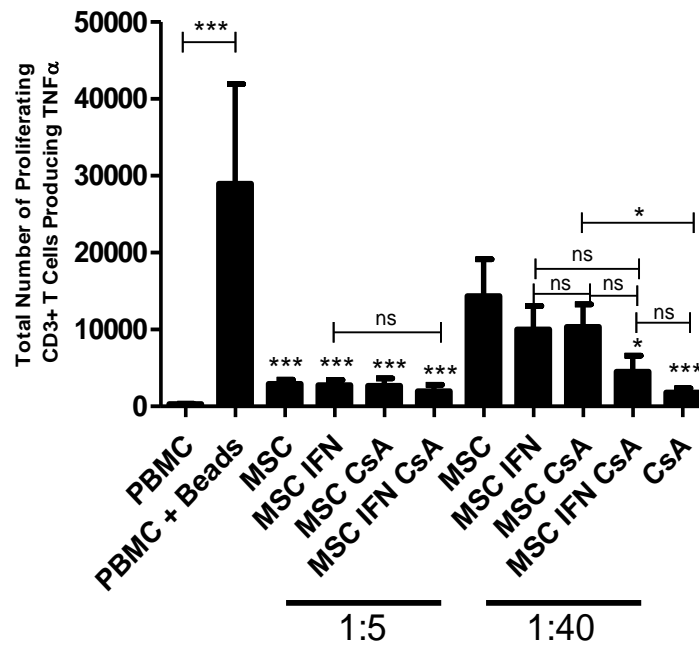
Figure 3.6. Licensed MSC with CsA significantly suppress the number of CD3$^+$ IFNγ^+ T cells at 1:5 ratio. T cell proliferation assays were carried out exactly as described before in figure 3.4, where PBMC labelled with cell proliferation dye eFluor® 670 were used to assess cytokine production by proliferating T cells. On day four, cells were harvested and stained with fluorescent antibody CD3 and fluorescent dye 7AAD to measure viable CD3$^+$ cells. These cells were fixed, permeabilised, and stained intracellularly with fluorescent antibody for IFNγ and analysed by flow cytometry. The assay was performed on three MSC donors from passages 5-7 against two PBMC donors (n=6). Statistical analysis was carried out using unpaired student t-test where * <0.05, ** <0.01 and *** <0.001. Stars with no bar are in comparison to the PBMC group.

Figure 3.7. Licensed MSC with CsA significantly suppress the number of CD3$^+$ TNFα T cells. T cell proliferation assays were carried out exactly as described in Fig 3.4, where PBMC labelled with Cell Proliferation Dye eFluor® 670 were used to assess cytokine production by proliferating T cells. On day four, cells were harvested and stained with fluorescent antibody CD3 and fluorescent dye 7AAD to measure viable CD3$^+$ cells. The cells were fixed, permeabilised, and stained intracellularly with fluorescent antibody for TNFα and analysed by Flow Cytometry. The assay was performed on three MSC donors from passages 5-7 against two PBMC donors (n=6). Statistical analysis was carried out using unpaired student *t*-test where * <0.05 and *** <0.001. Stars with no bar are in comparison to the PBMC group.
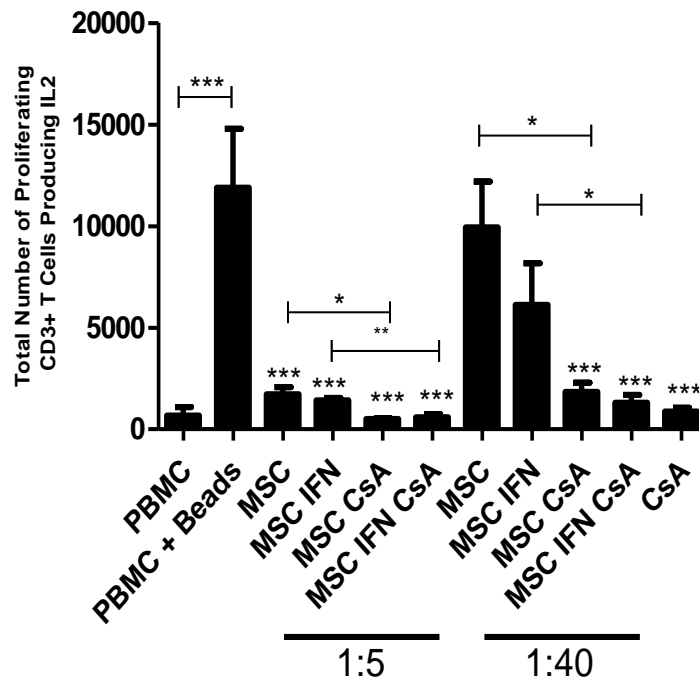
Figure 3.8. MSC does not hamper CsA suppression of CD3$^+$ IL2$^+$ T cells when used in combination *in vitro*. T cell proliferation assays were carried out exactly as described in Fig 3.4, where PBMC labelled with Cell Proliferation Dye eFluor® 670 were used to assess cytokine production by proliferating T cells. On day four, cells were harvested and stained with fluorescent antibody CD3 and fluorescent dye 7AAD to measure viable CD3$^+$ cells. The cells were fixed, permeabilised, and stained intracellularly with fluorescent antibody for IL2 and analysed by Flow Cytometry. The assay was performed on two MSC donors from passages 5-7 against two PBMC donors (n=4). Statistical analysis was carried out using unpaired student *t*-test where * <0.05, ** <0.01 and *** <0.001. Stars with no bar are in comparison to the PBMC group.

3.6. CsA REDUCED THE EXPRESSION OF CCL2 AND ICAM-1 BY MSC

MSC utilise a range of immunomodulatory agents to engage in their immunosuppressive functions. Chemoattraction of T cells in particular is thought to be required for MSC to exert their contact dependent immunosuppression mediated by short acting molecules like IDO and PGE-2 (Ren *et al*. 2008). The chemoattractant CCL2 and the adhesion molecule ICAM-1 are upregulated upon activation of MSC with TNFa or IFNγ (Krampera *et al*. 2006). MSC utilise ICAM-1 to allow cell-cell contact with T cells and blocking ICAM-1 function in MSC resulted in a significant reversal of MSC immunosuppressive function (Ren *et al.* 2010). To determine the direct effect of CsA on the regulation of CCL2 & ICAM-1, MSC were cultured in 6 well plates and stimulated with TNFα or IFNγ. RNA was isolated, cDNA was synthesised and used as a template for quantitative qPCR. Figure 3.9 A & B shows that TNFα increased the mRNA levels of CCL2 while IFNγ increased the mRNA expression of ICAM-1 in MSC. CsA alone had no effect on the mRNA levels of these immunomodulatory molecules. However, CsA reduced the mRNA levels of CCL2 and significantly reduced the mRNA levels of ICAM1 in MSC that were prestimulated with TNFα or IFNγ. CsA had no altering effect on the expression of ICAM-1 at the cell surface, as analysed by flow cytometry (Figure 3.9 C).
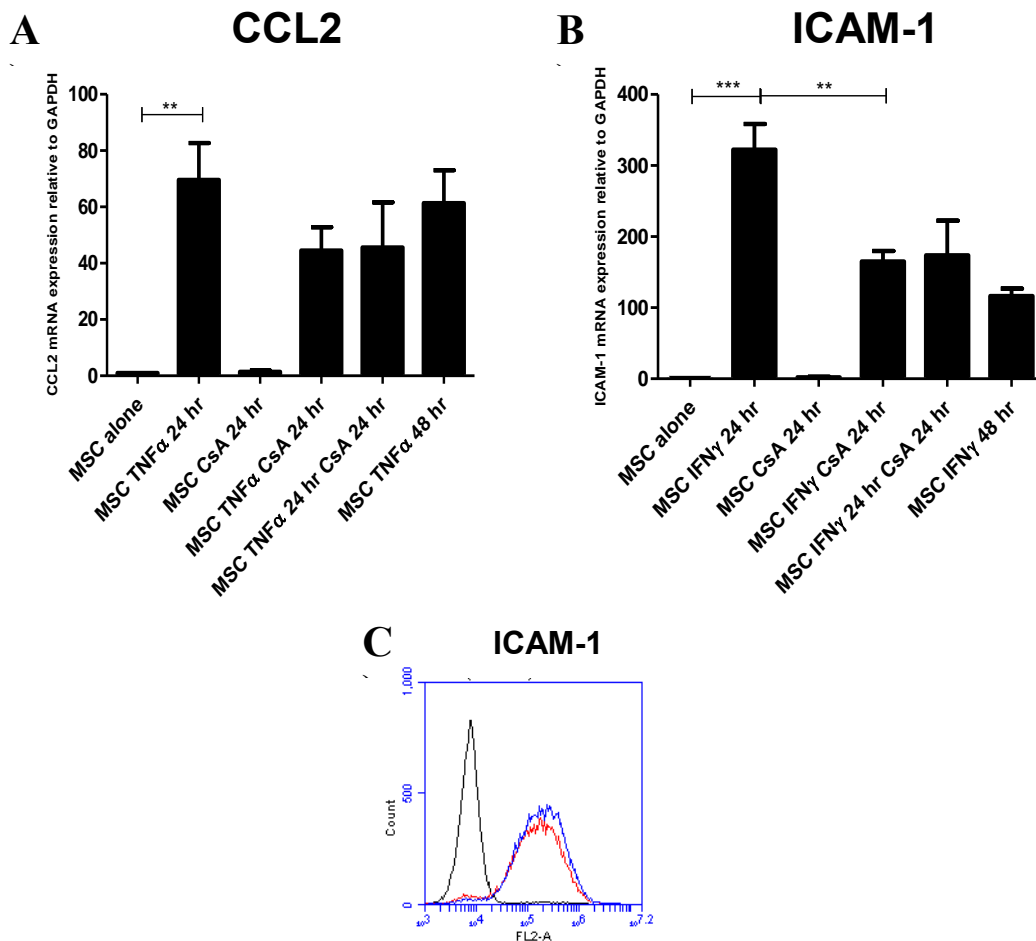
Figure 3.9. CsA reduced CCL2 and ICAM-1 mRNA expression in MSC while ICAM-1 at the cell surface of MSC was unchanged. Quantitative PCR (qPCR) analysis was carried out on MSC alone and following stimulation with TNFα (20 ng/ml) or IFNγ (50 ng/ml) and/or CsA (1 µg/ml) at different timepoints, 24 h or 48 h. RNA from each sample was extracted, cDNA was synthesised and used as a template for qPCR. CCL2 and ICAM-1 mRNA expression relative to the house keeping gene GAPDH **(A-B)**. These experiments were repeated using four MSC donors (n=4) and the results shown are representative of this. MSC stimulated with IFNγ for 48 h (red open histogram) or IFNγ for 24 h then CsA 24 h later (blue open histogram) were analysed for surface expression of ICAM-1 by flow cytometry **(C).** The black open histogram represents the isotype control. This was repeated using four MSC donors (passage 6-7). Statistical analysis was carried out using unpaired student *t*-test where ** <0.01 and *** <0.001.

3.7. CsA INCREASED EXPRESSION OF THE hMSC IMMUNOMODULATORY MEDIATOR CXCL9

Chemokine ligand 9 (CXCL9) is a T cell chemoattractant produced by MSC and it is regulated in response to inflammatory signals, such as IFNγ. To determine the direct effect of CsA on the regulation of CXCL9, MSC were cultured in 6 well plates and stimulated with IFNγ in the presence or absence of CsA. After two days, supernatant was collected to detect CXCL9 by ELISA and the cells were harvested for qPCR analysis. RNA was isolated, cDNA was synthesised and used as a template for qPCR. Figure 3.10 shows that IFNγ increased the mRNA expression of CXCL9 in MSC and CsA alone had no effect on this. Interestingly, CsA increased mRNA expression of CXCL9 in licensed MSC in comparison to licensed MSC alone. In line with this, licensed MSC even in the presence of CsA produced significantly increased levels of CXCL9 as detected by ELISA (Figure 3.10).

Further investigation was carried out on CXCL9 production by MSC and licensed MSC in the presence of CsA using a PBMC suppressor assay as an *in vitro* model of inflammation. MSC and licensed MSC were added to a co-culture assay with PBMC, exactly as described in section 3.4 and 3.5 using low (1:5) and high (1:40) MSC:PBMC ratios with CsA added accordingly. CsA significantly hampers the production of CXCL9 by MSC ($P < 0.01$), even after IFNγ licensing ($P < 0.01$) at 1:5 MSC:PBMC ratio. Surprisingly, this effect is reversed at 1:40 whereby MSC and licensed MSC significantly secreted CXCL9 into cell culture supernatant in the presence of CsA (both $P < 0.01$) (Figure 3.11). This data suggests that low dose MSC are unaffected by CsA and produce similar levels of CXCL9 as MSC or licensed MSC alone at 1:40. Figure 3.6 demonstrated that the co-cultures with higher T cell densities (1:40 ratios) have more CD3$^+$ IFNγ$^+$ T cells, it is likely that these cells provided a source of IFNγ and induced production of CXCL9 by MSC.
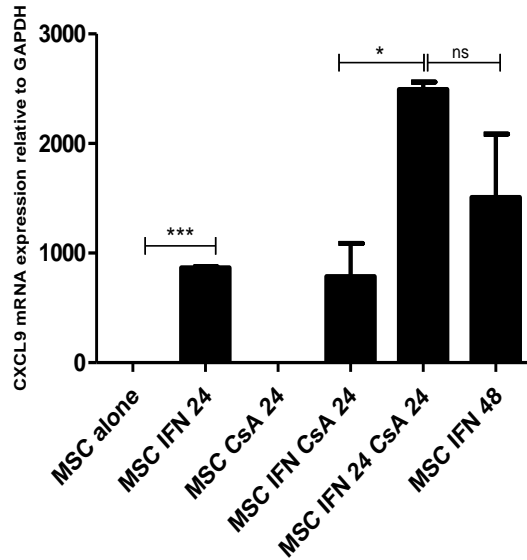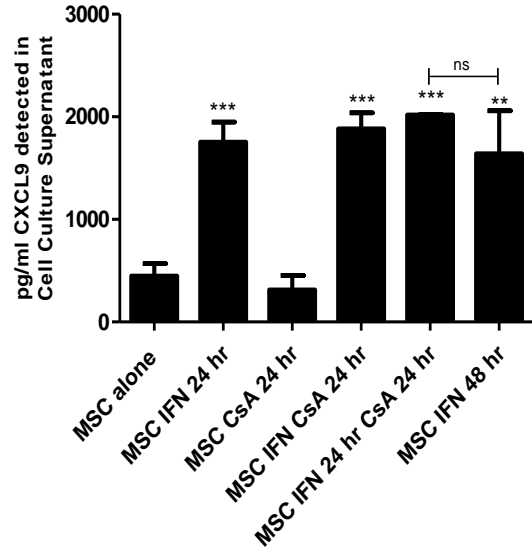
Figure 3.10. CsA enhanced CXCL9 mRNA but not protein expression by MSC post IFNγ stimulation. MSC were seeded at 2 x 10^5 per well in a 6 well plate and left alone or stimulated with IFNγ (50 ng/ml) and/or CsA (1 µg/ml) at different timepoints, 24h or 48h. After 48 hours, supernatant was collected for detection of CXCL9 by ELISA and the cells were collected for Quantitative PCR (qPCR) analysis. RNA from each sample was extracted, cDNA was synthesised and used as a template for qPCR. CXCL9 mRNA expression was relative to the house keeping gene GAPDH **(A)** CsA significantly increased the mRNA expression of CXCL9 after 24 hours of IFNγ prestimulation than by simultaneous stimulation of IFNγ and CsA (P < 0.05). **(B)** The concentration **of** CXCL9 was maintained by MSC stimulated with IFNγ in the presence of CsA. These experiments were repeated using four MSC donors (n=4) (passage 5-7) and the results shown are representative of this. Statistical analysis was carried out using unpaired student *t*-test where * <0.05, ** <0.01 and *** <0.001. Stars with no bar are in comparison to the MSC alone group.
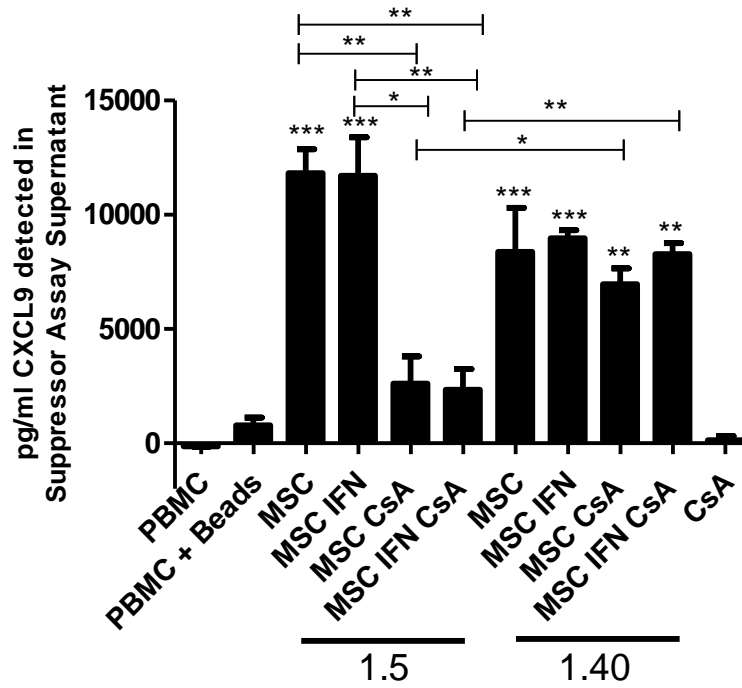
Figure 3.11. CsA suppression of CXCL9 was reversed in low dose MSC. T cell proliferation assays were carried out exactly as described in Fig 3.4. On day four, supernatant was collected for detection of CXCL9 by ELISA. CsA significantly hampered the production of CXCL9 by MSC (P < 0.01), even after IFNγ prestimulation (P < 0.01) at 1:5 MSC:PBMC ratio. This effect was reversed at 1:40 whereby MSC and MSC prestimulated with IFNγ significantly secreted CXCL9 into cell culture supernatant in the presence of CsA (both P < 0.01). The assay was performed on two MSC donors from passages 5-7 and two PBMC donors (n=4). Statistical analysis was carried out using unpaired student *t*-test where * <0.05, ** <0.01 and *** <0.001. Stars with no bar are in comparison to the PBMC group.

3.8. CsA ENHANCED IFNγ INDUCTION OF THE hMSC IMMUNOMODULATORY MEDIATOR IDO IN MSC

The tryptophan depleting enzyme IDO is regulated by IFNγ and has been shown to be altered in human MSC following treatment with steroids (Meisel *et al.* 2004; Ankrum *et al.* 2014; Chen *et al.* 2014). PGE2, derived from COX2, is produced by MSC following stimulation with TNFα and has been shown to be a significant factor in MSC suppression of alloresponses (Aggarwal & Pittenger 2005; English *et al.* 2007). To assess whether CsA has an impact on these soluble immune modulatory factors in MSC, MSC were stimulated with either IFNγ or TNFα and the expression of IDO and COX2 mRNA in MSC were examined. MSC mRNA expression of IDO was significantly increased following stimulation with IFNγ after 24 and 48 h (Figure 3.12). The addition of CsA increased mRNA expression of IDO in licensed MSC in comparison to licensed MSC alone (Figure 3.12). Although, IDO protein was not enhanced by CsA, the IFNγ induction of IDO production by licensed MSC was maintained in the presence of CsA, as illustrated by western blot (Figure 3.12). This data suggests that while IDO expression and production naturally increases upon exposure to IFNγ, additional conditioning by CsA resulted in a further increase of IDO mRNA expression and production. Further investigation of CsA enhancement of IDO by MSC was carried out by flow cytometry (gating strategy shown in Figure 3.13) following the same stimulations of IFNγ and CsA as above. Figure 3.14, shows that the percentage and number of MSC producing IDO was significantly increased after IFNγ stimulation. This induction of IDO by IFNγ was significantly enhanced by CsA after 24 h (Figure 3.14). This data suggests that CsA has a potential role to play in IFNγ signalling in MSC as it enhanced the MSC immunomodulatory mediator IDO following induction by IFNγ.

In the case of COX2, mRNA expression was increased with 24 and 48 h stimulation of TNFα as expected. However, the presence of CsA decreased COX2 mRNA expression in licensed MSC (Figure 3.15).
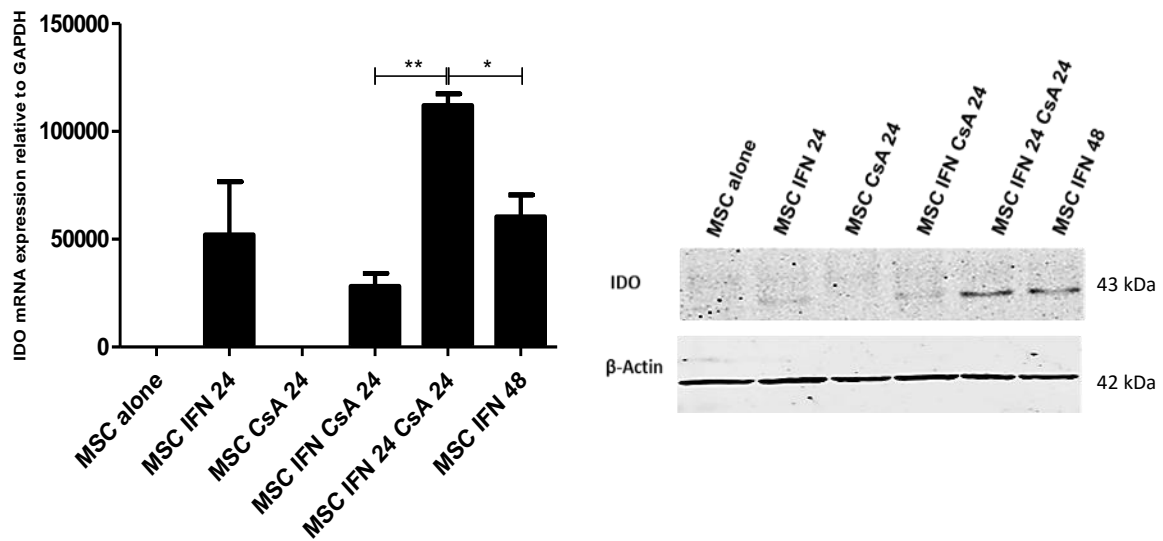

Figure 3.12. CsA enhanced IFNγ induction of IDO in human MSC. Quantitative PCR (qPCR) analysis was carried out on MSC alone or stimulated with IFNγ (50 ng/ml) and/or CsA (1 µg/ml) at different timepoints, 24h or 48h. RNA from each sample was extracted, cDNA was synthesised and used as a template for qPCR. Protein levels were measured by western blotting. CsA enhanced the mRNA expression and protein levels of IDO in MSC prestimulated with IFNγ in a time dependent manner. β-Actin was included as a loading control. These experiments were repeated using four MSC donors from passage 5-7 and the results shown are representative of this. Statistical analysis was carried out using unpaired student *t*-test where * <0.05 and ** <0.01.
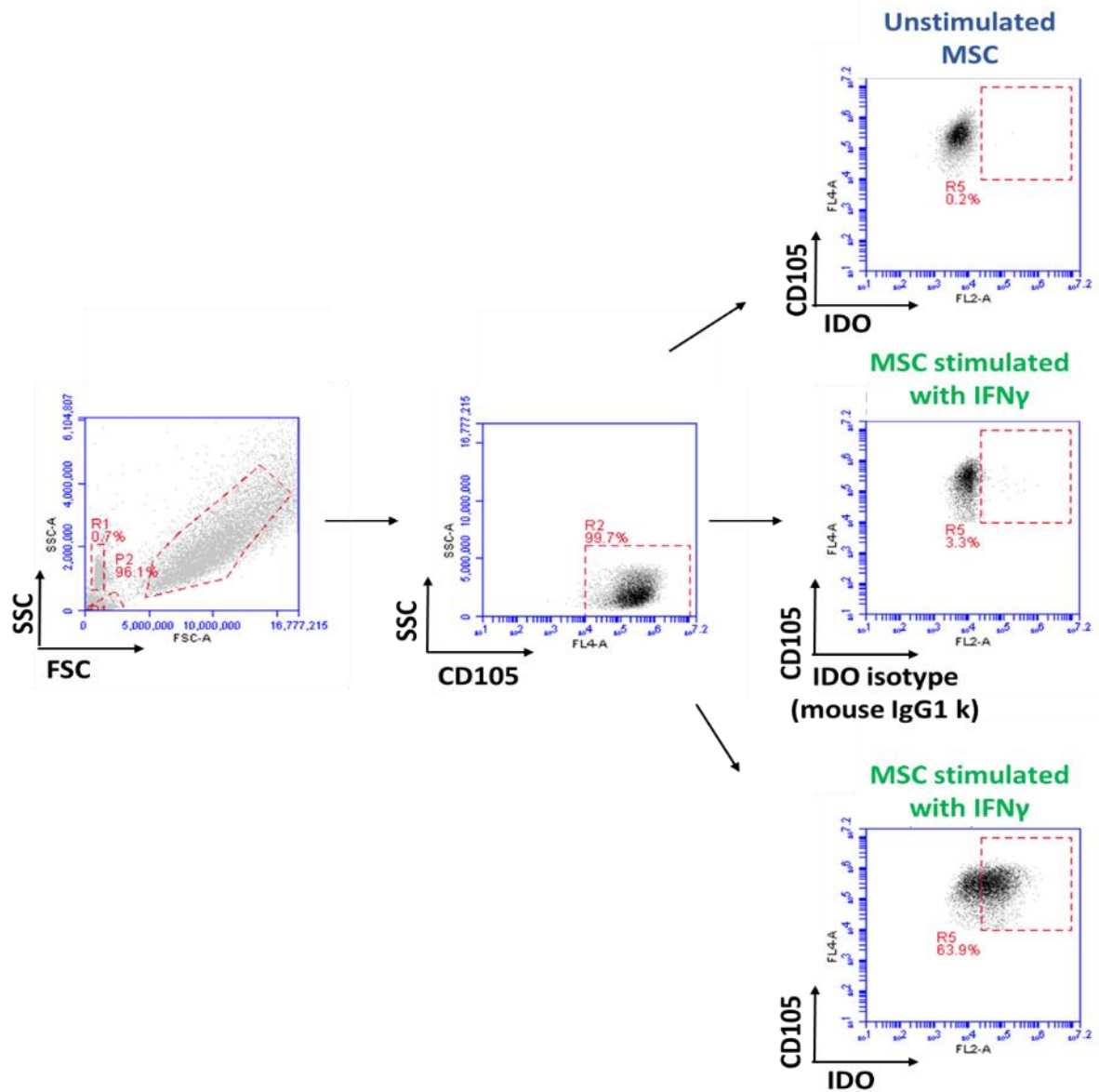
Figure 3.13. Representative example of gating strategy used to identify human CD105$^+$ MSC producing IDO. (A) Illustrates the gated MSC population from SSC against FSC plot, (B) represents the gating position for human CD105$^+$ (APC) expression within the MSC population, (C) illustrates the gating position for CD105$^+$ (APC) unstimulated MSC producing IDO (PE). (D) and (E) represent the CD105$^+$ MSC stimulated with IFNγ which were either stained with IDO isotype (PE) or antibody (PE) respectively. All other gating positions were determined using matching isotype controls.
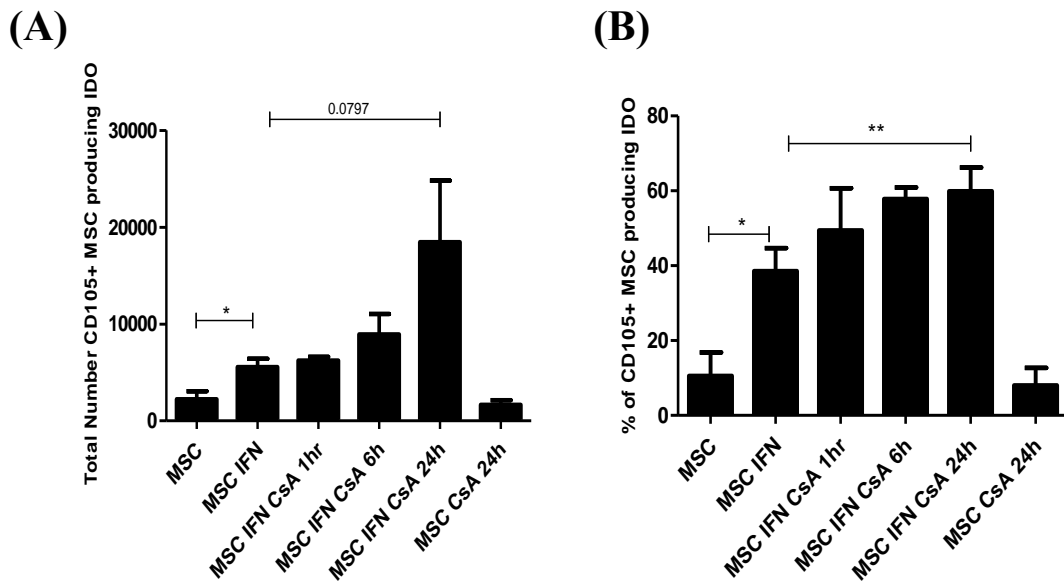
Figure 3.14. CsA significantly enhanced the percentage of MSC producing IDO after IFNγ induction in a time dependent manner. MSC were seeded at 2 x 10^5 per well in a 6 well plate. MSC were left unstimulated or stimulated with CsA (1 µg/ml) for 24 h only. As IDO is induced by IFNγ, MSC were stimulated with IFNγ (50 ng/ml) for 6h prior to the addition of CsA (1 µg/ml) added at either 24 h, 6 h, 1 h and 0h before all groups were harvested for analysis by intracellular flow cytometry at the same time. Graphical representation of the total number of human MSC producing IDO following stimulations with IFNγ and CsA (A). Graphical representation of the percentage of human MSC producing IDO following stimulations with IFNγ and CsA (B). The total number of human cells was assessed using counting beads during flow cytometry. n=5 per group (and 3 MSC donors). Statistical analysis was carried out using unpaired student *t*-test where * <0.05 and ** <0.01.
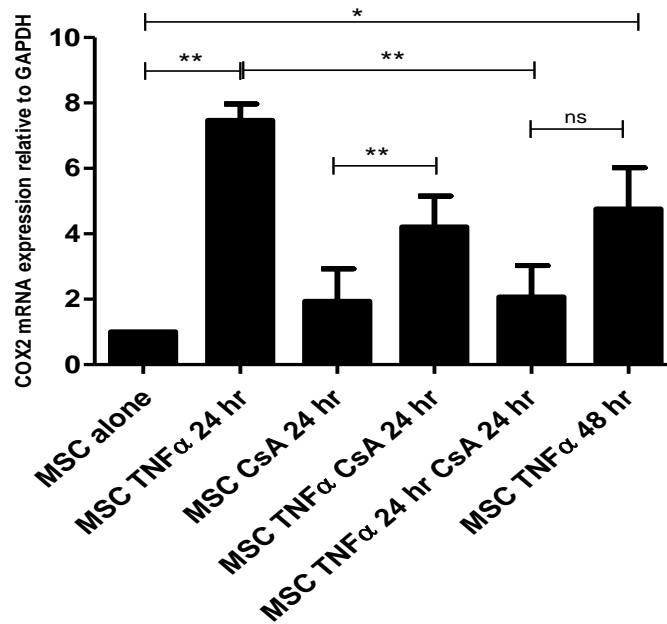
Figure 3.15. CsA impaired the up-regulation of COX2 mRNA expression in MSC following TNFα stimulation. Quantitative PCR (qPCR) analysis was carried out on MSC alone or stimulated with TNFα (20 ng/ml) and/or CsA (1 µg/ml) at different timepoints, 24h or 48h. RNA from each sample was extracted, cDNA was synthesised and used as a template for qPCR. COX2 mRNA expression was increased with 24 and 48 h stimulation of TNFα. The presence of CsA decreased COX2 mRNA expression in MSC prestimulated with TNFα than without CsA (P < 0.01). These experiments were repeated using four MSC donors (n=4) from passage 5-7 and the results shown are representative of this. Statistical analysis was carried out using unpaired student *t*-test where * <0.05 and ** <0.01.

3.9. CsA HAS AN INDIRECT INHIBITORY EFFECT ON THE IFNγ SIGNALLING REGULATOR SOCS1

Suppressor of cytokine signaling 1 (SOCS1) is a negative regulator of cytokine signal transduction and is known to play an important role in the regulation of IFNγ signalling (Yoshimura A.T *et. al* 2007). SOCS1 has recently been described as being a negative regulator of MSC immunosuppressive ability by reducing the expression of inducible nitric oxide synthase (iNOS) (Zhang *et al.* 2014). CsA is known to interfere with the inhibitory function of SOCS1 in cells infected with hepatitis c virus and rotavirus (Liu *et al* 2011; Shen *et al*. 2013). Notably, these viruses are dependent on IFN signalling for their replication. Throughout this chapter, CsA has been shown to enhance functionality of licensed MSC in suppressor assays (section 3.4) and amplify the production of IFNγ regulated mediators such as CXCL9 and IDO. Therefore, as SOCS1 has been described as a regulator of MSC immunosuppressive functions through IFNγ signalling, it is imperative to investigate the effect CsA has on SOCS1 signalling in MSC.

MSC were seeded into a 6 well plate (2 x 10^5 per well/2ml), stimulated with IFNγ and/or CsA and the protein levels of SOCS1, pSTAT1 and STAT1 were analysed by western blot (section 2.6) to assess the effect CsA has on this signalling pathway. At the mRNA level, CsA downregulated SOCS1 in MSC prestimulated with IFNγ for 24 h (Figure 3.16). Consistent with this, CsA also downregulated SOCS1 protein in MSC prestimulated with IFNγ in a time dependent manner (Figure 3.16). Notably, pSTAT1 and STAT1 protein levels were slightly increased in MSC that had been prestimulated with IFNγ before the addition of CsA (Figure 3.16). Interestingly, CsA added simultaneously with IFNγ had no inhibitory effect on SOCS1 mRNA or protein and CsA alone did not downregulate SOCS1 protein in MSC. This data suggests that SOCS1 inhibition of CsA is indirect and time dependent on IFNγ activation of MSC.
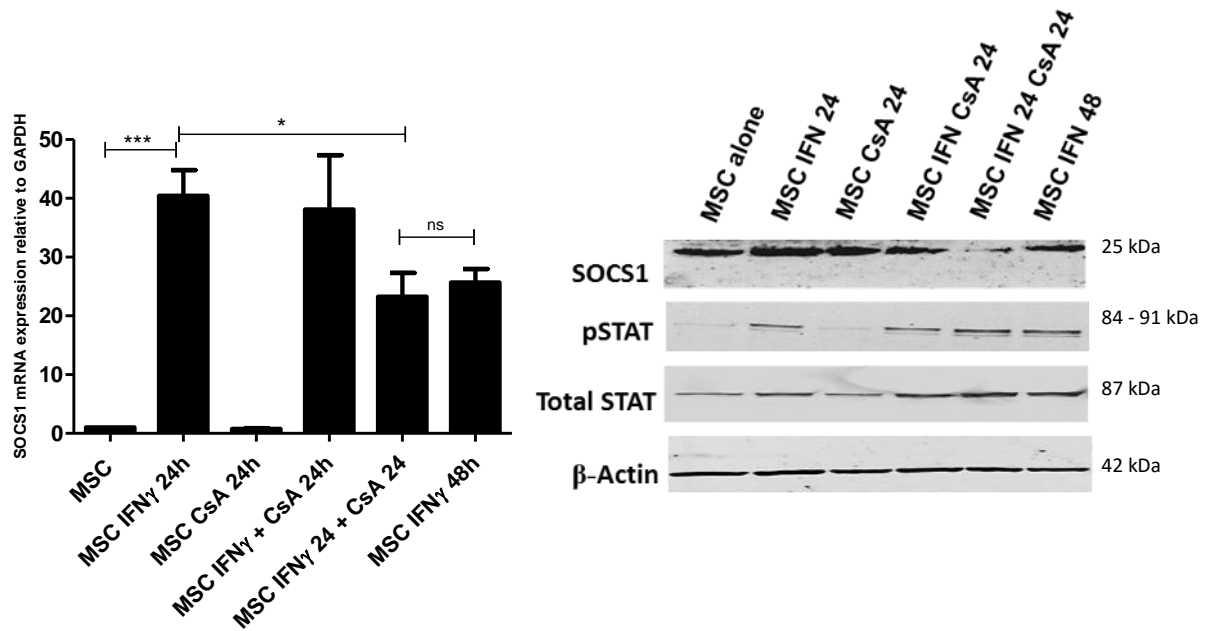
Figure 3.16. CsA inhibited SOCS1 in human MSC following IFNγ induction. Quantitative PCR (qPCR) analysis was carried out on MSC alone or stimulated with IFNγ (50 ng/ml) and/or CsA (1 µg/ml) at different timepoints, 24h or 48h. RNA from each sample was extracted, cDNA was synthesised and used as a template for qPCR. Protein levels were measured by western blotting. CsA decreased the mRNA expression and protein levels of SOCS1 in MSC prestimulated with IFNγ in a time dependent manner. The protein levels of pSTAT1 are increased in MSC that were prestimulated with IFNγ before the addition of CsA. β-Actin is included as a loading control. These experiments were repeated using four MSC donors (n=4) from passage 5-7 and the results shown are representative of this. Statistical analysis was carried out using unpaired student t-test where * <0.05 and *** <0.001.

3.10. SUMMARY

The main aims of this chapter were to 1) determine the influence of CsA on MSC characterisation and immunosuppressive ability, 2) to define the effects of CsA on the key immunomodulatory mediators of MSC and 3) to identify a mechanism by which CsA can influence key signal transduction events involved in MSC immunosuppression. The addition of CsA (100 ng/ml, 500 ng/ml & 1 µg/ml) for 24 and 48 h had no impact on MSC surface marker phenotype nor did it alter trilineage differentiation ability *in vitro* (Figures 3.1 – 3.3). Using a labelled cell proliferation co-culture assay, CsA was shown to have an inhibitory effect on MSC immunosuppressive ability at low PBMC densities (Figure 3.4). However, the prestimulation of MSC with IFNγ prior to the addition of CsA maintained immunosuppressive ability at 1:5 ratio and was enhanced at 1:40 in comparison to IFNγ alone (Figure 3.4).

In terms of suppression of cytokine production by $CD3^+$ T cells, MSC and CsA in combination displayed differential effects depending upon PBMC density in suppressor assays. At 1:5, CsA significantly enhanced licensed MSC suppression of $CD3^+$ $IFNγ^+$ T cells in comparison to MSC alone (Figure 3.6). While CsA alone significantly suppressed $CD3^+$ $IFNγ^+$ T cells, this capacity was significantly hampered when combined with MSC at high PBMC densities (1:40). These findings are similar for TNFα producing $CD3^+$ T cells, however at high PBMC density (1:40), licensed MSC significantly suppressed $CD3^+$ $TNFα^+$ T cells in combination with CsA with no significant differences to the potency of CsA alone (Figure 3.7). This suggests that licensing of MSC can facilitate a beneficial affiliation with CsA in suppressing $CD3^+$ $TNFα^+$ T cells. Additionally, MSC combined with CsA, display a significant suppression of $CD3^+$ $IL2^+$ T cells for both MSC and licensed MSC at 1:5 and 1:40 (Figure 3.8). This suggests that MSC have no hampering effect on CsA suppression of IL2 producing $CD3^+$ T cells. Collectively this data provides further evidence that MSC

are complex immunomodulators and their response is dependent on their inflammatory micro-environment. It is noteworthy that the cytokines IFNγ and TNFα are involved in MSC licensing and production of mediators such as CXCL9 were increased at high PBMC densities (Figure 3.11). This data also proposes that CsA uses different mechanisms to regulate these cytokines and, depending on inflammatory cues, MSC can hinder these processes.

The second part of this study was to define the effects of CsA on the key immunomodulatory mediators of MSC. CsA had no significant altering effect on CCL2 or ICAM1 (Figure 3.9). Licensed MSC in the presence of CsA displayed increased CXCL9 in comparison to licensed MSC alone at mRNA but not protein level (Figure 3.10). In the supernatant from PBMC suppressor assays, CsA significantly reduced CXCL9 production by MSC and licensed MSC at 1:5 but at 1:40, the concentration of CXCL9 by MSC and licensed MSC was not affected by CsA (Figure 3.11). The high levels of $CD3^+$ $IFNγ^+$ T cells at 1:40, as shown in figure 3.7, may have been a source for IFNγ licensing of MSC to induce CXCL9 production with no obstruction from CsA whereas at 1:5 the numbers of $CD3^+$ IFN^+ T cells (Figure 3.6) and IFNγ in the supernatant (Figure 3.5) are significantly lowered by CsA. This suggests that the co-addition of CsA at low PBMC densities provides an environment that is too suppressive for full MSC activation which resulted in less CXCL9 production. Whereas, at high PBMC densities, where the number of MSC is lower, the relative dose response from available IFNγ produced more potently suppressive MSC in the presence of CsA (Figure 3.4). Interestingly, IDO production was significantly enhanced by licensed MSC when in the presence of CsA at the mRNA and protein level (Figure 3.12). Futhermore, CsA significantly increased the percentage of MSC producing IDO following IFNγ induction (Figure 3.14)

All of these findings together suggest that the IFNγ signalling pathway must be active prior to CsA addition in order for MSC to become more potent immunomodulators in combination with CsA. Thus, MSC must be activated by IFNγ before a beneficial effect with CsA can be achieved *in vitro*.

Probing this pathway further, CsA has an inhibitory effect on SOCS1 expression in MSC resulting in a prolonged activation of the IFNγ pathway. This is evident as pSTAT1 and STAT1 protein levels are slightly increased in MSC that have been stimulated with IFNγ (24 h and 48 h) before the addition of CsA (Figure 3.16). The inhibition of SOCS1 by CsA was found only in licensed MSC as CsA alone had no inhibitory effect on basal levels of SOCS1 in resting MSC. This suggests that the inhibition is indirect as it is dependent on activation of the IFNγ pathway and therefore must involve other IFNγ inducible proteins. Here identifies a novel role for CsA in altering signal transduction in the IFNγ pathway of MSC which is pivotol for MSC to exert their immunosuppressive function.

CHAPTER 4

SMPILL® PROVIDES ENHANCED CSA EFFICACY IN A HUMANISED MOUSE MODEL OF AGVHD IN A TARGETED MANNER

4.1. INTRODUCTION

The development of graft versus host disease (GvHD) still represents a life threatening complication following allogeneic hematopoieic stem cell transplantation (HSCT). The disease manifests as a severe inflammatory condition affecting multiple organs, especially the gastrointestinal (GI) tract. For prophylaxis of aGvHD, CsA is administered for up to six months after allogeneic HSCT (Ruutu *et al.* 2014). CsA has also been reported to be effective in the treatment of established GvHD (Deeg *et al.* 1985; Ruutu *et al*. 2014). However, the metabolism of CsA in the GI tract has been shown to significantly affect it's bioavailability with CsA predominantly absorbed in the upper GI rather than the colon (Webber *et al.* 1992; Drewe *et al.* 1992). This suggests that there is a window for CsA absorption in the small intestine and that the length of the functionally intact small bowel is an important determinant of the oral dosage requirement of CsA. The added complications of damaged GI mucosa as a result of the conditioning regimen undergone by allogeneic HSCT patients could further influence CsA pharmacokinetics with reduced intestinal absorption (Kimura *et al.* 2010). Therefore, the variabilities of CsA absorption in HSCT patients could ultimately jeopardise the efficacy of GvHD prevention.

Humanised mouse models of aGvHD provide a platform from which novel therapies can be assessed and their performance of alleviating aGvHD can be investigated in a clinically relevant manner. Previous work within our research group contributed to the establishment of a robust and reproducible humanised mouse model of aGvHD based on transfusion of peripheral blood mononuclear cells (PBMCs) to immunodeficient NOD-SCID IL2 receptor gamma null (NSG) mice, first described by Pearson *et al.* (Pearson *et al*. 2008; Tobin *et al.* 2013). In this way, the disease is generated and sustained by human immune cells offering a more clinically relevant model of disease than murine models of aGvHD.

To enable efficacious oral drug therapy, adequate oral bioavailability must be achieved. Therefore, there is a need for an oral therapy capable of providing a modulated systemic and complete GI bioavailabilty. Sandimmune® and the more advanced Neoral® are oral formulations of CsA which were designed for this purpose. Neoral® in particular has been shown to enhance oral bioavailability of CsA more efficiently than Sandimmune® and reduce the variability in pharmacokinetic parameters within and between patients receiving CsA therapy (Parquet *et al*. 2000; Yocum *et al*. 2000). Although Neoral has provided an improvement to the variability of CsA bioavailability, it is an immediate releasing CsA formulation which results in rapid peaks and trough levels of CsA in the blood (Jorga *et al.* 2004). Therefore, CsA levels in the blood are maintained above threshold and ultimately contribute to unwanted systemic side effects and a potential limit to the beneficial GvL effect (Parquet *et al.* 2000; Kishi *et al*. 2005).

Our collaborators, Sigmoid Pharma Ltd., have developed a sophisticated drug delivery technology called SmPill® which encapsulates CsA into a multi-bead format where the outer coating controls the release of CsA. The beads are designed to release CsA via two formulations, immediate release beads and colonic release beads. These formulations deliver CsA systemically (immediate release) but also specifically target the GI tract (colonic release), where the two formulations combined expose the entire GI to CsA. The immediate release SmPill® formulation provides a slower release than Neoral® which permit modulated pharmacokinetic (PK) profiles, attaining adequate trough levels without the excessive PK profile associated with Neoral®. Also, it is hypothesised that this modulated systemic release formulation will release CsA over a longer time period than Neoral® and provide adequate levels of CsA to the small intestine leading to protection against small intestinal GvHD. As aGvHD is a multi organ inflammatory disease with the GI tract having a primary role in initiation, it is hypothesised that SmPill® will be an efficacious CsA therapy in the humanised mouse model of aGvHD.

The objectives of this chapter are laid out as follows:

- To optimise and assess the performance of the novel CsA formulation, SmPill® in the humanised model of aGvHD against conventional CsA therapies, Neoral® and Sandimmune®, and placebo controls.
- To determine if SmPill® therapy has the potential to benefit both GI and systemic GvHD in the humanised model.

4.2. DETERMINATION OF OPTIMAL SᴍPILL® DOSING SCHEDULE TO PROLONG SURVIVAL IN A HUMANISED MOUSE MODEL OF ᴀGᴠHD

This initial study sought to investigate if CsA delivered orally (SmPill® or Neoral® or Sandimmune®), intravenously (Sandimmune®) or intraperitoneally (Sandimmune®) alleviated aGvHD in this humanised model. The loading of CsA in the SmPill® immediate and colonic release beads collectively was approximately a 25 mg/kg dose. With this in mind and similar to published reports, all other CsA therapies were administered at 25mg/kg per dose (Gan *et al*. 2003; Hori *et al.* 2008; Perez *et al.* 2011). By keeping the dosage of CsA constant from day 1, the performance of each delivery method was assessed in terms of prolonging survival in the humanised aGvHD model.

NSG mice were conditioned with low dose whole body irradiation (2.4 Gy) and human PBMC (8×10^5 gram^{-1}) were injected via the tail vein on day 0 (Figure 4.1). In healthy non-GvHD control groups, NSG mice were irradiated and received sterile PBS in place of PBMC. CsA was delivered intravenously (Sandimmune® IV), intraperitoneally (Sandimmune®) and by oral gavage (Sandimmune® , Neoral®, SmPill®) for 6 daily doses (25mg/kg per dose) from day 1 (Figure 4.1). The SmPill® dosage consisted of 1 immediate and 1 colonic release CsA loaded beads each time, where the bead size ranged from 1.25-1.5mm. The development of aGvHD was monitored, in accordance with the local ethical committee guidelines at Maynooth University, and defined as total body weight loss of >15% of original starting weight with a series of clinical manifestations including posture, reduction in activity and fur condition. These parameters were scored by severity, where any mouse had a total body weight loss of >15% or accumulated a clinical score of 6 or more were considered to have severe aGvHD and euthanised.

After PBMC administration, weight loss and survival of each mouse was monitored every second day until day 9 and then every day for the remainder of the study (Figure 4.2).

As expected, the administration of PBS to irradiated NSG mice had no effect on survival or weight loss throughout the study (Figure 4.2). Irradiated NSG mice which received PBMC developed aGvHD with no mice surviving past day 14 (Figure 4.2 A). The administration of oral (Sandimmune®, Neoral®, SmPill®) and intraperitoneal (Sandimmune®) CsA therapy to irradiated NSG mice which received PBMC did not prolong the survival of these mice (Figure 4.2 A). Similarly, the weight loss displayed by these mice were in parallel with the irradiated NSG mice which received PBMC but no therapy (Figure 4.2 B). However, CsA therapy delivered intravenously (Sandimmune® IV) prolonged survival and significantly reduced weight loss in aGvHD mice (Figure 4.2).
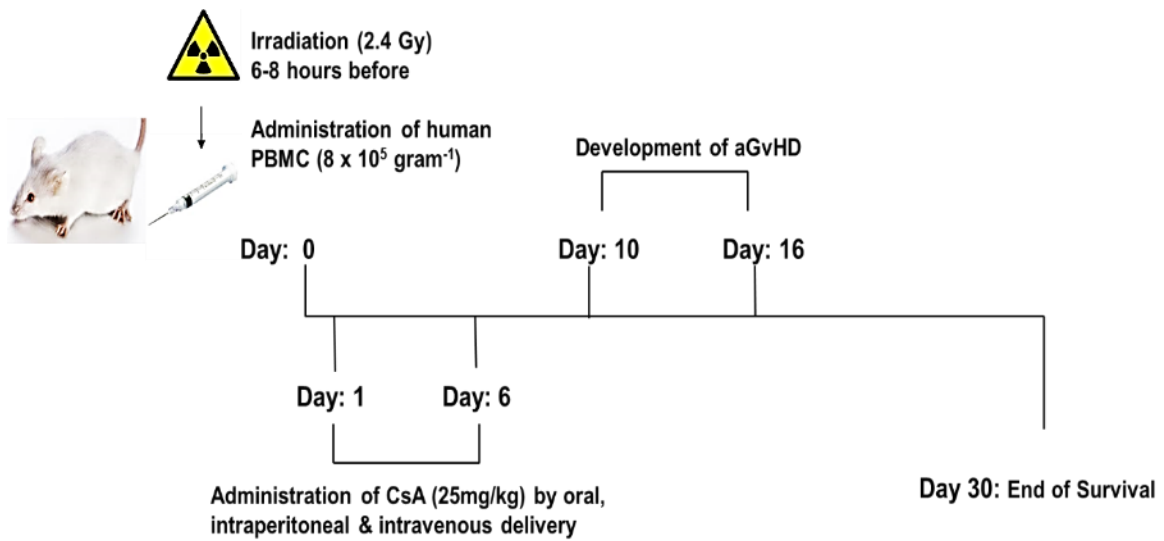
Figure 4.1. Development of a humanised mouse model of aGvHD to assess the performance of oral, intraperitoneal and intravenous CsA. NOD-SCID IL-2rγ^null (NSG) mice were exposed to a sub-lethal dose of gamma irradiation (2.4 Gy). 8×10^5 PBMC gram^{-1} or sterile PBS was then administered intravenously (300 µl) to each mouse via the tail vein on day 0. CsA was delivered intravenously (Sandimmune® IV), intraperitoneally (Sandimmune®) and by oral gavage (Sandimmune®, Neoral®, SmPill®) for 6 daily doses (25mg/kg per dose) from day 1. The SmPill® dosage consisted of 1 immediate and 1 colonic release CsA loaded beads each time. The development of aGvHD was monitored every second day until day 9 and then everyday thereafter by recording weight loss, appearance, posture and activity.
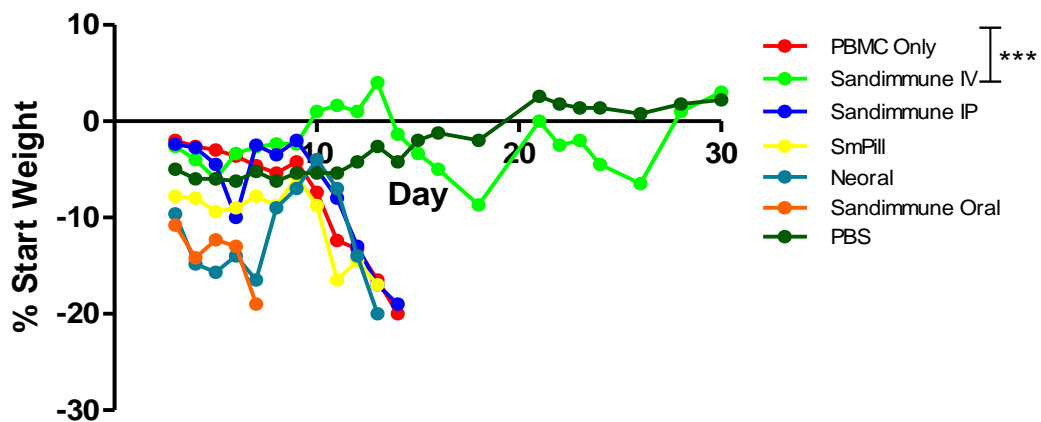
(A)
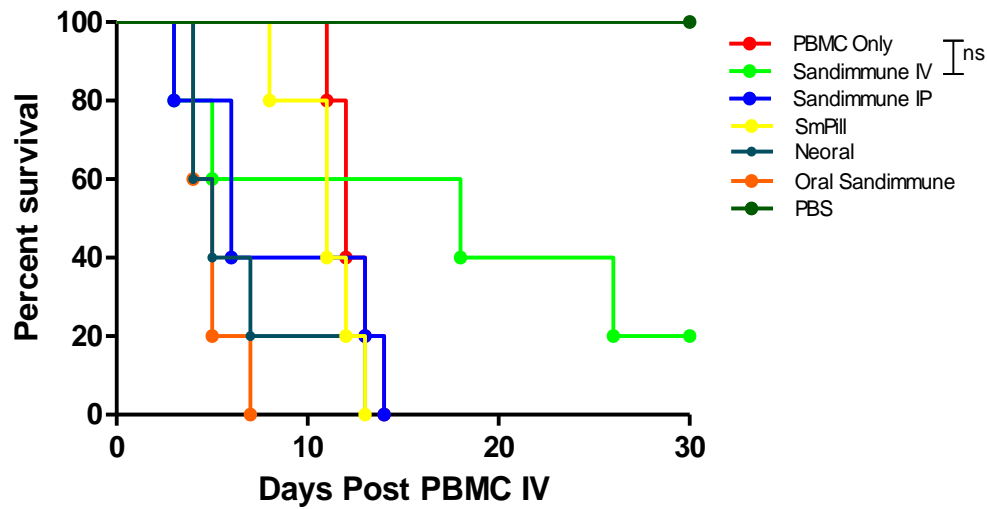
(B)

Figure 4.2. Sandimmune® IV prolonged survival and reduced weight loss in aGvHD mice after six daily doses from day 1. 8×10^5 human PBMC gram^{-1} were administered to irradiated NSG mice (2.4Gy) on day 0. CsA was delivered by intravenous (Sandimmune® IV), intraperitoneal (Sandimmune®) and oral (Sandimmune®, Neoral®, SmPill®) administration for 6 daily doses (25mg/kg per dose) from day 1. Transplanted mice were monitored every 2 days until day 9 and then every day for the duration of the experiment. n=5 mice for each group. Survival graphs for PBMC and Neoral® overlap with Sandimmune® IP and SmPill® respectively. PBMC group reached 0% at day 14 while Neoral® group reached 0% at day 13 (A). Statistical analysis was carried out using a Mantel-Cox test for the survival curve and unpaired student *t*-test for weight change where *** <0.001.

4.3. SmPILL® DELIVERY OF CsA SIGNIFICANTLY IMPROVED SURVIVAL AND REDUCED WEIGHT LOSS IN A HUMANISED MOUSE MODEL OF aGvHD

It has been reported that irradiation conditioning alone can severely impact mouse body weight (Saland *et al*. 2015). We therefore hypothesised that the initial weight loss as a result of the irradiation conditioning (2.4 Gy) could have been a factor contributing to reduced CsA absorption resulting in the failure of all oral and intraperitoneal CsA therapies in prolonging survival in GvHD mice (Figure 4.2.). Also, some SmPill® treated aGvHD mice were humanely euthanised due to tracheal damage as the beads delivered via oral gavage were not of optimal size.

Considering these factors, it was decided to refine the study by downsizing the number of study groups and utilise a different dosage strategy in terms of timing. The CsA study groups were reduced to Neoral® and Sandimmune® IV, as a comparator for SmPill® efficacy. The chosen start date of dosing was day 4 instead of day 1 as it was expected that mice would return to their respective start weights from this point. The bead size was also reduced from 1.25-1.5mm to 1-1.25mm for all other studies to prevent the possibility of further tracheal damage as a result of drug administration via gavage. As the 25 mg/kg dose delivered intravenously (Sandimmune® IV) prolonged survival and significantly reduced weight loss in the previous study (Figure 4.2), this concentration was used for remaining studies.

As before, NSG mice were irradiated (2.4 Gy) and human PBMC (8 x 10^5 gram^{-1}) were injected via the tail vein (Figure 4.3). Control groups were included by administering sterile PBS to irradiated NSG mice. For this study, CsA was delivered intravenously (Sandimmune® IV), and by oral gavage (Neoral® and SmPill®) for 3 doses (25mg/kg per

dose) from day 4 (Figure 4.3). Transplanted mice were monitored closely and the survival and weight loss of each mouse was recorded (Figure 4.4).

NSG mice that received human PBMC but no therapy developed aGvHD consistently and there was no survival of mice after day 14 (Figure 4.4 A). These mice exhibited significant weight loss in comparison to PBS healthy controls (Figure 4.4 B). In line with figure 4.2, the administration of Sandimmune® IV on day 4, 8 and 12 resulted in prolonged survival and significant reduction in weight loss in comparison to untreated aGvHD mice (Figure 4.4). The administration of SmPill® on day 4, 8 and 12 significantly prolonged survival and reduced weight loss in aGvHD mice (Figure 4.4). Three doses of Neoral® failed to prolong survival or reduce weight loss in aGvHD (Figure 4.4).

The efficacy of SmPill® CsA was investigated further by administering five doses of CsA (25 mg/kg) in the humanised aGvHD model (Figure 4.5). The model was set up exactly as described before but with five doses of CsA for each therapy (Figure 4.5). Placebo beads (containing no CsA) were included in the study as a vehicle control. The administration of PBMC (8×10^5 $gram^{-1}$) to NSG mice resulted in progression of aGvHD by which 30% of untreated mice remained on day 12 and all were sacrificed by day 17 (Figure 4.6 A). Consistent with all previous studies, Sandimmune® IV significantly prolonged survival and significantly reduced weight loss in aGvHD mice. Five doses of Neoral® reduced weight loss and prolonged survival in aGvHD mice, however there was no significant differences in comparison to untreated aGvHD mice (Figure 4.6). SmPill® was shown to significantly reduce weight loss and prolong survival in aGvHD mice with up to 60% survival at the end point of the study (Figure 4.6). GvHD mice who received placebo beads in place of CsA therapy succumbed to aGvHD with all mice sacrificed from this group by day 18 (Figure 4.6 A).
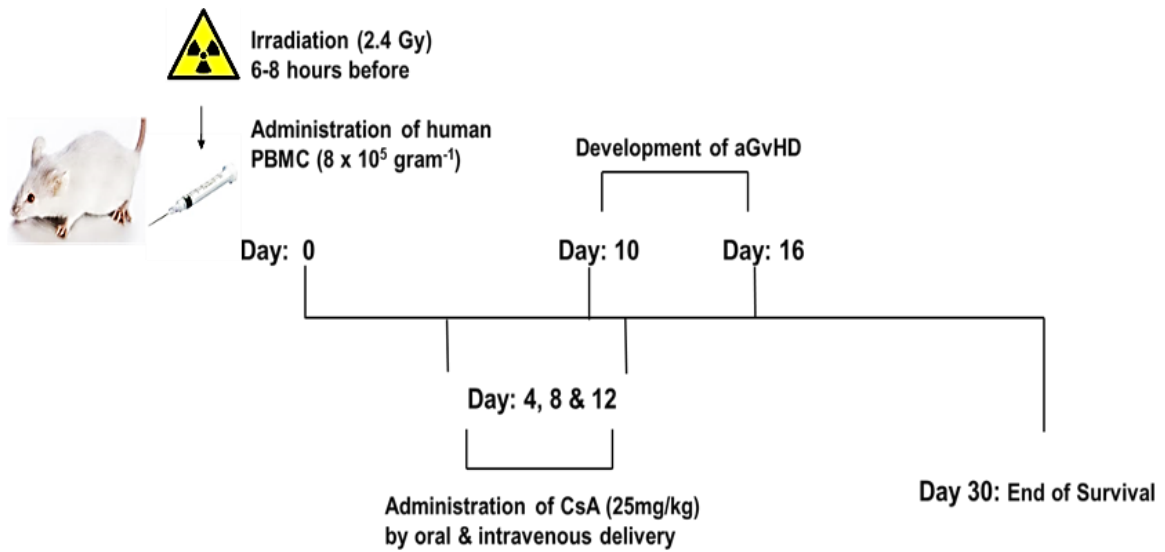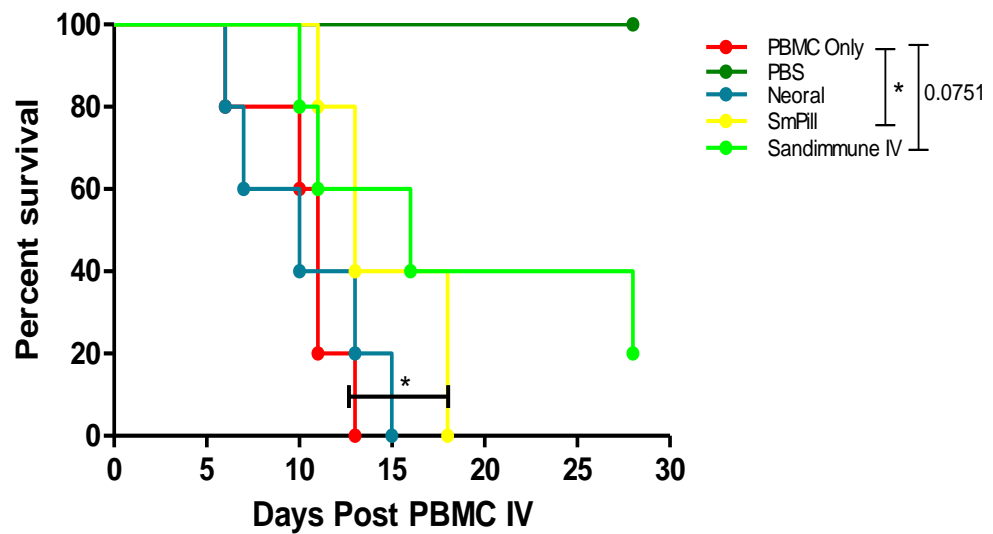
Figure 4.3. Development of a humanised mouse model of aGvHD to assess the performance of smaller formulated SmPill® CsA beads with delivery from day 4. NOD-SCID IL-2rγ^{null} (NSG) mice were exposed to a sub-lethal dose of gamma irradiation (2.4 Gy). 8×10^5 PBMC gram^{-1} or sterile PBS was then administered intravenously (300 µl) to each mouse via the tail vein on day 0. CsA was delivered by intravenous (Sandimmune® IV) and oral (Neoral®, SmPill®) administration for 3 doses (25mg/kg per dose) every 4 days from day 4. The SmPill® dosage consisted of 1 immediate and 1 colonic release CsA loaded beads each time. The development of aGvHD was monitored every second day until day 9 and then everyday thereafter by recording weight loss, appearance, posture and activity.
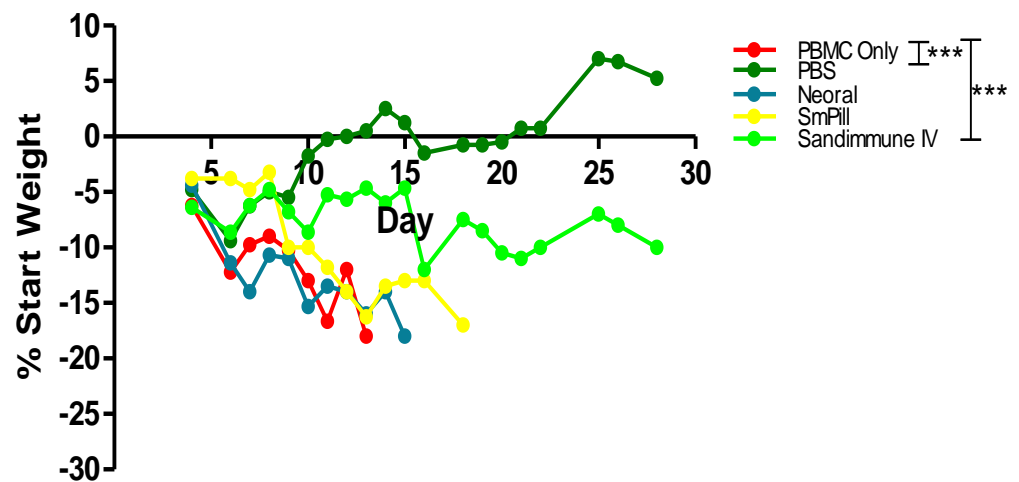
(A)

(B)

Figure 4.4. SmPill® therapy significantly prolonged survival and reduced weight loss in aGvHD mice after dosing (25mg/kg) on day 4, 8 and 12. 8×10^5 human PBMC gram^{-1} were administered to irradiated NSG mice (2.4Gy) on day 0. CsA was delivered by intravenous (Sandimmune® IV) and oral (Neoral®, SmPill®) administration for 3 doses (25mg/kg per dose) every 4 days from day 4. Transplanted mice were monitored every 2 days until day 9 and then every day for the duration of the experiment. n=5 mice for each group. Statistical analysis was carried out using a Mantel-Cox test for the survival curve and unpaired student *t*-test for weight change where * <0.05 and *** <0.001.
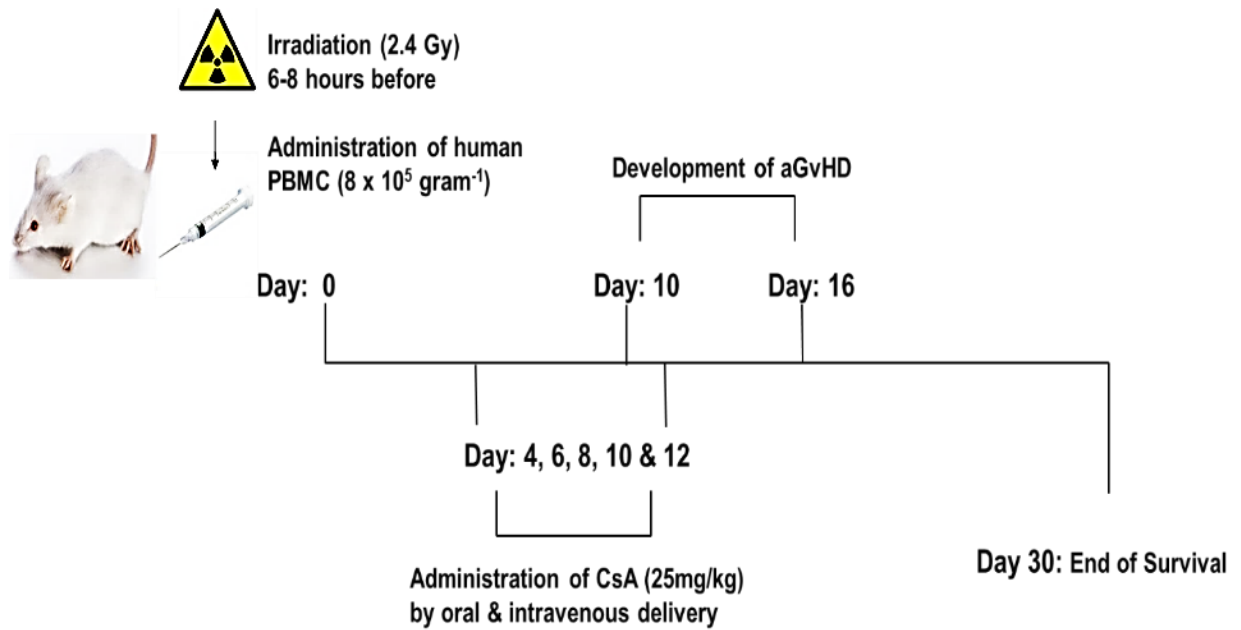
Figure 4.5. Development of a humanised mouse model of aGvHD to assess the performance of SmPill® CsA with more frequent delivery from day 4. NOD-SCID IL-2rγ^{null} (NSG) mice were exposed to a sub-lethal dose of gamma irradiation (2.4 Gy). 8 x 10^5 PBMC gram^{-1} or sterile PBS was then administered intravenously (300 µl) to each mouse via the tail vein on day 0. CsA was delivered intravenously (Sandimmune® IV) and by oral gavage (Neoral®, SmPill®) for 5 doses (25mg/kg per dose) every 2 days from day 4. The SmPill® dosage consisted of 1 immediate and 1 colonic release CsA loaded beads each time. Placebo SmPill® beads without CsA were also delivered every 2 days from day 4. The development of aGvHD was monitored every second day until day 9 and then everyday thereafter by recording weight loss, appearance, posture and activity.

(A)
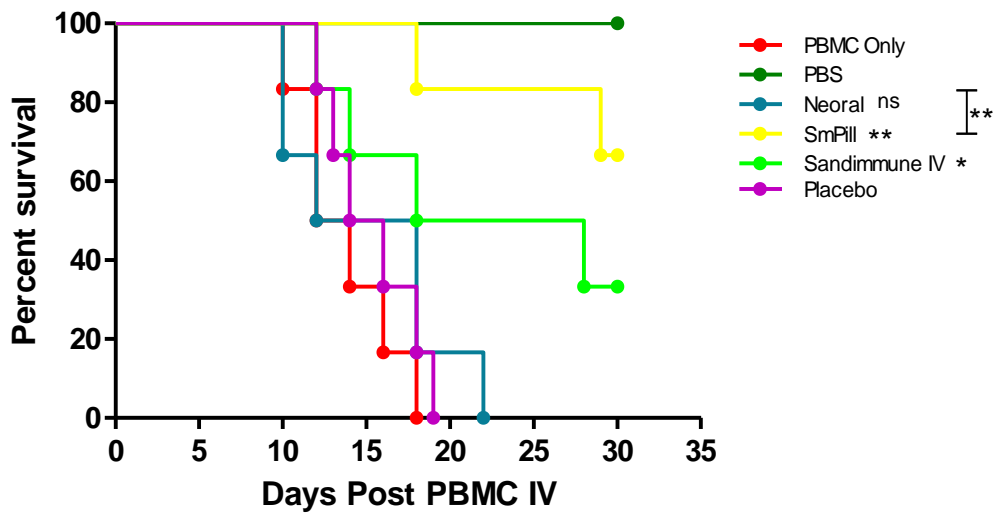
(B)
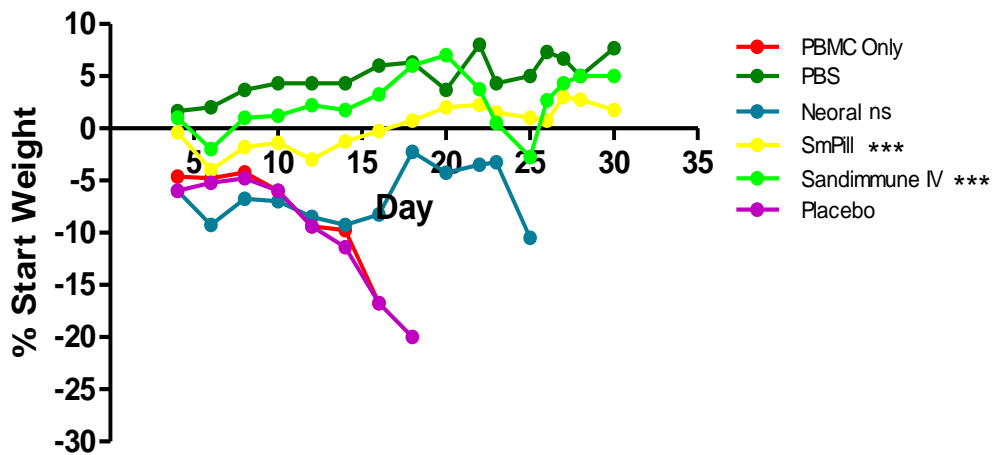
Figure 4.6. SmPill® therapy significantly prolonged survival and reduced weight loss in aGvHD mice after dosing (25mg/kg) on day 4, 6, 8, 10 and 12. 8×10^5 human PBMC gram^{-1} were administered to irradiated NSG mice (2.4Gy) on day 0. CsA was delivered intravenously (Sandimmune® IV) and by oral gavage (Neoral®, SmPill®) for 5 doses (25mg/kg per dose) every 2 days from day 4. Placebo SmPill® beads without CsA were also delivered every 2 days from day 4. Transplanted mice were monitored every 2 days until day 9 and then every day for the duration of the experiment. n=6 mice for each group. Statistical analysis was carried out using a Mantel-Cox test for the survival curve and unpaired student *t*-test for weight change where * <0.05, ** <0.01 and *** <0.001. Stars with no bar are in comparison to the PBMC group.

4.4. SmPILL® DELIVERY OF CsA SIGNIFICANTLY IMPROVED PATHOLOGY IN THE TISSUES OF aGvHD MICE

Acute GvHD is a multi-organ inflammatory disease which mainly affects the liver, lung, colon and small intestine. As shown in figure 4.6, the combination of immediate release and gastrointestinally targetted CsA (via SmPill® beads) significantly prolonged the survival and significantly reduced weight loss associated with aGvHD. It is hypothesised that delivering CsA in a multiformatted way will achieve a more efficacious aGvHD therapy as CsA is distributed systemically and gastrointestinally. Therefore, histological analysis was carried out to compare SmPill® efficacy against the efficacy of Neoral® (GI absorbed CsA) and systemically infused Sandimmune® IV in alleviating aGvHD pathology in these organs. As in the previous experiment, NSG mice were irradiated and received PBMC (8 x 10^5 gram^{-1}) on day 0. CsA therapies were administered as five doses (25 mg/kg per dose) via oral gavage (Neoral®, SmPill®) or intravenously (Sandimmune® IV) in the humanised aGvHD model (Figure 4.5). Day 13 was selected for harvest, as significant aGvHD pathology is evident in the lung, liver, small intestine and colon at this time point (Tobin *et al.* 2013). aGvHD target organs were harvested and placed in formalin for histological analysis.

Tissue sections were stained with H&E and the histological aGvHD score was evaluated for each treatment group according to the criteria described in section 2.10.4 (Tobin *et al*. 2013). Irradiation and PBS administration had no adverse effect on liver architecture of control mice as the tissue appeared normal with no lymphocyte infiltration (l) or endothelialitis (Figure 4.7). After aGvHD development, untreated mice receiving PBMC only had a significant increase in lymphocyte infiltration and endothelialitis particularly in the hepatic ducts when compared to PBS control mice (Figure 4.7 A & B). SmPill® therapy significantly reduced liver pathology with a significant reduction in lymphocyte infiltration

and endothelialitis of hepatic ducts (Figure 4.7 A & B). Neoral® and Sandimmune® IV had very similar effects to SmPill® on alleviating signs of GvHD in the liver. As expected, GvHD mice that received a placebo control displayed similar liver pathology to untreated mice (Figure 4.7 A & B).

Histological analysis of lung sections found that PBS control mice exhibited healthy lung architecture with regular air spaces and no cellular infiltration (Figure 4.7A). However, after PBMC delivery, the characteristics of aGvHD lungs classified as lymphocyte infiltration (l) and thickening of epithelial airways (t) were significantly evident in comparison to PBS controls (Figure 4.7 A & B). Following treatment with SmPill® and Sandimmune® IV, lymphocyte infiltration was substantially lowered with a marked reduction in the airway epithelium thickness (Figure 4.7 A & B). Neoral® therapy did not improve lung pathology in aGvHD mice which resulted in no significant change in histological scoring of aGvHD (Figure 4.7 A & B). GvHD mice that received placebo treatment displayed similar lung pathology to that of untreated mice (Figure 4.7 A & B).

GvHD pathology of the colon was determined by lymhocyte infiltration (l), crypt distortion and ulceration of colonic mucosa (u). Irradiated PBS control mice displayed an intact epithelium with well-defined gland lengths and no lymphocyte infiltration in the mucosa (Figure 4.8 A). SmPill® therapy significantly reduced GvHD pathology in the colon with a significant reduction in lymphocyte infiltration and maintenance of a well-defined epithelium in comparison to untreated or placebo treated mice (Figure 4.8 A & B). The GvHD pathology in the colon of Sandimmune® IV treated mice displayed similar characteristics to SmPill® treated mice, whereas Neoral® therapy did not improve colon pathology significantly (Figure 4.8 A & B).

Histological analysis of small intestine sections showed that GvHD mice exhibited characteristics of aGvHD which included lymphocyte infiltration (l) and villous destruction

or blunting (v) (Figure 4.8 A & B). PBS control mice exhibited normal small intestinal tissue morphology with no accumulation of infiltrating cells. However, PBMC mice that received no CsA therapy displayed frequent villi destruction and blunting accompanied by infiltrating lymphocytes (Figure 4.8 A & B). GvHD mice that received SmPill® and Sandimmune® IV were shown to have similar effects in improving small intestine pathology. Both of which significantly reduced the level of villi destruction and lymphocyte infiltration into the lamina propria (Figure 4.8 A & B). Although less significantly, Neoral® treatment resulted in less villi destruction with reduced signs of infiltrating lymphocytes (Figure 4.8 A & B). Showing similarity to PBMC only mice, the placebo treatment group displayed frequent levels of villi destruction and blunting accompanied by infiltrating lymphocytes (Figure 4.8 A & B).

The histological findings suggest that CsA delivered by SmPill® mediates significant protection in the liver, lung, small intestine and colon as illustrated by less aGvHD pathology in these organs. Expectedly, the systemically absorbed Sandimmune® IV was significantly efficacious in protecting each of the target organs from aGvHD progression. In terms of oral CsA therapy, Neoral® significantly alleviated signs of aGvHD in the liver and small intestine, however, Neoral® was not effective in reducing aGvHD pathology in the lung and colon. This suggests that CsA is not as effectively distributed using Neoral® in comparison to SmPill® or Sandimmune® IV. The data advocates for the requirement for oral CsA therapies to be released in a multiformatted way (SmPill®) for the protection of systemic and GI organs in aGvHD.

(A)

	Liver		Lung	
	100X	**400X**	**100X**	**400X**
PBS (Healthy)				
PBMC (GvHD)				
SmPill®				
Neoral®				
Sandimmune® IV				
Placebo				
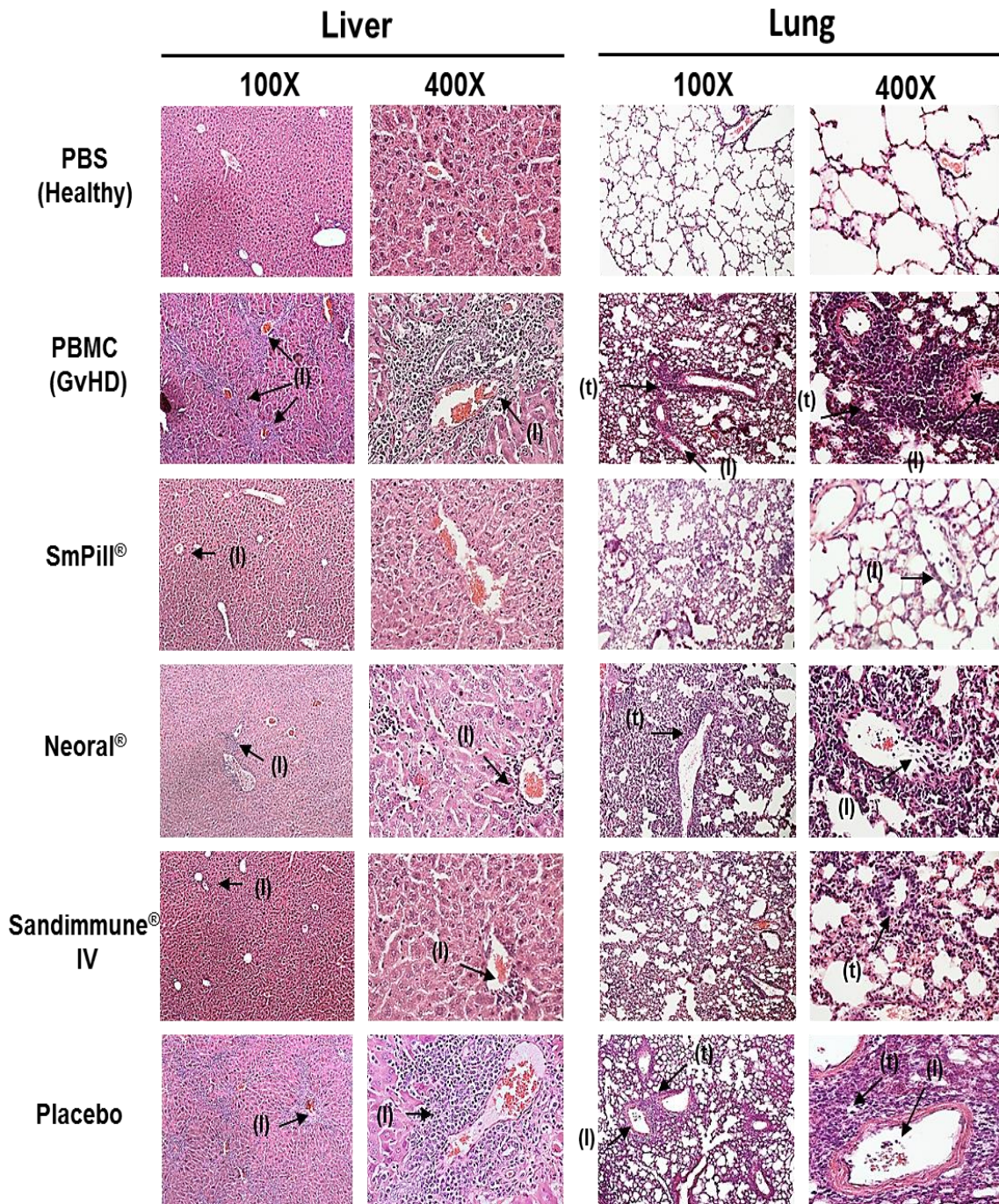
(B)
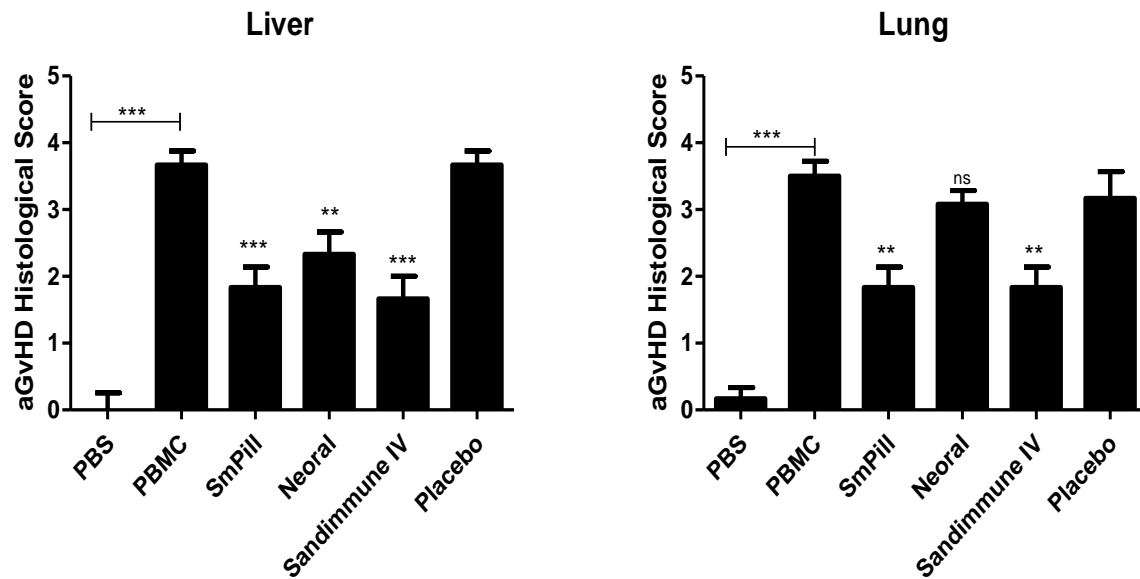
Figure 4.7. SmPill® therapy significantly reduced pathology and lowered infiltration in the liver and lung of aGvHD mice. The aGvHD model was set up exactly as described in figure 4.5. Tissue samples were harvested on day 13, formalin fixed, paraffin embedded and stained with H&E (A). Representative images were analysed for lymphocyte infiltration (l) and thickening of epithelial airways (t) and displayed for each group. Images were captured at 100X and 400X. A well defined aGvHD histological scoring system as described in section 2.10.4 was carried out blinded and used to determine the level of aGvHD development between the groups in the liver and lung (B). n=6 per group (2 PBMC donors). Statistical analysis was carried out using the unpaired student t-test where * <0.05, ** <0.01 and *** <0.001. * with no bar are in comparison to the PBMC group.

(A)

(B)

Figure 4.8. SmPill® therapy significantly decreased occurance of ulceration in the colon and reduced villi destruction in the small intestine of aGvHD mice. The aGvHD model was set up exactly as described in figure 4.5. Tissue samples were harvested on day 13, formalin fixed, paraffin embedded and stained with H&E (A). Representative images were analysed for lymphocyte infiltration (l), villi destruction (v) and ulceration of the colonic mucosa (u) and displayed for each group. Images were captured at 100X and 400X. A well defined aGvHD histological scoring system as described in section 2.10.4 was carried out blinded and used to determine the level of aGvHD development between the groups in the colon and small intestine (B). n=6 per group (2 PBMC donors). Statistical analysis was carried out using the unpaired student *t*-test where * <0.05, ** <0.01 and *** <0.001. Stars with no bar are in comparison to the PBMC group.
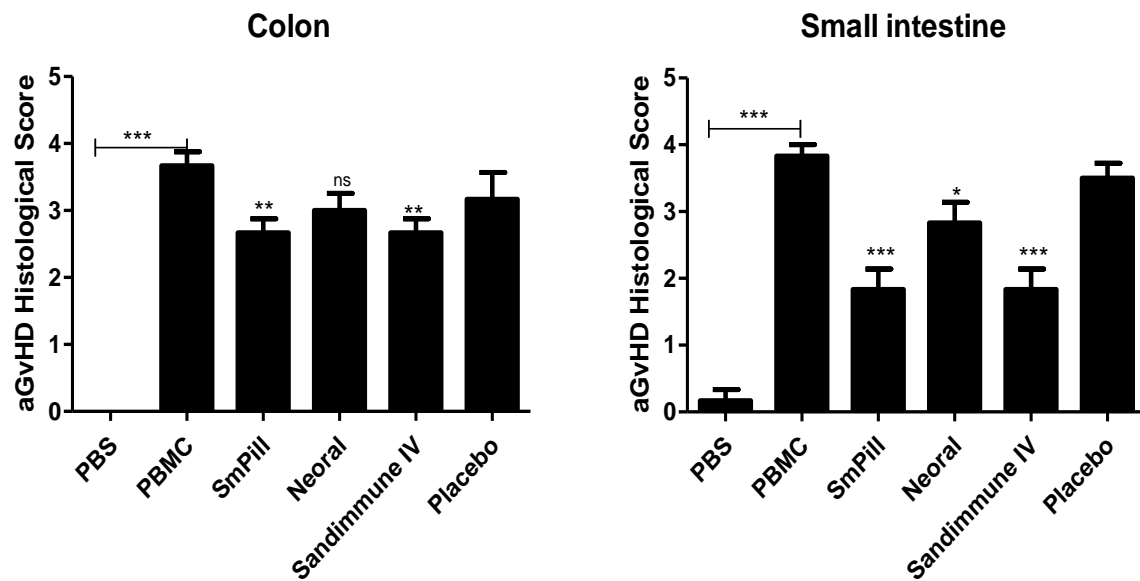
4.5. SMPILL® DELIVERY OF CsA SIGNIFICANTLY REDUCED PROINFLAMMATORY CYTOKINES IN THE GI OF aGvHD MICE

Acute GvHD is a disease driven by donor T cells following the recognition of patient HLA as foreign. The production of proinflammatory cytokines mediated by these effector T cells are a hallmark of aGvHD pathology. There have been numerous studies showing how proinflammatory cytokines such as IL1β, IFNγ, IL2, IL6, IL17 and IL23 contribute to the severity of aGvHD (Antin & Ferrara 1992a; Kappel *et al*. 2009). The GI tract is a principle target organ where pre-conditioning damage leads to the release of inflammatory mediators required for propagating the "cytokine storm" which, in turn, can amplify systemic disease (Antin & Ferrara 1992a). Accordingly, it is hypothesised that reducing the levels of these proinflammatory cytokines in the GI will control cytokine dysregulation and block the "cytokine storm" from heightening the systemic disease. Therefore for this study, the effect of SmPill® therapy on the production of these proinflammatory cytokines specifically in the small intestine and colon (GI tract) of aGvHD mice was analysed. Using the same model set up as described in figure 4.5., small intestine and colon tissue were harvested, snap frozen and homogenates were used to detect the levels of IL1β, IFNγ, IL2, IL17, IL6 and IL23 by ELISA.

In the small intestine, there was a significant increase in the levels of all the cytokines with the exception of IFNγ in the mice that received PBMC on day 0 compared to the PBS control mice (Figure 4.9). SmPill® therapy significantly decreased the levels of all proinflammatory cytokines with the exception of IFNγ (levels were reduced but not significantly) in the small intestine of aGvHD mice in comparison to untreated aGvHD mice (Figure 4.9). In comparison to placebo controls, SmPill® significantly reduced the levels of these cytokines in the small intestine with the exception of IL17. There was a reduction in the levels of IL1β and IL17 with a significant reduction in the levels of IL6 and IL23 in the

small intestine of aGvHD mice following Sandimmune® IV therapy (Figure 4.9). Neoral® reduced the levels of IFNγ, IL2, IL17, IL6 and IL23 with a significant decrease in IL1β detected in the small intestine of aGvHD mice. The placebo treated group had a similar cytokine profile to the untreated aGvHD mice except the levels of IFNγ were enhanced and IL17 was slightly reduced following placebo treatment, however these differences were not significant (Figure 4.9).

IL1β, IFNγ, IL2, IL17, IL6 and IL23 were significantly increased in the colons of aGvHD mice in comparison to PBS controls (Figure 4.10). Similar to the findings in the small intestine, SmPill® therapy significantly decreased the levels of all proinflammatory cytokines examined in the colon of aGvHD mice in comparison to untreated aGvHD mice (Figure 4.10). Sandimmune® IV lowered the levels of IL6 along with significant reduction in the detection of IL1β, IL17 and IL23 in the colon of aGvHD mice (Figure 4.10). Levels of IFNγ and IL2 remained unchanged in the colon of aGvHD mice that received Sandimmune® IV therapy. IL6 and IL23 were reduced by Neoral® therapy with a significant reduction in IL1β detected in the colon of aGvHD mice (Figure 4.10). However, levels of IFNγ, IL2 and IL17 were not reduced by Neoral®. Following placebo treatment, aGvHD mice had similar high levels of IFNγ and IL2 with slight decreases in IL1β, IL6, IL17 and IL23 in comparison to non treated GvHD mice. Moreover, there was no significant reductions in cytokine levels following SmPill® treatment in comparison to placebo treated controls.

This data indicated that SmPill® was a more efficient therapy in delivering CsA to the GI as it was better at reducing the levels of cytokines associated with aGvHD in the small intestine and colon compared to Neoral® or Sandimmune® IV. This is reflective of the histological findings in figure 4.8 B, where SmPill® and Sandimmune® IV were protective in the small intestine and colon but Neoral® failed to significantly reduce tissue damage.

Small Intestine

Figure 4.9. SmPill® CsA significantly reduced proinflammatory cytokines detected in the small intestine of aGvHD mice. The aGvHD model was set up exactly as described in figure 4.5. Tissue samples were harvested on day 13, immediately snap frozen and stored at -80°C. Homogenates were prepared and ELISA was used to detect proinflammatory cytokines (IL1β, IFNγ, IL2, IL17, IL6 and IL23). Concentration of cytokine is expressed as pg cytokine per mg tissue protein (normalised by bradford protein assay). n= 6 per group. Statistical analysis was carried out using unpaired student *t*-test where * <0.05, **<0.01 and *** <0.00

Colon
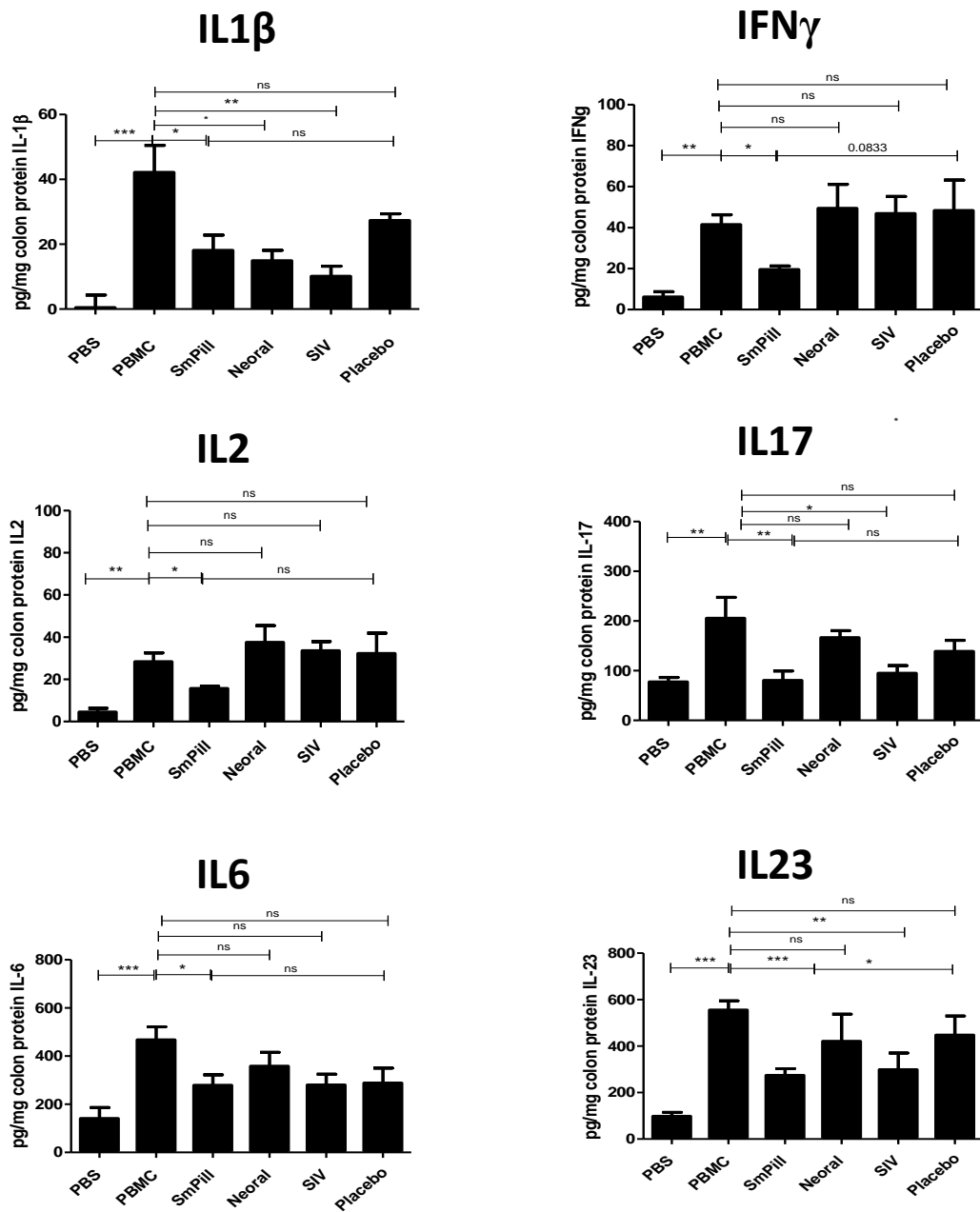
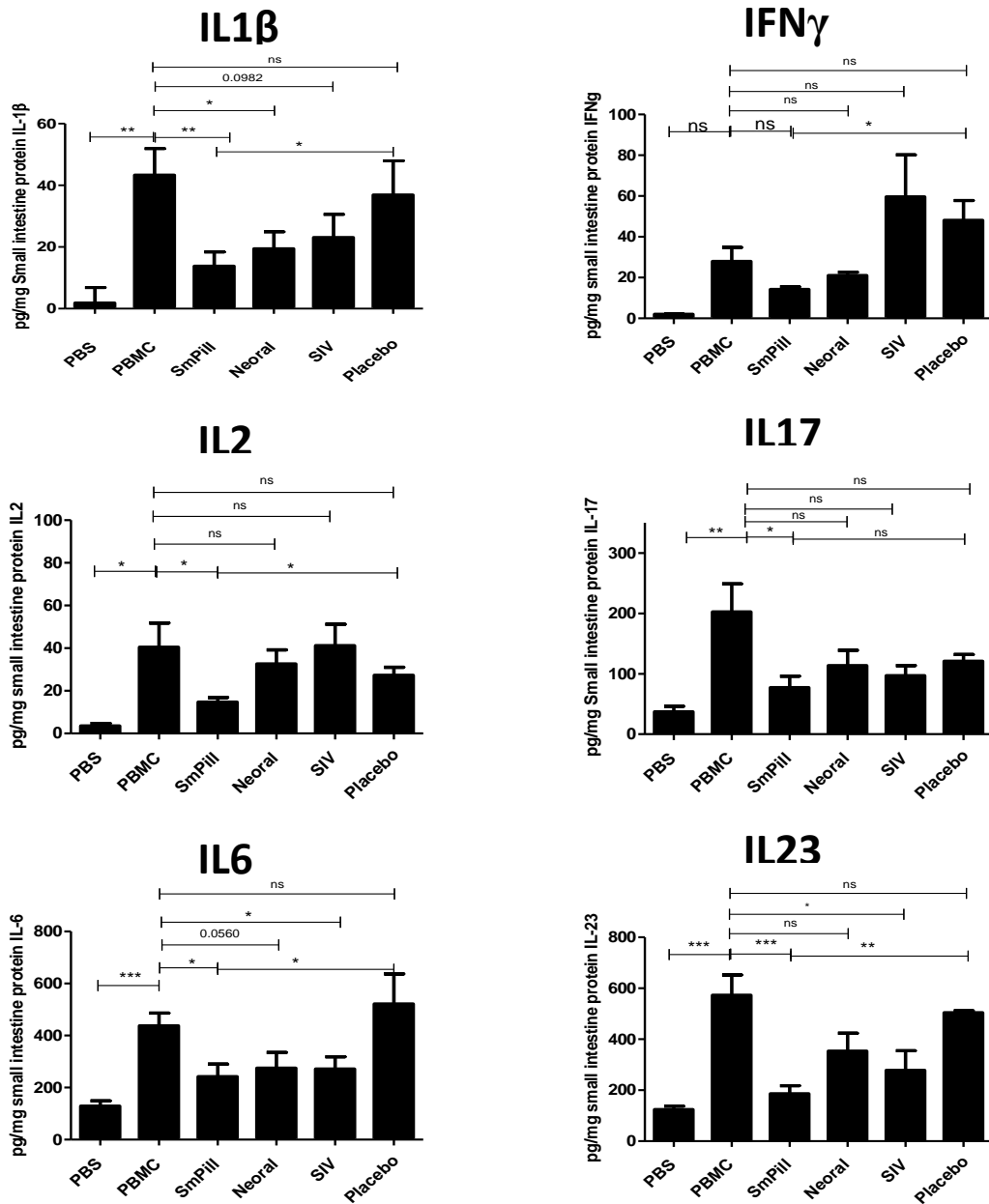**Figure 4.10. SmPill® CsA significantly reduced proinflammatory cytokines detected in the colon of aGvHD mice.** The aGvHD model was set up exactly as described in figure 4.5. Tissue samples were harvested on day 13, immediately snap frozen and stored at -80°C. Homogenates were prepared and ELISA was used to detect proinflammatory cytokines (IL1β, IFNγ, IL2, IL17, IL6 and IL23). Concentration of cytokine is expressed as pg cytokine per mg tissue protein (normalised by bradford protein assay). n=6 per group. Statistical analysis was carried out using unpaired student *t*-test where * <0.05, ** <0.01 and *** <0.001.

4.6. SMPILL® THERAPY SIGNIFICANTLY REDUCED TNFα PRODUCING T CELLS IN THE SPLEEN, LIVER AND LUNG OF aGvHD MICE

TNFα has been characterised as having a key role in the initiation and maintenance of aGvHD (Ferrara *et al*. 2009; Korngold *et al*. 2003). It is involved in activation and proliferation pathways of T cells, the main cellular effectors in aGvHD, and has direct effects leading to apoptosis of aGvHD tissues (Antin & Ferrara 1992; Stuber *et al.* 1999). Therefore, the effect that SmPill® therapy has on the development of human TNFα producing CD4$^+$ and CD8$^+$ T cells during aGvHD was analysed in the spleen, liver and lung of aGvHD mice using intracellular flow cytometry. The efficacy of Neoral® and Sandimmune® IV in reducing the numbers of TNFα producing CD4$^+$ and CD8$^+$ T cells was also analysed as a comparison. PBS and placebo controls were also included in the study.

On day 13 after PBMC administration, human CD4$^+$ and CD8$^+$ T cells were examined in the spleen from all groups of aGvHD mice. Using the gating strategy as described in figure 4.11, the potential for TNFα production was analysed in these cells by intracellular flow cytometry. As expected, there was a significant increase in the number of CD4$^+$ and CD8$^+$ T cells producing TNFα in the spleens of aGvHD mice that received no therapy (Figure 4.12). SmPill® therapy was most efficacious and significantly decreased the number of CD4$^+$ and CD8$^+$ T cells producing TNFα in the spleen of aGvHD mice in comparison to untreated aGvHD mice (Figure 4.12). There was a reduction in the numbers of CD4$^+$ T cells producing TNFα with a significant reduction in the numbers of CD8$^+$ T cells producing TNFα in the spleen of aGvHD mice following Sandimmune® IV therapy (Figure 4.12). Neoral® therapy reduced the number of CD4$^+$ and CD8$^+$ T cells producing TNFα in the spleen of aGvHD mice, however not significantly (Figure 4.12). The number of TNFα producing CD4$^+$ and CD8$^+$ T cells recovered in the spleen from the placebo treated group

were similar to that of the untreated aGvHD mice where no significant differences were detected (Figure 4.12).

In addition, the total number of TNFα producing CD4$^+$ and CD8$^+$ T cells in the liver was investigated. Figure 4.13 shows that significantly increased numbers of CD4$^+$ and CD8$^+$ liver T cells from placebo treated or untreated aGvHD mice produced TNFα. Here, SmPill® and Neoral® were more efficacious than Sandimmune® IV as the total number of TNFα producing CD4$^+$ T cells were significantly reduced by these therapies but not Sandimmune® IV (Figure 4.13). All CsA therapies reduced the number of CD8$^+$ TNFα$^+$ T cells, however not significantly (Figure 4.13).

Similarly, in the lung, there was a significant increase in the number of CD4$^+$ and CD8$^+$ T cells producing TNFα from placebo treated or untreated aGvHD mice in comparison to healthy PBS controls (Figure 4.14). All CsA therapies reduced the number of TNFα producing CD4$^+$ and CD8$^+$ T cells however, Sandimmune® IV was most effective as it significantly reduced CD4$^+$ TNFα$^+$ T cells. This data suggests that SmPill® and Neoral® offer similar protection in the lung in this context.

The complete dataset suggests that SmPill® was a more efficacious oral CsA therapy than Neoral® as it significantly reduced TNFa production by CD4$^+$ T cells in the systemic organs (spleen and liver) in a similar, if not better, manner to Sandimmune® IV therapy. It is also likely that the significant reduction in pathology in the liver and lung observed in figure 4.7 could be as a result of the reduction in TNFα producing T cells by SmPill® therapy in these organs.
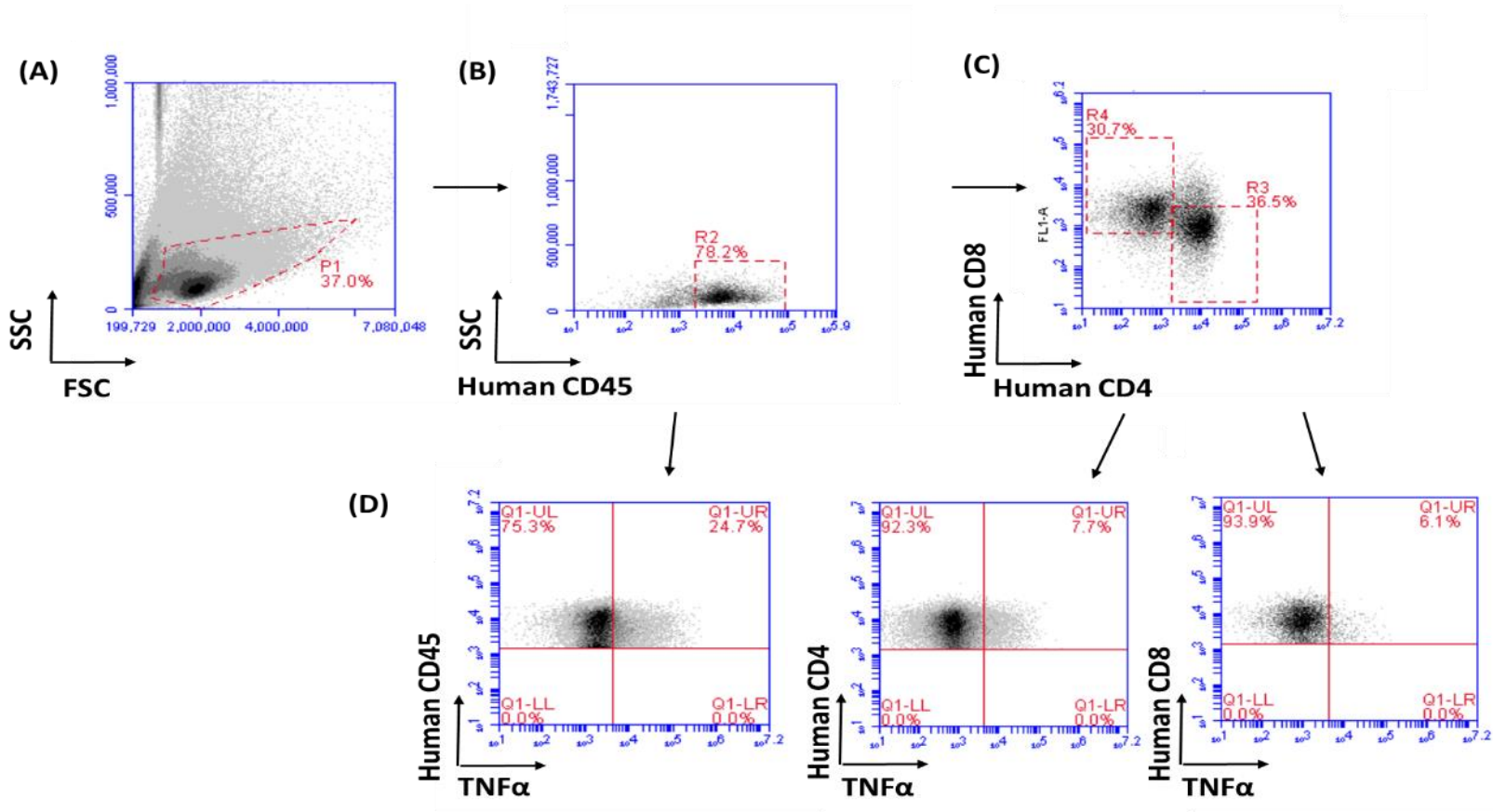
Figure 4.11. Representative example of gating strategy used to identify human CD45⁺ CD4⁺ and CD8⁺ T cells producing TNFα. (A) Illustrates the gated lymphocyte population from SSC against FSC plot, (B) represents the gating position for human CD45⁺ (PerCP) expression within the lymphocyte population, (C) illustrates the gating position for CD4 (APC) and CD8 (FITC) expression within the CD45⁺ population and (D) represents the gating position for the total CD45⁺, CD45⁺ CD4⁺ and CD45⁺ CD8⁺ T cells producing TNFα. All gating positions were determined using matching isotype controls

Spleen

Figure 4.12. SmPill® therapy significantly reduced the total number of TNFα producing CD4+ and CD8+ T cells in the spleen of aGvHD mice. The aGvHD model was set up exactly as described in figure 4.5. Cells were recovered on day 13, stimulated with 100 ng/ml PMA, 1 µg/ml iononmycin and 1X Brefeldin A for 4 h and analysed by intracellular flow cytometry. Graphical representation of the total number of human TNFα producing CD45+ CD4+ and CD8+ T cells recovered in the spleen. CD4+ and CD8+ T cell TNFα production is represented in (A) and (B) respectively. The total number of human cells was assessed using counting beads during flow cytometry. n=6 per group (2 PBMC donors). Statistical analysis was carried out using unpaired student *t*-test where * <0.05, ** <0.01 and *** <0.001.
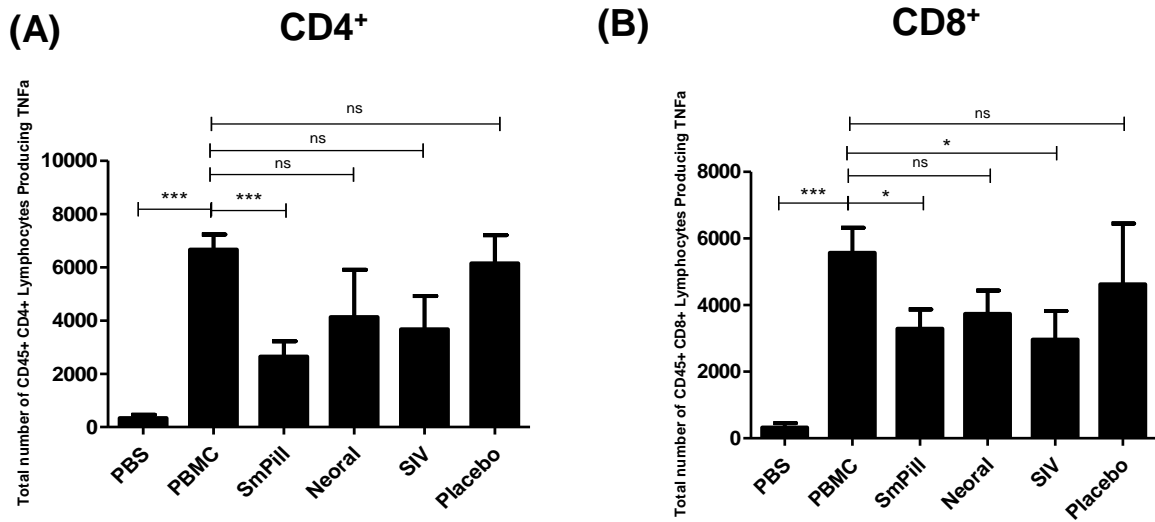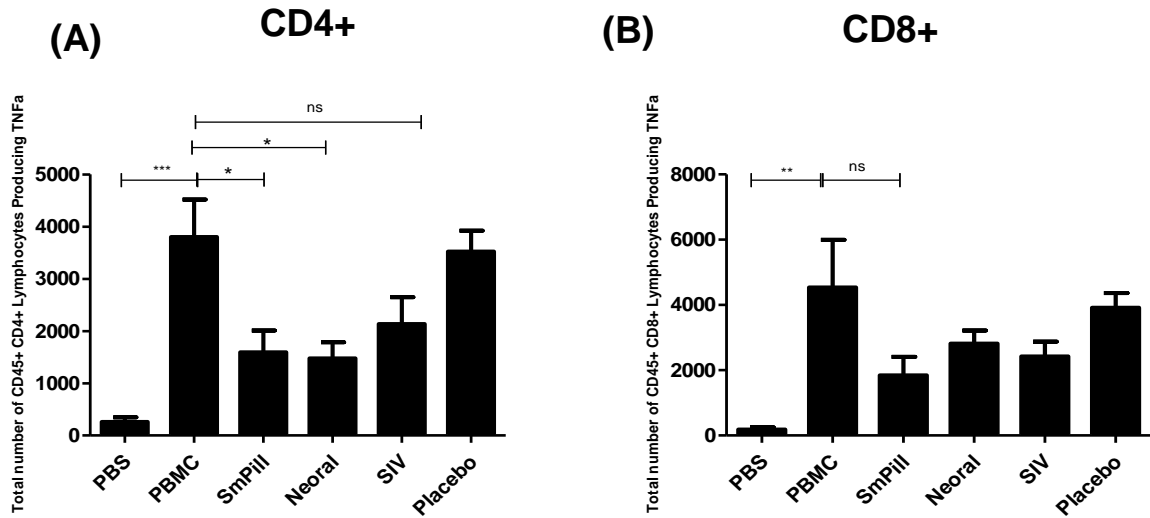
Liver

Figure 4.13. SmPill® therapy significantly reduced the total number of TNFα producing CD4+ T cells in the liver of aGvHD mice. As described in figure 4.5, the aGvHD model was set up. Cells were recovered on day 13, stimulated with 100 ng/ml PMA, 1 µg/ml iononmycin and 1X Brefeldin A for 4 h and analysed by intracellular flow cytometry. Graphical representation of the total number of human TNFα producing CD45+ CD4+ and CD8+ T cells recovered in the liver. CD4+ and CD8+ T cell TNFα production is represented in (A) and (B) respectively. The total number of human cells was assessed using counting beads during flow cytometry. n=6 per group (2 PBMC donors). Statistical analysis was carried out using unpaired student *t*-test where * <0.05, ** <0.01 and *** <0.001.

Lung

(A) CD4⁺

(B) CD8⁺
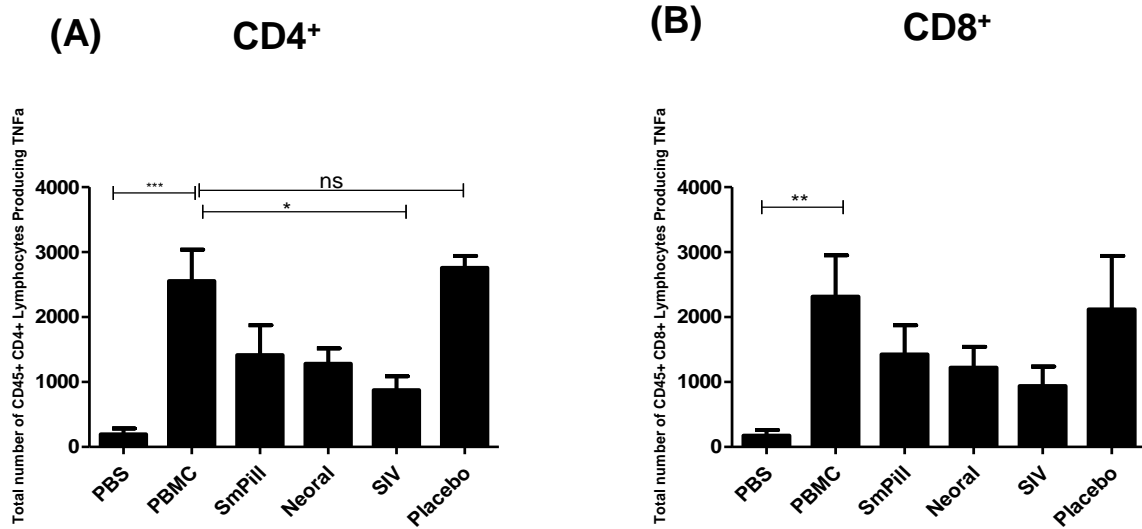
Figure 4.14. Sandimmune® IV was most efficacious in treating the lung as it significantly reduced the total number of TNFα producing CD45⁺ cells in aGvHD mice. Following development of aGvHD, as detailed in figure 4.5. Cells were recovered on day 13, stimulated with 100 ng/ml PMA, 1 µg/ml iononmycin and 1X Brefeldin A for 4 h and analysed by intracellular flow cytometry. Graphical representation of the total number of human TNFα producing CD45⁺ CD4⁺ and CD8⁺ T cells recovered in the lung. CD4⁺ and CD8⁺ T cell TNFα production is represented in (A) and (B) respectively. The total number of human cells was assessed using counting beads during flow cytometry. n=6 per group (2 PBMC donors). Statistical analysis was carried out using unpaired student t-test where * <0.05, ** <0.01 and *** <0.001.

4.7. SUMMARY I

This section presents the use of a robust and clinically relevant model of aGvHD for optimising the delivery schedule of the novel CsA therapy, SmPill®. Due to initial post-irradiation weight loss, early dosing of oral therapies from day 1 proved to be ineffective in this model of aGvHD (figure 4.2). Furthermore, the optimal SmPill® bead size was determined to be within the range of 1-1.25mm and used at this size for all other studies where there were no cases of tracheal damage as a result of drug administration via gavage. Day 4 represented an adequate start day for CsA dosing (Figure 4.4) and the administration of 5 doses (25 mg/kg per dose) of SmPill® on day 4, 6, 8, 10 and 12 was shown to be most effective at significantly prolonging survival and reducing weight loss during aGvHD (Figure 4.6). Accordingly, this dosing schedule was deemed optimal for efficacy of SmPill® delivery and was used for further investigations of SmPill® performance throughout this chapter.

Using this optimised dosing schedule of SmPill® in this humanised mouse model of aGvHD, the performance of SmPill® was assessed against another oral (Neoral®) and intravenous (Sandimmune® IV) CsA therapy using appropriate controls. As expected, Sandimmune® IV provided significant protection to all aGvHD target organs systemically or in the GI (Figure 4.7 and 4.8). SmPill® was a more effective oral CsA therapy than Neoral® as it was significantly effective in reducing aGvHD pathology in all the target organs including the lung and colon (Figure 4.7 B and 4.8 B). This suggests that oral CsA is more effectively distributed using SmPill® rather than Neoral® as it mediates protection of systemic and GI organs in aGvHD comparable to that of Sandimmune® IV. This protection from SmPill® is likely mediated through the modulated bioavailability systemically in addition to a more sustained GI bioavailability in comparison to Neoral®.

Looking more closely at GI protection, the efficacy of these CsA therapies in reducing proinflammatory cytokines involved in aGvHD severity (IL1β, IFNγ, IL2, IL6, IL17 and IL23) was analysed. SmPill® was more efficacious in significantly reducing the levels of each of these cytokines associated with aGvHD in the small intestine and colon compared to Neoral® or Sandimmune® IV. This suggests SmPill® was more efficient in delivering CsA to the GI resulting in enhanced protection (Figure 4.9 and 4.10).

In terms of systemic protection, the effect of these CsA therapies on the development of human TNFα producing CD4$^+$ and CD8$^+$ T cells during aGvHD was analysed in the spleen, liver and lung of aGvHD mice. SmPill® was shown to be a more efficacious oral CsA therapy than Neoral® as it significantly reduced TNFa producting CD4$^+$ T cells in the systemic organs (spleen and liver) in a similar, and some cases better, manner than Sandimmune® IV therapy (Figure 4.12 and 4.13). However, SmPill® and Neoral® exhibit similar efficacy in the lung (Figure 4.14).

Collectively, this data suggests that SmPill® provides an enhanced oral CsA therapy in comparison to Neoral® whereby systemic and GI protection is maintained during aGvHD. This enhancement may be a result of decreased IL1β, IFNγ, IL2, IL6, IL17 and IL23 in the GI and reduced TNFα production systemically.

4.8. SPECIFIC COMBINATIONS OF SᴍPILL® CsA BEAD FORMULATION SIGNIFICANTLY PROLONGED SURVIVAL AND REDUCED WEIGHT LOSS IN ᴀGᴠHD

Throughout this chapter, 5 doses of SmPill® (25 mg/kg per dose) from day 4 was shown to be effective in prolonging survival and reducing the pathology associated with aGvHD in this humanised model. SmPill® was delivered in the form of two beads each time, 1 bead that released CsA immediately and 1 bead where CsA release was sustained in order to target the colon. To investigate the potential of these beads further, different combinations were delivered to aGvHD mice to explore the systemic and GI effects mediated by these beads.

As before, NSG mice were irradiated (2.4 Gy) and human PBMC (8 x 10^5 gram^{-1}) were injected via the tail vein (Figure 4.15). Control groups were included by administering sterile PBS to irradiated NSG mice. For this study, CsA was delivered intravenously (Sandimmune® IV), and by oral gavage (Neoral® and SmPill®) for 5 doses (25mg/kg per dose) from day 4 (Figure 4.15). Different SmPill® CsA formulation combinations based specifically on either immediate release of CsA or colonic release were compared to the efficacy of 1 immediate and 1 colonic release combination used in all previous experiments (Figure 4.6 – 4.14). SmPill® formulation combinations were assigned to groups of mice and delivered by gavage as outlined in figure 4.15 B. Transplanted mice were monitored closely and the survival and weight loss of each mouse was recorded (Figure 4.16).

Acute GvHD mice who received no therapy significantly lost weight and succumbed to aGvHD with all mice sacrificed from this group by day 14 (Figure 4.16 A). Figure 4.16 shows that all healthy PBS mice survived and maintained a healthy weight above their start weight for the duration of the experiment. In consistence with all previous studies, Sandimmune® IV significantly prolonged survival with a median survival time (MST) of 24

days, however there was no significant differences when compared to SmPill® (1 immediate + 1 colonic) or Neoral® (Figure 4.16 A). While Sandimmune® IV significantly reduced weight loss in aGvHD mice, SmPill (1 immediate + 1 colonic) was significantly better in doing so (Figure 4.16 B). Neoral® therapy prolonged survival with an MST of 19 days and reduced weight loss in aGvHD mice, although SmPill® (1 immediate + 1 colonic) was significantly better with an MST of 29 days.

There were differences between the combinations of SmPill® therapy. 1 immediate release bead significantly prolonged the survival of aGvHD mice to day 19 (MST) and significantly reduced weight loss in comparison to untreated aGvHD mice (Figure 4.16). 1 colonic bead significantly prolonged the survival of aGvHD mice to day 25 (MST) and reduced weight loss while 2 colonic beads reduced weight loss in aGvHD mice however, only prolonged survival to day 15.5 (MST) (Figure 4.16). SmPill® in the form of 1 immediate and 1 colonic bead, was shown to significantly reduce weight loss and significantly prolong survival in aGvHD mice with up to 60% survival at the time of experiment completion (29 days MST) (Figure 4.16) just as it was the case in figure 4.6. This suggests that the 1 immediate and 1 colonic bead is the most efficacious SmPill® formulation in significantly prolonging the survival and significantly reducing the weight loss experienced by aGvHD mice.

(A)
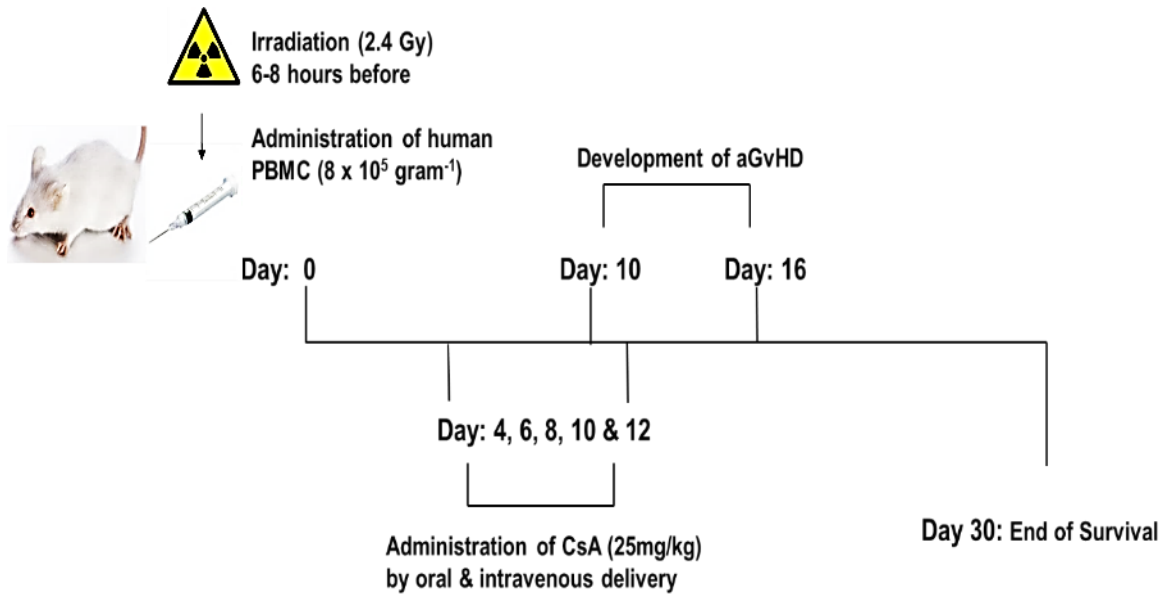
(B)

SmPill® CsA loaded Beads as follows;
1 immediate release (1 IR)
1 colonic release (1C)
2 colonic release (2C)
1 immediate + 1 colonic release (1+1)

Figure 4.15. Assessments of multiple SmPill® CsA formulation combinations in the humanised mouse model of aGvHD. NOD-SCID IL-2rγ^{null} (NSG) mice were exposed to a sub-lethal dose of gamma irradiation (2.4 Gy). 8 x 10^5 PBMC gram^{-1} or sterile PBS was then administered intravenously (300 µl) to each mouse via the tail vein on day 0. CsA was delivered intravenously (Sandimmune® IV) and by oral gavage (Neoral®, SmPill®) for 5 doses (25mg/kg per dose) every 2 days from day 4. Different SmPill® CsA formulation combinations were assigned and delivered by gavage to groups of mice as outlined in (B). n=12 per group (2 PBMC donors). The development of aGvHD was monitored every second day until day 9 and then everyday thereafter by recording weight loss, appearance, posture and activity.

(A)

(B)
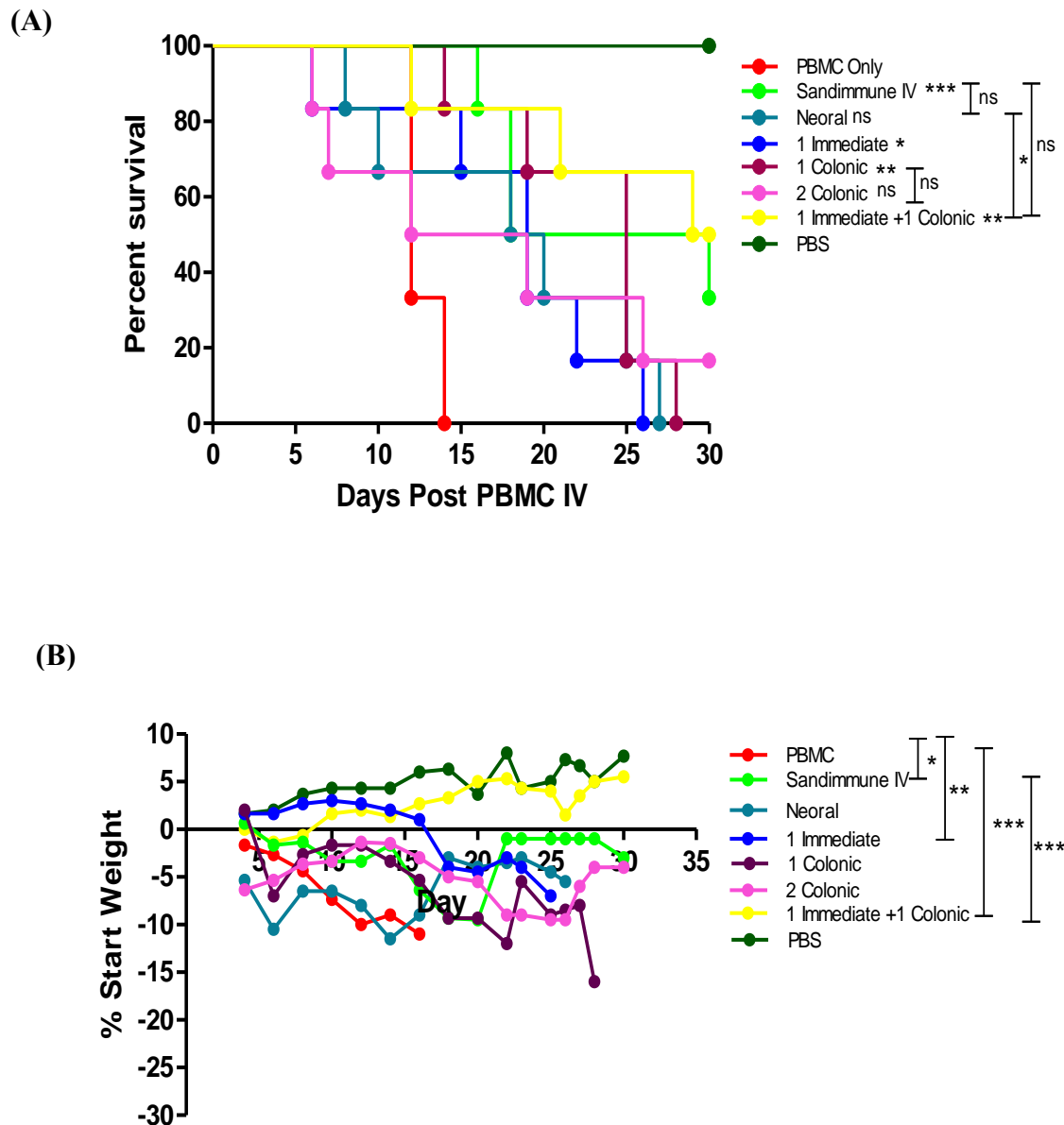
Figure 4.16. SmPill® CsA significantly prolonged survival and reduced weight loss in aGvHD mice after doses (25mg/kg) on day 4, 6, 8, 10 and 12. 8 x 10⁵ human PBMC gram⁻¹ were administered to irradiated NSG mice (2.4Gy) on day 0. CsA was delivered intravenously (Sandimmune® IV) and by oral gavage (Neoral®, SmPill®) for 5 doses (25mg/kg per dose) every 2 days from day 4. Different SmPill® CsA formulation combinations were assigned to groups of mice (n=6 per group for survival). Transplanted mice were monitored every 2 days until day 9 and then every day for the duration of the experiment. n=6 mice for each group. Statistical analysis was carried out using a Mantel-Cox test for the survival curve and unpaired student *t*-test for weight change where * <0.05, ** <0.01 and *** <0.001. * with no bar are in comparison to the PBMC group.

4.9. SᴍPɪʟʟ® CsA FORMULATIONS IMPROVED PATHOLOGY AND REDUCED APOPTOSIS IN THE TISSUES OF ᴀGᴠHD MICE IN A TARGETED MANNER

The main target organs involved in the pathology of this humanised mouse model of aGvHD include the liver, lung, colon and small intestine. As shown in figure 4.16 A and consistent with previous findings (Figure 4.6 A), SmPill® in the form of 1 immediate and 1 colonic release bead significantly prolonged the survival and significantly reduced weight loss associated with aGvHD. However, there were changes in efficacy when different combinations of SmPill® which targeted systemic (1 immediate) or GI (1 or 2 colonic) tissues were used. Therefore to probe further, histological analysis was carried out on systemic and GI GvHD tissues to compare GvHD pathology across all SmPill® combinations and appropriate comparators, Neoral® and Sandimmune® IV. As in the previous studies, NSG mice were irradiated and received PBMC (8×10^5 gram^{-1}) on day 0. CsA therapies were administered as five doses of CsA (25 mg/kg per dose) from day 4 via oral gavage (Neoral®, SmPill®) or intravenously (Sandimmune® IV) in the humanised aGvHD model (Figure 4.15). On day 13, where there is significant aGvHD pathology evident, the lung, liver, small intestine and colon were harvested and placed in formalin for histological analysis.

Tissue sections were stained with H&E and the histological aGvHD score was evaluated in a blinded manner for each treatment group, just as in figure 4.7 and 4.8, according to the criteria described in section 2.10.4 (Tobin *et al*. 2013). Irradiation and PBS administration had no negative effect on liver architecture of control mice as the tissue appeared normal with no lymphocyte infiltration (l) or endothelialitis (Figure 4.17). After aGvHD development, untreated mice had a significant increase in lymphocyte infiltration and endothelialitis particularly in the hepatic ducts when compared to PBS control mice (Figure 4.17 A & B). Neoral® reduced the infiltration of cells but endothelialitis remained

visible in the liver sections of aGvHD mice. Sandimmune® IV significantly reduced endothelialitis of hepatic ducts with lowered cell infiltration visible (Figure 4.17 A & B). All SmPill® therapies, with the exception of 1 immediate bead alone, significantly reduced liver pathology with a significant reduction in lymphocyte infiltration and endothelialitis of hepatic ducts (Figure 4.17 A & B). The most significant therapeutic was the 1 immediate and 1 colonic bead combination.

Histological analysis of lung sections found that PBS control mice exhibited healthy lung architecture with regular air spaces and no cellular infiltration (Figure 4.17A). However, after PBMC delivery, the characteristics of aGvHD lungs classified as lymphocyte infiltration (l) and thickening of epithelial airways (t) were significantly evident in comparison to PBS control (Figure 4.17 A & B). Following treatment with Sandimmune® IV, lymphocyte infiltration was significantly lowered with a significant reduction in the airway epithelium thickness (Figure 4.17 A & B). Neoral® therapy did not significantly improve lung pathology in aGvHD mice which resulted in no significant change in histological scoring of aGvHD (Figure 4.17 A & B). In contrast to the observations made in the liver, SmPill® therapies containing 1 immediate bead significantly reduced the thickening of epithelial airways with less lymphocyte infiltration than untreated aGvHD in comparison to both colonic bead therapies where there was still evidence of lymphocyte infiltration and thickening of epithelial airways (Figure 4.17 A & B).

Histological analysis of small intestine sections showed that GvHD mice exhibited characteristics of aGvHD which included lymphocyte infiltration (l) and villous destruction or blunting (v) (Figure 4.18 A & B). PBS control mice exhibited normal small intestinal tissue morphology with no accumulation of infiltrating cells. However, PBMC mice that received no CsA therapy displayed frequent villi destruction and blunting accompanied by infiltrating lymphocytes (Figure 4.18 A & B). Sandimmune® IV was most significant at

reducing the level of villi destruction and lymphocyte infiltration into the lamina propria than the other therapies (Figure 4.18 A & B). Less significantly, Neoral® treatment also resulted in less villi destruction with reduced signs of infiltrating lymphocytes (Figure 4.18 A & B). As Neoral® is mainly absorbed in the upper small intestine, it is likely that the small intestine is exposed to a reducing gradient of CsA from the stomach to the ileum. All SmPill® therapies, with the exception of 1 colonic bead alone, significantly reduced villi destruction with a significant reduction in lymphocyte infiltration (Figure 4.18 A & B).

GvHD pathology of the colon was determined by lymphocyte infiltration (l), crypt distortion and ulceration of colonic mucosa (u). Irradiated PBS control mice displayed an intact epithelium with well-defined gland lengths and no lymphocyte infiltration in the mucosa (Figure 4.18 A). The GvHD pathology in the colon of Sandimmune® IV treated mice were significantly healthier than untreated mice, whereas Neoral® therapy did not improve colon pathology significantly (Figure 4.18 A & B). The SmPill® therapies containing 1 immediate and 1 colonic or 2 colonic beads significantly reduced GvHD pathology in the colon with a significant reduction in lymphocyte infiltration and maintenance of a well-defined epithelium in comparison to untreated aGvHD mice (Figure 4.18 A & B). However, 1 colonic bead alone was less significant in reducing ulceration in the colon mucosa and 1 immediate bead alone was not significant at all in reducing this pathology associated with colon aGvHD (Figure 4.18 A&B).

This data displays evidence of how targeted CsA delivery differentially protects systemic and GI aGvHD tissues. The combination of 1 immediate + 1 colonic SmPill® formulation was shown to give the most significant protection in the liver and lung and protection in these systemic tissues is reduced when CsA is targeted directly to the GI only (1 or 2 colonic). Similarly, in the small intestine or colon, the 1 immediate + 1 colonic SmPill® formulation was shown to give significant protection whereas CsA delivered

systemically only (1 immediate) was not protective in the GI. This shows that in order to provide protection in systemic and GI tissues simultaneously, SmPill® formulated CsA must be delivered both systemically and to the GI.

Given that the target organs in aGvHD mice displayed features of severe inflammation with obvious signs of damage to tissue architecture, the potential for apoptotic tissue damage was analysed. While apoptotic damage can be found in each of the target organs, the purpose of this experiment was to directly compare protection obtained, systemically or GI locally, as a result of targeting CsA treatment in this manner. As the small intestine and colon both exhibit similar features of apoptosis (Washington & Jagasia 2009), the small intestine was selected to compare against the lung.

To detect apoptosis in the lung and small intestine, a commercially available TUNEL assay kit was used, as described in section 2.10.3. The TUNEL assay detects DNA fragmentation as a result of apoptosis and emits a green fluorescent light as shown in (Figure 4.19). DAPI was used as a nuclear stain and it emits blue fluorescent light. Positive controls for apoptotic damage were set up using DNase treated non GvHD tissue (Figure 4.19). The capacity for SmPill® and other CsA therapies, Neoral® and Sandimmune® IV to alleviate apoptotic damage associated with aGvHD was analysed.

The TUNEL assay revealed that lung sections from untreated aGvHD mice had detectable apoptotic damage (Figure 4.19). Apoptosis was not detected in lung sections from PBS control mice. Sandimmune® IV therapy alleviated apoptotic damage in the lungs of aGvHD mice. Consistent with the H&E histological analysis, Neoral® had no efficacy in reducing the apoptotic damage in the lungs of aGvHD mice. The 1 or 2 colonic bead SmPill® therapies also had little efficacy in reducing damage caused by apoptosis in the lungs of aGvHD mice. However, the 1 immediate and the 1 immediate + 1 colonic bead SmPill® therapies reduced apoptosis in aGvHD lung tissue (Figure 4.19). Importantly, these

observations are consistent with H&E histological findings and highlight that with targeted GI delivery of CsA (1 or 2 colonic beads), systemic protection in the lung is lost (Figure 4.17).

Apoptotic damage was also observed in the small intestine of aGvHD mice but not in PBS control mice (Figure 4.19). Sandimmune® IV therapy was shown to reduce but not completely alleviate apoptotic damage in the small intestine of aGvHD mice (Figure 4.19). Similar to the H&E histological analysis, Neoral® had some efficacy in reducing the apoptotic damage in the small intestine of aGvHD mice (Figure 4.19). The 1 immediate and 1 colonic bead SmPill® therapies had similar efficacy as Neoral® in reducing damage caused by apoptosis in the small intestine of aGvHD mice. However, the 2 colonic and the 1 immediate + 1 colonic bead SmPill® therapies were most efficacious in reducing the apoptosis detectable in aGvHD small intestine (Figure 4.19). These data are similar to the H&E histological findings and highlight that with systemic delivery of CsA (1 immediate bead), GI protection in the small intestine is lost (Figure 4.18). These findings further highlight the importance of optimal CsA delivery for the alleviation of pathology in a multi system disease like aGvHD.

(A)

	Liver		Lung	
	100X	**400X**	**100X**	**400X**
PBS (Healthy)				
PBMC (GvHD)		(l)		(l) (t)
1 Immediate		(t)		(l)
1 Colonic		(l)		(t)
2 Colonic		(l)		(t)
1 Immediate + 1 Colonic		(l)		(l)
Neoral®		(l)		(l)
Sandimmune® IV		(l)		(t)

156
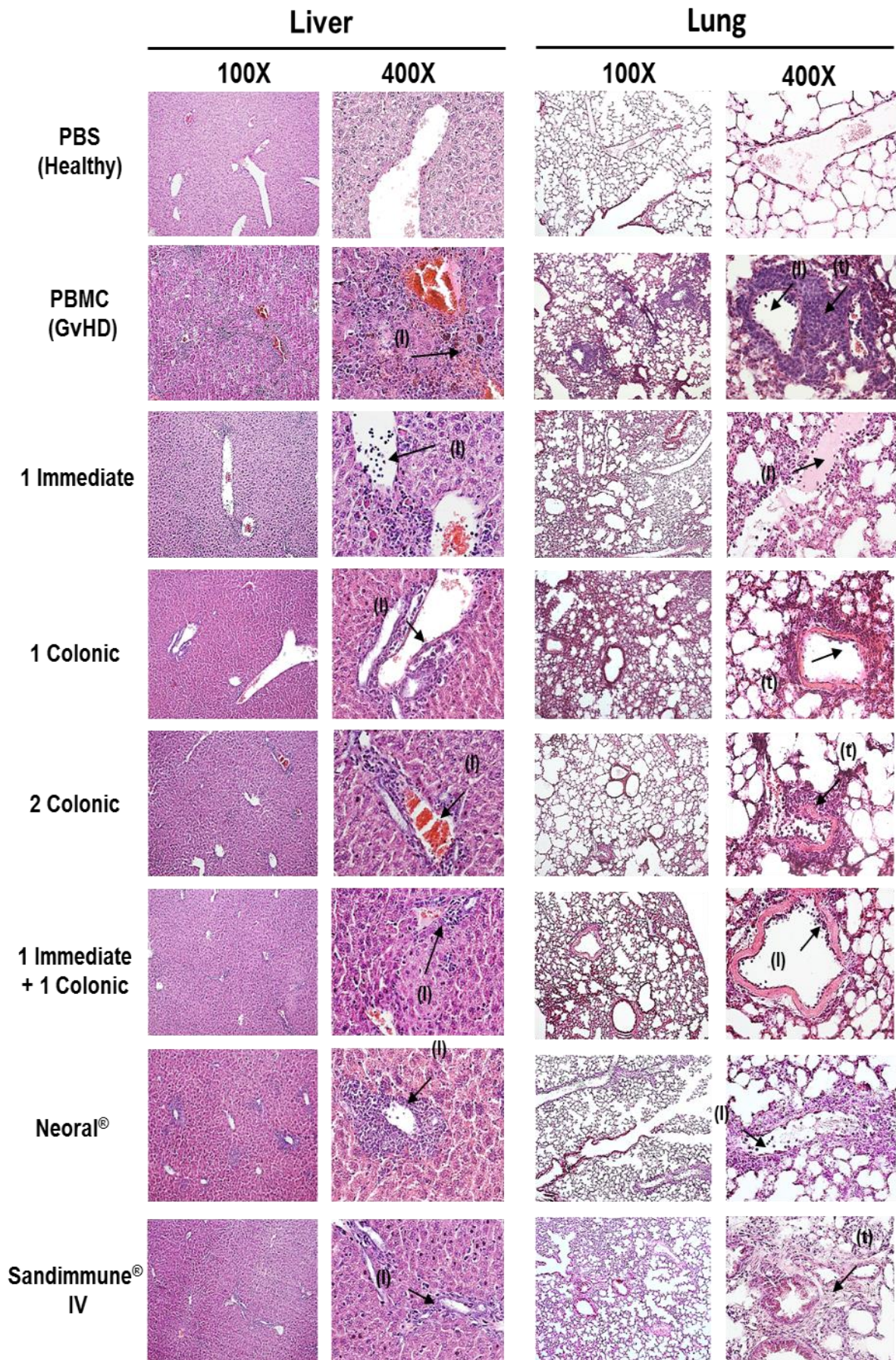
(B)
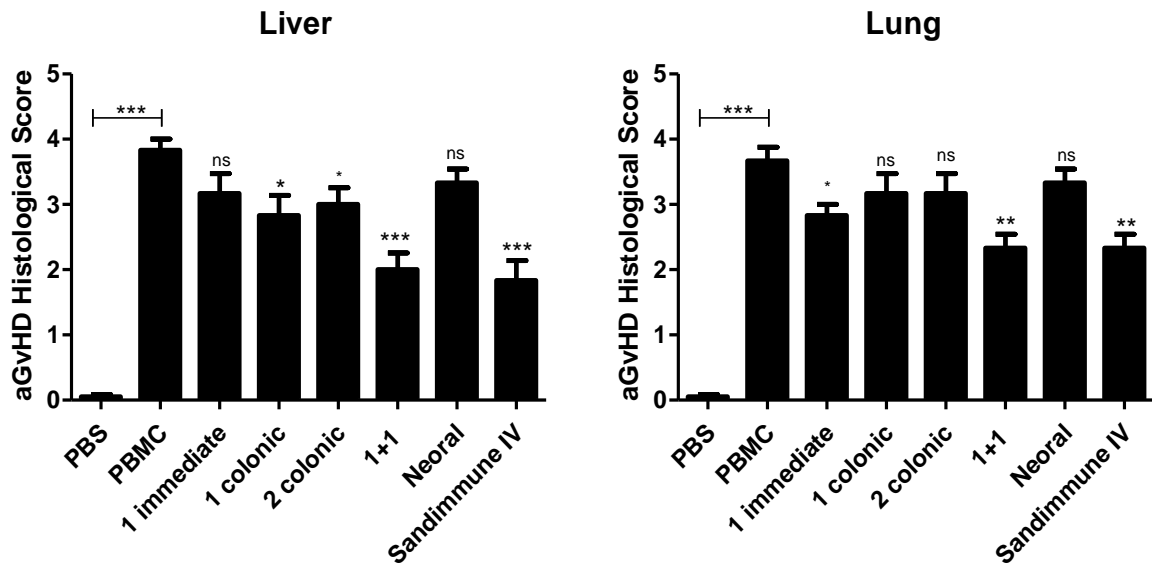
Figure 4.17. The significant reduction of pathology and lowered infiltration in the liver and lungs of aGvHD mice by SmPill® therapy is dependent on specific targeted combinations. The aGvHD model was set up exactly as described in figure 4.15. Tissue samples were harvested on day 13, formalin fixed, paraffin embedded and stained with H&E (A). Representative images were analysed for lymphocyte infiltration (l) and thickening of epithelial airways (t) and displayed for each group. Images were captured at 100X and 400X. A well defined aGvHD histological scoring system was carried out in a blinded manner and used to determine the level of aGvHD development between the groups in the liver and lung (B). n=6 per group (2 PBMC donors). Statistical analysis was carried out using the unpaired student *t*-test where * <0.05, ** <0.01 and *** <0.001. * with no bar are in comparison to the PBMC group.

(A)

	Small Intestine		Colon
	100X	**400X**	**400X**
PBS (Healthy)			
PBMC (GvHD)		(v)	(u)
1 Immediate		(v)	(u)
1 Colonic		(v)	(u)
2 Colonic		(v)	(u)
1 Immediate + 1 Colonic		(v)	(u)
Neoral®		(v)	(u)
Sandimmune® IV			(u)

(B)

Figure 4.18. The reduction of villi destruction in the small intestine and decreased occurrence of ulceration in the colon of aGvHD mice by SmPill® therapy is dependent on GI targeted combinations. The aGvHD model was set up exactly as described in figure 4.15. Tissue samples were harvested on day 13, formalin fixed, paraffin embedded and stained with H&E (A). Representative images were analysed for lymphocyte infiltration (l), villi destruction (v) and ulceration of the colonic mucosa (u) and displayed for each group. Images were captured at 100X and 400X. A well defined aGvHD histological scoring system was carried out in a blinded manner and used to determine the level of aGvHD development between the groups in the small intestine and colon (B). n=6 per group (2 PBMC donors). Statistical analysis was carried out using the unpaired student *t*-test where * <0.05, ** <0.01 and *** <0.001. * with no bar are in comparison to the PBMC group.
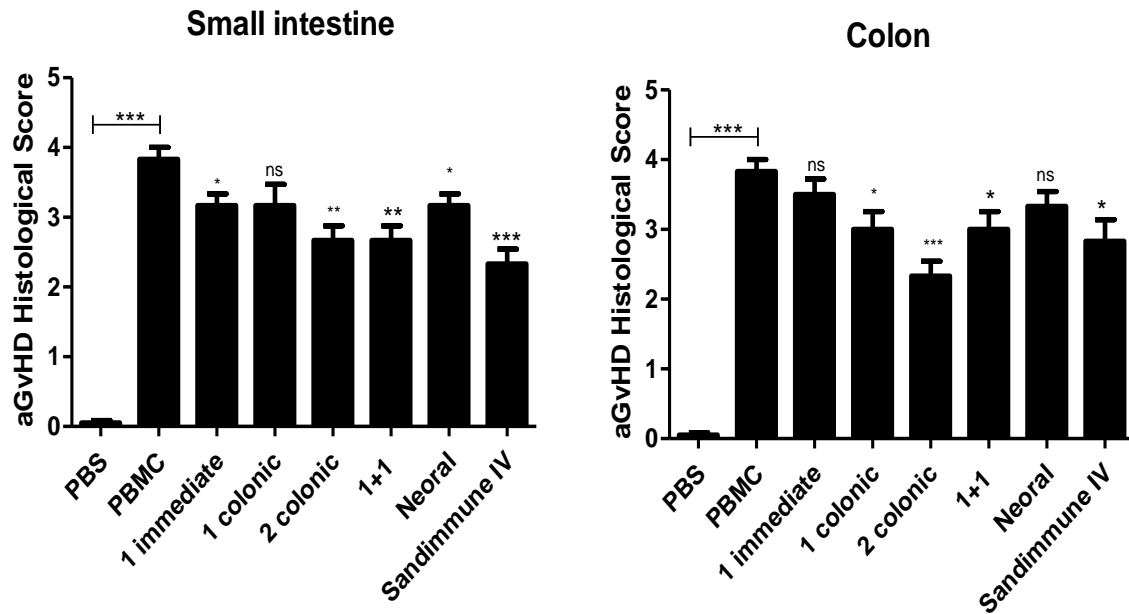
Figure 4.19. The reduction of apoptosis in the lung and small intestine of aGvHD mice by SmPill® therapy is dependent on specific targeted combinations. The aGvHD model was set up exactly as described in figure 4.15. Tissue samples were harvested on day 13, formalin fixed, paraffin embedded and TUNEL assay was carried out using a commercially available kit as described in section 2.10.3. TUNEL assay detects DNA fragmentation as a result of apoptosis and emits a green fluorescent light. DAPI was used as a nuclear stain and emits blue fluorescent light upon binding to AT regions of DNA. Positive controls for apoptotic damage were set up using DNase treated non GvHD tissue. Representative images are displayed. Images were captured at 100X using a flourescent microscope. n=6 per group (2 PBMC donors).

4.10. ENGRAFTMENT OF HUMAN PBMC IN THE aGvHD MODEL WAS NOT SIGNIFICANTLY ALTERED BY ANY SmPILL® CsA FORMULATION

For a HSCT transplant to be successful, it is imperative that donor hematopoietic cells engraft efficiently in order to reconstitute a functional immune system and maintain the graft versus leukemia effect. This means that there is a requirement for novel aGvHD treatments to have no impairment on engraftment. To determine the effect of all CsA therapies, used throughout this chapter, on the engraftment of human $CD4^+$ and $CD8^+$ T cell populations, spleens, livers, lungs and GI tracts (small intestine and colon combined) were harvested on day 13 post PBMC transfusion, mechanically digested and analysed as described in detail in section 2.9. Density gradient centrifugation was used to isolate pure human lymphocyte populations from the tissues of aGvHD mice. These single cell suspensions were examined for the expression of human $CD45^+$, $CD4^+$ and $CD8^+$ by flow cytometry using the gating strategy illustrated in figure 4.11.

The administration of all CsA therapies, SmPill® Neoral® and Sandimmune® IV, had no significant effect on the total number or percentage of human $CD45^+$, $CD4^+$, $CD8^+$ T cells recovered from the spleen, liver, lungs or GI tract of aGvHD mice, 13 days after PBMC infusion (Figure 4.20 -4.23). While there were some increases or decreases in the total number of human $CD45^+$, $CD4^+$, $CD8^+$ T cells detected in spleen, lung and GI tract, these slight alterations were not significant. This suggests that CsA does not impair the engraftment of human lymphocytes in the organs of aGvHD mice.

Spleen

Figure 4.20. SmPill®, Neoral® and Sandimmune® IV did not impair engraftment of CD45+, CD4+ and CD8+ human lymphocytes in the spleens of aGvHD mice. The aGvHD model was set up exactly as described in figure 4.15. On day 13, tissue samples were harvested, mechanically digested and single cell suspensions were analysed for the expression of CD45+, CD4+ and CD8+ by flow cytometry. Statistical analysis was carried out using one way ANOVA Tukey Multiple Comparison Test and unpaired student t-test in comparison to the PBMC group.
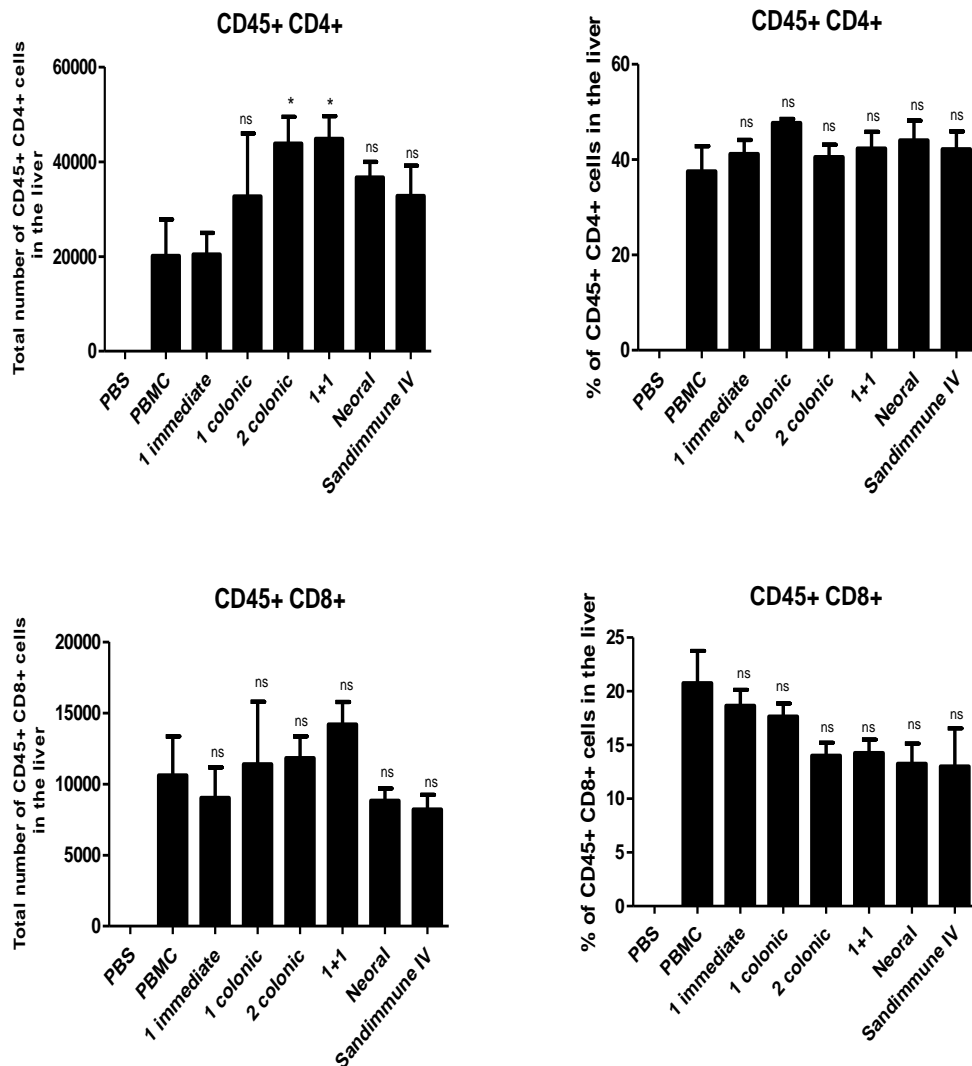
Liver

Figure 4.21. SmPill®, Neoral® and Sandimmune® IV did not impair engraftment of CD45+, CD4+ and CD8+ human lymphocytes in the livers of aGvHD mice. The aGvHD model was set up exactly as described in figure 4.15. On day 13, tissue samples were harvested, mechanically digested and single cell suspensions were analysed for the expression of CD45+, CD4+ and CD8+ by flow cytometry. Statistical analysis was carried out using one way ANOVA Tukey Multiple Comparison Test and unpaired student *t*-test in comparison to the PBMC group.
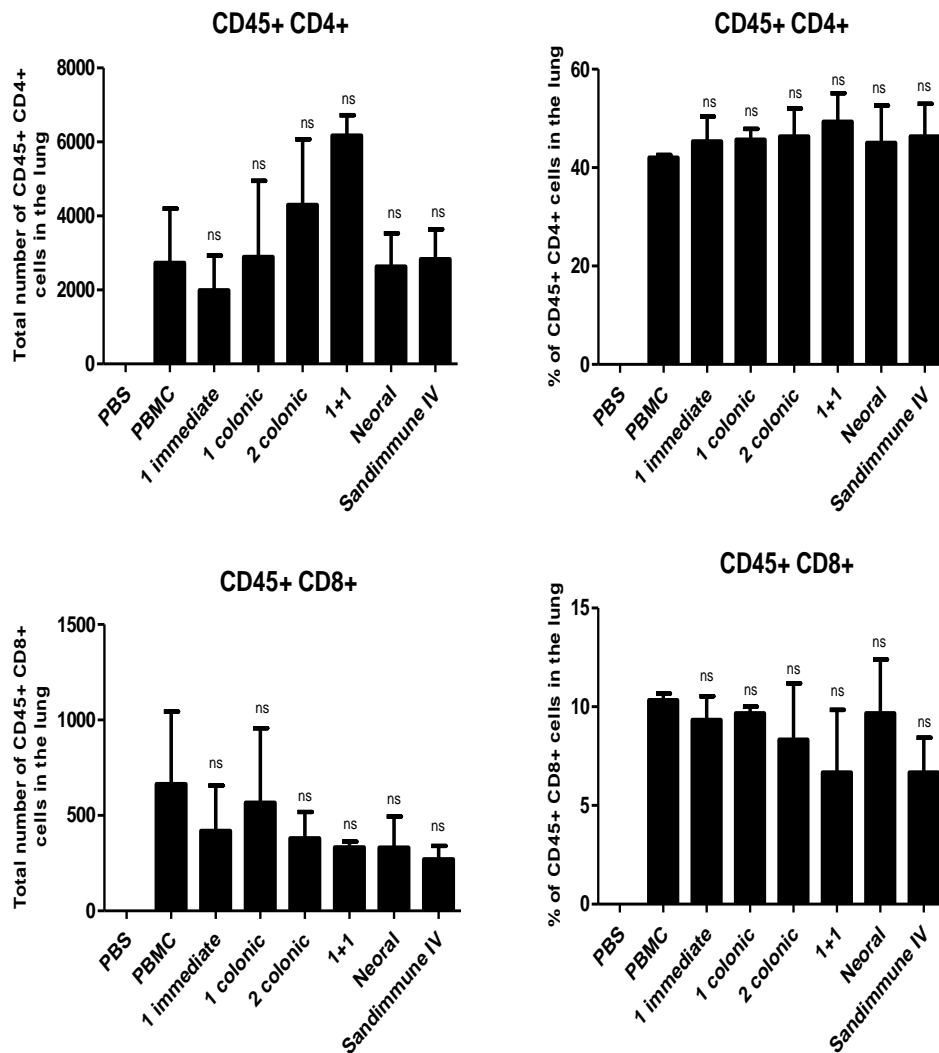
Lung

Figure 4.22. SmPill®, Neoral® and Sandimmune® IV did not impair engraftment of CD45+, CD4+ and CD8+ human lymphocytes in the lungs of aGvHD mice. The aGvHD model was set up exactly as described in figure 4.15. On day 13, tissue samples were harvested, mechanically digested and single cell suspensions were analysed for the expression of CD45+, CD4+ and CD8+ by flow cytometry. Statistical analysis was carried out using one way ANOVA Tukey Multiple Comparison Test and unpaired student *t*-test in comparison to the PBMC group.
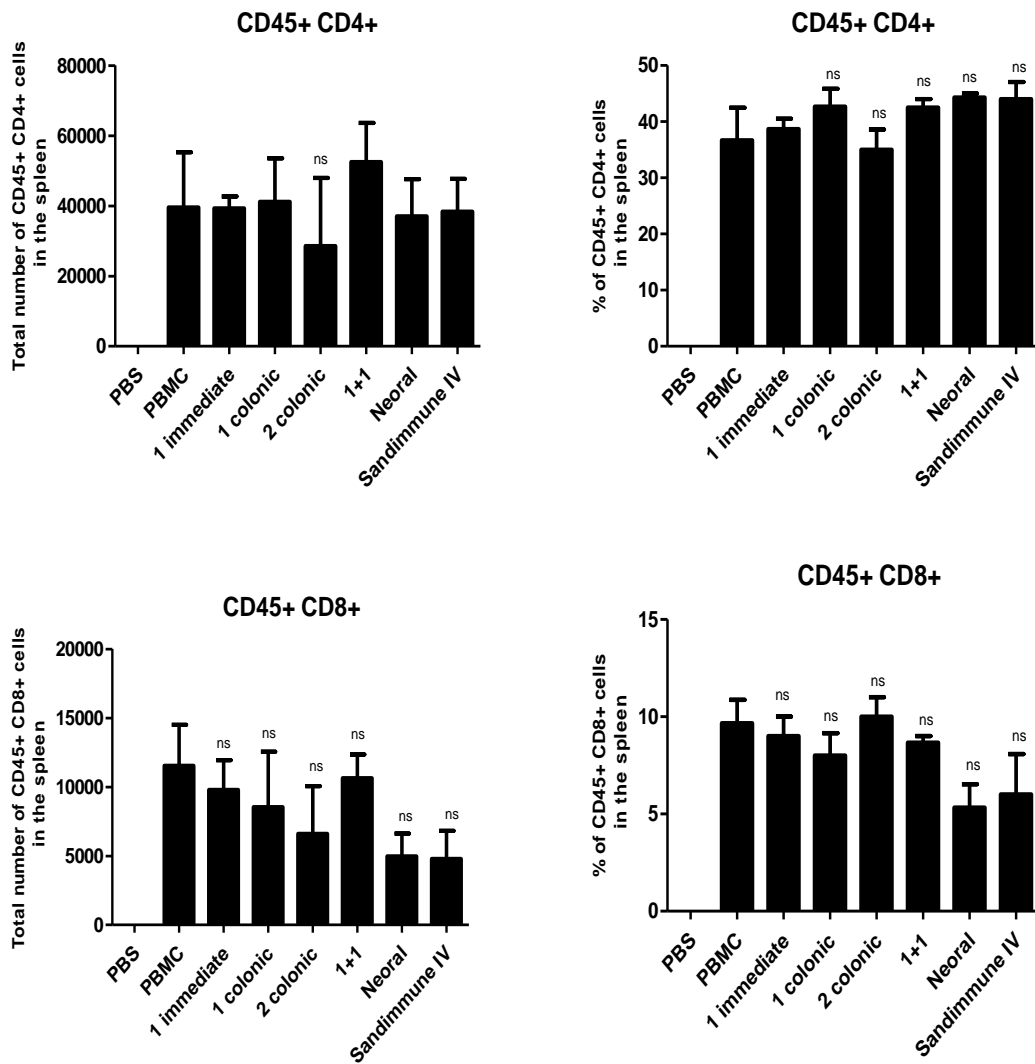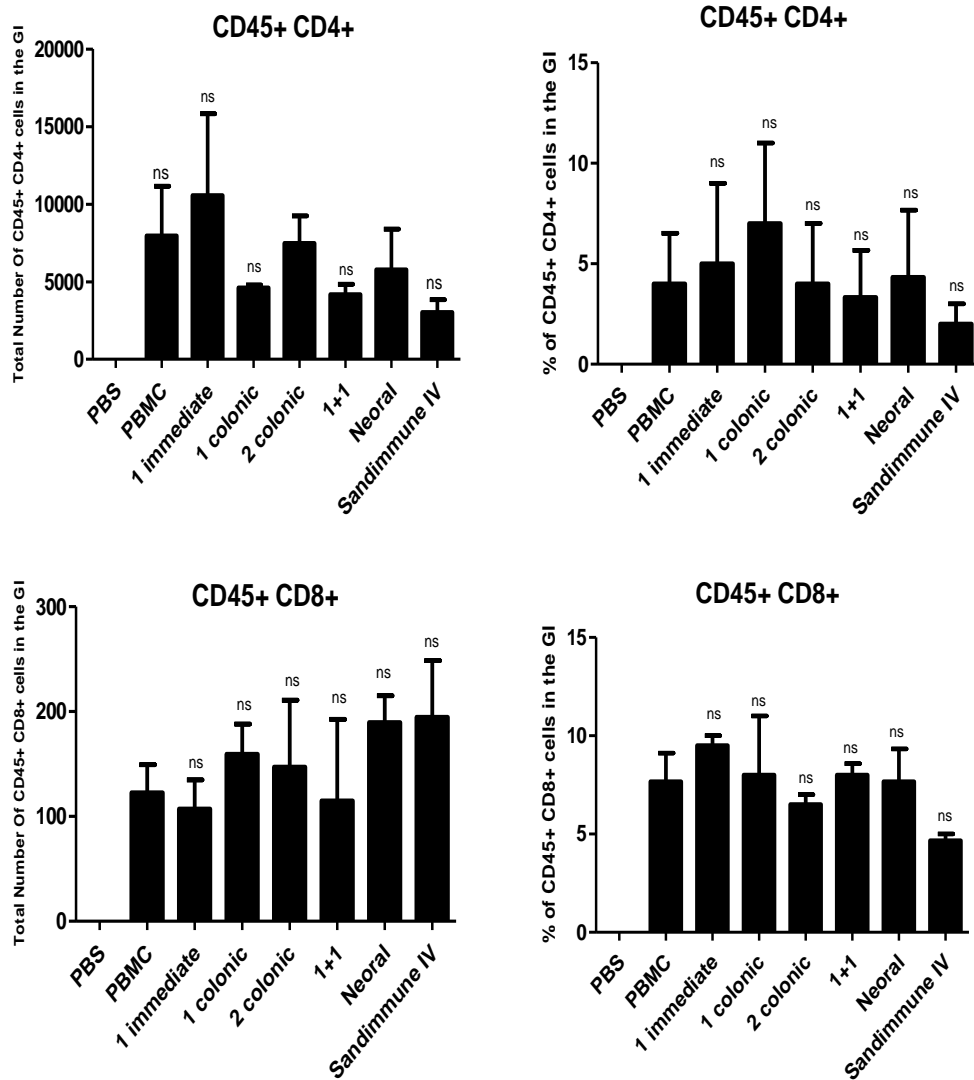
Figure 4.23. SmPill®, Neoral® and Sandimmune® IV did not impair engraftment of CD45⁺, CD4⁺ and CD8⁺ human lymphocytes in the GI tract of aGvHD mice. The aGvHD model was set up exactly as described in figure 4.15. On day 13, tissue samples were harvested, digested using collagenase and single cell suspensions were analysed for the expression of CD45⁺, CD4⁺ and CD8⁺ by flow cytometry. Statistical analysis was carried out using one way ANOVA Tukey Multiple Comparison Test and unpaired student *t*-test in comparison to the PBMC group.

4.11. SᴍPILL® CsA BEAD FORMULATIONS SIGNIFICANTLY REDUCED PROINFLAMMATORY CYTOKINES DETECTED IN ᴀGᴠHD TISSUES IN A TARGETED MANNER

As already mentioned in section 4.5, the production of proinflammatory cytokines mediated by the effector T cells, following patient HLA recognition, are a major feature of aGvHD pathology. SmPill® therapy, in the form of 1 immediate and 1 colonic bead, has already been shown to reduce, in some cases significantly, the proinflammatory cytokines IL1β, IFNγ, IL2, IL17, IL6 and IL23 in the small intestines and colon of aGvHD mice (Figure 4.9 and 4.10). To further our knowledge on the systemic and GI therapeutic effects of SmPill® therapy, cytokine profiles for the liver, lung and spleen along with the colon and small intestine were determined. Different combinations of SmPill® beads were assessed to demonstrate the targeting efficacy of SmPill® in delivering CsA to systemic and GI organs.

Using the model set up as described in figure 4.15, splenocytes were isolated from the tissue, single cell suspensions were cultured *in vitro*, stimulated with 100 ng/ml PMA and 1 µg/ml ionomycin for 72 hours and IFNγ, TNFα, IL2 and IL17 were detected in supernatants by ELISA. The liver, lung, colon and small intestine were also harvested, snap frozen and homogenates were used to detect the levels of IL1β, IFNγ, IL2, IL17, IL6 liver by ELISA.

In the splenocyte *ex vivo* culture, there was significant levels of IFNγ, TNFα, IL2 and IL17 detected in the supernatants from untreated aGvHD mice in comparison to PBS healthy controls (Figure 4.24 and Table 4.1). Sandimmune® IV and Neoral® therapy both significantly reduced the levels of IFNγ but not as significantly as the SmPill® therapy combinations, 2 colonic or 1 immediate + 1 colonic bead. The levels of TNFα were reduced in the splenocyte supernatants of all treatments with the SmPill® therapy combinations, 2 colonic or 1 immediate + 1 colonic being most significant (Figure 4.24). All of the CsA

treatments significantly reduced the levels of IL2 in the splenocyte supernatants with the exception of Sandimmune® IV and 1 immediate SmPill® bead. The levels of IL17 detected in splenocyte supernatants were reduced by all CsA treatments with the SmPill® therapy combinations, 2 colonic or 1 immediate + 1 colonic bead being most significant (Figure 4.24).

In liver homogenates collected from aGvHD mice, the levels of IL2 were significantly reduced by all CsA treatments with the exception of Neoral® and the 1 immediate release SmPill® bead therapy (Figure 4.25). The levels of IL17 and IFNγ detected in liver homogenates were also significantly reduced with the exception of Neoral® therapy (Figure 4.25). All of the CsA treatments reduced the levels of IL6 while only the SmPill® combinations of 2 colonic beads or 1 immediate + 1 colonic beads significantly reduced IL1β in liver homogenates obtained from aGvHD mice (Figure 4.25). This data is summarised in table 4.2.

The cytokine profile from lung homogenates showed how the levels of IL2 were all significantly reduced by all CsA treatments (Figure 4.26). The levels of IL17 were found to be decreased in lung homogenates of aGvHD mice by all SmPill® therapies but not Neoral® or Sandimmune® IV. All of the CsA therapies reduced the amount of IL1β and IL6 in the lungs of aGvHD mice with the exception of 1 colonic bead SmPill® therapy. The SmPill® therapy combinations of 2 colonic beads or 1 immediate + 1 colonic bead were efficacious in an equal manner to Neoral® in reducing IFNγ detectable in the lung (Figure 4.26). This cytokine profile is broken down in table 4.3.

Figure 4.27 outlines the cytokine profile of colon homogenates. The SmPill® combination of 1 immediate bead alone failed to significantly reduce any of the proinflammatory cytokines tested (Figure 4.27). Sandimmune® IV significantly reduced levels of IL2 and IL17 while Neoral® significantly lowered IL2, IL17 and IL1β in the colon

homogenates (Figure 4.27). The SmPill® therapy combinations of 2 colonic beads or 1 immediate + 1 colonic bead were most effective at targetting the colon and reducing IFNγ, IL2, IL17, IL1β and IL6 detected in the colon (Figure 4.27). Table 4.4 summarises this data.

The cytokine profile (Table 4.5) in the small intestine determined that all CsA therapies significantly reduced IL1β and IL6 (Figure 4.28). However, there were differences detectable in the other cytokines. All CsA therapies reduced the levels of IL2, however the 1 + 1 SmPill® combination was significantly efficacious (Figure 4.28). The 1 + 1 SmPill® combination and other GI targeting CsA therapies (1 or 2 colonic beads) significantly reduced IL17 in a similar manner to Sandimmune® IV (Figure 4.28). All SmPill® formulations were significant in decreasing levels of IFNγ, whereas Sandimmune® IV and Neoral® were not.

This data demonstrates further that SmPill® is efficacious at targeting CsA delivery and a balanced combination such as 1 immediate and 1 colonic release bead can provide protection in both systemic and GI tissues. This was characterised by the reduction in proinflammatory cytokines in systemic or GI tissues in the humanised aGvHD model. Interestingly, there was significant protection in the lung where 2 colonic beads were delivered as CsA therapy in aGvHD mice (Table 4.3). This supports the concept of the GI as being a principal organ involved in determining aGvHD severity and by targeting the colon, in particular, there were shielding effects systemically whereby proinflammatory cytokines in the lung were significantly reduced.

Spleen
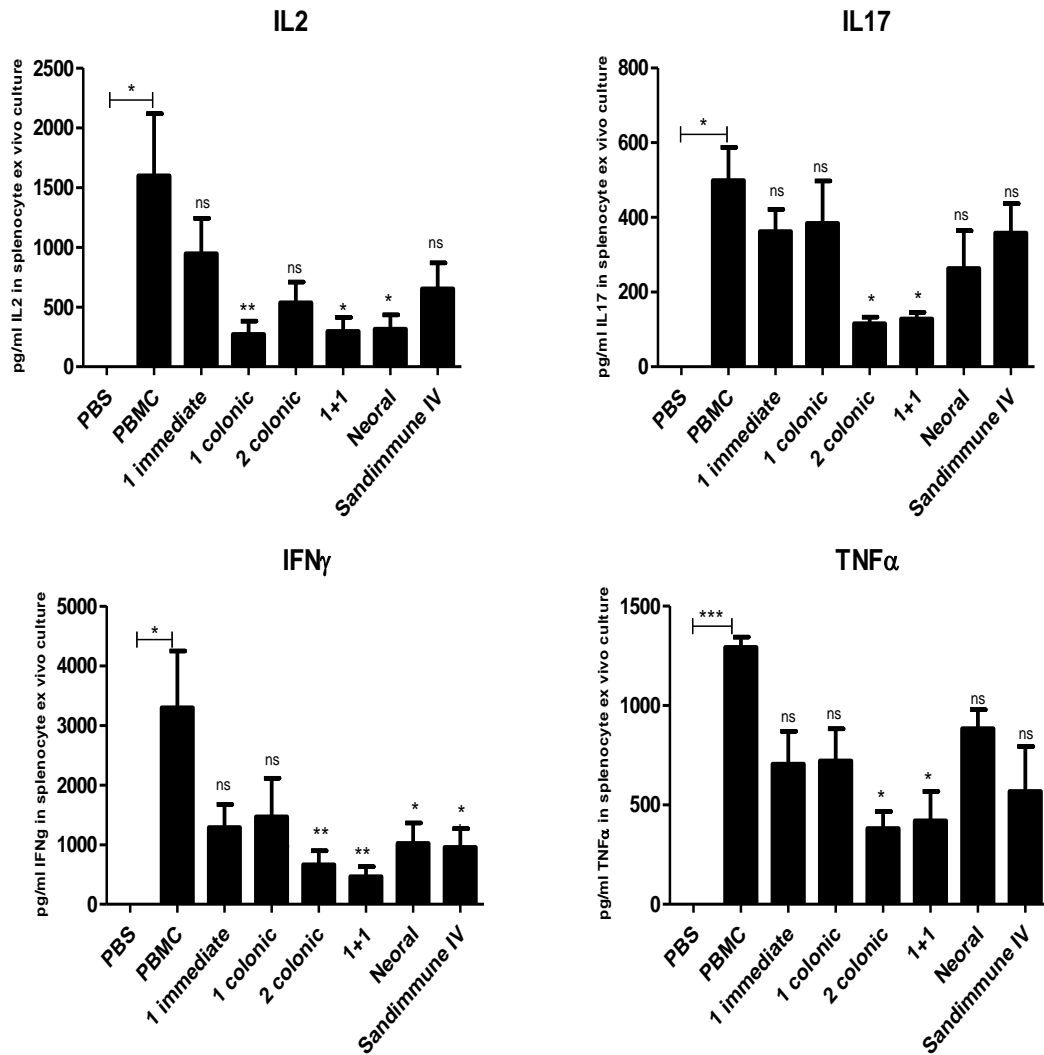
Figure 4.24. SmPill® formulations targeting the GI were significantly better at reducing proinflammatory cytokines detected in the spleens of aGvHD mice. The aGvHD model was set up exactly as described in figure 4.15. Tissue samples were harvested on day 13, single cell suspensions were cultured *in vitro* and stimulated with 100 ng/ml PMA and 1 µg/ml ionomycin for up to 72 hours. Supernatants were collected and ELISA was used to detect proinflammatory cytokines (IFNγ, TNFα, IL2 and IL17). Statistical analysis was carried out using using one way ANOVA Tukey Multiple Comparison Test where * <0.05, ** <0.01 and *** <0.001. Stars with no bar are in comparison to the PBMC group.

Liver

Figure 4.25. SmPill® formulations targeting the GI were most significant at reducing proinflammatory cytokines detected in the liver of aGvHD mice. The aGvHD model was set up exactly as described in figure 4.15. Tissue samples were harvested on day 13, immediately snap frozen and stored at - 80 C. Homogenates were prepared and ELISA was used to detect proinflammatory cytokines (IL2, IL17, IL1β, IL6 and IFNγ). Concentration of cytokine is expressed as pg cytokine per mg tissue protein as normalised by bradford protein assay. Statistical analysis was carried out using using one way ANOVA Tukey Multiple Comparison Test where * <0.05, ** <0.01 and *** <0.001. Stars with no bar are in comparison to the PBMC group.
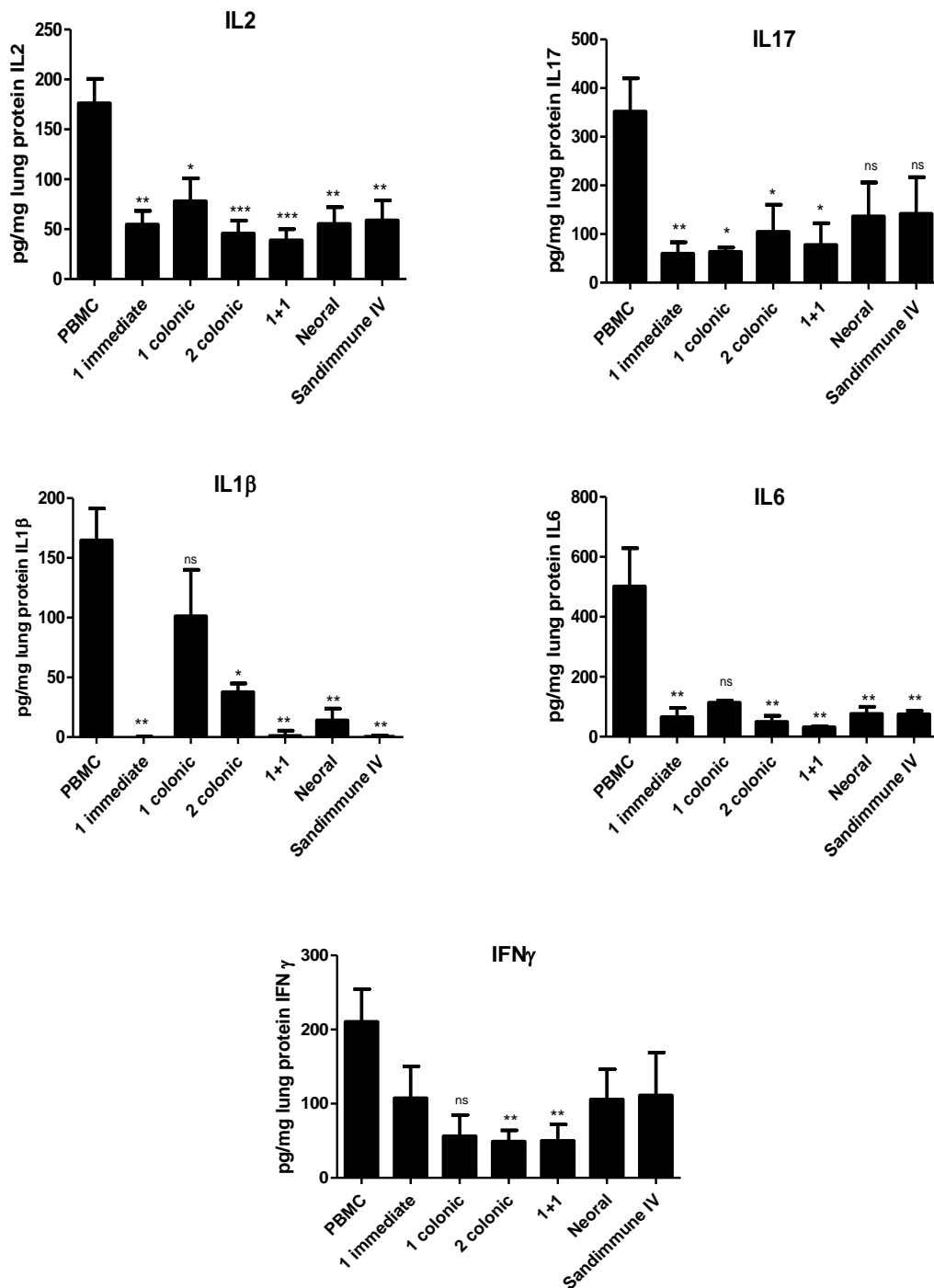
Figure 4.26. All SmPill® formulations significantly reduced proinflammatory cytokines detected in the lungs of aGvHD mice. The aGvHD model was set up exactly as described in figure 4.15. Tissue samples were harvested on day 13, immediately snap frozen and stored at - 80 C. Homogenates were prepared and ELISA was used to detect proinflammatory cytokines (IL2, IL17, IL1β, IL6 and IFNγ). Concentration of cytokine is expressed as pg cytokine per mg tissue protein as normalised by bradford protein assay. Statistical analysis was carried out using using one way ANOVA Tukey Multiple Comparison Test where * <0.05, ** <0.01 and *** <0.001. Stars with no bar are in comparison to the PBMC group.
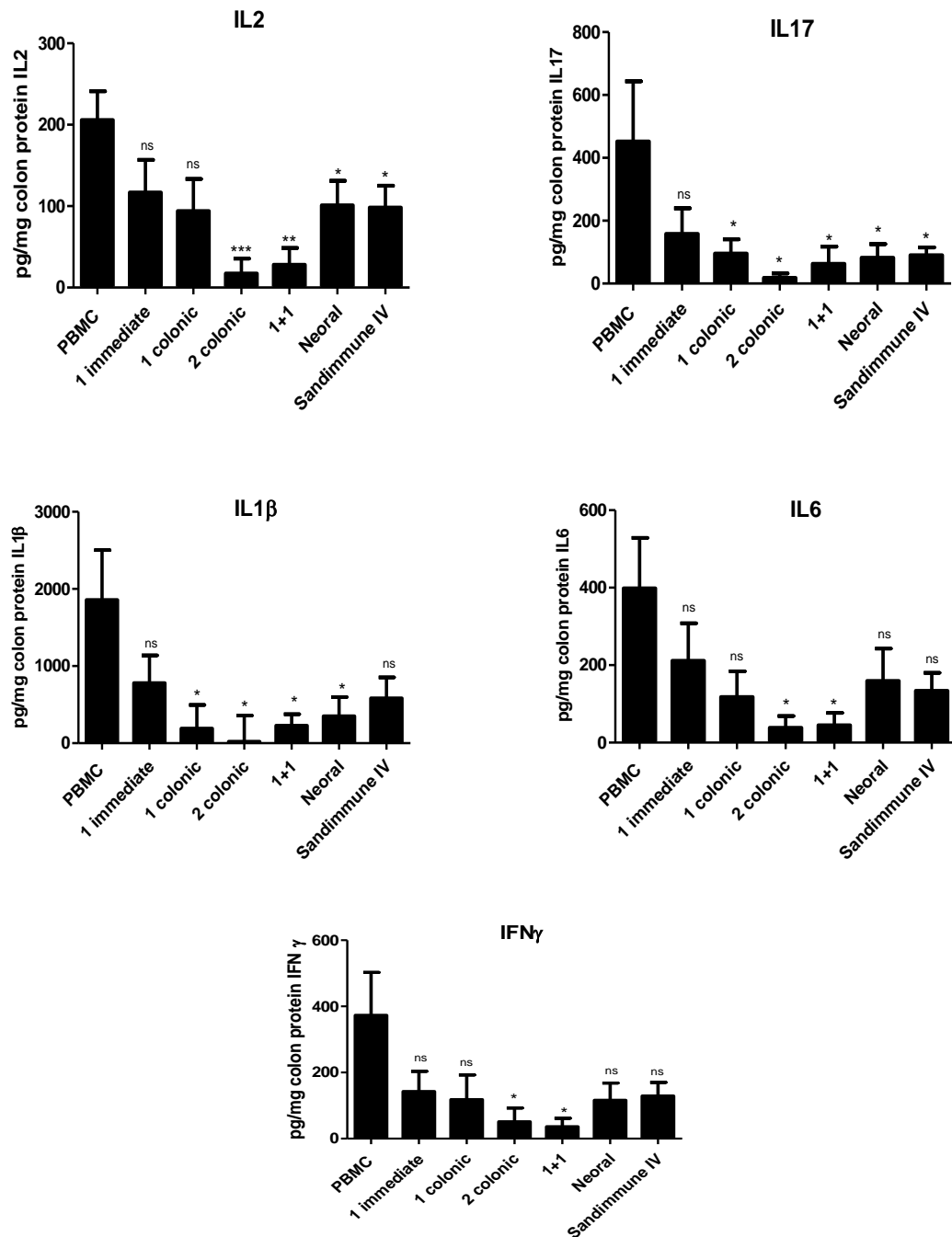
Colon

Figure 4.27. GI targeted SmPill® formulations significantly reduced proinflammatory cytokines detected in the colon of aGvHD mice. The aGvHD model was set up exactly as described in figure 4.15. Tissue samples were harvested on day 13, immediately snap frozen and stored at - 80 C. Homogenates were prepared and ELISA was used to detect proinflammatory cytokines (IL2, IL17, IL1β, IL6 and IFNγ). Concentration of cytokine is expressed as pg cytokine per mg tissue protein as normalised by bradford protein assay. Statistical analysis was carried out using using one way ANOVA Tukey Multiple Comparison Test where * <0.05, ** <0.01 and *** <0.001. Stars with no bar are in comparison to the PBMC group.
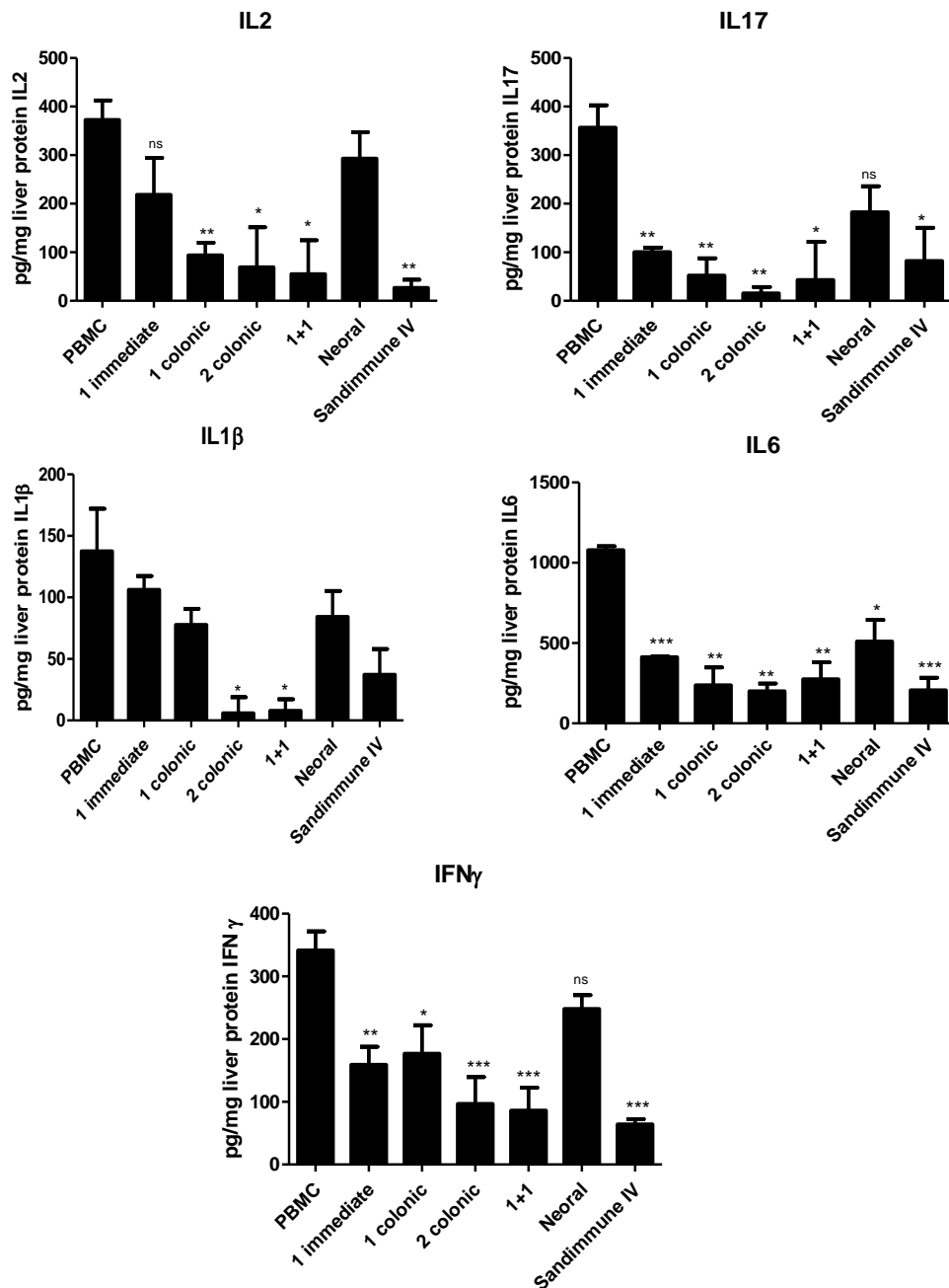
Small Intestine

Figure 4.28. GI targeted SmPill® formulations significantly reduced proinflammatory cytokines detected in the small intestine of aGvHD mice. The aGVHD model was set up exactly as described in figure 4.15. Tissue samples were harvested on day 13, immediately snap frozen and stored at - 80 C. Homogenates were prepared and ELISA was used to detect proinflammatory cytokines (IL2, IL17, IL1β, IL6 and IFNγ). Concentration of cytokine is expressed as pg cytokine per mg tissue protein as normalised by bradford protein assay. Statistical analysis was carried out using using one way ANOVA Tukey Multiple Comparison Test where * <0.05, ** <0.01 and *** <0.001. Stars with no bar are in comparison to the PBMC group.

Table 4.1 Proinflammatory cytokine profile in the spleen

	1 Immediate	1 colonic	2 colonic	1 + 1	Neoral®	Sandimmune® IV
IL2	↓[5]	**[6]	↓	*[7]	*	↓
IL17	↓	↓	*	*	↓	↓
IFNγ	↓	↓	**	**	*	*
TNFα	↓	↓	*	*	↓	↓

Table 4.2 Proinflammatory cytokine profile in the liver

	1 Immediate	1 colonic	2 colonic	1 + 1	Neoral®	Sandimmune® IV
IL2	↓	**	*	*	↓	**
IL17	**	**	**	*	↓	*
IL1β	↓	↓	*	*	↓	↓
IL6	***[8]	**	**	**	*	***
IFNγ	**	*	***	***	↓	***

Table 4.3 Proinflammatory cytokine profile in the lung

	1 Immediate	1 colonic	2 colonic	1 + 1	Neoral®	Sandimmune® IV
IL2	**	*	***	***	**	**
IL17	**	*	*	*	↓	↓
IL1β	**	↓	*	**	**	**
IL6	**	↓	**	**	**	**
IFNγ	↓	↓	**	**	**	↓

---

[5] Denotes a reduction in test group where significance was not obtained using one way ANOVA Tukey Multiple Comparison Test.

[6] Denotes statistical significance using one way ANOVA Tukey Multiple Comparison Test. where ** <0.01

[7] Denotes statistical significance using one way ANOVA Tukey Multiple Comparison Test. where * <0.05

[8] Denotes statistical significance using one way ANOVA Tukey Multiple Comparison Test.where *** <0.001

Table 4.4 Proinflammatory cytokine profile in the colon

	1 Immediate	1 colonic	2 colonic	1 + 1	Neoral®	Sandimmune® IV
IL2	↓	↓	***	**	*	*
IL17	↓	*	*	*	*	*
IL1β	↓	*	*	*	*	↓
IL6	↓	↓	*	*	↓	↓
IFNγ	↓	↓	*	*	↓	↓

Table 4.5 Proinflammatory cytokine profile in the small intestine

	1 Immediate	1 colonic	2 colonic	1 + 1	Neoral®	Sandimmune® IV
IL2	↓	↓	↓	*	↓	↓
IL17	↓	*	*	*	↓	*
IL1β	***	***	***	***	***	***
IL6	***	***	***	***	***	***
IFNγ	*	*	*	**	↓	↓

4.12. SMPILL® CSA BEAD FORMULATIONS SIGNIFICANTLY REDUCED TNFα PRODUCING T CELLS IN THE TISSUES AND CIRCULATING TNFα IN SERUM OF ᴀGᴠHD MICE IN A TARGETED MANNER

TNFα plays a role in all phases of aGvHD pathophysiology, as detailed in Chapter 1, from the early phase of host APC activation through to tissue damage where the GI tract in particular is most susceptible. In mouse models of GvHD, inhibiting TNFα was shown to be protective in the gut with reduced occurence of apoptosis (Brown *et al.* 1999; Stuber *et al.* 1999). Earlier in this chapter, SmPill® therapy, in the form of 1 immediate and 1 colonic bead, was shown to significantly reduce the number of TNFα producing CD4$^+$ and CD8$^+$ T cells in the spleen, lung and liver of aGvHD mice (Figure 4.12 – 4.14). Next we sought to further characterise the influence of different SmPill® formulations on delivering CsA systemically or targeting the GI by measuring the production of TNFα by CD4$^+$ and CD8$^+$ T cells in target organs and in the serum of aGvHD mice.

NSG mice were irradiated and PBMC were administered as before. CsA was delivered intravenously (Sandimmune® IV), and by oral gavage (Neoral® and SmPill®) for 5 doses (25mg/kg) from day 4 (Figure 4.15). Different SmPill® CsA formulation combinations were assigned and delivered by gavage to groups of mice as outlined in figure 4.15 B. On day 13 after PBMC administration, following the gating strategy as described in figure 4.11, human CD45$^+$ cells were recovered from the spleen, liver, lungs and GI tract (small intestine and colon combined) and the potential for TNFα production by human CD4$^+$ and CD8$^+$ T cells was analysed by intracellular flow cytometry.

As expected and observed previously, aGvHD mice that received no therapy had significantly higher numbers and percentages of CD4$^+$ and CD8$^+$ T cells producing TNFα in the spleen (Figure 4.29). SmPill® therapies which included 1 or 2 colon beads were most efficacious and significantly decreased the number of TNFα producing CD45$^+$ CD4$^+$ cells,

however the number and percentage of and CD8$^+$ T cells producing TNFα in the spleen were not significantly reduced by any of the CsA therapies (Figure 4.29). However, the 1 immediate + 1 colonic SmPill$^®$ significantly reduced both the number of CD4$^+$ and CD8$^+$ T cells producing TNFα in the spleen. This is consistent with figure 4.12, where this combination was already shown to significantly reduced the number of TNFα producing CD4$^+$ and CD8$^+$ T cells in the spleen.

In the liver, all groups of CsA treatments significantly reduced the percentage of CD4$^+$ T cells producing TNFα while Neoral$^®$ and 1 immediate + 1 colonic SmPill$^®$ therapy were the only CsA treatments to fail to significantly reduce the numbers of CD45$^+$ CD4$^+$ T cells producing TNFα (Figure 4.30). In addition, all CsA treatment groups equally reduced the number and percentage of CD45$^+$ CD8$^+$ T cells producing TNFα in the liver of aGvHD mice (Figure 4.30).

In the lungs, Neoral$^®$ and the 1 immediate + 1 colonic SmPill$^®$ therapy significantly reduced both the number and percentage of CD45$^+$ CD4$^+$ T cells producing TNFα (Figure 4.31). Interestingly, the 2 colonic SmPill$^®$ therapy also significantly reduced the percentage of CD45$^+$ CD4$^+$ T cells producing TNFα (Figure 4.31). This supports findings in section 4.11 where there is evidence of GI targeted CsA having systemic therapeutic effects (Figure 4.26). Surprisingly, none of the CsA treatments had a significant effect on the number and percentage of CD45$^+$ CD8$^+$ T cells producing TNFα (Figure 4.31).

The optimisation of a protocol to isolate lymphocytes from the small intestine and colon (combined as GI tract for optimal cell recovery), detailed in section 2.9.4, enabled the analysis of the number and percentage of CD45$^+$ CD4$^+$ and CD8$^+$ T cells producing TNFα in the GI tract for the first time. Figure 4.32 shows that there is was a significant number and percentage of CD45$^+$ CD4$^+$ and CD8$^+$ T cells producing TNFα present in the GI tract of untreated aGvHD mice in comparison to PBS controls. All CsA therapies, with the

exception of Neoral® and 1 colonic SmPill® therapy, were effective at significantly reducing the number but not percentage of CD45$^+$ CD4$^+$ T cells producing TNFα in the GI tract (Figure 4.32). All CsA therapies significantly reduced the percentage but not the number of CD45$^+$ CD8$^+$ T cells producing TNFα with varying efficacy in the GI tract (Figure 4.32).

The level of circulating TNFα was significantly reduced by all CsA therapies with the exception of Neoral® (Figure 4.33). Collectively, this data suggests that delivery of SmPill® via different combinations can result in variable efficacy within systemic and GI specific organs in terms of suppression of TNFα producing CD45$^+$ CD4$^+$ and CD8$^+$ T cells.

Spleen

Figure 4.29. The significant reduction in the total number and percentage of TNFα producing CD4$^+$ and CD8$^+$ T cells in the spleen of aGvHD mice is mediated by immediate and GI targeted SmPill® therapy. The aGvHD model was set up exactly as described in figure 4.15. Cells were recovered on day 13, stimulated with 100 ng/ml PMA, 1 µg/ml iononmycin and 1X Brefeldin A for 4 h and analysed by intracellular flow cytometry. Graphical representation of the total number of human TNFα producing CD45$^+$ CD4$^+$ cells recovered in the spleen (A). CD45$^+$ CD8$^+$ T cell TNFα production is represented in (B). The total number of human cells was assessed using counting beads during flow cytometry. n=6 per group (2 PBMC donors). Statistical analysis was carried out in comparison to the PBMC group using unpaired student *t*-test where * <0.05, ** <0.01 and *** <0.001.
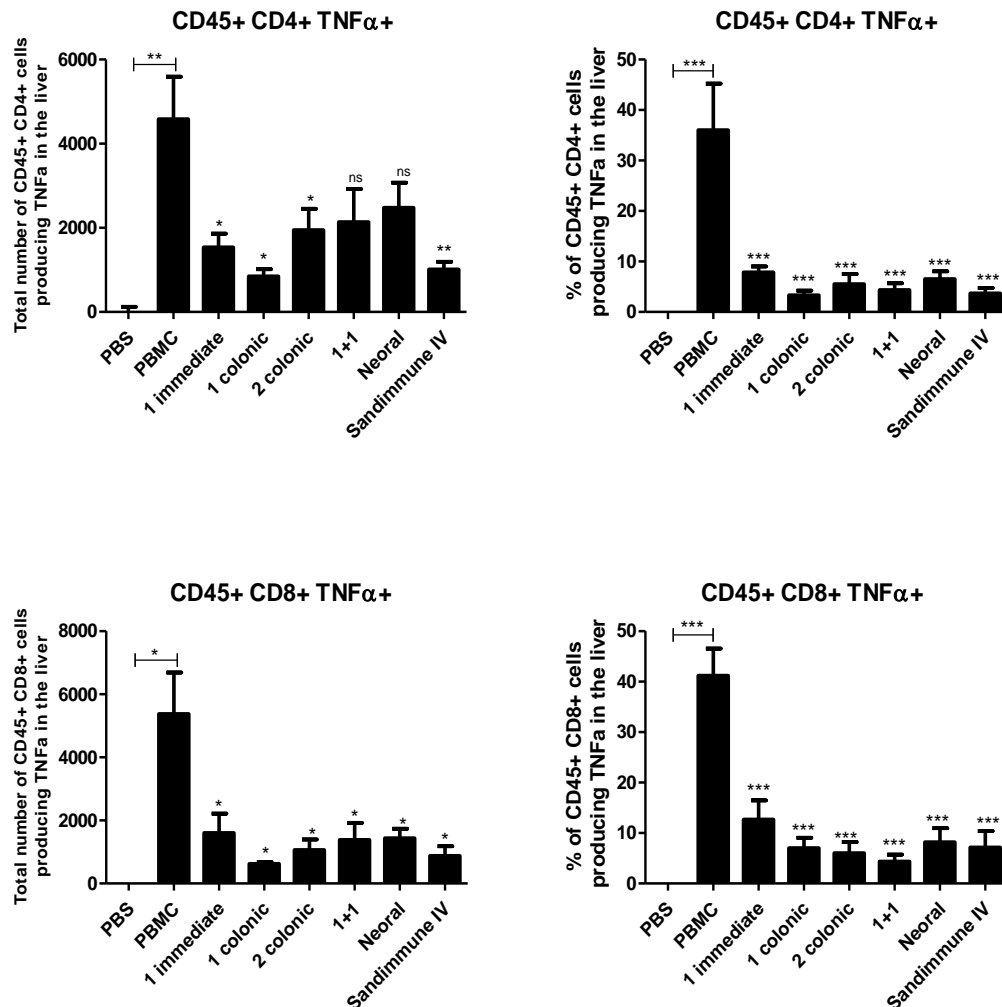
Liver

Figure 4.30. All CsA therapies significantly reduced the total number and percentage of TNFα producing CD4+ and CD8+ T cells in the liver of aGvHD mice. The aGvHD model was set up exactly as described in figure 4.15. Cells were recovered on day 13, stimulated with 100 ng/ml PMA, 1 µg/ml iononmycin and 1X Brefeldin A for 4 h and analysed by intracellular flow cytometry. Graphical representation of the total number of human TNFα producing CD45+ CD4+ cells recovered in the liver (A). CD45+ CD8+ T cell TNFα production is represented in (B). The total number of human cells was assessed using counting beads during flow cytometry. n=6 per group (2 PBMC donors). Statistical analysis was carried out in comparison to the PBMC group using unpaired student t-test where * <0.05, ** <0.01 and *** <0.001.
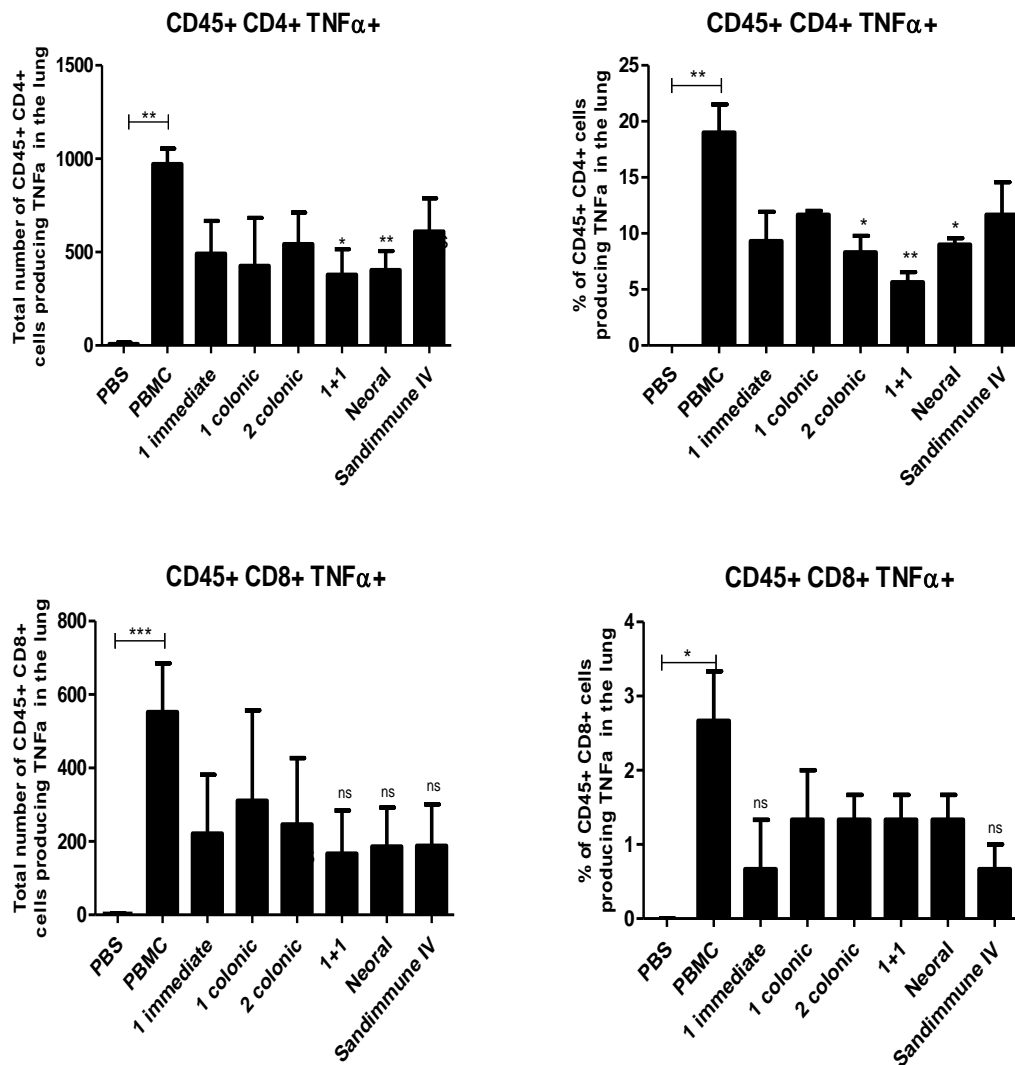
Lung

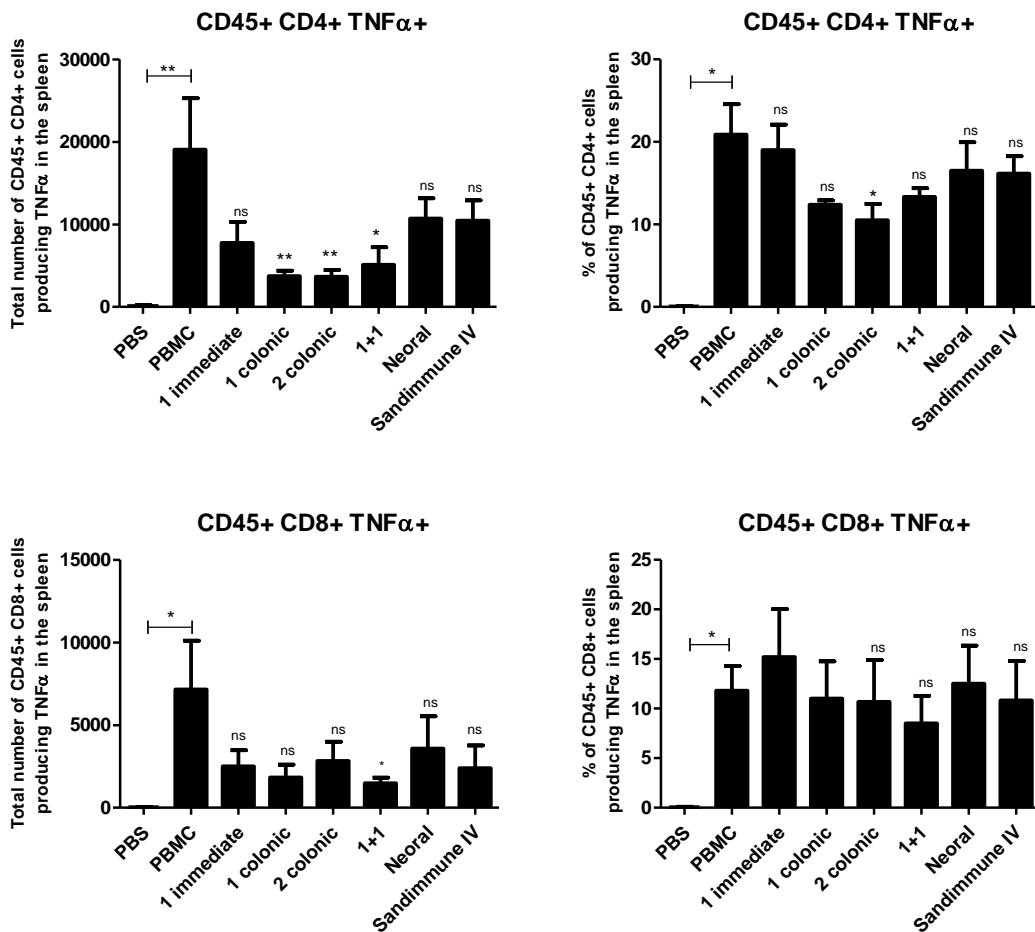**Figure 4.31. The significant reduction in the total number and percentage of TNFα producing CD4+ and CD8+ T cells in the lung of aGvHD mice is mediated by immediate and GI targeted SmPill® therapy.** The aGvHD model was set up exactly as described in figure 4.15. Cells were recovered on day 13, stimulated with 100 ng/ml PMA, 1 µg/ml iononmycin and 1X Brefeldin A for 4 h and analysed by intracellular flow cytometry. Graphical representation of the total number of human TNFα producing CD45+ CD4+ cells recovered in the lung (A). CD45+ CD8+ T cell TNFα production is represented in (B). The total number of human cells was assessed using counting beads during flow cytometry. n=6 per group (2 PBMC donors). Statistical analysis was carried out in comparison to the PBMC group using unpaired student *t*-test where * <0.05, ** <0.01 and *** <0.001.

GI Tract
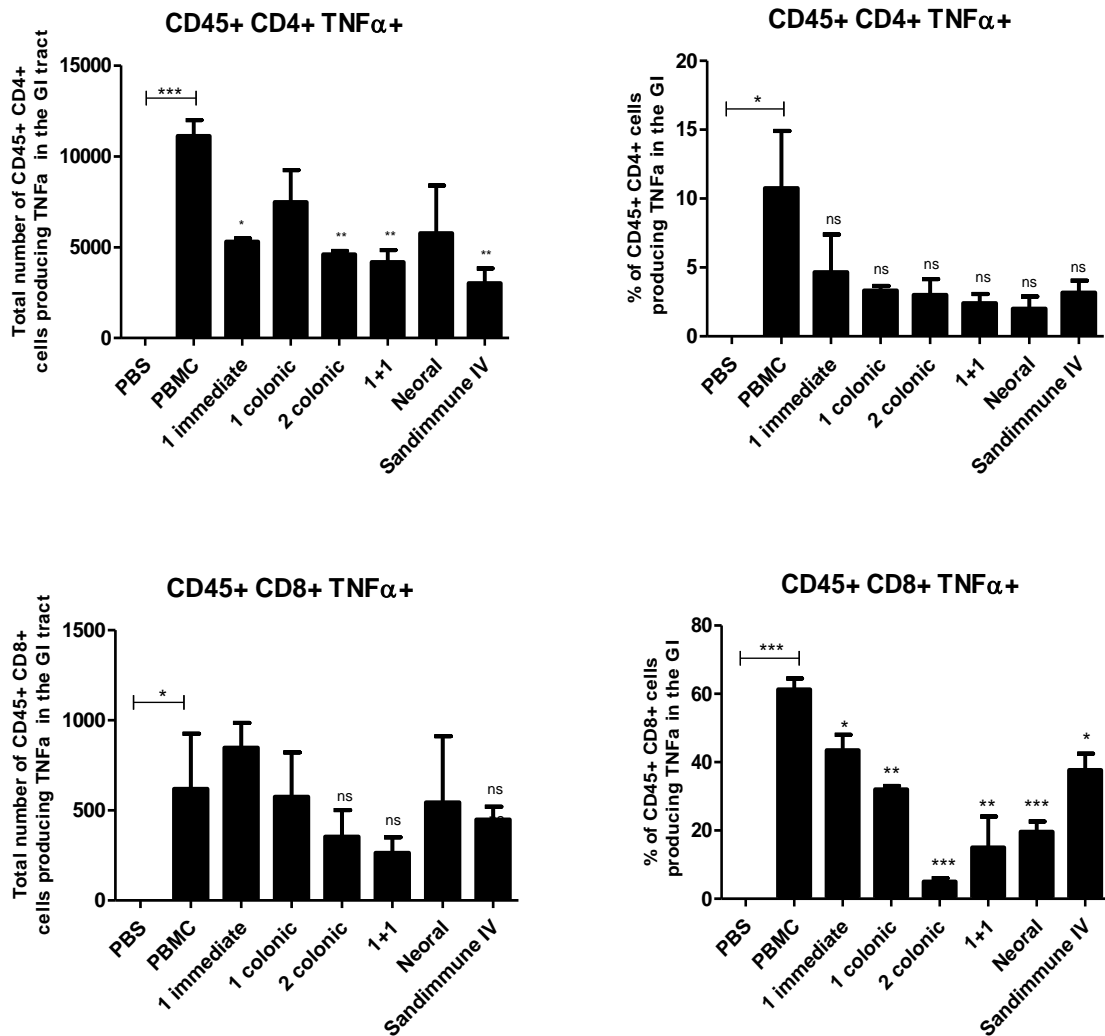
Figure 4.32. The significant reduction in the total number and percentage of TNFα producing CD4+ and CD8+ T cells in the GI of aGvHD mice is mediated by GI targeted SmPill® therapy. The aGvHD model was set up exactly as described in figure 4.15. Cells were recovered on day 13, stimulated with 100 ng/ml PMA, 1 μg/ml iononmycin and 1X Brefeldin A for 4 h and analysed by intracellular flow cytometry. Graphical representation of the total number of human TNFα producing CD45+ CD4+ cells recovered in the GI tract (A). CD45+ CD8+ T cell TNFα production is represented in (B). The total number of human cells was assessed using counting beads during flow cytometry. n=6 per group (2 PBMC donors). Statistical analysis was carried out in comparison to the PBMC group using unpaired student t-test where * <0.05, ** <0.01 and *** <0.001.
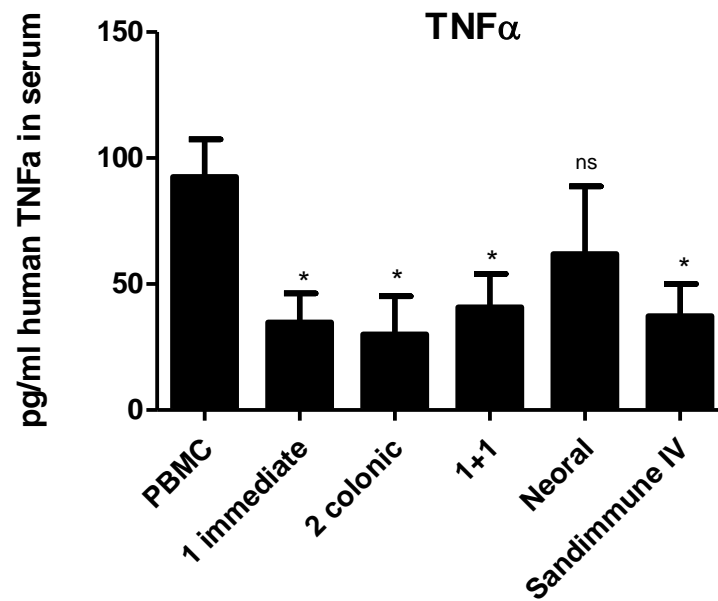
Figure 4.33. All SmPill® therapies and Sandimmune® IV significantly reduced the levels of TNFα in the serum of aGvHD mice. The aGvHD model was set up as described in figure 4.15. On day 13, facial bleeds were performed on PBS control mice (not detected), aGvHD mice and aGvHD mice that received different CsA therapies. The total level of circulating human TNFα was analysed in the serum of aGvHD mice using ELISA. n=6 per group (2 PBMC donors). Statistical analysis was carried out in comparison to the PBMC group using unpaired student *t*-test where * <0.05.

## 4.13. REGULATORY T CELLS IN aGvHD MICE WERE NOT SIGNIFICANTLY ALTERED BY ANY COMBINATION OF SMPILL ® CsA FORMULATION

One of the main candidates emerging as a strategy for the management of aGvHD is the exploitation of regulatory T cell (Treg) functions for immunotherapy. IL2 has been shown to play an important role in Treg homeostasis (Yates *et al*. 2007). CsA is an inhibitor of calcineurin, which hinders IL2 production and has been previously reported to compromise the number of peripheral $CD4^+$ $CD25^+$ $FoxP3^+$ T cells in GvHD mice (Coenen *et al*. 2007). Considering this, the effect that SmPill® therapy has on Treg during aGvHD was investigated in the humanised mouse model. In particular, the potential differences between immediate release and targeted GI release of CsA might have a determining effect on the effect of CsA on Treg systemically. The capacity to control the distribution of CsA in specific tissues, in this case the GI tract, may have a sparing effect on systemic Treg (i.e. those outside the GI tract).

Acute GvHD mice treated with CsA therapies or untreated were sacrificed on day 13 and the spleens, lungs, livers and GI tract were harvested for analysis. Human Treg cells were defined as $CD4^+$ $CD25^+$ $FoxP3^+$ after gating on the human $CD45^+$ cells recovered from the tissues and determined by intracellular flow cytometry. Recent findings have shown the importance of using other markers such as CD127 in defining T reg populations (Liu *et al.* 2006). However, the limitation for this study was access to a flow cytometer capable of detecting more than 4 colours.

Very small populations of Treg cells were present in all of the organs harvested. Interestingly the total number or percentage of human Treg cells was not significantly altered in the spleen or lungs by any of the CsA therapies administered as 5 doses every second day from day 4-12 (Figure 4.34). While figure 4.34 shows a reduction in the number of Tregs in the lung, these changes are not significant. Similarly, in the liver and GI tract, there is no

effect on the percentage of Tregs. Where the total number of Tregs are reduced, these are not significant (Figure 4.35). These results suggest that CsA has no signficant effect on the number and percentage of Tregs, as defined as CD4$^+$ CD25$^+$ FoxP3$^+$, during aGvHD and that these cells are detectable in the tissues associated with aGvHD inflammation.
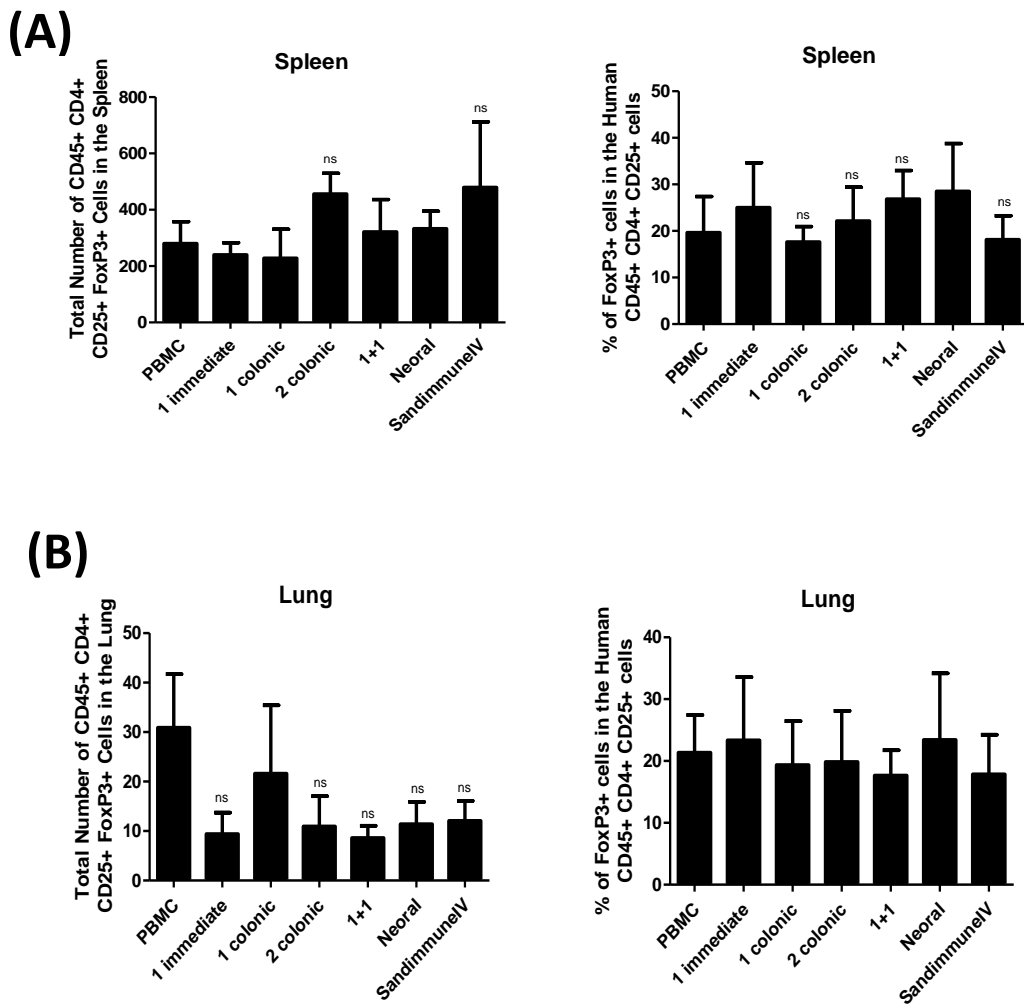
Figure 4.34. All formulations of SmPill® had no significant effect on the number and percentage of Treg cells in the spleen and lung of aGvHD mice. The aGvHD model was set up exactly as described in figure 4.15. Cells were recovered on day 13. Human Treg cells were defined as CD4⁺ CD25⁺ FoxP3⁺ after gating on the human CD45⁺ cells and analysed by intracellular flow cytometry. Graphical representation of the total number and percentage of human Treg cells recovered from the spleen (A) and lung (B). The total number of human cells was assessed using counting beads during flow cytometry. n=6 per group (2 PBMC donors). Statistical analysis was carried out in comparison to the PBMC group using one way ANOVA Tukey Multiple Comparison Test and unpaired student *t*-test.

Figure 4.35. All formulations of SmPill® had no significant effect on the number and percentage of Treg cells in the liver and GI of aGvHD mice. The aGvHD model was set up exactly as described in figure 4.15. Cells were recovered on day 13. Human Treg cells were defined as CD4+ CD25+ FoxP3+ after gating on the human CD45+ cells and analysed by intracellular flow cytometry. Graphical representation of the total number and percentage of human Treg cells recovered from the liver (A) and GI (B). The total number of human cells was assessed using counting beads during flow cytometry. n=6 per group (2 PBMC donors). Statistical analysis was carried out in comparison to the PBMC group using one way ANOVA Tukey Multiple Comparison Test and unpaired student *t*-test.

4.14. NFAT ACTIVITY IS SIGNIFICANTLY REDUCED IN THE LUNG AND LIVER OF ᴀGᴠHD MICE BY SᴍPILL ® THERAPY

The well characterised mechanism of action of CsA, as detailed in chapter 1, is dependent upon the inhibition of calcineurin, whereby the transcription factor NFAT fails to dephosphorylate and transmigrate into the nucleus to activate expression of genes such as IL2 (Liu *et al.* 1991). On this basis, we hypothesised that a good predictor of CsA efficacy can be obtained through measuring NFAT activity, specifically the active NFATc1 isoform, in the tissues of aGvHD mice. Active NFAT was determined as being the NFATc1 detected within T cells recovered from tissues of aGvHD mice.
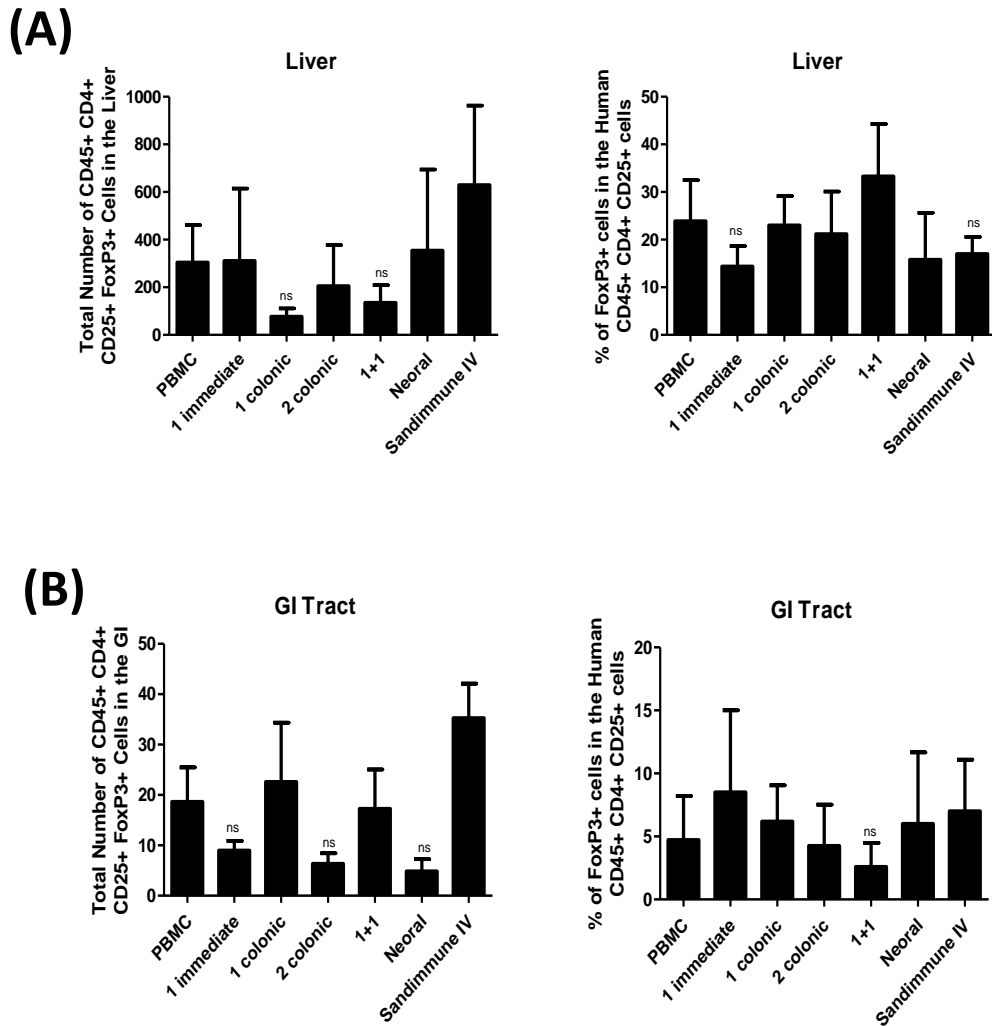
Acute GvHD mice treated with CsA therapies or untreated were sacrificed on day 13 and the spleens, lungs, livers and GI tract were harvested for analysis. Single cell suspensions were prepared and active NFATc1 detected in the nucleus of $CD45^+ CD3^+$ T cells was quantified using nuclear intracellular staining protocols. In the spleen, NFAT activity was reduced by all treatments but none were significant in doing so (Figure 4.36). However, in the lung, all treatments significantly reduced the mean fluorescence intensity of active NFATc1, suggesting that there is sufficient CsA delivered to the lung by all treatments (Figure 4.36). The systemic infusion of Sandimmune® IV was most significant in reducing active NFAT in the lung (Figure 4.36).

In the GI tract, all SmPill® therapies reduced the mean fluorescence intensity of NFATc1 in the nucleus of $CD3^+$ T cells, however Sandimmune® IV was significant in doing so (Figure 4.37). In the liver, NFAT activity was significantly reduced by all therapies with the 1 immediate + 1 colonic SmPill® therapy, Neoral® and Sandimmune® IV being the most significant (Figure 4.37). This data suggests that there is similar reduced NFAT activity in all of the tissues by the different targeted deliveries of CsA with significant decreases observed in the lung and liver of aGvHD mice.

(A) Spleen

(B) Lung
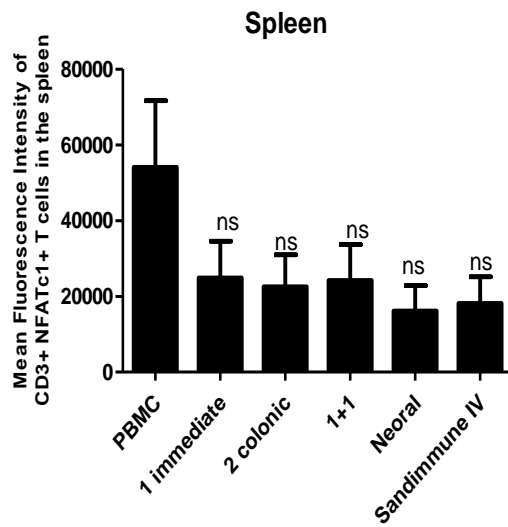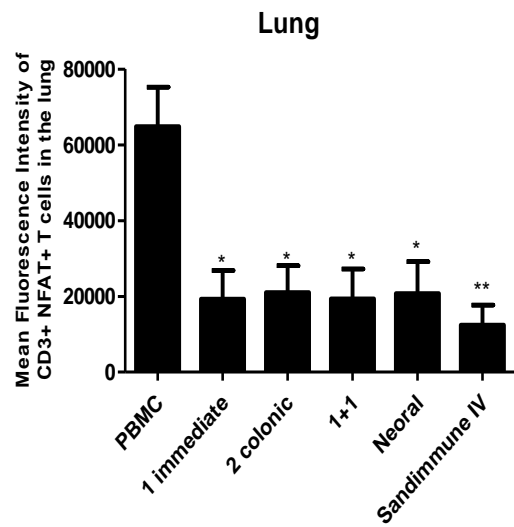
Figure 4.36. SmPill® significantly reduced the mean fluorescence intensity of CD3$^+$ T cells expressing active NFATc1 in the lungs of aGvHD mice. The aGvHD model was set up exactly as described in figure 4.15. Cells were recovered on day 13 and analysed by nuclear intracellular flow cytometry. Graphical representation of the mean flourescence intensity of NFATc1 in CD3$^+$ T cells recovered from the spleen (A) and lung (B). The total number of human cells was assessed using counting beads during flow cytometry. n=4 per group (2 PBMC donors). Statistical analysis was carried out in comparison to the PBMC group using unpaired student t-test where * <0.05 and ** <0.01.
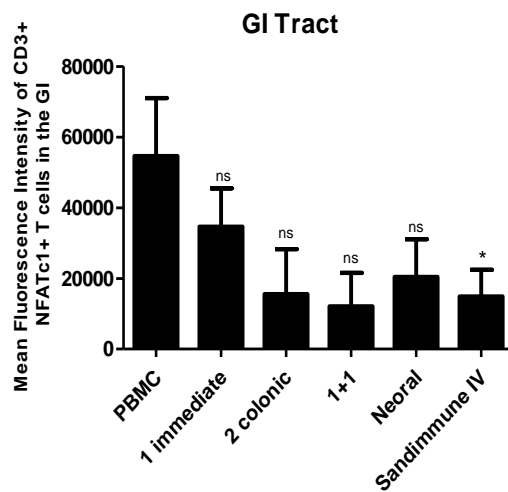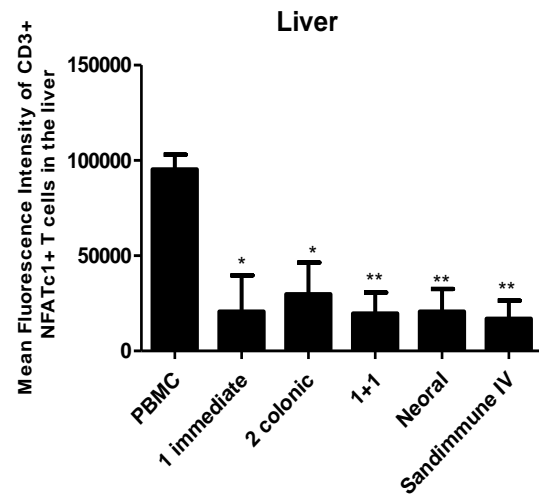
Figure 4.37. All CsA therapies significantly reduced the mean fluorescence intensity of active NFATc1 in CD3$^+$ T cells in the liver of aGvHD mice. The aGvHD model was set up exactly as described in figure 4.15. Cells were recovered on day 13 and analysed by nuclear intracellular flow cytometry. Graphical representation of the mean flourescence intensity of NFATc1 in CD3$^+$ T cells recovered from the GI tract (A) and liver (B). The total number of human cells was assessed using counting beads during flow cytometry. n=4 per group (2 PBMC donors). Statistical analysis was carried out in comparison to the PBMC group using unpaired student t-test where * <0.05 and ** <0.01.

.

4.15.   SUMMARY II

The main objectives of this chapter were to 1) to assess the performance of the novel CsA formulation, SmPill® in the humanised model of aGvHD and 2) to determine if SmPill® therapy has the potential to benefit both GI and systemic GvHD in the humanised model. This section presents more evidence of SmPill® being a significantly better oral CsA therapy than Neoral® where the survival of aGvHD mice was significantly improved and their weight loss was significantly reduced using the 1 immediate and 1 colonic bead combination (Figure 4.16).   Interestingly, delivery of either 1 immediate or 1 colonic alone significantly prolonged survival in aGvHD mice also (Figure 4.16 A).   This suggests that both systemic and GI targeted delivery of CsA can be efficacious in their own right.

Investigating systemic and GI protection by SmPill®, histological analysis revealed that targeted SmPill® delivery of CsA differentially protects systemic or GI organs from aGvHD associated tissue damage and apoptosis (Figures 4.17 – 4.19). The 1 immediate and 1 colonic bead combination gave the most significant protection in the liver and lung, however this protection is reduced when 1 or 2 colonic beads are given instead (Figures 4.17 and 4.19). Similarly, the significant protection in the GI mediated by the 1 immediate + 1 colonic combination is lost when 1 immediate is given alone (Figures 4.18 and 4.19). This highlights how CsA is poorly absorbed in the GI and a sustained release of the drug using SmPill® technology is necessary for optimal GI protection.

Probing systemic and GI protection by SmPill® further, cytokine analysis in the spleen, lung, liver, small intestine and colon confirmed that SmPill® delivery of CsA differentially protects systemic or GI organs from aGvHD. The 1 immediate and 1 colonic combination provided significant reduction in proinflammatory cytokines across all systemic and GI specific organs, as summarised in table 4.1 – 4.5. The 1 immediate alone provided significant reduction in the proinflammatory cytokines detected in the liver and lung,

however protection in the colon was not significant (Figures 4.25 – 4.27). Unexpectedly, in addition to GI there was systemic protection from proinflammatory cytokines mediated by 2 colonic beads alone, as summarised in tables 4.1 – 4.5. This reinforces the primary role the GI plays in the aGvHD response and this data suggests that targeted delivery of CsA can provide systemic protection by means of proinflammatory cytokine reduction in the spleen, liver and lung.

Next we characterised the influence of these different SmPill® formulations on delivering CsA systemically or targeting the GI further by measuring the production of TNFα by CD4$^+$ and CD8$^+$ T cells in target organs and in the serum of aGvHD mice. These findings supported both the histological findings and cytokine analysis and affirmed the hypothesis that TNFα production by T cells in systemic and GI tissues is regulated by specific targeted combinations of SmPill®. The 1 immediate + 1 colonic combination proved to be significantly effective systemically and in the GI (Figures 4.29 – 4.33).

Importantly, the effect that SmPill® formulations have on Treg, defined as CD4$^+$ CD25$^+$ FoxP3$^+$ cells, engraftment in aGvHD mice was analysed. It was revealed that the number and percentage of Tregs recovered from aGvHD tissues was not significantly changed by any CsA therapy compared to untreated aGvHD mice (Figures 4.34 and 4.35).

As CsA is known to reduce NFAT activity through calcineurin inhibition, this characteristic of CsA was assessed in all the SmPill® formulations as a means of further determining efficacy of targeted delivery. All of the SmPill® formulations reduced active NFAT in CD3$^+$ T cells recovered from the GI and significantly in the lung and liver (Figure 4.36 and 4.37). This data suggests that there is similar NFAT activity within these tissues and that each SmPill® formulation regulates this activity in a comparable manner.

Collectively the data in this section provides a thorough evaluation into SmPill® efficacy as a therapeutic intervention for aGvHD with a specific focus on targeted delivery

to systemic organs and GI organs. The results of which determined that a balanced efficacy is required for optimal management of a multi-system disease like aGvHD and the 1 immediate and 1 colonic SmPill® combination provided significant protection in each of the target organs in aGvHD.

CHAPTER 5

MSC REQUIRE PRE-LICENSING FOR EFFICACY WITH SMPILL® IN A HUMANISED MOUSE MODEL OF AGVHD

5.1. INTRODUCTION

The use of MSC as a cellular therapy for inflammatory diseases such as acute GvHD was first suggested by Lee *et al*. and has since garnered considerable interest owing to their potent immunosuppressive and immune evasive properties (Lee *et al.* 2002; Ryan *et al.* 2005; Tobin *et al*. 2013). Le Blanc *et al*. were the first to demonstrate the striking clinical efficacy of MSC as an allogeneic cell therapy for patients with steroid resistant grade IV GvHD, however the precise mechanisms employed by MSC to mediate their effect was not determined (Le Blanc *et al*. 2004). Despite the clear potential of MSC therapy, the impact of this cellular therapy for aGvHD has provided mixed results from clinical trials (Le Blanc *et al.* 2008; Kebriaei *et al.* 2009; Martin *et al.* 2010). As discussed in more detail in Chapter 1, most phase II trials have provided encouraging results, however, while a number of Phase III trials have been completed, there has been no published study to date showing comparable efficacy to that of the initial study led by Le Blanc *et al*. This is likely due to the variations in preparation, dosing, frequency of MSC infusion, donor source, culture conditions and the lack of understanding of MSC fate post infusion (Ankrum & Karp 2010; Herrmann & Sturm 2014). Moreover, there remains a lack of understanding on the influence of immunosuppressive drugs on MSC therapeutic efficacy in aGvHD.

The use of immunosuppressive drugs has resulted in significant increases in survival and provided huge improvements to the standard of living for GvHD patients (Van Lint *et al.* 2006; MacMillan *et al*. 2002). In particular CsA, has been reported to be effective in the treatment of established GvHD and is currently recommended throughout Europe (Parquet *et al*. 2000; Finke *et al.* 2009; Ruutu *et al.* 2014). However, as discussed in Chapter 1, there are problems associated with CsA such as nephrotoxicity, variable bioavailability and increased risk of infection from long term immunosuppression. The introduction of a combination therapy consisting of MSC and CsA for aGvHD in the clinic has the potential

to overcome these issues. The intrinsic pro-reparative properties of MSC should reduce these harmful side effects and the immune regulatory capacity of MSC would support the use of a lower dose of CsA. However, one of the major challenges in successfully translating MSC therapy into the clinic is due to the lack of understanding of the interactions of MSC with immunosuppressive drugs such as CsA.

MSC and CsA have been reported as having synergistic suppressive effects of T cell proliferation *in vitro* (K Le Blanc *et al*. 2004; Maccario *et al*. 2005; Shi *et al*. 2011). Findings from Chapter 3 support this and determined that synergy is dependent on the activation status of MSC where prestimulating MSC with IFNγ facilitated synergism with CsA *in vitro*. However, murine models of transplantation have shown how MSC and CsA have negative interactions whereby low dose CsA in combination with MSC accelerated allograft rejection in these models (Inoue *et al.* 2006; Jia *et al.* 2012).

Established models of inflammatory disease provide a rich environment of IFNγ/TNFα which activate MSC and supports their efficacy as immunomodulators. Previous work within our research group demonstrated that timing of MSC administration and proinflammatory cytokine levels *in vivo* are critical for MSC effectiveness as immunosuppressive agents in aGvHD (Tobin *et al*. 2013). As CsA significantly suppressed proinflammatory cytokines in the tissues of this aGvHD model (Chapter 4) the next step requires the establishment of optimal conditions for MSC and CsA co-therapy *in vivo*. On this basis and building on findings obtained in chapter 3, the efficacy of prestimulating MSC with IFNγ before CsA treatment warrants further investigation *in vivo* using this humanised mouse model of aGvHD. Furthermore, many patients undergoing HSCT transplant will have undergone a prophylaxis regimen involving CsA immunosuppression, therefore emphasizing the clinical relevance of this investigation.

Therefore, the aims of this chapter are to investigate the synergy of MSC and CsA *in vivo* and to define the optimal conditions for their efficacy as a co-therapy in aGvHD. As in chapter 4, a robust and reproducible humanised mouse model will be used as a platform to make these assessments of therapeutic interventions in aGvHD and achieve these aims.

The objectives of this chapter are outlined as follows:

- Determine if MSC and SmPill® are efficacious as a co-therapy for aGvHD

- Investigate if pre-licensing MSC with IFNγ (MSCγ) enhances MSC and SmPill® co-therapy

- Examine the effects of oral (SmPill®) and intravenous (Sandimmune® IV) routes of CsA administration on the efficacy of MSC and MSCγ therapy and vice versa

- Elucidate the conditions for optimal efficacy of MSC and CsA co-therapy for aGvHD.

5.2. MSCγ AND SᴍPILL® CO-THERAPY SIGNIFICANTLY PROLONGED SURVIVAL AND REDUCED WEIGHT LOSS IN ᴀGᴠHD MICE

Throughout chapter 4, SmPill® and Sandimmune® IV therapy were shown to significantly prolong survival and reduce weight loss in a humanised model of aGvHD. Previous research from our laboratory demonstrated that MSC and IFNγ stimulated MSC (MSCγ) prolonged the survival and reduced pathology of aGvHD mice (Tobin *et al.* 2013). Therefore, the next step was to firstly investigate if MSC and CsA are efficacious as a co-therapy in aGvHD and secondly if pre-licensing MSC (MSCγ) would further enhance the co-therapy in prolonging survival and preventing aGvHD progression.

As before, NSG mice were irradiated (2.4 Gy) and injected with PBMC (8 x 10^5 gram^{-1}) or PBS via tail vein injection. MSC\MSCγ therapy (6.4 x 10^4 gram^{-1}) was delivered intravenously on day 6. CsA therapy was administered intravenously (Sandimmune® IV) or by oral gavage (SmPill®) for 5 doses (25mg/kg per dose) from day 4 (Figure 5.1 A). Treatment groups were assigned as outlined in figure 5.1 B. Transplanted mice were closely monitored as before and the survival and weight loss of each mouse recorded (Figure 5.1).

NSG mice which received PBMC consistently developed aGvHD with a median survival time (MST) of 11.5 days with none surviving past day 15 (Figure 5.2 – 5.4). While, all therapies alone significantly prolonged survival and reduced weight loss in aGvHD mice (Figure 5.2), SmPill® was the most efficacoius therapy in terms of survival and weight loss. Mice treated with SmPill® alone had an MST of 22 days which was significantly better than MSC treatment, where the MST was 16.5 days (Figure 5.2 A). MSCγ alone and Sandimmune® IV prolonged survival in a similar manner to SmPill® where the MST for MSCγ and Sandimmune® IV were 19.5 and 19 days, respectively (Figure 5.2 A). In terms of weight loss, SmPill® was significantly better than both MSC therapies and Sandimmune® IV at reducing weight loss in aGvHD mice (Figure 5.2 B). Sandimmune® IV therapy

resulted in significantly less weight loss than MSC but was comparable to the weight loss experienced by aGvHD mice that received MSCγ therapy (Figure 5.2 B).

The co-treatment of MSC and SmPill® (14.5 days MST) did not significantly enhance survival of aGvHD mice (Figure 5.3 A). While the MSC and SmPill® combined therapy (14.5 days MST) had no significant difference in survival to MSC alone (16.5 days MST), it was significantly less efficacious than SmPill® alone (22 days MST) (Figure 5.3 A). However, pre-licensed MSC (MSCγ) in combination with SmPill® was a significantly better co-therapy with an MST of 16.5 days and prolonged survival in a similar manner to either therapy alone (Figure 5.3 A). In relation to weight loss, the combined treatment of SmPill® with resting MSC or MSCγ did not significantly reduce weight loss in aGvHD mice and both combinations were significantly less efficacious than SmPill® alone but similar to either single MSC therapy (Figure 5.3 B). This suggests that MSC hamper the efficacy of SmPill®. While pre-licensing of MSC is better than resting MSC for co-treatment with SmPill®, SmPill® was most efficacious when administered alone.

Sandimmune® IV combined with MSC significantly enhanced the survival of aGvHD mice to 27 days (MST) with similar efficacy to Sandimmune® IV alone (19 days MST) but was significantly better than MSC alone (16.5 days MST (Figure 5.4 A). The MSCγ and Sandimmune® IV co-therapy also significantly prolonged survival in aGvHD mice with an MST of 18 days which displayed similar efficacy compared to the single therapies Sandimmune® IV (19 days MST) and MSCγ (19.5 days) (Figure 5.4 A). Sandimmune® IV combined with either MSC or MSCγ significantly reduced weight loss in aGvHD mice in a similar manner to Sandimmune® alone (Figure 5.4 B). However, the combination of Sandimmune® IV with MSC resulted in significantly less weight loss than MSC alone (Figure 5.4 B). This suggests that Sandimmune® IV and MSC can be efficacious without the requirement of MSC pre-licensing for co-treatment.

(A)
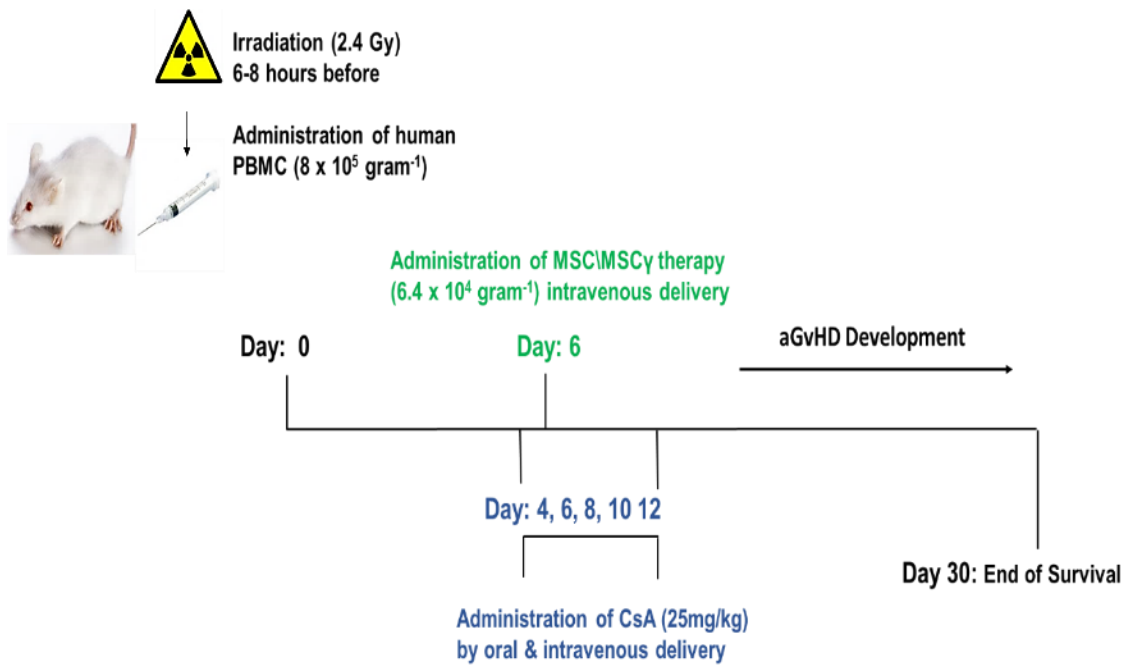
(B)

Mice were assigned as follows;
MSC on day 6
MSCγ on day 6
SmPill® on day 4,6,8,10,12
Sandimmune® IV on day 4,6,8,10,12
MSC on day 6 + SmPill® on day 4,6,8,10,12
MSC on day 6 + Sandimmune® IV on day 4,6,8,10,12
MSCγ on day 6 + SmPill® on day 4,6,8,10,12
MSCγ on day 6 + Sandimmune® IV on day 4,6,8,10,12

Figure 5.1. Assessing the performance of MSC therapy against and in combination with CsA therapy using the humanised mouse model of aGvHD. NOD-SCID IL-2rγ[null] (NSG) mice were exposed to a sub-lethal dose of gamma irradiation (2.4 Gy). 8×10^5 PBMC gram[-1] or sterile PBS was then administered intravenously (300 µl) to each mouse via the tail vein on day 0 (A). MSC\MSCγ therapy (6.4×10^4 gram[-1]) was delivered intravenously on day 6. CsA therapy was administered intravenously (Sandimmune® IV) or by oral gavage (SmPill®) for 5 doses (25mg/kg per dose) from day 4. The SmPill® dose consisted of 1 immediate and 1 colonic release CsA loaded bead each time. Mice were assigned treatment groups as outlined in (B). The development of aGvHD was monitored every second day until day 9 and then everyday thereafter by recording weight loss, appearance, posture and activity.

(A)
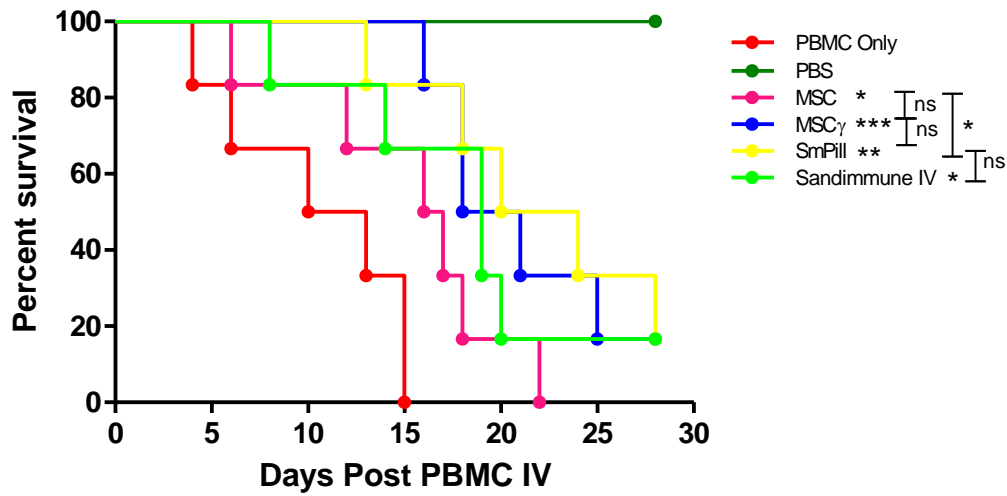
(B)
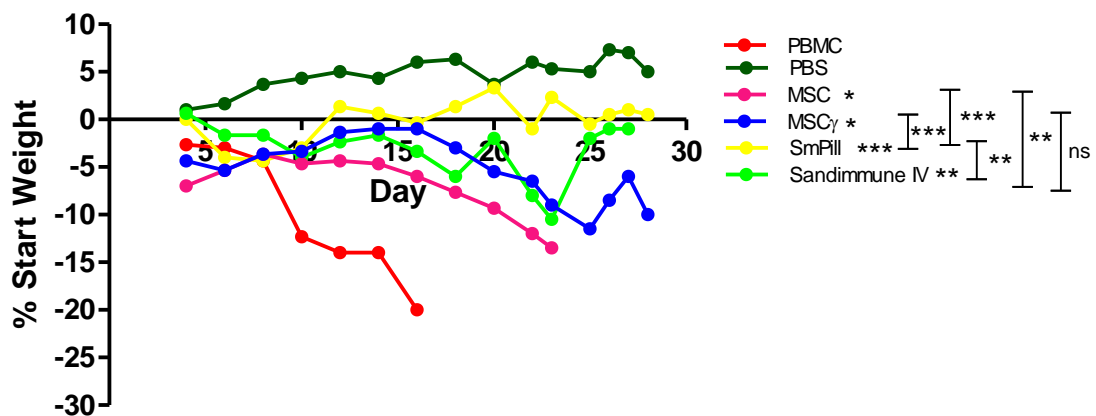
Figure 5.2. All therapies alone significantly prolonged survival and reduced weight loss in aGvHD mice. 8×10^5 human PBMC gram^{-1} were administered to irradiated NSG mice (2.4Gy) on day 0. 6.4×10^4 human MSC or MSCγ gram^{-1} were administered on day 6. CsA was delivered intravenously (Sandimmune® IV) and by oral gavage (SmPill®) for 5 doses (25mg/kg per dose) every 2 days from day 4. Transplanted mice were monitored every 2 days until day 9 and then every day for the duration of the experiment. Graphical presentation of survival curve (A), and percentage weight change of aGvHD mice (B). n=6 mice for each group. Statistical analysis was carried out using a Mantel-Cox test for the survival curve and unpaired student *t*-test for weight change where * <0.05, ** <0.01 and *** <0.001. Stars with no bar are in comparison to the PBMC group.

Figure 5.3. IFNγ licensing of MSC was required for efficacy with SmPill® co-therapy in significantly prolonging survival in aGvHD mice. 8×10^5 human PBMC gram^{-1} were administered to irradiated NSG mice (2.4Gy) on day 0. 6.4×10^4 human MSC or MSCγ gram^{-1} were administered i.v. on day 6. CsA was delivered by oral gavage (SmPill®) for 5 doses (25mg/kg per dose) every 2 days from day 4. Transplanted mice were monitored every 2 days until day 9 and then every day for the duration of the experiment. Graphical presentation of survival curve (A), and percentage weight change of aGvHD mice (B). n=6 mice for each group. Statistical analysis was carried out using a Mantel-Cox test for the survival curve and unpaired student t-test for weight change where * <0.05, ** <0.01 and *** <0.001. Stars with no bar are in comparison to the PBMC group.

(A)
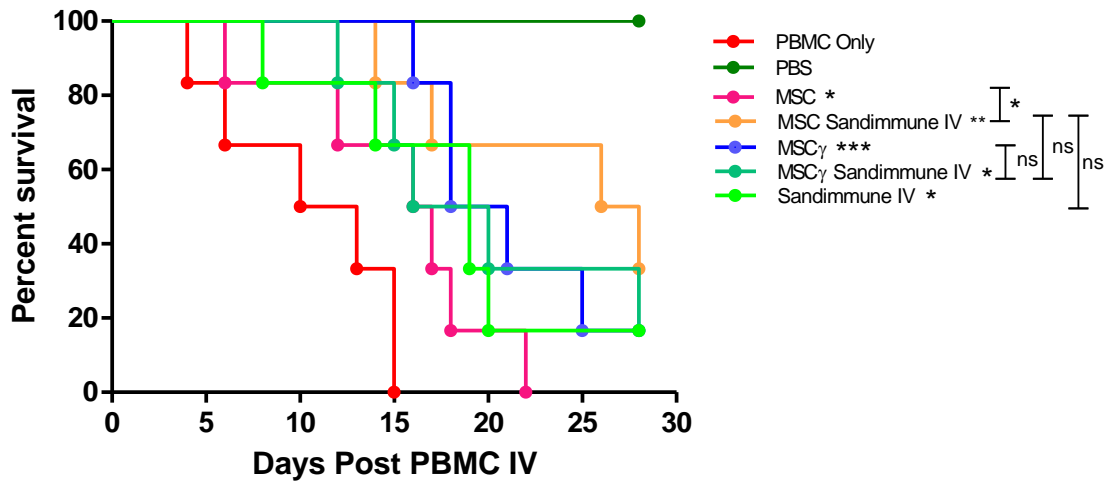
(B)
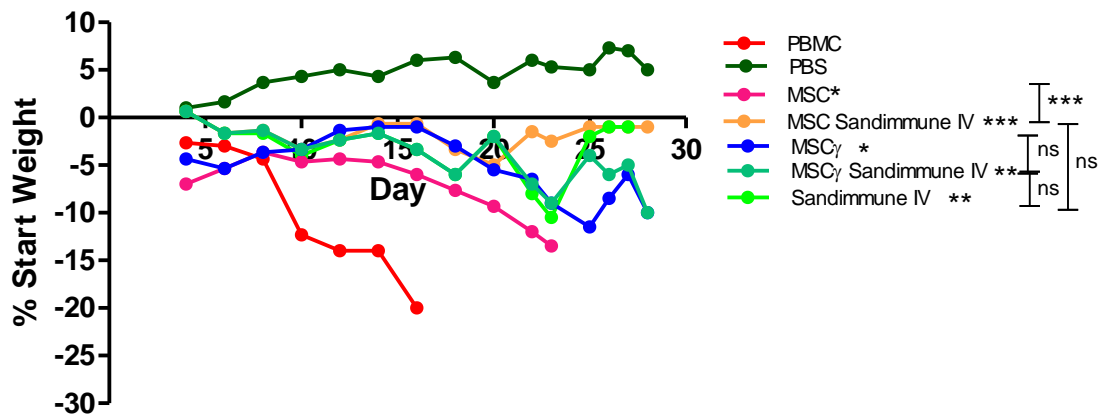
Figure 5.4. Sandimmune® IV significantly enhanced resting MSC therapy where survival was prolonged and weight loss reduced in aGvHD mice. 8×10^5 human PBMC gram^{-1} were administered to irradiated NSG mice (2.4Gy) on day 0. 6.4×10^4 human MSC or MSCγ gram^{-1} were administered on day 6. CsA was delivered intravenously (Sandimmune® IV) for 5 doses (25mg/kg per dose) every 2 days from day 4. Transplanted mice were monitored every 2 days until day 9 and then every day for the duration of the experiment. Graphical representation of survival curve (A), and percentage weight change of aGvHD mice (B). n=6 mice for each group. Statistical analysis was carried out using a Mantel-Cox test for the survival curve and unpaired student t-test for weight change where * <0.05, ** <0.01 and *** <0.001. Stars with no bar are in comparison to the PBMC group.

5.3. MSCγ AND SᴍPILL® CO-THERAPY SIGNIFICANTLY IMPROVED PATHOLOGY AND REDUCED APOPTOSIS IN THE TISSUES OF ᴀGᴠHD MICE

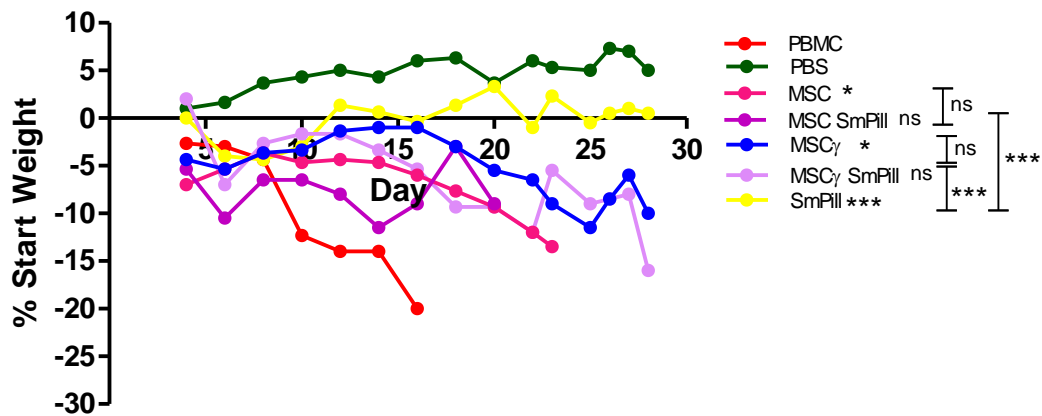The liver, lung, small intestine and colon are the principle target organs in aGvHD. The efficacy of SmPill® and Sandimmune® IV in improving aGvHD pathology was demonstrated earlier in chapter 4. Figure 5.3 and 5.4 show that MSC and CsA therapies alone significantly prolonged survival in aGvHD mice, however, there were significant differences when they were combined as a co-therapy. Therefore, histological analysis was carried out on aGvHD target organs to investigate further the efficacy of these co-treatments with MSC or CsA alone.

Formalin fixed tissue sections were stained with H&E and the histological aGvHD score was evaluated for each treatment group, according to the criteria described in section 2.10.4 (Tobin *et al*. 2013). Irradiation and PBS administration did not adversely affect liver pathology as measured by lymphocyte infiltration (l) and thickening of hepatic veins (t) (Figure 5.5 A). PBMC mice displayed significant periportal infiltration of mononuclear cells with evidence of hepatic portal vein thickening (Figure 5.5 A). Treatment with resting MSC reduced hepatic portal inflammation but this was not significant (Figure 5.5 A) whereas MSCγ therapy significantly lowered lymphocyte infiltration into the hepatic veins (Figure 5.5 A). Consistent with the findings in chapter 4, SmPill® and Sandimmune® IV therapy significantly reduced liver pathology. Both CsA treatments were more protective in the liver than MSC but their efficacy was comparable to that of MSCγ therapy (Figure 5.5). The administration of resting MSC significantly hampered SmPill® efficacy (Figure 5.5 B). However, the IFNγ activation of MSC (MSCγ) before administration with SmPill® significantly alleviated this effect (Figure 5.5 B). Interestingly, this was not the case when resting MSC or MSCγ was combined with Sandimmune® IV, as both combinations had no

significant differences in efficacy in comparison to Sandimmune® IV therapy alone (Figure 5.5 B).

PBS control mice demonstrated no adverse effect on lung architecture as evaluated by lymphocyte infiltration around peribronchial spaces (l) and the thickening of airway epithelium (t) (Figure 5.5 A). Following aGvHD development, PBMC mice exhibited a significant cluster of lymphocyte infiltrate around peribronchial spaces with corroborating evidence of airway epithelium thickening (Figure 5.5 A). Administration of resting MSC or MSCγ significantly reduced lymphocyte infiltration and thickening of airway epithelium (Figure 5.5 B). Sandimmune® IV treatment alone significantly reduced lung pathology in a similar manner to MSC and MSCγ, however SmPill® therapy was the most effective single treatment for lung pathology. Similar to the findings in the liver sections, the administration of resting MSC significantly hampered SmPill® efficacy (Figure 5.5 B). Again, the IFNγ activation of MSC (MSCγ) before administration with SmPill® significantly alleviated this effect (Figure 5.5 B). Combination therapies of Sandimmune® IV with resting MSC or MSCγ had no significant differences in comparison to Sandimmune® IV therapy alone and both co-therapies significantly reduced lung inflammation around the small arteries and veins (Figure 5.5).

GvHD pathology in the small intestine was characterised as destruction or blunting of villi (v). The administration of PBS resulted in no alterations to the structure of villi (Figure 5.6 A), whereas GvHD (PBMC) mice displayed significant changes in pathology with destruction and blunting of villi frequently evident (Figure 5.6 B). Sandimmune® IV alone resulted in a significant reduction of villi blunting in the small intestine of aGvHD mice in a similar manner to MSC, however MSCγ was more effective with SmPill® being most efficacious single therapy in this case. (Figure 5.6 B). When MSC/MSCγ was used in combination with SmPill® or Sandimmune® IV, there was no significant differences in

efficacy (Figure 5.6 B). This suggests that there is no enhancement over single therapies but importantly, MSC therapies did not negatively impact CsA therapies and vice versa.

In the colon, GvHD pathology was measured by the occurance of ulceration in the crypts of colonic mucosa (u). This ulceration was due to the infiltration of lymphocytes which distorted the structure of the crypts and encouraged formation of abscesses. PBS control mice displayed features of healthy colonic crypt structure with normal gland architecture (Figure 5.6 A). However, GvHD (PBMC) mice manifested signs of aGvHD pathology in the colon with significant crypt ulceration or hyperplasia as a result of lymphocyte infiltration (Figure 5.6 A). Resting MSC had no significant effect on reducing aGvHD pathology in the colon, however, MSCγ significantly improved pathology (Figure 5.6 B). While SmPill® therapy alone was significantly efficacious in reducing signs of aGvHD in the colon, the combination of SmPill® with MSCγ had comparable efficacy to SmPill® or MSCγ alone. However, the combination of SmPill® with resting MSC was not significant in reducing colon pathology (Figure 5.6 B). The GvHD pathology in the colon of Sandimmune® IV treated mice were similar to mice who received SmPill® therapy and there were no significant changes to Sandimmune® IV efficacy when combined with resting MSC or MSCγ (Figure 5.6 B).

This data displays evidence of how CsA in combination with MSC can provide differential protection to systemic and GI aGvHD tissues which is dependent on CsA delivery and MSC activation status. SmPill® combined with MSCγ provided a more favourable therapy in the liver and lung than combination with MSC. However, the co-treatment of Sandimmune® IV with either MSC therapy provided systemic protection in an equal manner. In the GI tissues, there was similar protection provided by Sandimmune® IV when combined with either MSC therapy. However, MSCγ and SmPill® co-therapy was significantly better than MSC and SmPill® co-therapy in the GI tissues. In general, both

MSC therapies were more efficacious when they were combined with either CsA therapy. These findings suggest that licensed MSC are better suited with SmPill® for systemic and GI treatment than resting MSC. However, there was no enhancement in combining MSCγ therapy with SmPill® and this suggests that SmPill® is a more suitable therapy administered on its own. It also suggests that Sandimmune® IV can be combined with either MSC therapy for systemic and GI protection.

MSC and MSCγ alone were more efficacious in preventing tissue damage in the lungs and small intestine than the liver and colon of aGvHD mice. The effects of a systemic (Sandimmune® IV) or GI targeted (SmPill®) CsA on the effectiveness of MSC treatment were probed further by comparing apoptotic damage in these tissues. To detect apoptosis in the lung and small intestine, a commercially available TUNEL assay kit was used, as described in section 2.11.3. The TUNEL assay revealed that lung sections from untreated aGvHD mice had detectable apoptotic damage (Figure 5.7). Apoptosis was not detected in lung sections from PBS control mice. Treatment with resting MSC reduced apoptosis while MSCγ therapy further mitigated apoptotic damage in the lung. Consistent with chapter 4, Sandimmune® IV and SmPill® therapy were shown to alleviate apoptotic damage in the lungs of aGvHD mice. The combination of Sandimmune® IV CsA with resting MSC and MSCγ attenuated apoptotic damage in the lung in comparison to untreated aGvHD mice (Figure 5.7). However, SmPill® protection from apoptotic lung damage was impaired by resting MSC but not MSCγ. Importantly, these observations are supportive of the H&E histological findings (Figure 5.5).

Apoptotic damage was also observed in the small intestine of aGvHD mice but not in PBS control mice (Figure 5.7). Treatment with both resting MSC and MSCγ reduced apoptotic damage in the small intestine of aGvHD mice (Figure 5.7). However, SmPill® therapy displayed an exceptional reduction of apoptosis in the small intestine. When used

in combination with SmPill®, MSCγ were just as efficacious but resting MSC hampered the effectiveness of SmPill® (Figure 5.7). There were no significant changes to Sandimmune® efficacy when combined with resting MSC or MSCγ as all treatments reduced apoptotic damage in an equal manner (Figure 5.7). These findings are also consistent with H&E histological findings (Figure 5.6).

Together the data highlights the importance of MSC pre-licensing for combined efficacy with SmPill® therapy for the alleviation of pathology in aGvHD. Interestingly, pre-licensing of MSC was not required for combined efficacy with Sandimmune® IV which suggests that delivery of CsA via oral (targeted to GI tract) or intravenous routes (systemic) has an impact on MSC therapeutic efficacy. Overall, these findings suggest that MSC has a negative impact on SmPill® therapy which is consistant with the survival and weight loss data.

(A)

	Liver		Lung	
	100X	**400X**	**100X**	**400X**
PBS (Healthy)				
PBMC (GvHD)				
MSC				
MSCγ				
SmPill®				
MSC + SmPill®				
MSCγ + SmPill®				
Sandimmune® IV				
MSC + Sandimmune® IV				
MSCγ + Sandimmune® IV				
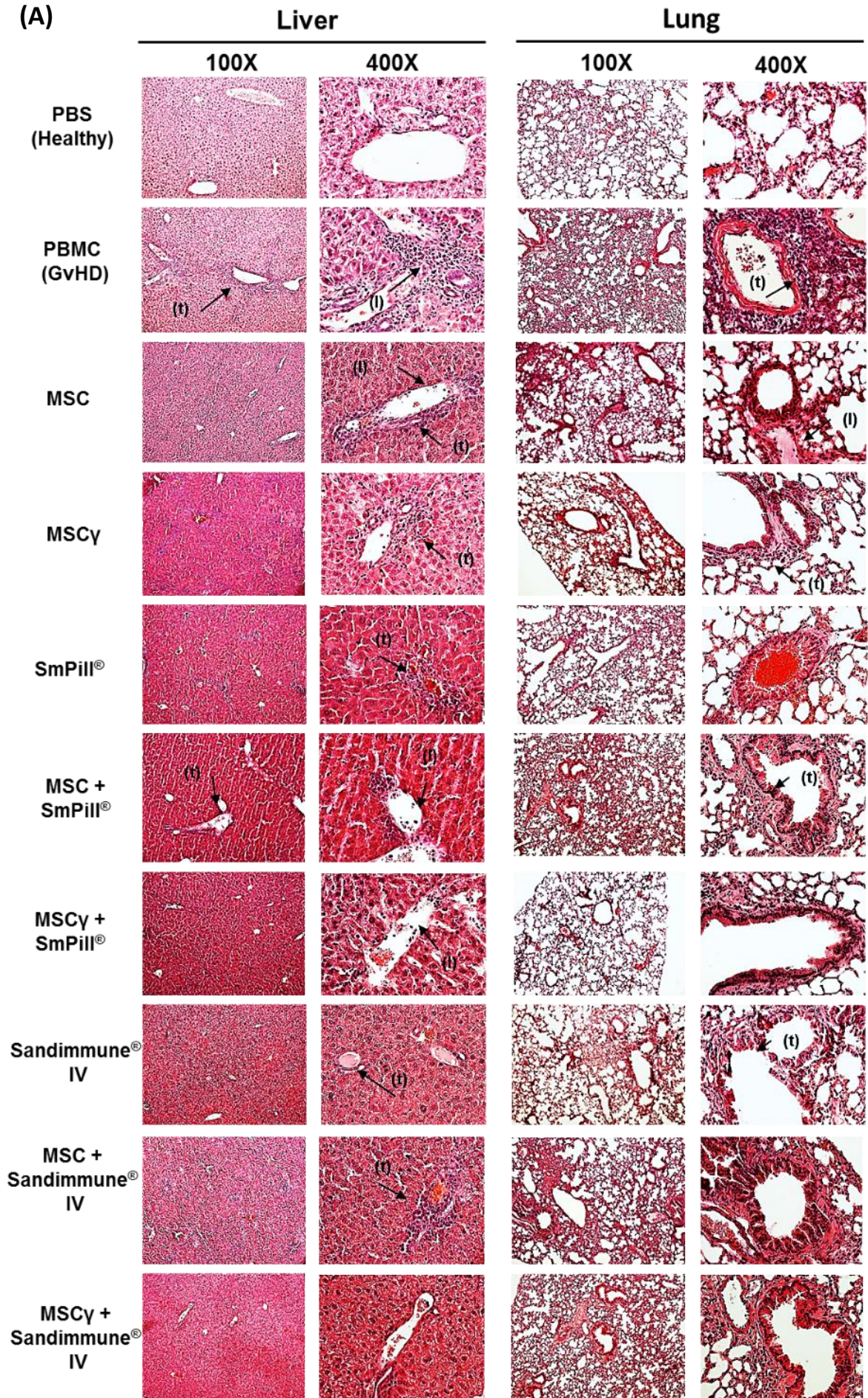
(B)

Figure 5.5. Resting MSC significantly reduced SmPill® therapeutic efficacy in alleviating pathology in the liver and lung of aGvHD mice. The aGvHD model was set up as described in figure 5.1. Tissue samples were harvested on day 13, formalin fixed, paraffin embedded and stained with H&E (A). Representative images were analysed for lymphocyte infiltration (l) and thickening of epithelial airways or hepatic veins (t) and displayed for each group. Images were captured at 100x and 400x. A well defined aGvHD histological scoring system as detailed in section 2.10.4, was carried out in a blinded fashion and used to determine the level of aGvHD development between the groups in the liver and lung (B). n=6 per group (2 MSC donors, 2 PBMC donors). Statistical analysis was carried out using the unpaired student *t*-test where * <0.05, ** <0.01 and *** <0.001. Stars with no bar are in comparison to the PBMC group.

(A)

	Small Intestine 400X	Colon 400X
PBS (Healthy)		
PBMC (GvHD)	(v)	(u)
MSC	(v)	(u)
MSCγ	(v)	
SmPill®	(v)	
MSC + SmPill®		(u)
MSCγ + SmPill®		
Sandimmune® IV	(v)	(u)
MSC + Sandimmune® IV		
MSCγ + Sandimmune® IV		(u)

212
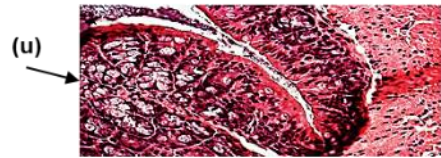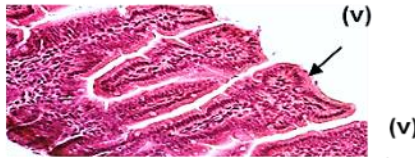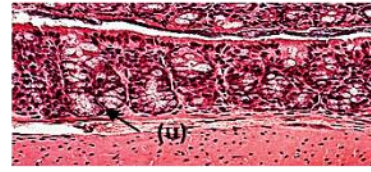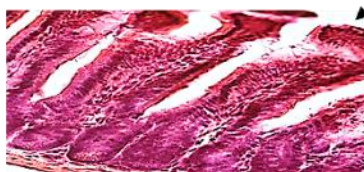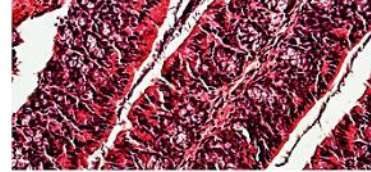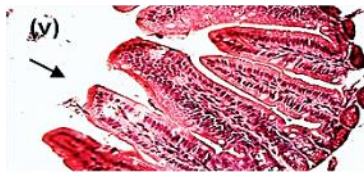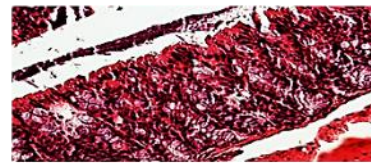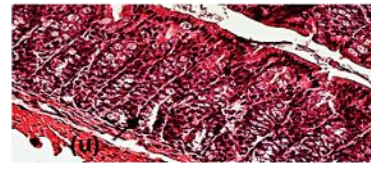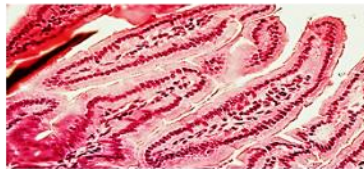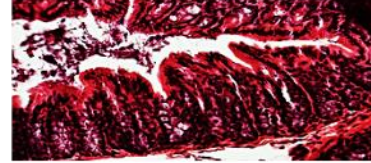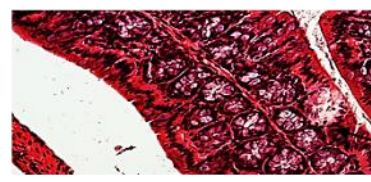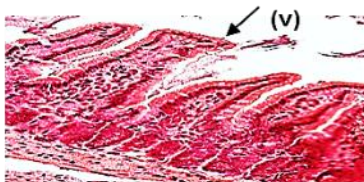
(B)

Figure 5.6. MSC and CsA co-therapies were efficacious in reducing pathology in small intestine and colon of aGvHD mice. The aGvHD model was set up as described in figure 5.1. Tissue samples were harvested on day 13, formalin fixed, paraffin embedded and stained with H&E (A). Representative images displayed for each group were analysed for villi destruction (v) and ulceration of the colonic mucosa (u). Images were captured at 400x. A well defined aGvHD histological scoring system, as detailed in section 2.10.4, was carried out in a blinded fashion and used to determine the level of aGvHD development between the groups in the small intestine and colon (B). n=6 per group (2 MSC donors, 2 PBMC donors). Statistical analysis was carried out using the unpaired student *t*-test where * <0.05, ** <0.01 and *** <0.001. Stars with no bar are in comparison to the PBMC group.

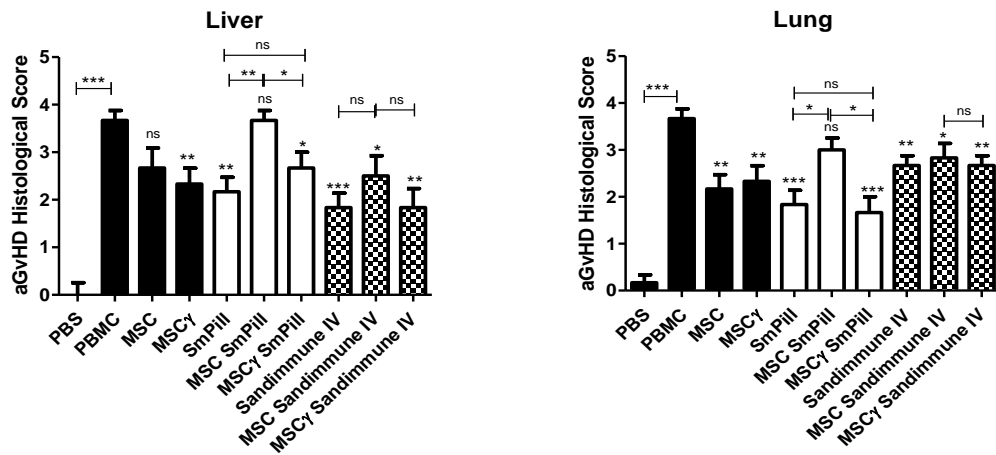|	Lung		Small Intestine	
	DAPI	TUNEL	DAPI	TUNEL
PBS (Healthy)				
PBMC (GvHD)				
MSC				
MSCγ				
SmPill®				
MSC + SmPill®				
MSCγ + SmPill®				
Sandimmune® IV				
MSC + Sandimmune® IV				
MSCγ + Sandimmune® IV				
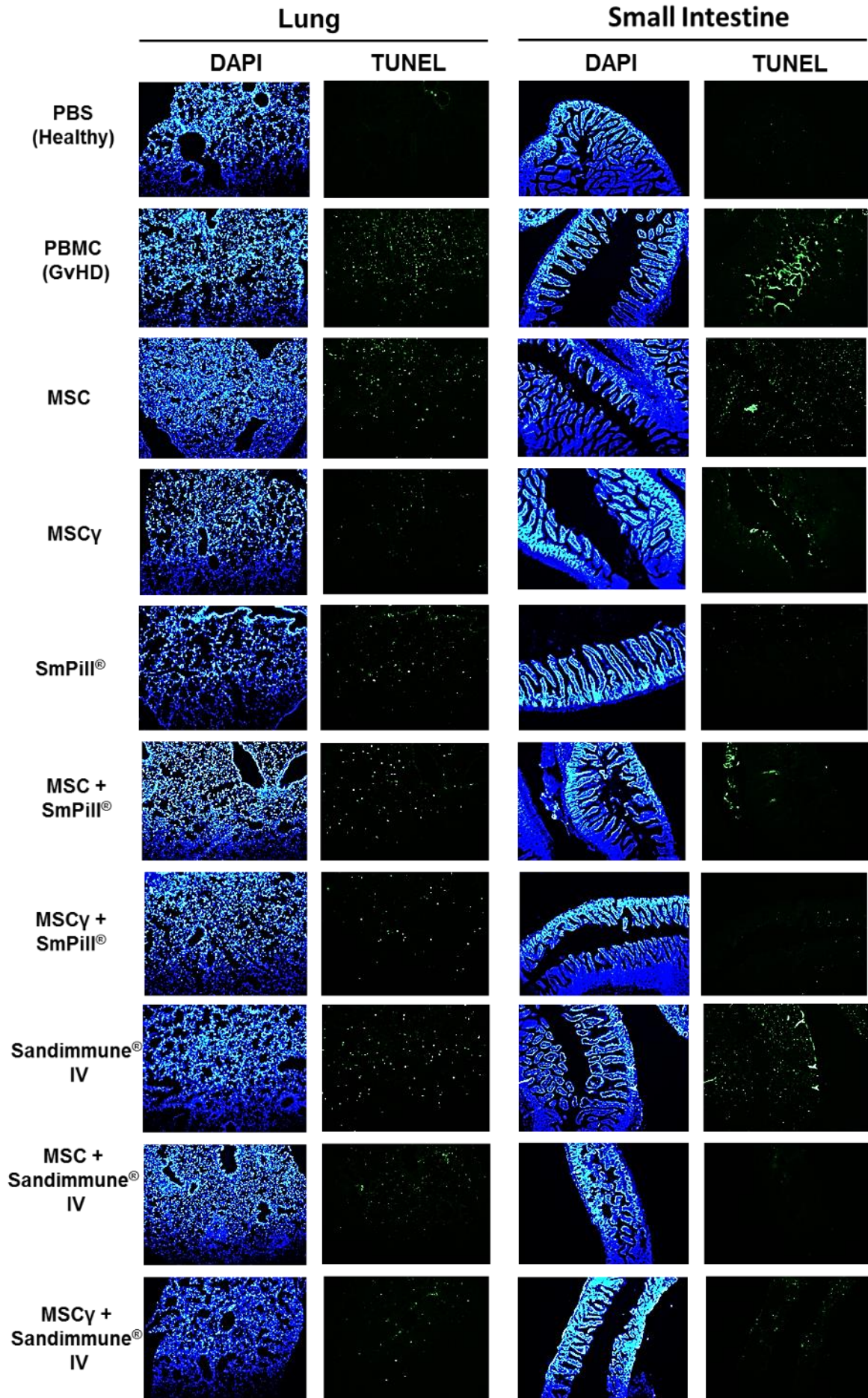
Figure 5.7. Resting MSC significantly reduced SmPill® therapeutic efficacy in reducing apoptosis in the lungs of aGvHD mice. The aGvHD model was set up as described in figure 5.1. Tissue samples were harvested on day 13, formalin fixed, paraffin embedded and TUNEL assay was carried out using a commercially available kit as described in section 2.10.3. TUNEL assay detects DNA fragmentation as a result of apoptosis and emits a green fluorescent light. DAPI was used as a nuclear stain and emits blue fluorescent light upon binding to AT regions of DNA. Representative images are displayed. Images were captured at 100x using a flourescent microscope. n=6 per group (2 MSC donors, 2 PBMC donors).

5.4. DELIVERY OF CsA WITH MSC DICTATED CO-THERAPY EFFICACY OF CYTOKINE MANAGEMENT IN ALL aGVHD TISSUES

The proinflammatory cytokine cascade is a hallmark of aGvHD. There are multiple proinflammatory cytokines associated with aGvHD and each play a role in causing direct tissue damage to target organs, as displayed in section 5.3, by stimulating mature donor T cells and recruiting additional donor mononuclear effector cells (Antin & Ferrara 1992). Hence, if cytokine dysregulation can be controlled in the target organs there will be less tissue damage and the aGvHD response can be effectively managed. Throughout chapter 4, GI targeted (SmPill®) and systemic (Sandimmune® IV) CsA were shown to reduce, in some cases significantly, the proinflammatory cytokines IL1β, IFNγ, IL2, IL17 and IL6 differentially in the tissues of aGvHD mice. As previously described, the immunosuppressive phenotype of MSC is favoured in the presence of proinflammatory cytokines such as IFNγ and TNFα where the mode of action is triggered by the diseased tissue environment. It is therefore important for the efficacy of MSC to retain this immunosuppressive property when combined with GI targeted (SmPill®) or systemic (Sandimmune® IV) CsA.

Using the same model as described in figure 5.1, spleen cells were isolated from the tissue, single cell suspensions were cultured *in vitro*, stimulated with 100 ng/ml PMA and 1 μg/ml ionomycin for 72 hours and IFNγ, TNFα, IL2 and IL17 were detected in supernatants by ELISA. The liver, lung, small intestine and colon tissue were also harvested, snap frozen and homogenates were used to detect the levels of IL1β, IFNγ, IL2, IL17, IL6 and TNFα by ELISA.

In the splenocyte *ex vivo* culture, resting MSC or MSCγ therapy alone reduced the levels of IFNγ and TNFα with significant suppression of IL2 and IL17 (Figure 5.8). Consistent with findings from chapter 4, Sandimmune® IV and SmPill® therapy significantly reduced the

levels of IFNγ, TNFα, IL2 and IL17 (Figure 5.8). Both resting MSC and MSCγ significantly reduced all of these cytokines when used in combination with Sandimmune® IV (Figure 5.8). However, resting and licensed MSC significantly hampered the reduction of IL2 and TNFα by SmPill® in the splenocyte culture while MSCγ improved SmPill® reduction of IL17 (Figure 5.8).

In the liver, resting MSC or MSCγ therapy alone significantly reduced the levels of IL2, IL17, IL1β, IFNγ and TNFα (Figure 5.9). Similar to results shown in chapter 4, SmPill® and Sandimmune® IV treatment alone signifiantly suppressed all of these cytokines in the liver of aGvHD mice (Figure 5.9). When these CsA therapies were combined with resting MSC or MSCγ, these cytokines remained reduced in the liver but in some cases signifance was lost (Figure 5.9).

The cytokine profile from lung homogenates revealed that resting MSC and MSCγ alone significantly suppressed the levels of IL2, IL17, IL1β, IL6, IFNγ and TNFα (Figure 5.10). The combination of MSC or MSCγ with CsA did not have a negative impact of therapeutic efficacy as each of the therapies significantly reduced these proinflammatory cytokines in lung homogenates with no significant differences between groups (Figure 5.10). These results are consistent with H&E histological findings as almost all treatment groups were efficacious in reducing pathology in the lung (Figure 5.5).

In the small intestine, resting MSC and MSCγ alone were shown to significantly reduce IFNγ and TNFα (Figure 5.11). In most cases, there was no significant differences in efficacy when CsA was combined with MSC or MSCγ. However, the combination of resting MSC with SmPill® resulted in a significant impairment of SmPill® effectiveness at suppressing TNFα (Figure 5.11). However, the combination of Sandimmune® IV with resting MSC was significantly better at reducing IFNγ in comparison to MSC alone (Figure 5.11). As the levels

of IFNγ are reduced to a similar level by Sandimmune® IV alone, it is likely that this suppression is mediated by CsA without obstruction from MSC therapy. This data suggests that the delivery route and more likely the bioavailability of CsA can have differential effects on resting MSC and the potential for co-therapy efficacy reflects this.

In colon homogenates, MSC and MSCγ alone significantly supressed levels of IL1β, IL6 and IFNγ (Figure 5.12). Interestingly, when both were combined with SmPill® and Sandimmune® IV there was no negative impact on the effectiveness of the co-therapies in comparison to their singular counterparts as there was no significant differences between them in any of the cytokine levels detected (Figure 5.12).

The differences in the efficacy of all the treatments reflects the dysregulated nature and complexity of these cytokines in aGvHD. The data suggests that management of these cytokines by each of these therapies varies between systemic and GI tissues. This is likely due to the differences in the activation status of MSC and the relative bioavailability of CsA in these tissues, depending on oral or intravenous route of administration. All of these findings are summarised in tables 5.1 – 5.5.

Spleen
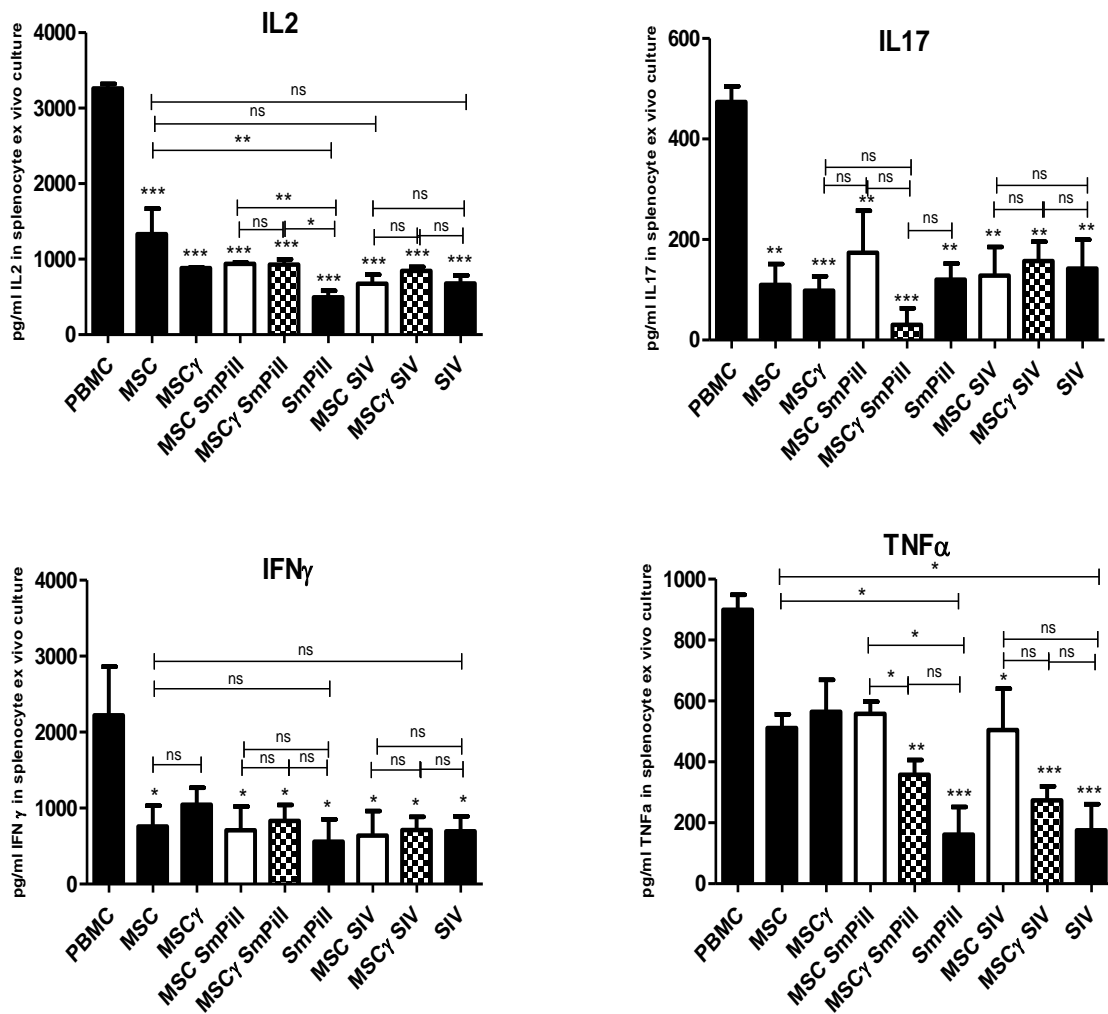
Figure 5.8. Resting MSC significantly hampered the reduction of IL2 and TNFα by SmPill® in the spleen of aGvHD mice. The aGvHD model was set up as described in figure 5.1. Tissue samples were harvested on day 13, single cell suspensions were cultured *in vitro* and stimulated with 100 ng/ml PMA and 1 µg/ml ionomycin for up to 72 hours. Supernatants were collected and ELISA was used to detect proinflammatory cytokines (IL2, IL17, IFNγ, and TNFα). n=6 per group (2 MSC donors, 2 PBMC donors). Statistical analysis was carried out using one way ANOVA Tukey Multiple Cmparison Test and unpaired student *t*-test where * <0.05, ** <0.01 and *** <0.001. Stars with no bar are in comparison to the PBMC group.

219
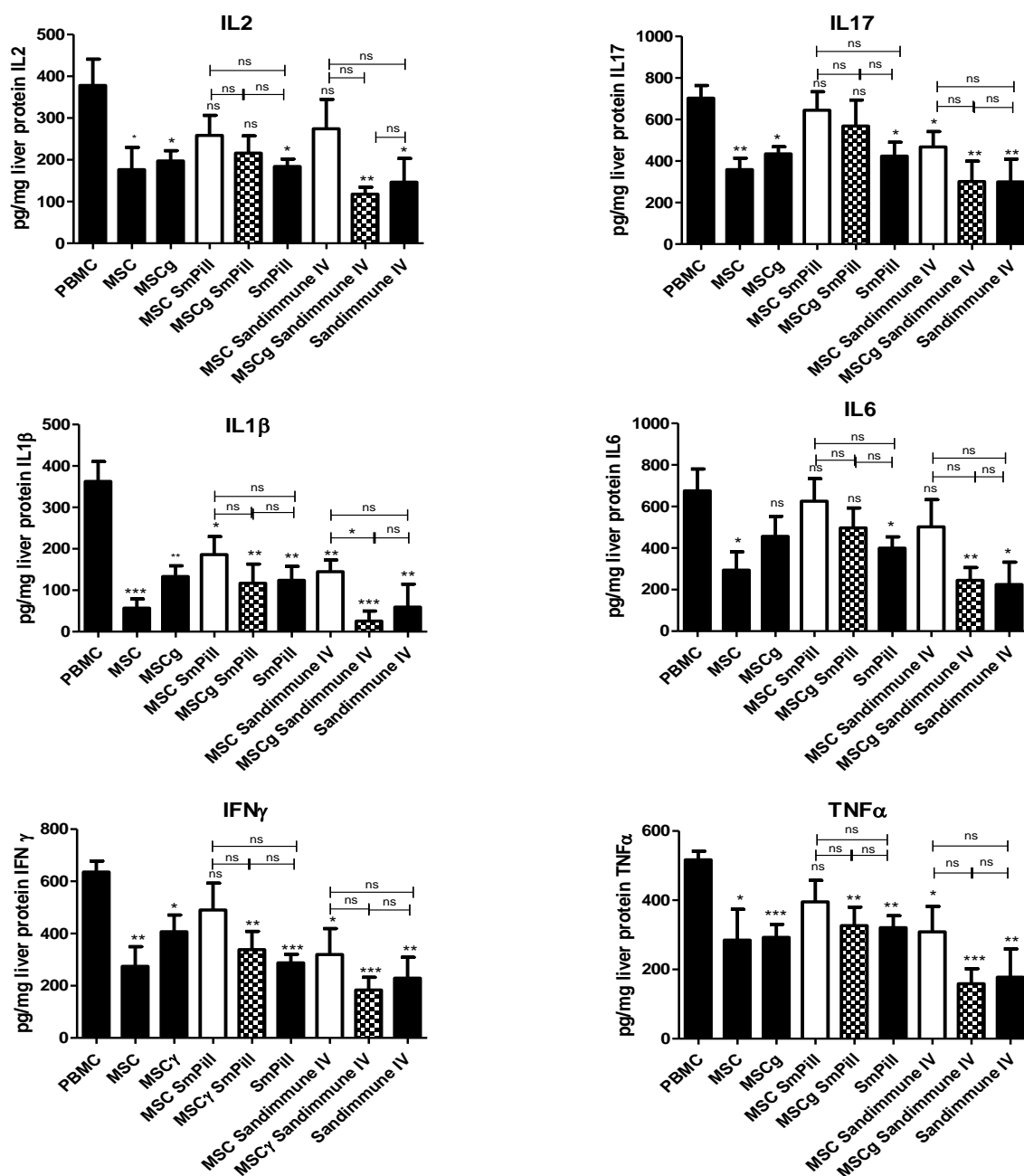
Liver

Figure 5.9. MSC and CsA single therapies were more efficacious than co-therapies in reducing proinflammatory cytokines detected in the liver of aGvHD mice. The aGvHD model was set up as described in figure 5.1. Tissue samples were harvested on day 13, immediately snap frozen and stored at - 80 C. Homogenates were prepared and ELISA was used to detect proinflammatory cytokines (IL2, IL17, IL1β, IL6, IFNγ and TNFα). Concentration of cytokine is expressed as pg cytokine per mg tissue protein as normalised by bradford protein assay. n=6 per group (2 MSC donors, 2 PBMC donors). Statistical analysis was carried out using unpaired student t-test where * <0.05, ** <0.01 and *** <0.001. Stars with no bar are in comparison to the PBMC group.
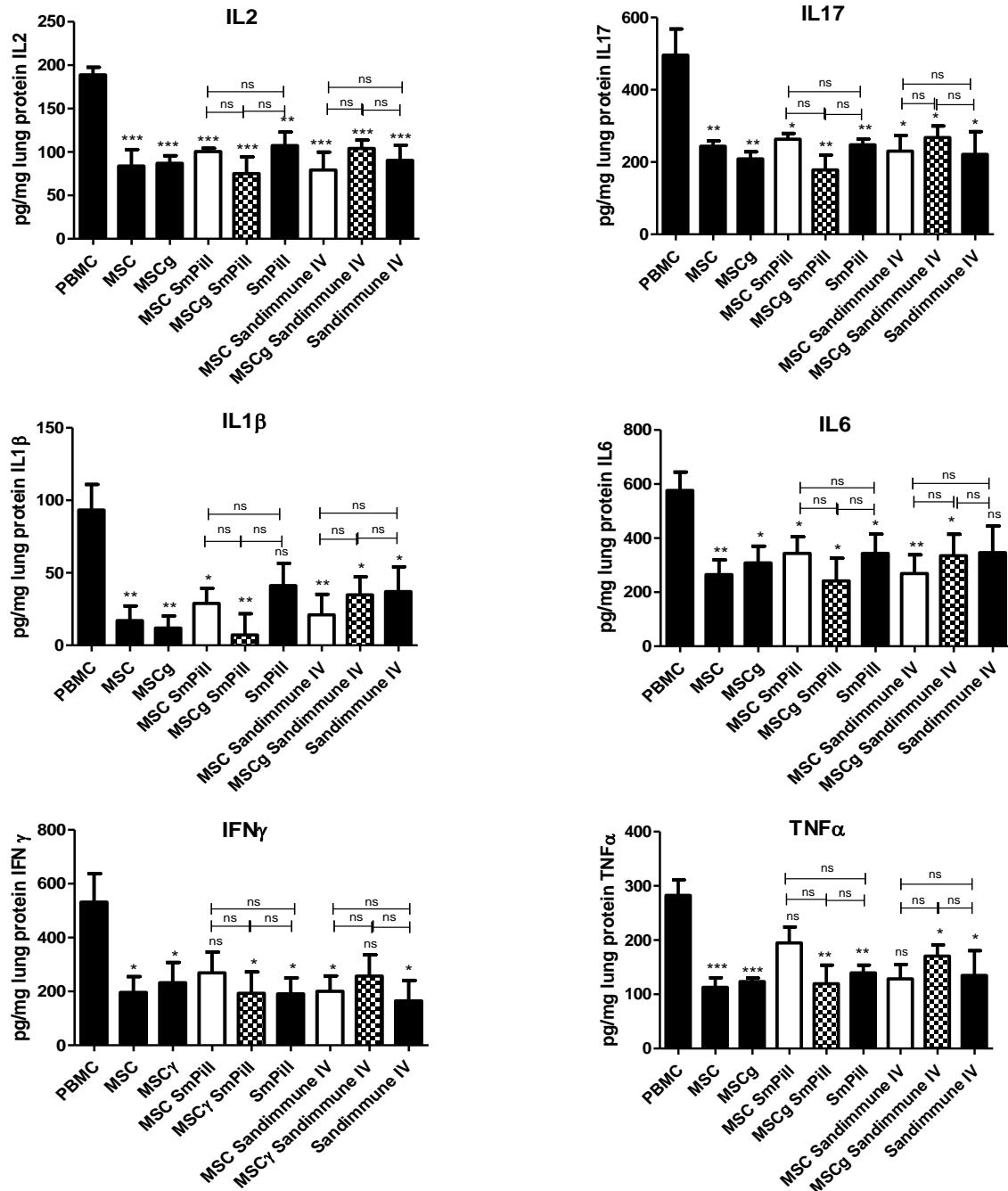
Lung

Figure 5.10. MSC and CsA co-therapies provide no significant enhancement at reducing proinflammatory cytokines in comparison to single therapies in the lungs of aGvHD mice. The aGvHD model was set up as described in figure 5.1. Tissue samples were harvested on day 13, immediately snap frozen and stored at - 80 C. Homogenates were prepared and ELISA was used to detect proinflammatory cytokines (IL2, IL17, IL1β, IL6, IFNγ and TNFα). Concentration of cytokine is expressed as pg cytokine per mg tissue protein as normalised by bradford protein assay. n=6 per group (2 MSC donors, 2 PBMC donors). Statistical analysis was carried out using unpaired student *t*-test where * <0.05, ** <0.01 and *** <0.001. Stars with no bar are in comparison to the PBMC group.
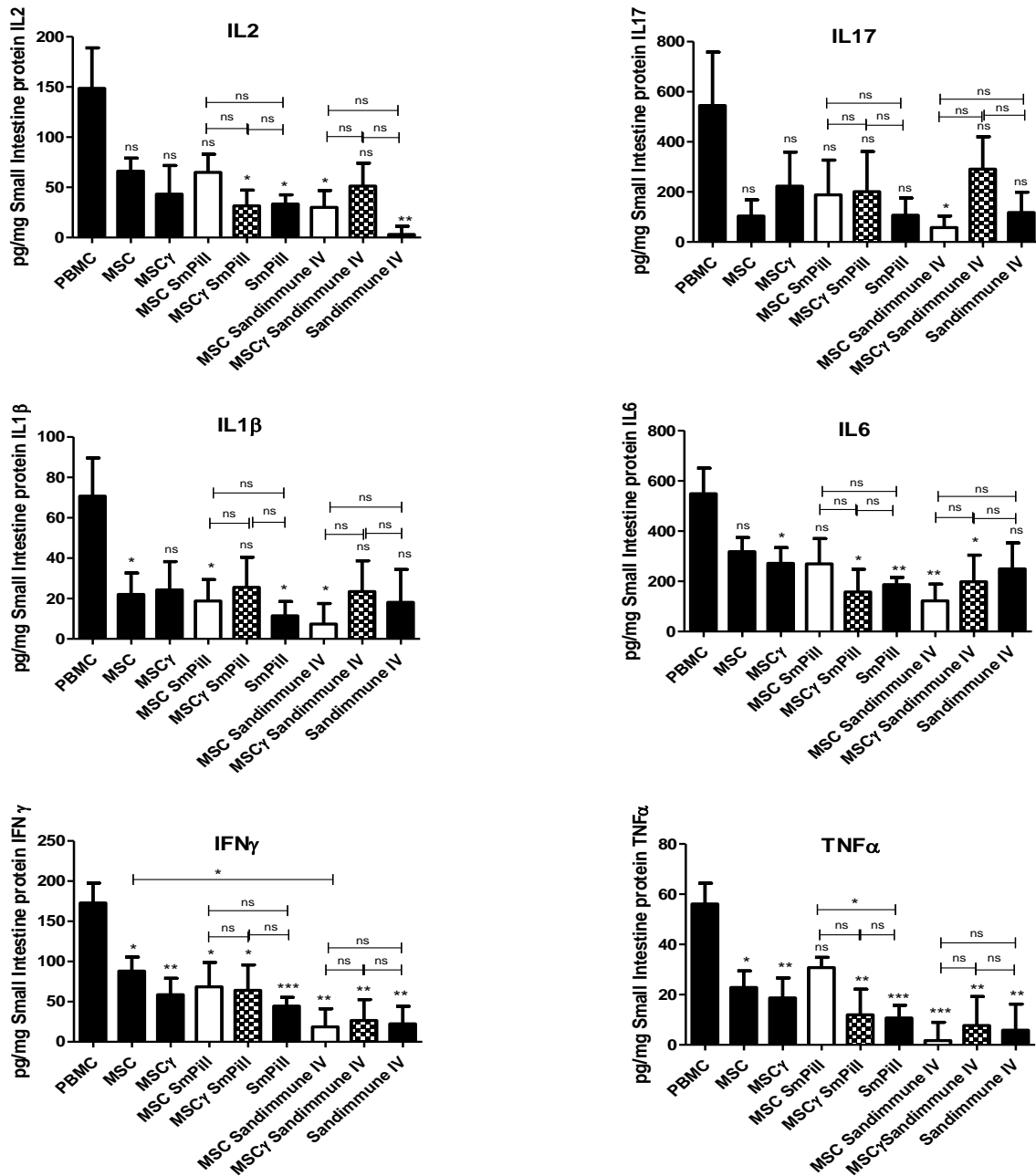
Small Intestine

Figure 5.11. Efficacy of MSC and CsA co-therapy is dependent on CsA delivery route for significant reduction of IFNγ or TNFα in the small intestine of aGvHD mice. The aGvHD model was set up as described in figure 5.1. Tissue samples were harvested on day 13, immediately snap frozen and stored at - 80 C. Homogenates were prepared and ELISA was used to detect proinflammatory cytokines (IL2, IL17, IL1β, IL6, IFNγ and TNFα). Concentration of cytokine is expressed as pg cytokine per mg tissue protein as normalised by bradford protein assay. n=6 per group (2 MSC donors, 2 PBMC donors). Statistical analysis was carried out using unpaired student *t*-test where * <0.05, ** <0.01 and *** <0.001. Stars with no bar are in comparison to the PBMC group.

Colon

Figure 5.12. MSC had no negative impact on the efficacy of CsA at reducing proinflammatory cytokines detected in the colon of aGvHD mice. The aGvHD model was set up as described in figure 5.1. Tissue samples were harvested on day 13, immediately snap frozen and stored at - 80 C. Homogenates were prepared and ELISA was used to detect proinflammatory cytokines (IL2, IL17, IL1β, IL6, IFNγ and TNFα). Concentration of cytokine is expressed as pg cytokine per mg tissue protein as normalised by bradford protein assay. n=6 per group (2 MSC donors, 2 PBMC donors). Statistical analysis was carried out using unpaired student *t*-test where * <0.05, ** <0.01 and *** <0.001. Stars with no bar are in comparison to the PBMC group.

Table 5.1 Cytokine profile in the spleen

	MSC	MSCγ	MSC SmPill®	MSCγ SmPill®	SmPill®	MSC S IV	MSCγ S IV	S IV
IL2	***[9]	***	***	***	***	***	***	***
IL17	**[10]	***	**	***	**	**	**	**
IFNγ	*[11]	↓	*	*	*	*	*	*
TNFα	↓	↓	↓[12]	**	***	*	***	***

Table 5.2 Cytokine profile in the liver

	MSC	MSCγ	MSC SmPill®	MSCγ SmPill®	SmPill®	MSC S IV	MSCγ S IV	S IV
IL2	*	*	↓	↓	*	↓	**	*
IL17	**	*	↓	↓	*	*	**	**
IL1β	***	**	*	**	**	**	***	**
IL6	*	↓	↓	↓	*	↓	**	*
IFNγ	**	*	↓	**	***	*	***	**
TNFα	*	***	↓	**	**	*	***	**

Table 5.3 Cytokine profile in the lung

	MSC	MSCγ	MSC SmPill®	MSCγ SmPill®	SmPill®	MSC S IV	MSCγ S IV	S IV
IL2	***	***	***	***	**	***	***	***
IL17	**	**	*	**	**	*	*	*
IL1β	**	**	*	**	↓	**	*	*
IL6	**	*	*	*	*	**	`*	↓
IFNγ	*	*	↓	*	*	*	↓	*
TNFα	***	***	↓	**	**	↓	*	*

---

[9] Denotes statistical significance using student *t*-test where *** <0.001
[10] Denotes statistical significance using student *t*-test where ** <0.01
[11] Denotes statistical significance using student *t*-test where * <0.05
[12] Denotes a reduction in test group where significance was not obtained using student *t*-test.

Table 5.4 Cytokine profile in the small intestine

	MSC	MSCγ	MSC SmPill®	MSCγ SmPill®	SmPill®	MSC S IV	MSCγ S IV	S IV
IL2	↓	↓	↓	*	*	*	↓	**
IL17	↓	↓	↓	↓	↓	*	↓	↓
IL1β	*	↓	*	↓	*	*	↓	↓
IL6	↓	*	↓	*	**	**	*	↓
IFNγ	*	**	*	*	***	**	**	**
TNFα	*	**	↓	**	***	***	**	**

Table 5.5 Cytokine profile in the colon

	MSC	MSCγ	MSC SmPill®	MSCγ SmPill®	SmPill®	MSC S IV	MSCγ S IV	S IV
IL2	↓	↓	↓	↓	↓	↓	↓	↓
IL17	↓	*	*	↓	*	↓	*	*
IL1β	*	**	**	***	**	*	***	*
IL6	*	**	**	**	**	*	**	**
IFNγ	*	**	**	*	*	↓	↓	*
TNFα	↓	*	*	*	**	*	*	*

5.5. MSCγ ENHANCED SANDIMMUNE® IV SUPPRESSION OF TNFα PRODUCING CD4+ AND CD8+ T CELLS IN THE SPLEEN AND LUNG OF ᴀGᴠHD MICE

TNFα is involved in all stages of GvHD pathophysiology, making TNFα inhibition an attractive target for GvHD prevention and treatment. Throughout section 5.4, the co-treatment of MSC and CsA was shown to reduce the levels of total TNFα within all of the tissues of aGvHD mice in a similar manner. However, in section 5.3, there were significant differences between co-therapies and CsA alone in alleviating tissue damage associated with aGvHD pathology in the liver and lung. Also, resting MSC was shown to impair SmPill® anti-apoptotic efficacy to a greater degree in the lung than the small intestine (Figure 5.7). Subsequently, with donor T cells being the prime source of TNFa, the spleen, liver and lung were selected to quantify the production of TNFα by human CD4+ and CD8+ and examine efficacy of co-therapies in these tissues further.

Human CD4+ and CD8+ T cells were recovered from the spleen, liver and lungs from untreated and all treatment groups of aGvHD mice 13 days after PBMC administration. The potential for each treatment group to reduce the number or percentage of TNFα producing human CD4+ and CD8+ T cells during aGvHD was analysed by intracellular flow cytometry. The number of CD4+ and CD8+ T cells producing TNFα was reduced by both MSC and MSCγ alone in each of the tissues, however not significantly (Figures 5.13 – 5.15). There were no significant differences in efficacy when either MSC treatment was combined with SmPill® in the spleen and lung. However, in the liver, the efficacy of SmPill® at reducing the number of TNFα producing CD4+ and CD8+ T cells was significantly hampered by resting MSC (Figure 5.14). Similarly, SmPill® suppression of CD8+ TNFa T cells was significantly impaired by MSCγ in the liver (Figure 5.14).

With systemic CsA (Sandimmune® IV) there was beneficial suppressive effects of the number of $CD4^+$ and $CD8^+$ T cells producing TNFα in some of the tissues analysed (Figure 5.13 – 5.15). In contrast to the GI targeted CsA treatment (SmPill®), the efficacy of Sandimmune® IV was enhanced by MSCγ in the spleen and lung but not the liver of aGvHD mice (Figure 5.13 and 5.15). Notably, this data is preliminary (n=3) and additional experiments are required to reinforce these findings. However, this data supports findings throughout this chapter that suggest that activation status of MSC can facilitate beneficial suppressive effects with CsA.

Spleen
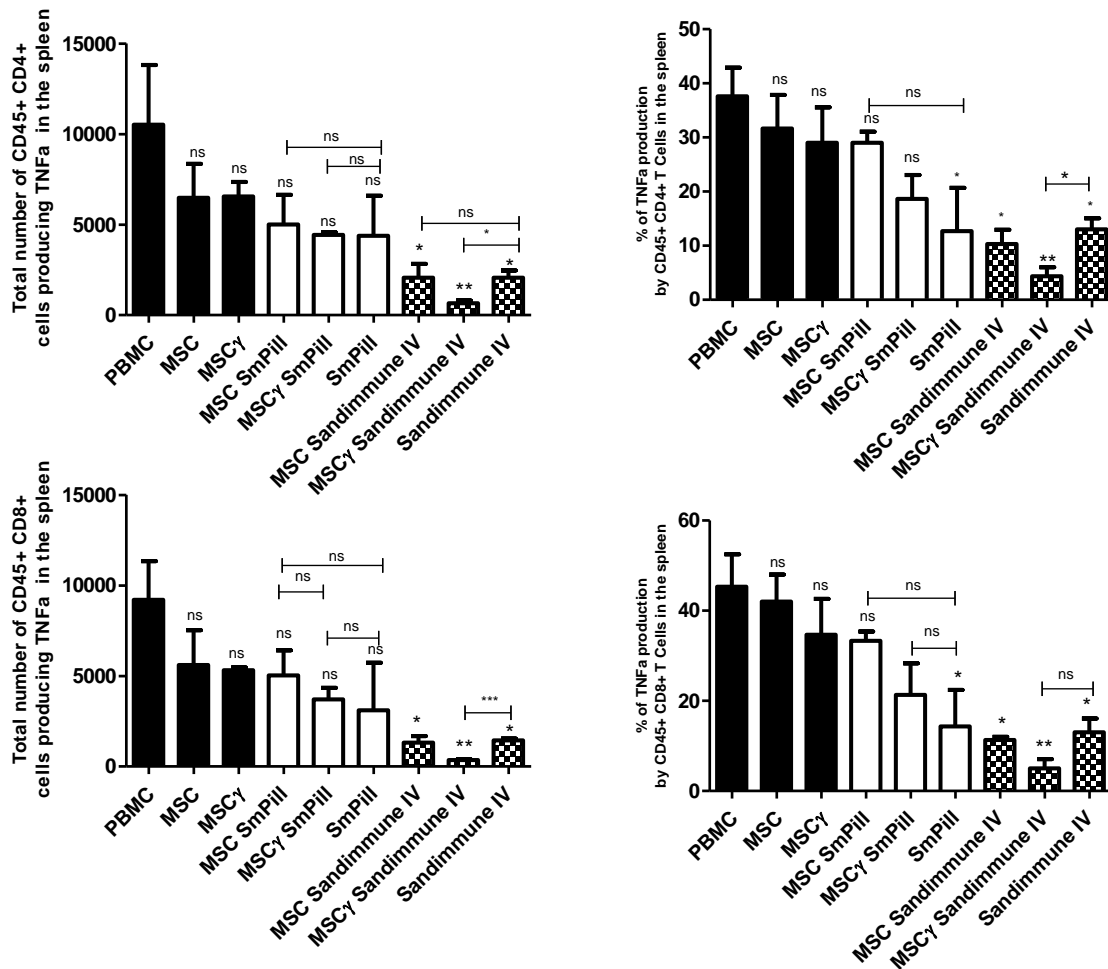
Figure 5.13. Sandimmune® IV and MSCγ co-therapy significantly reduced the total number and percentage of CD4+ TNFα+ and CD8+ TNFα+ T cells in the spleen of aGvHD mice. The aGvHD model was set up as described in figure 5.1. Cells were recovered on day 13, stimulated with 100 ng/ml PMA, 1 µg/ml iononmycin and 1X Brefeldin A for 4 h and analysed by intracellular flow cytometry. Graphical representations of the total number and percentage of human TNFα producing CD45+ CD4+ and CD8+ T cells recovered in the spleen. The total number of human cells was assessed using counting beads during flow cytometry. n=3 per group (1 PBMC donor). Statistical analysis was carried out using one way ANOVA Tukey Multiple Cmparison Test and unpaired student *t*-test where * <0.05, ** <0.01 and *** <0.001. Stars with no bar are in comparison to the PBMC group.
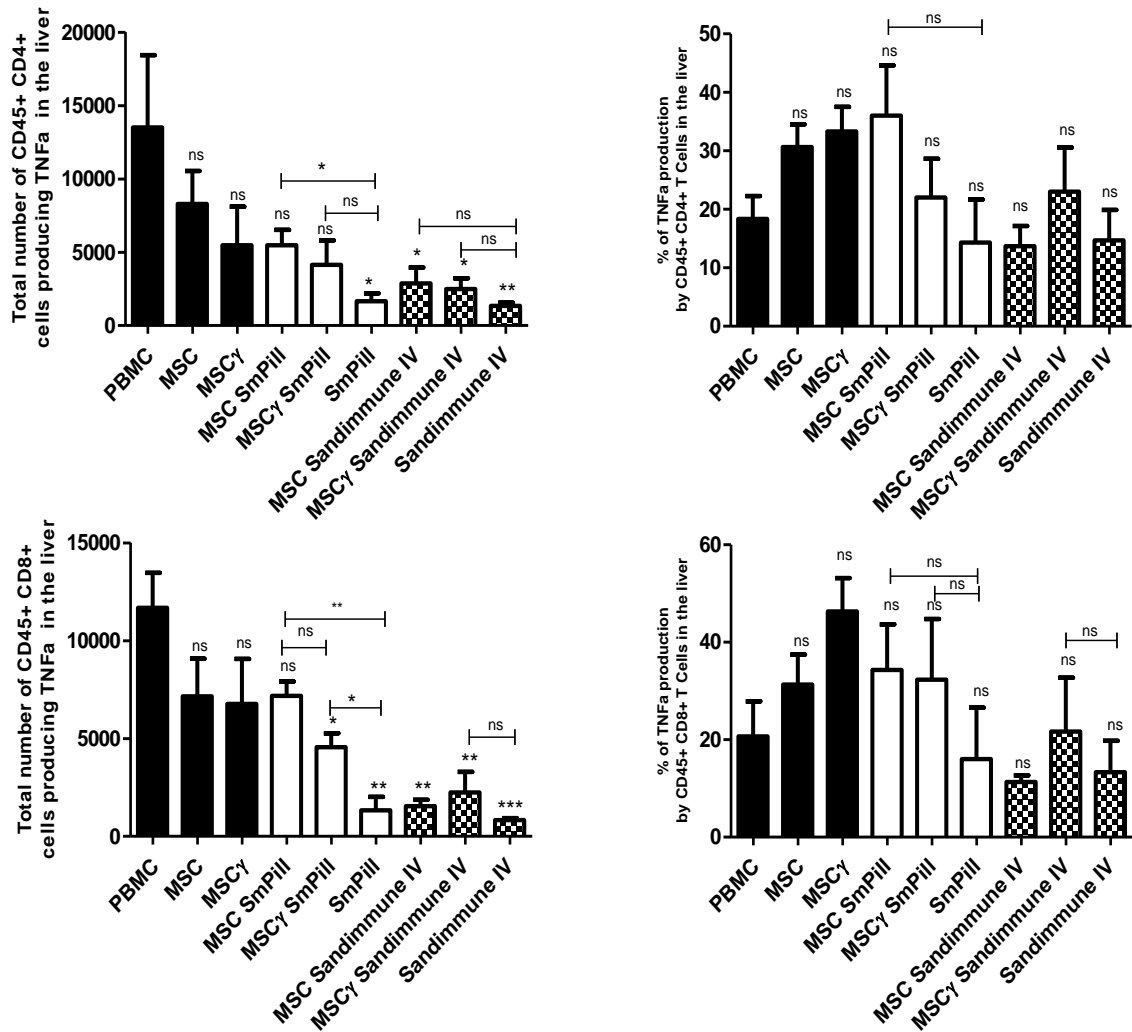
Liver

Figure 5.14. MSC significantly hampers SmPill® efficacy at reducing the total number of CD4+ TNFα+ and CD8+ TNFα+ T cells in the liver of aGvHD mice. The aGvHD model was set up as described in figure 5.1. Cells were recovered on day 13, stimulated with 100 ng/ml PMA, 1 µg/ml iononmycin and 1X Brefeldin A for 4 h and analysed by intracellular flow cytometry. Graphical representations of the total number and percentage of human TNFα producing CD45+ CD4+ and CD8+ T cells recovered in the liver. The total number of human cells was assessed using counting beads during flow cytometry. n=3 per group (1 PBMC donor). Statistical analysis was carried out using one way ANOVA Tukey Multiple Cmparison Test and unpaired student *t*-test where * <0.05, ** <0.01 and *** <0.001. Stars with no bar are in comparison to the PBMC group.
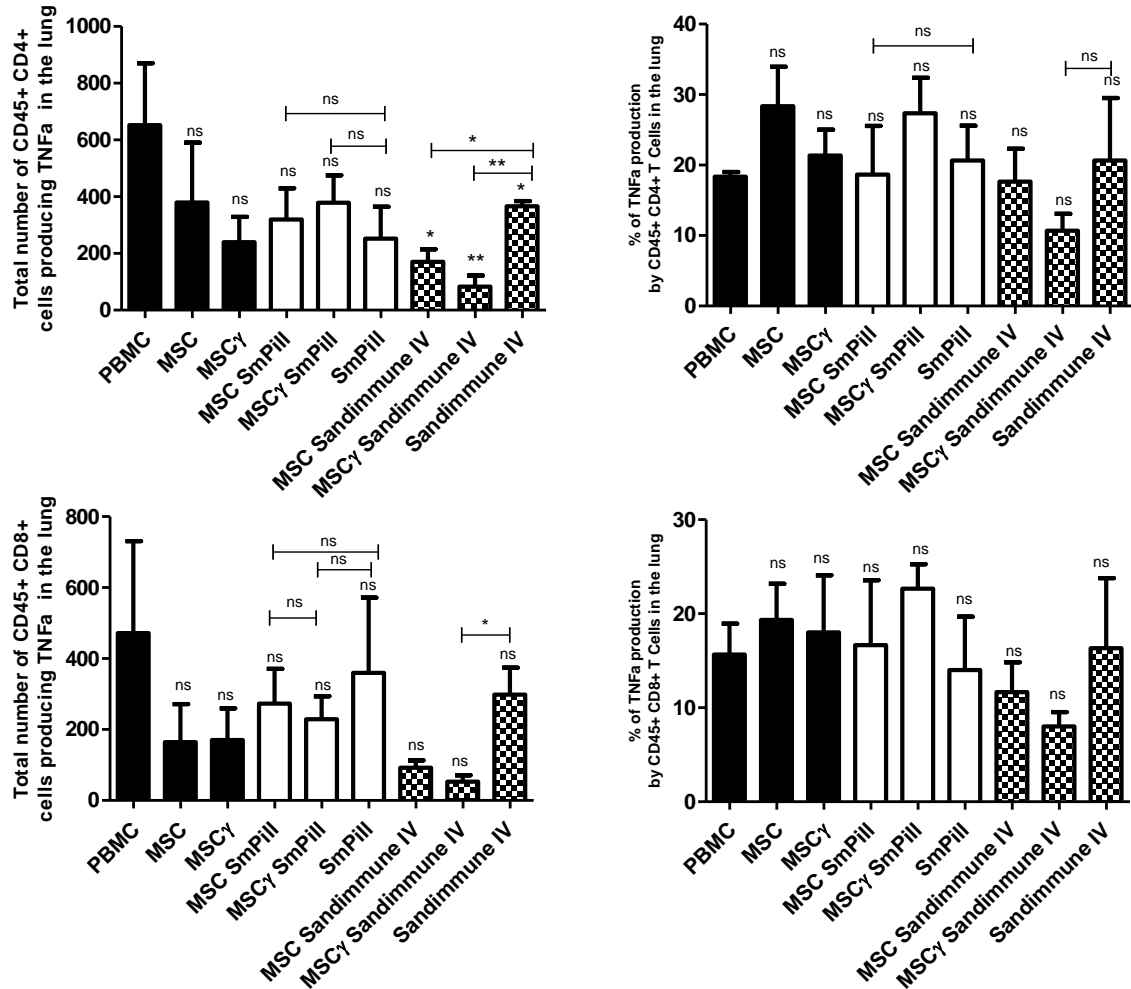
Lung

Figure 5.15. MSC significantly enhanced Sandimmune® IV efficacy in reducing the total number of CD4⁺ TNFα⁺ T cells in the lung of aGvHD mice. The aGvHD model was set up as described in figure 5.1. Cells were recovered on day 13, stimulated with 100 ng/ml PMA, 1 µg/ml iononmycin and 1X Brefeldin A for 4 h and analysed by intracellular flow cytometry. Graphical representations of the total number and percentage of human TNFα producing CD45⁺ CD4⁺ and CD8⁺ T cells recovered in the lung. The total number of human cells was assessed using counting beads during flow cytometry. n=3 per group (1 PBMC donor). Statistical analysis was carried out using one way ANOVA Tukey Multiple Cmparison Test and unpaired student *t*-test where * <0.05, ** <0.01 and *** <0.001. Stars with no bar are in comparison to the PBMC group.

5.6. ENHANCEMENT OF REGULATORY T CELLS BY RESTING MSC IN ᴀGVHD WAS SIGNIFICANTLY HAMPERED BY SANDIMMUNE® IV

Regulatory T (Treg) cells are potent suppressors of immune responses and provide potential to mitigate the severity of aGvHD by promoting immunological tolerance. In chapter 4, Tregs were shown to engraft in this humanised model of aGvHD and CsA treatment had no significant effect on the number of Tregs recovered from the tissues of aGvHD mice (Figure 4.34 and 4.35). Previous unpublished data from this laboratory established that MSC increased the number of Treg in the liver and lung in this humanised aGvHD model (Healy 2015, Thesis). To that end, the effect of CsA on MSC ability to increase the number of Treg in the spleen, liver and lung in this aGvHD model was assessed.

Acute GvHD mice treated with MSC and CsA therapies or untreated, as outlined in figure 5.1 B, were sacrificed on day 13 and the spleens, lungs and livers were harvested for analysis. Human Treg cells were defined as $CD4^+$ $CD25^+$ $FoxP3^+$ after gating on the human $CD45^+$ cells recovered from the tissues and determined by intracellular flow cytometry. Small populations of Treg cells were present in all of the organs harvested, particularly in the lung.

The number of Tregs was increased by resting MSC and MSCγ in the spleen, liver and lung (Figure 5.16). Co-treatment of resting MSC or MSCγ with SmPill® resulted in no significant changes in the number or percentage of Tregs recovered. However, Sandimmune® IV significantly hampered the ability of resting MSC to increase the number of Tregs in the spleen of aGvHD mice (Figure 5.16 B). CsA treatments alone did not significantly reduce the numbers of Tregs in comparison to untreated aGvHD mice, systemic infusion of CsA (Sandimmune® IV) has a negative impact on MSC. However, this data is preliminary (n=3) and will need to be repeated to confirm these observations. Nonetheless, this data suggests that GI targeted (SmPill®) CsA has sparing effects on MSC enhancement of Treg numbers in

systemic aGvHD tissues. However, it is important to note that there is no enhancement in the number of Tregs when MSC are combined with SmPill®.
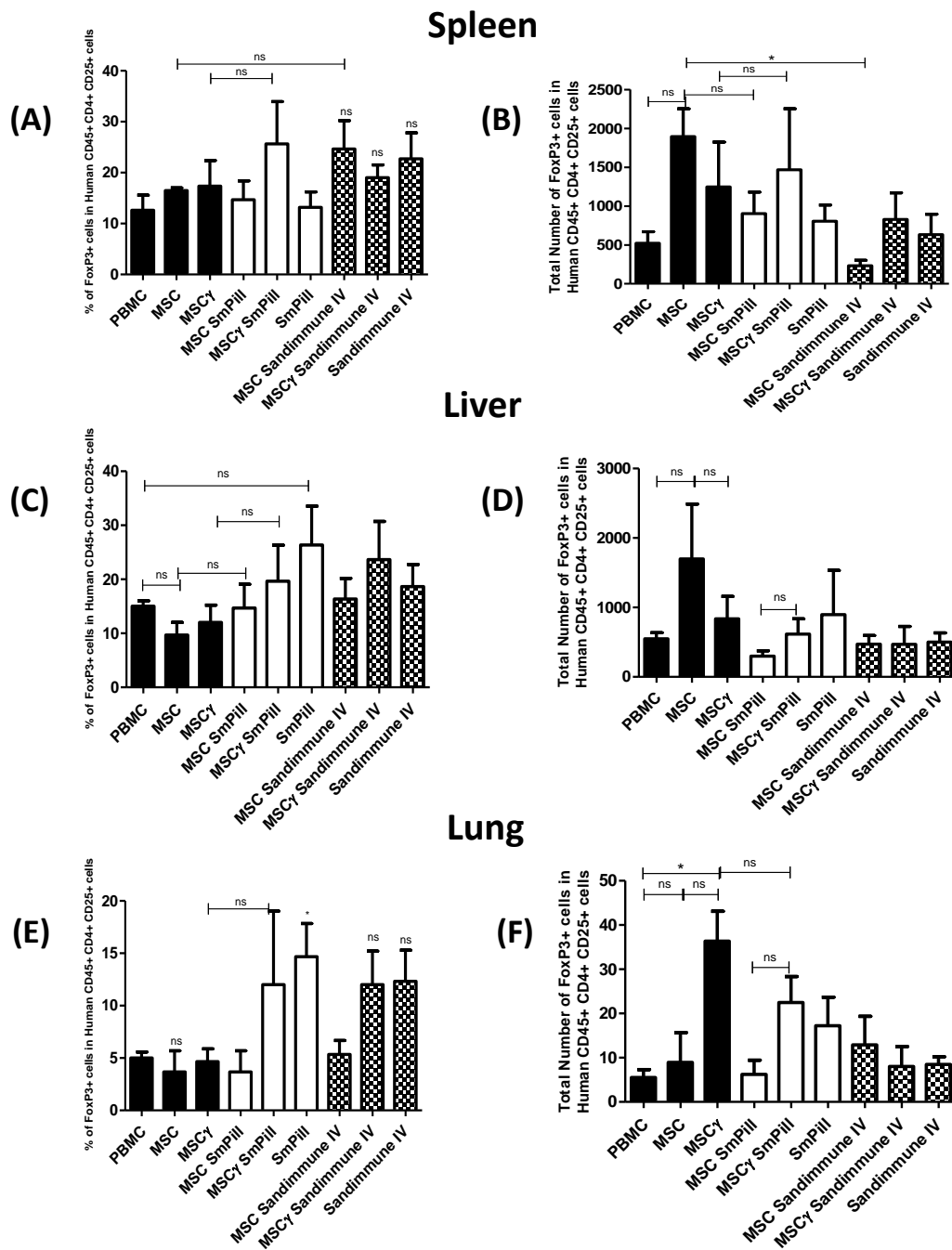
Figure 5.16. Sandimmune® IV significantly reduced resting MSC's enhancement of the number of Tregs in the spleen aGvHD mice. The aGvHD model was set up exactly as described in figure 5.1. Cells were recovered on day 13. Human Treg cells were defined as $CD4^+ CD25^+ FoxP3^+$ after gating on the human $CD45^+$ cells and analysed by intracellular flow cytometry. Graphical representation of the total number and percentage of human Treg cells recovered from the spleen (A, B), liver (C, D) and lung (E, F). The total number of human cells was assessed using counting beads during flow cytometry. n=3 per group (1 PBMC donor). Statistical analysis was carried out using unpaired student t-test where * <0.05. * with no bar are in comparison to the PBMC group.

5.7. SUMMARY

Throughout this chapter studies were designed to 1) determine if CsA and MSC are efficacious as a co-therapy in aGvHD, 2) define the role MSC activation status plays in partnership with CsA and 3) examine the effect of CsA delivery on MSC potency in aGvHD therapy. Following these investigations, this chapter adds significant knowledge on our understanding of the efficacy of co-therapy consisting of MSC and CsA and presents a framework from which suitable conditions for co-treatment of MSC and CsA can be adopted for aGvHD therapy.

In terms of survival, GI targeted CsA (SmPill®) effectiveness proved to be significantly impaired by resting MSC (Figure 5.3). However, this negative effect was significantly ameliorated when MSC were pre-licensed with IFNγ (Figure 5.3). Contrastingly, intravenous CsA (Sandimmune® IV) efficacy was not affected by resting MSC or enhanced by MSCγ (Figure 5.4). This data suggests that the activation status for MSC is important for optimal performance with GI targeted CsA (SmPill®) but not for systemic CsA (Sandimmune® IV).

Following a similar trend, tissue damage in the target organs of aGvHD mice was greatly diminished when SmPill® was combined with MSCγ rather than resting MSC (Figures 5.5 – 5.6). However, Sandimmune® IV was effective at reducing pathology in the tissues when combined with either resting MSC or MSCγ (Figures 5.5 - 5.6). The observations made in relation to apoptosis in the lung and small intestine support H&E histological data (Figure 5.7). These similar findings suggest that pre-licensing of MSC was required for combined efficacy with SmPill® but not Sandimmune® IV. Therefore, delivery of CsA via oral (targeted to GI tract) or intravenous routes (systemic) had an impact on MSC therapeutic efficacy.

For further investigation, cytokine profiles in aGvHD tissues following these treatments were analysed. Figures 5.8 – 5.12, confirmed that activation status of MSC and relative

bioavailability of CsA had varying effects on cytokine levels in systemic and GI tissues. Resting MSC was shown to weaken SmPill® efficacy of IL2 and TNFα reduction in the spleen (Figure 5.8). In the small intestine, there was further verification that MSC and CsA co-therapy efficacy was dependent on delivery of CsA, as Sandimmune® IV and MSC significantly reduced the levels of IFNγ to levels similar to Sandimmune® IV alone while co-treatment of SmPill® with MSC significantly mitigated reduction of TNFα (Figure 5.11). While a significant level of cytokine suppression was maintained by MSC and Sandimmune® IV co-therapy in the liver and colon, there was no significant enhancement of efficacy in comparison to single therapies (Figure 5.9 and 5.12).

Further evidence of MSC activation status impacting CsA efficacy was exposed in section 5.5, where TNFα production from CD4+ and CD8+ T cells were quantified following all treatments. Here, resting MSC and MSCγ were shown to significantly hamper SmPill® effectiveness of reducing TNFα production from CD4+ and CD8+ T cells in the liver (Figure 5.14). While the efficacy of Sandimmune® IV in this regard was enhanced by either MSC or MSCγ in the spleen and lungs (Figure 5.13 and 5.15).

Interestingly, SmPill® spared MSC capacity to enhance Tregs *in vivo* as the co-treatment did not significantly reduce the number of Tregs in the spleen, liver or lungs of aGvHD mice (Figure 5.16). Contrastingly, Sandimmune® IV significantly reduced MSC enhancement of Treg in the spleen (Figure 5.16).

This chapter in its entirety has provided evidence of MSC and CsA as having both positive and negative suppressive effects *in vivo* and has outlined the conditions by which this was facilitated by means of MSC activation or delivery method of CsA. This knowledge can be translated to inform better design of a combined cellular therapy and pharmacotherapy approach for aGvHD treatment.

CHAPTER 6

DISCUSSION

Since its inception, the field of MSC research has grown exponentially from Friedenstein's early discoveries to the vast therapeutic applications of these cells currently being examined in clinical trials. Early studies indicated potential use for MSC in regenerative medicine (Ashton *et al*. 1980; Pittenger *et al*. 1999; Orlic *et al*. 2001; Quarto *et al*. 2001). However, studies displaying MSC ability to modulate inflammation and immune cell function in an allogeneic setting placed MSC at the forefront of cellular therapy development (Bartholomew *et al*. 2002; Di Nicola *et al*. 2002; Aggarwal & Pittenger 2005). Their homing ability and capacity for secreting immunomodulatory soluble factors coupled with their immune evasive properties present MSC as an attractive cellular therapy against inflammatory and immune mediated diseases.

Clinical studies have demonstrated the beneficial potential of MSC as a cell therapy, particularly in aGvHD, solid organ transplantation, Crohn's disease and rheumatoid arthritis (Kebriaei *et al*. 2009; Dahlke *et al*. 2009; Duijvestein *et al*. 2010; Liang *et al*. 2012). Despite these advances, there are numerous issues obstructing the routine implementation of this cellular therapy. These issues are mainly surrounding the dosing schedule of MSC, culture/expansion methods of MSC, the source, potency and immunogenicity of MSC donors paired with the lack of understanding of MSC mechanisms of action *in vivo*. In addition, a major limitation for the incorporation of MSC therapy to treatment schedules for aGvHD is that lack of understanding about the interactions of MSC with immunosuppressive drugs.

CsA has proved to be a powerful immunosuppressant in HSCT medicine, where it can be used as a prophylaxis and a second line treatment in HSCT. Steroid resistance is the leading cause of first line treatment failure in aGvHD and CsA has proved useful as a salvage therapy (Deeg *et al*. 1985; Parquet *et al*. 2000; Finke *et al*. 2009; Ruutu *et al*. 2014). However, little is known about the direct interactions of CsA with MSC in terms of the impact they pose on each others immunosuppressive capacity. While there are numerous *in vitro* and *in vivo* studies

reporting beneficial effects of CsA in combination with MSC (Le Blanc *et al*. 2004; Maccario *et al*. 2005; Zhang *et al*. 2007; Pischiutta *et al*. 2014), there are equal numbers of studies showing CsA as having a negative impact on MSC immunosuppressive ability and vice versa (Inoue *et al.* 2006; Buron *et al*. 2009; Eggenhofer *et al.* 2011; Jia *et al*. 2012). This suggests that the interaction between CsA and MSC immunosuppressive activity is multifactorial and that there are no key mechanisms defined as of yet. Therefore, the aim of this thesis was to firstly characterise the direct interactions of MSC and CsA and elucidate the mechanisms by which these interactions occur *in vitro* and *in vivo*. Secondly to establish the efficacy of a novel and more clinically applicable CsA treatment by means of optimal targeted delivery in a humanised model of aGvHD.

In chapter 3, the interactions of CsA and MSC were assessed *in vitro.* Firstly, the effect of CsA on MSC characterisation and differential ability was explored and the presence of CsA had no impact on MSC surface marker phenotype nor did it alter trilineage differentiation ability *in vitro*. This ruled out any potential negative effects CsA had on MSC morphology, phenotype, characterisation and capacity to undergo differentiation.

The ability of MSC to suppress the adaptive immune system is a key feature in the development of MSC therapy. In particular, MSC have been shown to have dynamic interactions on T cells via cell contact or through secreted soluble factors in the context of specific environmental cues (Di Nicola et al. 2002; English et al. 2007; Ren et al. 2008; Krampera et al. 2006). CsA also targets T cells and is a potent T cell immunosuppressive drug that suppresses the production of IL2 as a result of calcineurin inhibition (Liu et al. 1991; Flanagan et al. 1991). Thus it was necessary to elucidate MSC and CsA interactions in terms of T cell suppression as this likely has implications for their combined use in transplant settings. Therefore, the next investigation was to assess the interaction of CsA on MSC immunosuppressive ability *in vitro*. Using a proliferation dye dilution co-culture assay, CsA

was shown to have an inhibitory effect on MSC immunosuppressive ability when MSC are present at a ratio of 1 MSC to 5 PBMC (1:5). This finding is supported by Buron *et al* (2009) who showed that CsA anatagonised the suppressive effects of MSC at 1:5 and 1:10 ratios. Le Blanc *et al* (2004) observed that CsA only added slightly to the inhibitory effect of MSC at 1:9 ratio. Maccario *et al*. (2005) showed that CsA and MSC combined had synergistic suppressive effects in a mixed lymphocyte culture. Notably, in that study CsA was added at 50 ng/ml whereas in our study 1 µg/ml CsA was added which would explain these differences. However, at a high MSC:PBMC density (1:40) MSC were shown to be significantly more suppressive with CsA than MSC alone. This is in line with findings of Buron *et al* (2009) who found that MSC and CsA were more suppressive than MSC alone at 1:20 ratio.

It is noteworthy that MSC alone can provide significant suppression of T cell proliferation in a dose dependent manner, therefore these findings suggest that it is more useful to combine CsA with MSC at a ratio of 1 MSC to 40 PBMC (1:40) as positive effects are more apparent. This is an important finding as the ratio of PBMC to MSC *in vivo* will be high, particularly in inflammatory disease models. It is also likely that the concentration of CsA (1 µg/ml) used in these assays was too high and didn't provide MSC with sufficient pro-inflammatory cues to become suppressive at the 1:5 ratio. IFNγ has been shown by others to be critical to activate MSC into an immunosuppressive phenotype (Krampera et al. 2006; English et al. 2007; Polchert et al. 2008). Elegant studies utilising IFNγ (-/-) T cells or neutralising antibodies have demonstrated the key role played by IFNγ in this context (Polchert et al. 2008; Sheng et al. 2008; Wang Lei et al.2013). This study showed that CsA significantly reduced the level of IFNγ in the supernatant and significantly suppressed the number of CD3$^+$ T cells producing IFNγ in this 1:5 suppressor assay. Thus, MSC in the presence of CsA were less potent with impaired suppressive ability due to a lack of IFNγ presence in the co-culture. Using the same co-culture assay, the prestimulation of MSC with IFNγ (MSCγ) prior to the

addition of CsA was required to maintain immunosuppressive ability at 1:5 ratio. This supports the above studies and suggests that licensing of MSC plays a key role in facilitating beneficial effects of MSC and CsA co-treatment.

CsA or MSCγ treatments alone have similar T cell suppressive effects at the 1:40 ratio. Interestingly, when CsA was combined with MSCγ at 1:40 this resulted in a more potent suppressive response than MSCγ alone or CsA alone. This proposes that CsA can enhance the potency of MSCγ, which others have observed in the case of steroids and MSCγ co-treatment (Ankrum *et al.* 2014). In the Ankrum *et al.* study, there was no evidence of enhanced MSCγ potency over that of resting MSC following combination with budesonide as MSC + budesonide and MSCγ + budesonide groups resulted in 60% of proliferating PBMC at 1:16 ratio. Moreover, the authors failed to show significant suppression by these combination groups in comparison to PBMC only group (80% proliferation) at 1:16 ratio. Our study used counting beads to specifically enumerate the proliferation of $CD3^+$ T cells in the PBMC co-culture and is the first study to show significant enhancement of MSCγ when combined with CsA at 1:40 ratio. However the possibility that CsA, present in these treatment groups, mediated the suppressive effect observed cannot be ruled out in this case. Recently, Girdlestone *et al.* have shown how MSC pretreated with CsA and rapamycin were more suppressive in PBMC co-cultures without the presence of the drugs in the co-culture (Girdlestone *et al.* 2015). This supports our findings and shows that CsA does enhance MSC potency directly but when both are added to the co-culture, CsA reduces the number of $CD3^+$ T cells producing IFNγ (which we have shown), affecting MSC activation indirectly.

These findings highlight that the dose of CsA can have an impact on MSC activation and subsequent suppressive ability which make it an important consideration to make when translating these *in vitro* findings to an *in vivo* setting. More importantly, this data suggests

that the efficacy of MSC therapy may be impaired in patients who have undergone a prophylaxis regimen with CsA.

Pro-inflammatory cytokine production is one of the driving forces used by T cells to mediate an inflammatory environment. MSC suppression of T cell proliferation *in vitro* also corresponds to reduced IFNγ, TNFα and IL2 (Aggarwal & Pittenger 2005; Prasanna *et al*. 2010; Patel *et al*. 2010). Similarly, CsA has been shown to significantly reduce these cytokines and the number of immune cells producing them (Tramsen et al. 2014; Haider et al. 2008). Therefore the effect of CsA on this immunosuppressive feature of MSC was investigated.

Surprisingly, MSC and MSCγ significantly suppressed the levels of TNFα in the supernatant of suppressor assays (containing whole PBMC) but IFNγ and IL2 levels were unchanged. These findings were not expected as they are not entirely similar to the published studies (Aggarwal & Pittenger 2005; Prasanna *et al*. 2010; Patel *et al*. 2010) where MSC were shown to suppress levels of IFNγ, TNFα and IL2, however differences in PBMC stimulus (Phytohaemagglutinin used in Aggarwal & Pittenger study and Prasanna study) and MSC:PBMC ratio (1:50 in Patel study) may account for these variances. Also, the Aggarwal & Pittenger study used purified subpopulations of immune cells whereas this study used whole PBMC population for assessment. Interestingly, MSC and licensed MSC significantly suppressed the levels of IFNγ, TNFα and IL2 when combined with CsA. However, as CsA alone significantly suppressed these cytokines, it could therefore be suggested that this anti-inflammatory effect was mediated by CsA without obstruction from MSC in doing so. Nonetheless, this data shows that MSC does not hamper CsA suppression of IFNγ, TNFα and IL2 *in vitro*.

Although, measuring cytokine levels in supernatant provides an overall view of cytokine concentration, it does not provide any detail of cytokines being produced at the

cellular level. Therefore the next approach was to assess the number of T cells producing these cytokines to draw further conclusions about the interactions of MSC and CsA on T cell suppression. MSC in combination with CsA were shown to have differential effects on CD3$^+$ T cell cytokine production depending upon PBMC density in the suppressor assays. At both low and high densities, MSC do not negatively impact CsA suppression of IL2 producing CD3$^+$ T cells. This is an important result as IL2 has been known for a long time to be one of the main cytokines suppressed by CsA and this data shows that MSC does not interfere with the conventional suppressive mechanism of CsA (Kaufmann *et al.* 1984; Liu *et al.* 1991; Flanagan *et al.* 1991).

Following the results obtained in the suppressor assays where CsA hampered MSC suppressive ability at low PBMC density (1 MSC : 5 PBMC), it was expected that CsA would inhibit MSC suppression of TNFα and IFNγ producing CD3$^+$ T cells. However, this was not the case. At low densities, there was similar levels of suppression of TNFα and IFNγ producing CD3$^+$ T cells across all groups but at high PBMC densities (1 MSC : 40 PBMC), MSC hampered CsA suppression of TNFα and IFNγ producing CD3$^+$ T cells. Importantly, MSCγ did not significantly impair CsA suppressive ability. Dan Shi *et al.* have shown that human adipose derived MSC combined with CsA significantly reduced the levels of IL2 and IFNγ in the supernatant of a T cell co-culture (Shi *et al.* 2011). However, this study used PHA instead of CD3/CD28 activation, used isolated T cells as opposed to whole PBMC population and 50 ng/ml CsA in place of 1 μg/ml CsA as in our study. The authors showed that the suppressive effect was mediated by Jagged-1 mediated inhibition of NF-κB signalling (Shi *et al* 2011). However, the precise role CsA has on this inhibition is unclear as MSC on their own were capable of inhibiting NF-κB signalling through Jagged-1 (Shi *et al* 2011).

Our study shows that the beneficial effect of MSC and CsA co-treatment for the suppression of the CD3$^+$ T cell population (within the PBMC co-culture) at high densities (1

242

MSC: 40 PBMC) is being mediated through the suppression of IL2 producing CD3$^+$ T cells and not IFNγ or TNFα producing CD3$^+$ T cells. However, the negative effect of MSC on CsA suppression of TNFα producing CD3$^+$ T cells is mitigated by licensed MSC suggesting that licensing of MSC can facilitate a beneficial affiliation with CsA in suppressing CD3$^+$ TNFα$^+$ T cells at high densities. This is the first study to report the potential for beneficial combination of IFNγ licensed MSC with CsA in the context of immunosuppression. Collectively this data provides further evidence that MSC are complex immunomodulators and their response is dependent on their inflammatory micro-environment. This data also proposes that CsA uses different mechanisms to regulate these cytokines and, depending on inflammatory cues, MSC can hinder these processes.

It is of interest that the cytokines IFNγ and TNFα are involved in MSC licensing, and production of mediators such as CXCL9 (protein) were increased at high PBMC densities by all groups of MSC irrespective of IFNγ licensing or CsA addition. The high levels of CD3$^+$ IFNγ$^+$ T cells at the 1:40 ratio may have been a source for IFNγ licensing of MSC to induce CXCL9 production with no obstruction from CsA whereas at 1:5 the numbers of CD3$^+$ IFN$^+$ T cells and IFNγ in the supernatant are significantly lowered by CsA. This suggests that the co-addition of CsA at low PBMC densities provides an environment that is too suppressive for full MSC activation which resulted in less CXCL9 production. Whereas, at high PBMC densities, where the number of MSC is lower, the relative dose response from available IFNγ produced more potently suppressive MSC in the presence of CsA. While these results seem paradoxical, they may be explained and supported by the findings of Ren *et al.,* (2008) and others. These studies demonstrate that MSC must encounter some level of IFNγ arising from initial T cell activation subsequently leading to the induction of MSC immunosuppressive function before they shut down its production (Cuerquis *et al.* 2014). It also shows that MSC are receptive to their micro-environment and require a threshold of IFNγ and TNFα to facilitate

immunosuppression as opposed to the targeted potent immunosuppressive nature of CsA. While it is suggested here that MSC hamper CsA immunosuppressive ability *in vitro*, there may be a protective regulatory role mediated by MSC *in vivo* and this may be useful in a patient setting where long term immunosuppression by CsA has been shown to have harmful side effects such as susceptibility to infection or nephrotoxicity (Tharayil John *et al*. 2003; Parekh *et al.* 2004). In a model of ischaemia reperfusion injury, MSC were shown to alleviate kidney fibrosis in CsA immunosuppressed rats (Alfarano *et al.* 2012). Hence, MSC have been shown to display reparative rather than immunosuppressive activity and this may play a supportive role with CsA *in vivo*.

MSC utilise a range of immunomodulatory agents to engage in their immunosuppressive functions. To probe further the dynamic interactions of CsA and MSC, the direct effects of CsA on the key immunomodulatory mediators of MSC were defined *in vitro*. Chemoattraction of T cells in particular is thought to be required for MSC to exert their contact dependent immunosuppression mediated by short acting molecules like IDO and PGE-2 (Ren *et al.* 2008), importantly CsA had no altering effect on MSC production of CCL2 or CXCL9. Reports demonstrating the effect of CsA on MSC production of these chemokines are lacking in the literature. In a lung allograft model, CsA administered with anti-CXCL9 prevented acute lung allograft rejection in comparison to CsA alone (Belperio *et al*. 2003). This implies that the effect of CsA on CXCL9 is negligible as a neutralising antibody was required to reduce levels of CXCL9 in this case.

Similarly, in a model of renal transplantation, the levels of CCL2 in the serum were unchanged by CsA (Yao & Yu 2009). These studies show that CsA has no altering effects on these chemokines in these settings and support the lack of effect observed by CsA on MSC chemokine production. It is important to note here that while this study investigated the direct

effect of CsA on MSC chemokine production, CCL2 and CXCL9, it didn't explore the effect of CsA on T cell migratory capacity to these chemokines.

Interestingly, CsA has been shown to upregulate chemokines such as CXCL12 in other cell types such as trophoblasts and decidual stromal cells through the activation of mitogen-activated protein kinase/extracellular signal-regulated kinase (MAPK/ERK) signalling (Du *et al.* 2012; Zhao *et al.* 2012; Wang *et al*. 2013; Meng *et al.* 2012). Although, CsA has been shown to upregulate CXCL12 by these cells, pre-treatment of T cells with CsA inhibited their migration towards CXCL12 (Datta *et al.* 2006). This raises questions surrounding the effect of CsA on MSC and T cell cross-talk and chemoattraction. While this was not investigated here, this is an area which calls for future investigation as MSC produce CXCL12 to maintain the haematopoietic niche and combination with CsA may have important implications for patients receiving HSCT in terms of engraftment (Hou *et al.* 2010; Ehninger & Trumpp 2011).

CsA was also shown to inhibit DC migration towards CCL3 and CCL19, however the administration of exogenous PGE2 reversed the effects of CsA on DC migration (Chen *et al.* 2004). The effect of CsA on PGE2 production by MSC was explored in this study, however the use of a competitive ELISA for a short lived lipid such as PGE2 consistently presented saturated samples making it impossible to determine differences between samples, as a result the data was excluded. However, CsA significantly impaired COX-2 mRNA even when MSC were prelicensed with TNFα. As COX-2 regulates PGE2 production it is hypothesised that PGE2 is likely downregulated by CsA. However, this has yet to be confirmed at the lipid level.

While this effect of CsA on MSC is poorly documented in the literature, CsA was shown to inhibit PGE2 induced CCL2 secretion in mast cells (Nakayama *et al*. 2006), reduce COX-2 mRNA and PGE2 production in macrophage (Attur *et al.* 2000) and Chen *et al.* showed that COX-2 mRNA expression was reduced in DC. Therefore, CsA can inhibit PGE2

production in many immune cells and it is likely that a similar scenario occurs in MSC. The lack of reports on this in the literature highlights a significant gap in our understanding of the direct interactions of CsA on MSC-PGE2 mediated immunosuppression.

IDO is an important mediator used by MSC to suppress T cell proliferation *in vitro* through the depletion of tryptophan (Francois *et al.* 2012). It is upregulated by inflammatory cytokines and has been described as being an "on-off' switch that determines the outcome of immunomodulation by MSC where targeting it allows manipulation of the plasticity of MSC-mediated immunomodulation (Wang *et al.* 2014). The functional relevance of IDO activity has been shown by the use of the specific inhibitor 1-Methyl-L-tryptophan, which restored alloresponsiveness and supported a model where IDO, produced by MSC, exerted its effect through the local accumulation of tryptophan metabolites rather than through tryptophan depletion *in vitro* (Ryan *et al*. 2007). Following this, the ISCT have suggested that the IDO response should be central when investigating MSC potency *in vitro* (Krampera *et al*. 2013; Galipeau *et al*. 2016).

Therefore, the effect of CsA on IDO production by MSC was assessed *in vitro* and it was hypothesised that CsA would impair IDO production by MSC as immunosuppressive drugs including CsA were shownto do so by others (Schroecksnadel *et al*. 2011; Wang *et al*. 2014b; Chen *et al*. 2014). Unexpectedly, CsA significantly enhanced IDO production by prelicensed MSC at the mRNA and protein level. Futhermore, this enhancement by CsA was evident using a more quantifiable method, flow cytometry, where CsA was shown to significantly increase the percentage of MSC producing IDO following IFNγ induction in a time dependent manner. Importantly, CsA alone did not induce IDO production but when CsA was added 24 h after IFNγ it enhanced IFNγ induced IDO production.

Notably, when IFNγ and CsA were added to MSC simultaneously, this effect was not observed. These findings are supported by Ankrum *et al*., (2014) where IDO was shown to be enhanced in human MSC following treatment with IFNγ and subsequent steroids, budesonide and dexamethasone. It is important to distinguish that these were direct effects of CsA on MSC production of IDO following IFNγ prestimulation rather than effects observed in a PBMC co-culture assay. In this way, the stimulus for facilitating this effect was solely down to IFNγ and the IFNγ (but not TNFα) prelicensing of MSC was identified as being key for facilitating this effect.

All of the findings thus far have suggested an instrumental role for activation of the IFNγ signalling pathway in MSC for the maintaintenance or enhancement of immunomodulatory ability when combined with CsA *in vitro*. The interaction of CsA on IFNγ licensing of MSC in this study therefore supports the primacy of IFNγ in the MSC activation process as suggested by the ISCT (Krampera *et al*. 2013). Therefore, the next approach was to probe this pathway further and identify a mechanism by which this effect was being achieved *in vitro.*

Following a comprehensive review of existing literature to identify potential targets, suppressor of cytokine signaling 1 (SOCS1) was identified as an interesting candidate. SOCS1 is a negative regulator of cytokine signal transduction and is known to play an important role in the regulation of IFNγ signalling (Yoshimura A.T *et. al* 2007). It has recently been shown to negatively regulate the immunosuppressive ability of murine MSC by reducing the expression of inducible nitric oxide synthase (iNOS) (Zhang *et al*. 2014). This study showed that T cell proliferation was strikingly inhibited by MSC knocked down for SOCS1 by shRNA at 1:80 (MSC : T cells) ratio *in vitro* (Zhang *et al*. 2014). Therefore, as SOCS1 has been described as a regulator of MSC immunosuppressive functions through IFNγ signalling, it was imperative to investigate the effect CsA has on SOCS1 signalling in MSC.

CsA had an inhibitory effect on SOCS1 expression (at the protein level) in MSC resulting in preservation of the IFNγ pathway. This reduction in SOCS1 may correspond to slightly higher pSTAT1 protein levels in MSC that were licensed with IFNγ before CsA addition. Mounayar *et al*., showed that STAT1 overexpression in MSC strongly enhanced MSC suppression of T cells while downregulation of STAT1 abrogated MSC immunosuppressive ability *in vitro* (Mounayar *et al.* 2015). This places STAT1 as a critical signal for the induced production of IDO in MSC and we have shown how CsA can manipulate this pathway by inhibiting SOCS1 which subsequently maintained the phosphorylation of STAT1 *in vitro*. The inhibition of SOCS1 by CsA was found only in licensed MSC as CsA alone had no inhibitory effect on basal levels of SOCS1 in resting MSC which further supports the requirement for IFNγ to induce IDO production. SOCS1 overexpression has been shown to specifically inhibit STAT1 activation following Toll like receptor 3 (TLR3) stimulation in MSC with subsequent internalisation of chemokine receptor CXCR7 (Tomchuck *et al*. 2012). This study shows further how SOCS1 is an important regulator of MSC function whereby MSC migratory capacity is impaired when SOCS1 is overexpressed. These findings show that exploitation of SOCS1 inhibition by CsA would improve MSC therapy by enhancing the mobilisation of MSC into targeted sites of inflammation and enhance their potency via an IDO mediated mechanism.

The inhibition of SOCS1 by CsA in MSC is indirect as it is dependent on activation of the IFNγ pathway and therefore must involve other IFNγ inducible proteins. These findings are supported by others where CsA is known to interfere with the inhibitory function of SOCS1 in cells infected with hepatitis C virus and rotavirus (Liu *et al* 2011; Shen *et al.* 2013). Notably, these viruses are dependent on IFN signalling for their replication.

Interestingly, while SOCS1 is a negative regulator of STAT1, STAT1 was shown to regulate SOCS1 and the IFNγ induced expression of SOCS1 mRNA was eliminated in

fibroblasts lacking STAT1 (Saito *et al.* 2000). We have shown that while SOCS1 is reduced in MSCγ treated with CsA there is maintenance of pSTAT1 and STAT1 protein levels. This supports the theory that CsA could be inhibiting the transmigration of SOCS1 from the nucleus into the cytoplasm as it has been suggested that cyclophilin may capture CsA into the nucleus where it can target regulatory proteins or transcriptional control elements (Le Hir *et al.* 1995). However, this remains to be explored. Another likely explanation for the maintenance of pSTAT1 and STAT1 protein levels is the timing of CsA stimulation relative to this negative feedback loop process and suggests that the effect mediated by CsA is transient.

This study shows that the interaction of CsA on MSC immunosuppressive activity is multifactorial and beneficial effects are dependent on the activation of MSC through IFNγ priming. While there are numerous *in vitro* and *in vivo* studies reporting beneficial effects of CsA in combination with MSC (K Le Blanc et al. 2004; Maccario et al. 2005; Zhang et al. 2007; Pischiutta et al. 2014), there are equal numbers of studies showing CsA as having a negative impact on MSC immunosuppressive ability and vice versa (Inoue et al. 2006; Buron et al. 2009; Eggenhofer et al. 2011; Jia et al. 2012). These studies reported their observations without a mechanistic explanation to support their assumptions and failed to expose the role of IFNγ signalling in inducing an immunosuppressive phenotype in MSC when combined with CsA. We have shown conclusively for the first time that licensing of MSC is required for MSC to retain their suppressive function in the presence of CsA. We have also shown that CsA can enhance IDO production in licensed MSC through the inhibition of SOCS1.

However, the exact mechanism by which CsA is inhibiting SOCS1 remains unclear. Nonetheless, this identifies a novel role for CsA in maintaining signal transduction in the IFNγ pathway of MSC through the inhibition of SOCS1 which has consequences for the potency of MSC immunosuppressive function.

Chapter 3, extensively investigated the interactions of CsA and MSC *in vitro* and provided comprehensive findings regarding the influence of CsA on MSC immunosuppressive ability and vice versa. While many have reported on the immunosuppressive effects of CsA on MSC in terms of suppressive ability, there have been no reports or in-depth studies providing a mechanism to support such interactions. Notably, this chapter has defined the direct effects of CsA on the key immunomodulatory mediators of MSC and proposed a mechanism by which CsA can influence IFNγ signalling in MSC. These findings enhance our knowledge of how CsA interacts with MSC *in vitro* and provide a basis from which these investigations can be expanded upon *in vivo*.

However, the limitation with all *in vitro* studies is that they are manufactured systems designed to mimic a naturally occuring environment making it difficult to replicate such findings in more complex systems like *in vivo* settings. Importantly, these findings do represent an advance in our understanding of how CsA interacts with MSC, particularly identifying MSC activation and timing of CsA as being crucial for beneficial immunosuppressive functions which can be applied to *in vivo* pre-clinical models and clinical settings.
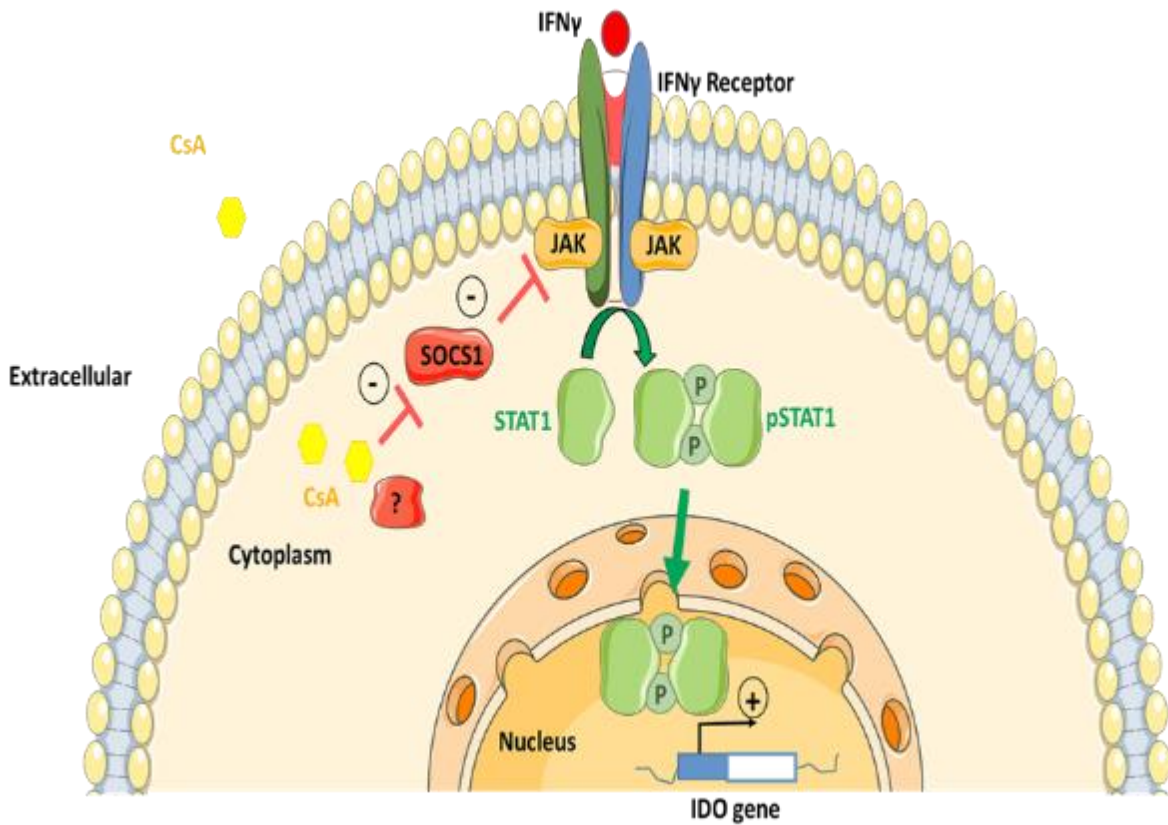
Figure 6.1 CsA enhances IFNγ induced IDO through a SOCS1 inhibitory mechanism.
IFNγ binds to and activates its cognate receptor (IFNγ receptor) triggering a cascade of signalling events that induce IDO. Kinases of the Janus Kinase (JAK) family are recruited and phosphorylate STAT1 leading to dimerisation. This complex can translocate to the nucleus and stimulate transcription of interferon regulated genes such as IDO, denoted by +. SOCS1 inhibits the catalytic activity of JAKs by binding to the activation loop of the catalytic domain thereby inhibiting phosphorylation of STAT1, translocation to the nucleus and subsequent stimulation of interferon regulated genes, denoted by -. CsA inhibits this SOCS1 induced negative loop, maintains IFNγ signalling through STAT1 and enhance the IFNγ induction of IDO, denoted by -. The protein marked "?" is an IFNγ induced protein, yet to be identified, which we suspect facilitates CsA inhibition of SOCS1 as CsA does not inhibit basal levels of SOCS1 in resting MSC.

The implementation of MSC therapy for routine clinical use has suffered a setback following the results of large scale phase III clinical trials. While there has been a number of reasons put forward to explain this failure, it is apparent that the lack of standardised approaches and conceptual understanding of MSC action is preventing this advancement. The application of MSC therapy for the treatment of aGvHD patients on the grounds of compassionate use provided the first ground breaking reports of the potential for MSC therapy in this setting.

Following academic led trials, Osiris Therapeutics produced MSC-like cells called Prochymal™ and investigated their therapeutic efficacy for aGvHD in clinical trials. In Phase II trials, Prochymal™ induced a successful response in a high percentage (77%) of aGvHD patients when used in combination with existing therapy, however, the Phase III clinical trial was deemed unsuccessful and failed to reach its primary endpoint (Martin *et al.* 2010). This study showed that MSC have a huge inter-donor variability in terms of their immunoregulatory function (Galipeau 2013). This variability has impeded the progress in MSC therapeutic application, due to the inability to determine how MSC modulate aGvHD and with difficulties in determining optimal treatment dose, timing and importantly, in identifying where it is not a suitable therapy. More importantly, the lack of understanding on the interactions of MSC with immunosuppressive drugs, particularly CsA, has prevented the routine incorporation of MSC therapy into prophylaxis or treatment schedules.

CsA is widely used for prophylaxis of aGvHD and it is also used as a salvage therapy where steroids have failed (Ruutu *et al.* 2014). Thus the importance of its application as a therapy for aGvHD and the relevance for defining its interaction with MSC is a key priority. However, the variability of CsA metabolism in the GI tract has been shown to significantly affect its bioavailability which poses implications on oral dosage requirements (Webber *et al.* 1992; Drewe *et al.* 1992). This prompted the development of a novel oral CsA delivery

technology, SmPill® by our collaborators (Sigmoid Pharma) for which the efficacy was established in a humanised model of aGvHD in chapter 4. Other problems associated with CsA include nephrotoxicity and increased risk of infection from long term immunosuppression (Halloran *et al.* 1999; Parekh *et al.* 2004). The introduction of a combination therapy consisting of MSC and CsA for aGvHD in the clinic has the potential to overcome these issues. The intrinsic pro-reparative properties of MSC should reduce these harmful side effects and the immune regulatory capacity of MSC would likely support the use of a lower dose of CsA. Moreover, a novel CsA treatment by means of optimal targeted delivery (SmPill®) can provide a more clinically applicable co-therapy. However, one of the major challenges in successfully translating MSC therapy into the clinic is due to the lack of understanding of the interactions of MSC with immunosuppressive drugs such as CsA.

Therefore, this thesis advocates that the elucidation of the interactions of MSC with both oral and intravenous CsA will provide a more successful and tailored approach to treating aGvHD. Understanding the influence of CsA on MSC activation and vice versa *in vivo* will aid in this process. Therefore the purpose of chapter 5 was to explore these interactions further and determine if CsA and MSC are efficacious as a co-therapy in aGvHD and define the role MSC activation plays in partnership with CsA.

The advancement of humanised models to study aGvHD has provided a clinically relevant setting by which the pathophysiology of the disease can be studied. What makes them more advantageous over mouse models of aGvHD is that they are designed to facilitate the engraftment of adult human immune cells within the mouse. These transplanted immune cells are activated in response to the xenogeneic recognition of murine MHC molecules (present on mouse tissues) and the subsequent activation and proliferation of human immune cells form the basis for aGvHD development. Thus, the cells driving the disease are human making this model clinically relevant and useful for assessing novel therapeutic interventions, including

human MSC for aGvHD. Another advantage is that the progression of aGvHD in these models is faster which reduce the time and costs associated with large scale *in vivo* studies. However, there are also some disadvantages associated with this model. Transplantation of human PBMC to immunodeficient mice require human APC to process mouse antigens and present them in the presence of MHC class II (Schroeder & DiPersio 2011). T cell recognition of MHC molecules is restricted by species as human T cell receptors don't recognise mouse MHC, therefore making this a CD4$^+$ T cell dependent model (Lucas *et al.* 1990). Moreover, DC migration to the lymph nodes may not function well in NSG mice due to the poor structure of their lymph nodes making it difficult to define the role of DC in aGvHD (Spranger *et al.* 2012).

While there are a number of humanised mouse models available to study aGvHD, the NSG model has been shown to be superior in terms of human PBMC engraftment compared to other models (Ali *et al.* 2012) and has been successfully established in the English lab for assessing the efficacy of MSC therapy (Tobin *et al.* 2013; Healy 2015). While this humanised mouse model was originally developed by Pearson *et al.*, extensive experimentation was carried out in the English lab to establish a robust and reproducible model of disease. Many approaches were undertaken to enhance this model, in particular the use of freshly isolated PBMC to the progression of PBMC isolated from buffy packs and subsequent normalisation of PBMC dose to the weight of each mouse (Tobin *et al.* 2013; Healy 2015). This facilitated the performance of large scale *in vivo* studies as the recovery of higher numbers of PBMC from buffy packs than freshly isolated samples could allow the inclusion of more mice per study and the normalisation of PBMC dose to the weight of each mouse provided a more consistent level of aGvHD development within each mouse. Subsequently, investigations into the efficacy of MSC therapy in this model of aGvHD led to the demonstration that MSC administered on day 7 could significantly prolong the survival of aGvHD mice (Tobin *et al.* 2013; Healy 2015). Tobin *et al.*, also demonstrated that timing of MSC administration and proinflammatory

cytokine levels *in vivo* are critical for MSC effectiveness as immunosuppressive agents in aGvHD (Tobin *et al.* 2013). On this basis and building on findings obtained in chapter 3, this humanised mouse model of aGvHD was used as a platform to assess the importance of prestimulating MSC with IFNγ before CsA treatment *in vivo*. Furthermore, many patients undergoing HSCT transplant will have undergone a prophylaxis regimen involving CsA immunosuppression, therefore emphasising the clinical relevance of this investigation. However, before this investigation was carried out, it was necessary to fully define the optimal dosing schedule of CsA and establish its efficacy within this humanised mouse model. A detailed study investigating the efficacy of CsA administered through oral, intravenous, or through targeted systemic or gastrointestinal delivery in the humanised mouse model of aGvHD was carried out.

Cyclosporine (CsA) has played an important role in the advancement of transplant medicine. With improved rates of acute rejection and graft survival rates at 1 (82%), 5 (69%) and 10 (54%) years, CsA has become a mainstay for modern immunosuppression for solid organ transplants and HSCT (Marcen *et al.* 2009; Ruutu *et al.* 2014). The specific T cell inhibitory activity of CsA make it an ideal therapy for a T cell driven disease like GvHD. For prophylaxis of aGvHD, CsA is administered for up to six months after allogeneic HSCT (Ruutu *et al.* 2014). Over the years, CsA has also been reported to be an effective second line treatment of established GvHD and is currently recommended throughout Europe (Deeg *et al.* 1985; Parquet *et al.* 2000; Finke *et al.* 2009; Ruutu *et al.* 2014). However, the metabolism of CsA in the GI tract has been shown to significantly affect bioavailability as its absorption is slow, variable and incomplete (Webber *et al.* 1992; Drewe *et al.* 1992). The added complications of damaged GI mucosa as a result of the conditioning regimen undergone by allogeneic HSCT patients could further influence CsA pharmacokinetics with reduced intestinal absorption (Kimura *et al.* 2010).

Much focus has been on efforts to enhance oral CsA bioavailability. Sandimmune®️ and the more advanced Neoral®️ are oral formulations of CsA which were designed for this purpose. Neoral®️ in particular has been shown to enhance oral bioavailability of CsA more efficiently than oral Sandimmune®️ and reduce the variability in pharmacokinetic parameters within and between patients receiving CsA therapy (Parquet *et al*. 2000; Yocum *et al.* 2000). As oral Sandimmune®️ is an oil-in-water emulsion, CsA absorption is affected by food intake and fat content, GI movements and bile secretion, however the microemulsion Neoral®️ formulation achieves a fast release of CsA at the site of absorption which improves the disolution of CsA in the GI tract, independent of food or bile secretion (Yocum *et al*. 2000; van Mourik *et al.* 1999). Although Neoral has provided an improvement to the variability of oral CsA bioavailability, it is an immediate releasing CsA formulation which results in rapid peaks and trough levels of CsA in the blood (Jorga *et al.* 2004). Therefore, CsA levels in the blood are maintained above thresholds and ultimately contribute to unwanted systemic side effects and a potential limit to the beneficial GvL effect (Parquet *et al.* 2000; Kishi *et al*. 2005). Also, CsA nephrotoxicity still presents as a side effect in the clinic which suggests that there is still interindividual variability in pharmacokinetics of CsA.

Our collaborators, Sigmoid Pharma Ltd., have developed a sophisticated drug delivery technology called SmPill®️ which encapsulates CsA into a multi-bead format where the outer coating controls the release of CsA. These formulations deliver CsA systemically (immediate release) but also specifically target the GI tract (colonic release), where the two formulations combined expose the entire GI to CsA (Figure 6.2). The immediate release SmPill®️ formulation provides a slower release than Neoral®️ which permits modulated pharmacokinetic (PK) profiles, attaining adequate trough levels without the excessive PK profile associated with Neoral®️. Therefore, it was hypothesised that this modulated systemic release formulation would release CsA over a longer time period than Neoral®️ and provide sustained levels of CsA

to the small intestine leading to protection against small intestinal GvHD. As aGvHD is a multi organ inflammatory disease with the GI tract having a primary role in initiation, it was hypothesised that SmPill® would be a more efficacious CsA therapy in the humanised mouse model of aGvHD.

Our humanised mouse model of aGvHD provided a platform from which these therapies were assessed and their performance of alleviating aGvHD was investigated in a clinically relevant manner. In parallel with this, the impact of oral and intravenous delivery of CsA on the GI tract or systemic tissues was explored in this model. The efficacy of each of these CsA therapies and of particular interest, SmPill®, was demonstrated in our humanised model for the first time.   As CsA is a mainstay prophylaxis treatment for aGvHD (Ruutu *et al.* 2014), our first approach was to begin dosing on day 1 on a daily basis to day 12 where aGvHD development is known to be established in our model (Tobin *et al.* 2013). The loading of CsA in the SmPill® immediate and colonic release beads collectively was approximately a 25 mg/kg dose. With this in mind and similar to published reports, all other CsA therapies were administered at 25mg/kg per dose (Gan *et al*. 2003; Hori *et al.* 2008; Perez *et al.* 2011). By keeping the dosage of CsA constant from day 1, the performance of each delivery method was assessed in terms of prolonging survival in the humanised aGvHD model. However, we found that this dosing schedule was not effective at prolonging survival of aGvHD mice and continuous weight loss was observed.

It has been reported that irradiation conditioning alone can severely impact mouse body weight (Saland *et al*. 2015). Thus, we hypothesised that the initial weight loss as a result of the irradiation conditioning (2.4 Gy) could have been a factor contributing to reduced CsA absorption resulting in the failure of all oral and intraperitoneal CsA therapies in prolonging survival in GvHD mice. In contrast Sandimmune® IV significantly prolonged the survival and reduced weight loss in this model. While this meant that the CsA dose of 25mg/kg was

effective in this model, it demonstrated how oral therapies are not very well tolerated in the early days following transplantion. This is similar to findings in the clinic, where patients who have received allogeneic HSCT are firstly given CsA intravenously and converted to oral therapy as tolerated (Jacobson et al. 2003). Another outcome from this initial study was in relation to the size of the SmPill® beads, where a number of mice treated with SmPill® were humanely euthanised due to tracheal damage as the beads delivered via oral gavage were not of optimal size.

Considering each of these factors, the study was refined by downsizing the number of study groups and utilising a different dosage strategy in terms of timing. The CsA study groups were reduced to Neoral® and Sandimmune® IV, as a comparator for SmPill® efficacy. In this way, valuable data was attained while reducing the number of mice, thus heightening the ethical standards of our study. Due to initial post-irradiation weight loss, early dosing of oral therapies from day 1 proved to be ineffective in this model of aGvHD. Day 4 represented an adequate start day (as mice had returned to baseline weight) for CsA dosing and the administration of 5 doses (25 mg/kg per dose) of SmPill® on day 4, 6, 8, 10 and 12 was shown to be most effective at significantly prolonging survival and reducing weight loss during aGvHD. Furthermore, the optimal SmPill® bead size was determined to be within the range of 1-1.25mm and used at this size for all other studies where there were no cases of tracheal damage as a result of drug administration via gavage. Accordingly, this dosing schedule was deemed optimal for efficacy of SmPill® delivery and was used for further investigations of SmPill® performance throughout this study.

As SmPill® was now optimised to prolong the survival and reduce weight loss associated with aGvHD. It was hypothesised that delivering CsA in a multiformatted way would achieve a more efficacious aGvHD therapy as CsA is distributed systemically and gastrointestinally. Therefore, our humanised model of aGvHD was used to test this hypothesis.

This study found that SmPill® prolonged survival and reduced weight loss in aGvHD mice in a comparable manner to Sandimmune® IV but with greater efficacy than Neoral®. Sandimmune® IV by its intravenous nature provides 100% bioavailability and therefore proved to be an efficacious treatment in our humanised model of this multi-organ disease, aGvHD. Whereas following oral administration, CsA absorption in the GI is affected by food intake, fat content and GI movements which can reduce the bioavailability to 30% (Beauchesne *et al.* 2007). Interestingly, we found SmPill® to be more efficacious than Neoral®. This shows that SmPill® is an advanced oral therapy, having comparable efficacy to its intravenous counterpart, Sandimmune® IV suggesting it can provide enhanced protection to this multi-organ disease, aGvHD.

This was evident in our histological findings where SmPill® provided a similar protective profile to that of Sandimmune® IV but was a more effective oral CsA therapy than Neoral®. The systemically absorbed Sandimmune® IV was significantly efficacious in protecting all of the target organs from aGvHD progression and SmPill® matched this efficacy. While Neoral® significantly alleviated signs of aGvHD in the liver and small intestine, it was not effective in reducing aGvHD pathology in the lung and colon. This suggests that CsA is not as effectively distributed using Neoral® in comparison to SmPill® or Sandimmune® IV. This is likely due to the immediate CsA releasing nature of Neoral® which resulted in reduced CsA bioavailability reaching the colon (Jorga *et al.* 2004). Whereas, the colonic release SmPill® beads were designed to provide a sustained release via a slow colon transit time to permit complete and sustained colon tissue bioavailabilty.

In relation to the lung, Neoral® is associated with rapid peaks and trough levels of CsA in the blood which need to be maintained (Jorga *et al.* 2004). Therefore, our dosing schedule where CsA was administered every second day may not have been optimal for Neoral® which lead to inefficient lung protection. Whereas, SmPill® was designed specifically to provide a

sustained release of CsA from the immediate release beads providing protection to both systemic and intestinal tissues which would explain the differences between these two oral CsA therapies. In a study using magnetic nanoparticles as a delivery system for CsA, it was found that this targeted carrier of CsA was efficacious in reducing pathology in aGvHD mice (Zhou *et al*. 2011). However, Zhou *et al*., did not use clinically relevant CsA comparator controls such as Neoral® and Sandimmune® IV, instead they administered CsA by intraperitoneal injection for comparison to their delivery system.

Proinflammatory cytokine production drives the progression of aGvHD where the cytokine network may function as a common pathway mediating target organ damage (Antin & Ferrara 1992). There have been numerous studies showing how proinflammatory cytokines such as IL1β, IFNγ, IL2, IL6, IL17 and IL23 contribute to the severity of aGvHD (Antin & Ferrara 1992a; Kappel *et al*. 2009). The GI tract in particular plays a key role in the initiation of systemic aGvHD through the propagation of a "cytokine storm" as a result of bacterial translocation from the disruption of the physical barrier in the GI (Antin & Ferrara 1992; Ferrara & Reddy 2006). Therefore, the primacy of the GI tract as a target organ in aGvHD has focused experimental approaches aiming to reduce GI damage by fortification of the GI mucosal barrier using novel "cytokine shields" such as IL11 or keratinocyte growth factor (Hill & Ferrara 2000).

Our humanised model of aGvHD was used to examine the effect of SmPill® on the production of these cytokines (IL1β, IFNγ, IL2, IL6, IL17 and IL23) by human PBMC in the GI tract. Importantly, SmPill® was more efficacious in significantly reducing the levels of proinflammatory cytokines involved in aGvHD severity in the small intestine and colon than Neoral® and Sandimmune® IV. Thus providing more evidence that SmPill® was a superior CsA therapy as it was more efficient in delivering CsA to the GI resulting in enhanced protection. These cytokines have been detected in the serum of aGvHD patients where

abundance of these cytokines directly correlated with aGvHD severity (Fujii *et al*. 2006). This shows how SmPill® can provide a more clinically useful CsA treatment as it was more effective here than CsA treatments currently used in the clinic.

As TNFα is a hallmark of aGvHD, the ability of these therapies to reduce the production of TNFα during aGvHD was investigated. In particular, donor T cell derived TNFα has been shown to contribute to GvHD (Schmaltz et al. 2002; Borsotti et al. 2007). Therefore, in terms of systemic protection, the effect of these CsA therapies on the development of human TNFα producing CD4$^+$ and CD8$^+$ T cells during aGvHD was analysed in the spleen, liver and lung of aGvHD mice. SmPill® was shown to be a more efficacious oral CsA therapy than Neoral® as it significantly reduced TNFa producing CD4$^+$ T cells in the systemic organs (spleen and liver) in a similar, and some cases better, manner than Sandimmune® IV therapy.

However, SmPill® and Neoral® exhibited similar efficacy in the lung. Collectively, the histological and cytokine data provided evidence that SmPill® is an enhanced oral CsA therapy in comparison to Neoral® whereby systemic and GI protection is maintained during aGvHD. This enhancement may be a result of decreased IL1β, IFNγ, IL2, IL6, IL17 and IL23 in the GI and reduced TNFα production systemically. Targeting TNFα production as a therapy for aGvHD has already provided encouraging results in prolonging the survival of NSG aGvHD mice (King *et al*. 2009) and in the clinic where the use of moAbs that specifically target TNFα production, such as Etanercept or Infliximab, have proved to be efficacious second line aGvHD treatments (Horiuchi *et al*. 2010; Park *et al*. 2014). This places SmPill® in line with these treatments in terms of being an efficacious therapy for aGvHD by means of TNFα reduction from human PBMC in the tissues of aGvHD mice.

So far, we have provided evidence of the superior therapeutic efficacy of SmPill® in comparison to two CsA therapies already used in the clinic, Neoral® and Sandimmune® IV.

Following this, a number of methods were used to explore further how the different SmPill® bead formulations impact systemic and GI aGvHD in terms of engraftment kinetics, tissue apoptosis, cytokine profiles in systemic and GI tissues, Treg cell engraftment and NFAT activity. The different SmPill® bead formulations, as before, consisted of an immediate release bead (delivers CsA systemically) and a colonic release bead (specifically targets the GI tract). A particular interest here was to determine if the immediate SmPill® bead delivered alone could mediate protective effects in the GI in addition to systemic tissues and to examine if the colonic release bead cold mediate systemic effects as a result of targeting the GI in the humanised aGvHD model. By delivering the beads separately, the study provided a better indication of how efficacious they are in mediating protection in a targeted manner.

Five doses of SmPill® (25 mg/kg per dose) from day 4 was already shown to be effective in prolonging survival and reducing the pathology associated with aGvHD in this humanised mouse model. SmPill® was delivered in the form of two beads each time, 1 bead that released CsA immediately and 1 bead where CsA release was sustained in order to target the colon. To investigate the potential of these beads further, the immediate release and colonic release beads were delivered on their own to aGvHD mice and compared to their combined counterparts or Neoral® or Sandimmune® IV to explore the extent of systemic and GI protective effects mediated by these beads.

Consistent with earlier studies, the survival of aGvHD mice was significantly improved and weight loss was significantly reduced using the 1 immediate and 1 colonic bead SmPill® combination comparable to that of Sandimmune® IV but significantly better than Neoral®. Interestingly, delivery of either 1 immediate or 1 colonic bead alone significantly prolonged survival in aGvHD mice also. This shows that both systemic and GI targeted delivery of CsA can be efficacious in their own right. Moreover, these singular counterparts were more effective in prolonging survival and reducing weight loss than Neoral®. As the immediate

262

release beads do not release CsA as rapidly as the Neoral® solution, we hypothesise that it may provide broader GI tissue exposure from the luminal side and some of the systemically absorbed CsA will make its way to the colon tissue. In relation to the colonic release beads we hypothesised that, as the release initiates in the small intestine, there will be broad GI exposure with a small amount absorbed systemically. These findings are particularly interesting as aGvHD is a multi-organ disease which therefore requires a therapy capable of providing protection to each target organ affected. Due to the identification of the GI as a primary organ for aGvHD development in phase 1 (Hill & Ferrara 2000), we proposed that the early (from day 4) and GI targeted dosing of CsA (in the form of SmPill® colonic beads) provides protection at this phase of aGvHD development in the humanised mouse model. This prompted further investigation into the efficacy of systemic and GI protection by SmPill® to probe these hypotheses further.

Histological analysis revealed that targeted SmPill® delivery of CsA differentially protected systemic or GI organs from aGvHD associated tissue damage and apoptosis. The 1 immediate and 1 colonic bead combination facilitated the most significant protection in the liver and lung, however this systemic protection was reduced when only 1 or 2 colonic beads were administered. We also noted that the significant protection in the GI mediated by the 1 immediate + 1 colonic SmPill® combination was lost when 1 immediate bead was given alone. This highlighted the variability of total GI tissue bioavailability of CsA following the administration of immediate release alone whereas the colon release beads alone provided a sustained release through the colon which provided enhanced GI protection. CsA has been referred to as a "critical dosage drug" and its impact on calcineurin suggests a benefit from consistent and persistent exposure to CsA (Morris 2003). While the 1 immediate release and the 1 or 2 colonic beads administered alone could prolong survival and reduce weight loss, it is evident that the combination of the two is required for protection of each target organ

(systemically & gastrointestinally). Thus, the consistent and persistent dose of CsA, provided from the duo combination, provided a more impactful aGvHD therapy.

Probing systemic and GI protection by SmPill® further, cytokine profiles were established for the spleen, lung, liver, small intestine and colon. This confirmed that SmPill® delivery of CsA differentially protects systemic or GI organs from aGvHD. The 1 immediate and 1 colonic combination provided significant reduction in proinflammatory cytokines across all systemic and GI specific organs. Supporting the preferential systemic efficacy of the immediate release, the immediate release bead alone provided significant reduction in the proinflammatory cytokines detected in the liver and lung but protection in the colon was not significant. Interestingly, in addition to GI there was systemic protection from proinflammatory cytokines mediated by the 2 colonic bead therapy. This reinforces the primary role the GI plays in the aGvHD response and this data suggests that targeted delivery of CsA can provide systemic protection by means of proinflammatory cytokine reduction in the spleen, liver and lung.

This effect may be due to a reduction in DC migration from the GI as CsA has been shown to impair the migration of DC to CCL19 *in vitro* and inhibit the migration of DC from the skin to secondary lymphoid organs *in vivo* (Chen *et al.* 2004). Also, CsA has been shown to increase the homing of CD4$^+$ T effector cells to the colons of mice via upregulation of mucosal addressin cell adhesion molecule in a syngeneic mouse model of GvHD (Perez *et al.* 2011). Homing studies would enlighten this effect in our model and it is possible that with increased migration of CD4$^+$ T cells to the colon, CD4$^+$ T cell function could be impaired due to the sustained exposure of CsA concentration released from the SmPill® colonic bead. These studies support our findings and strengthen our hypothesis that proposes that targeted delivery of CsA to the GI can provide systemic protection.

As already mentioned, TNFα producing donor T cells contribute a major role in the development of GvHD (Schmaltz et al. 2002; Borsotti et al. 2007). TNFα plays a role in all phases of aGvHD pathophysiology, as detailed in Chapter 1, from the early phase of host APC activation through to tissue damage where the GI tract in particular is most susceptible. In mouse models of GvHD, inhibition of TNFα resulted in reduced intestinal pathology with reduced occurence of apoptosis (Brown *et al*. 1999; Stuber *et al.* 1999). This study already showed that SmPill® (1 immediate + 1 colonic) suppressed the number of CD4+ and CD8+ T cells producing TNFα in the spleen, liver and lung but didn't measure the number of CD4+ and CD8+ T cells producing TNFα in the GI. Therefore, this larger study with different combinations of SmPill® was carried out to investigate specific systemic and GI protection from TNFα producing CD4+ and CD8+ T cells mediated by 1 immediate or 1 colonic bead alone.

In this regard, we showed that the 1 immediate + 1 colonic combination proved to be significantly effective systemically and in the GI. This combination displayed similar efficacy to Neoral® in the GI but was more efficacious than Sandimmune® IV. Interestingly, the 1 immediate bead was efficacious in the GI tract while the 1 or 2 colonic beads were effective systemically (liver and lung) by means of reducing the number or percentage of TNFα production by T cells in each case. Others have shown that CsA uptake by DC to T cells resulted in suppressive effects (Muller *et al.* 1988), impaired DC capacity to stimulate allogenic and autologous T cells (Ciesek *et al*. 2005) and inhibited DC antigen presentation *in vivo* (Lee *et al*. 2007). The established concentration of CsA from the 1 immediate or the 1 colonic beads may be mediating these effects on DC resulting in the reduced number of TNFα T cells. Notably, the cells isolated in the small intestine and colon were combined and therefore it is possible that investigating the number of TNFα producing T cells in the colon alone would distinguish differences. These findings supported both the histological findings and cytokine

265

analysis and affirmed the hypothesis that TNFα producing T cells in systemic and GI tissues is regulated by specific targeted combinations of SmPill®.

Naturally occurring CD4+CD25+ Treg are pivotal for the maintenance of self-tolerance and in GvHD they can maintain tolerance to the matched host tissues but they can also react across MHC barriers and prevent the initiation of immune responses to host antigens (Trzonkowski *et al*. 2013). Tregs have been identified as a potential cell therapy for regulating aGvHD development (Taylor *et al.* 2002; Hoffmann *et al.* 2002; Edinger *et al*. 2003). Depletion or reduced engraftment of Treg has been shown to increase the progression and severity of aGvHD (Taylor *et al.* 2002). Also, in murine models of aGvHD, the infusion of donor derived Tregs at the time of allogeneic BMT prolonged their survival and reduced aGvHD associated pathology through an IL10 dependent mechanism (Hoffmann *et al.* 2002; Edinger *et al.* 2003). Importantly in HSCT patients, reduced Treg engraftment strongly correlated with aGvHD development, proposing the use of Tregs as a diagnostic/prognostic biomarker for aGvHD (Magenau *et al.* 2010; Fujioka *et al*. 2013; Danby *et al.* 2016).

With this in mind, the effect of each SmPill® formulation on the engraftment of CD4+ CD25+ FoxP3+ Treg in aGvHD mice was established. It was revealed that the number and percentage of Tregs recovered from aGvHD tissues was not significantly changed by any CsA therapy compared to untreated aGvHD mice. This was unexpected as CsA has been shown previously to reduce the number of of CD4+ CD25+ Tregs inmouse models of GvHD and in a skin transplant model (Zeiser *et al.* 2006; Coenen *et al.* 2007; Satake *et al*. 2014; Liu *et al.* 2014). However, our study warrants further experimentation as error bars were quite high in this dataset and suggests variations within our small sample size of n=6.

CsA is known to reduce NFAT activity through calcineurin inhibition and it has been shown to induce partial calcineurin inhibition that varies directly with the blood and tissue

levels which may be greater in some tissues due to higher drug accumulation (Halloran *et al.* 1999). Therefore it was hypothesised that the different SmPill® formulations would regulate NFAT differentially in systemic and GI tissues and would correlate to the relative CsA concentration in these tissues. In this way, targeted delivery of CsA to GI and systemic tissues can be measured and compared by the different SmPill® formulations in terms of NFAT activity as an indicator of calcineurin inhibition. Suprisingly, there was no significant differences between each of the SmPill® formulations as all of them reduced active NFAT in CD3$^+$ T cells recovered from the spleen, lung, liver and GI in a similar manner. This data suggests that there is similar NFAT activity within these tissues and that each SmPill® formulation regulates this activity in a comparable manner.

However, there are significant limitations in the sensitivity of measuring NFAT activity by flow cytometry. The nuclear translocation of NFAT defines NFAT activity and while an intracellular kit for nuclear detection was used to quantify NFAT, it does not differentiate or exclude cytoplasmic protein. Therefore, it is highly likely that this data is presenting nuclear and cytoplasmic NFAT. While there is a measurable reduction of NFAT by CsA, this method may not be sensitive enough to detect differences between each SmPill® formulation. Perhaps the use of confocal imaging or western blot of the different cellular fractions from the preparation of nuclear and cytoplasmic extracts from PBMC recovered from the tissues of aGvHD would enlighten differences between NFAT activity in systemic and GI tissues after targeted CsA delivery.

Chapter 4 has provided a thorough evaluation of SmPill® efficacy as a therapeutic intervention for aGvHD with a specific focus on targeted delivery to systemic and GI organs. This highly efficacious delivery system for CsA provides a stable and adequate concentration of CsA to mediate systemic and GI protection which reduced morbidity and mortality in

aGvHD mice. Thus, complications associated with systemic immunosuppression can be minimised making it highly applicable to the clinic. This study unequivocally demonstrates that a balanced efficacy is required for optimal management of a multi-system disease like aGvHD and the 1 immediate and 1 colonic SmPill® combination provided significant protection in each of the target organs in aGvHD. For the first time, we have shown that a novel CsA formulation, SmPill® provided safe and superior efficacy in comparison to routinely used CsA drugs, Neoral® and Sandimmune® IV in a humanised model of aGvHD. We have shown this enhanced efficacy using pre-clinical survival studies, histopathology and cytokine analysis and hypothesise that this enhancement over these conventional CsA drugs is mediated through targeted delivey to systemic and GI tissues (via 1 immediate and 1 colonic bead).

Therefore, making it a highly attractive candidate for routine clinical use for aGvHD treatment. Currently, our collabortaors are advancing a SmPill®-like product called CyCol® into Phase III clinical trials for ulcerative colitis. CyCol® was shown to be safe and well tolerated in over 100 mild to moderate patients over the four week treatment and four week follow up periods in the Phase II trial (Sigmoid Pharma Ltd. 2009). This formulation provides targeted CsA delivery to the colon in a similar manner to the colonic beads used in this study.
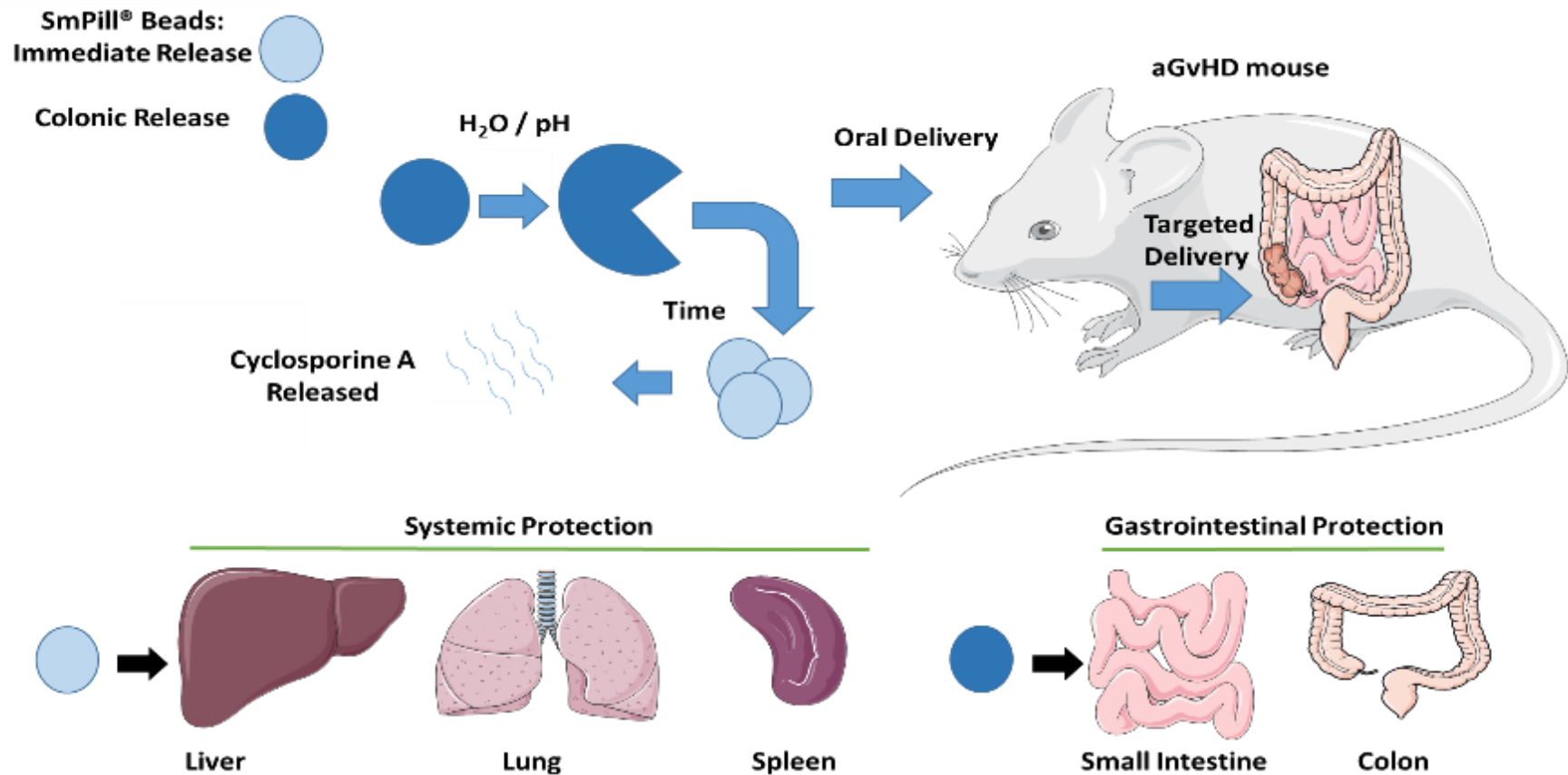
Figure 6.2 SmPill® technology provides systemic and gastrointestinal protection through targeted delivery in aGvHD mice. Cyclosporine A (CsA) is encapsulated in two formulations; immediate release and colonic release beads. The outer coatings of each bead protect inner SmPill® mini-spheres from gastrointestinal (GI) contents including stomach acid (pH), H_2O and digestive enzymes to facilitate targeted delivery to specific regions of the GI (small intestine or colon). CsA is maintained in its fully solubilised/active form for optimal pharmacological activity at target sites. The solubilised state is maintained throughout GI transit and released through the outer coatings providing systemic and GI protection to aGvHD mice following oral delivery.

Previous work within our research group demonstrated that timing of MSC administration and proinflammatory cytokine levels *in vivo* are critical for MSC effectiveness as immunosuppressive agents in aGvHD (Tobin *et al.* 2013). The findings from Tobin *et al.*, demonstrated the absolute requirement of MSC activation for therapeutic efficacy in this model of aGvHD (Tobin *et al.* 2013). This thesis furthered these findings, extending our knowledge about the requirement for IFNγ prestimulation before CsA (data from chapter 3). Chapter 4 clearly outlined the significant suppression of pro-inflammatory cytokines such as IFNγ following CsA administration in this aGvHD model. Based on these findings, it was hypothesised that MSC would require pre-stimulation with IFNγ to be efficacious in a combination therapy with CsA in this aGvHD model.

Firstly, the survival of aGvHD mice following treatment with MSC or MSCγ alone and in combination to SmPill® or Sandimmune® IV were explored. Similar to the findings of Tobin *et al.*, we have shown that MSC delivered on day 6 is efficacious in prolonging survival (16.5 days MST) and reducing weight loss in this aGvHD model. We have furthered these findings by showing that pre-licensing of MSC with IFNγ (MSCγ) were better at prolonging survival (19.5 days MST) and reducing weight loss in aGvHD mice. This demonstrated that MSCγ are more potent than MSC in aGvHD and prolong survival in a comparable manner to SmPill® (22 days MST) and Sandimmune® IV (19 days MST). In agreement with our hypothesis, the efficacy of oral CsA therapy (SmPill®) was impaired when co-administered with resting MSC. However, this negative impact on SmPill® efficacy was significantly ameliorated when pre-licensed MSC (MSCγ) were co-administered with SmPill®. Contrastingly, intravenous CsA (Sandimmune® IV) efficacy was not affected by resting MSC or enhanced by MSCγ. This data shows that the activation status for MSC is important for optimal performance with GI targeted CsA (SmPill®) but not for systemic CsA (Sandimmune® IV). We hypothesised that the rapid metabolism associated with intravenous CsA (Kimura *et al.* 2010) would not impact MSC

activation (i.e. requirement for IFNγ) when administered on day 6 as CsA was administered on day 4 and it is likely that by day 6 there would be levels of IFNγ sufficient to activate MSC. On the other hand, we hypothesised that the sustained CsA release associated with SmPill® prevented the activation of MSC (again likely linked to levels of IFNγ). Therefore, we wanted to explore this hypothesis by examining the mechanisms of interaction between CsA and MSC in terms of histopathology, cytokine profiles and Treg expansion in aGvHD mice.

The liver, lung, small intestine and colon are the principle target organs in aGvHD. The efficacy of SmPill® and Sandimmune® IV in improving aGvHD pathology and reducing apoptotic tissue damage was demonstrated in chapter 4. Consistent with these findings, SmPill® and Sandimmune® IV displayed comparable efficacy systemically while SmPill® provided superior GI protection to that of Sandimmune® IV. MSCγ provided significantly better protection to the liver and GI with less pathology than that of MSC treated mice and this correlates with the survival data. In terms of tissue apoptosis, MSCγ were more protective than MSC and Sandimmune® IV in the lung but similar in the small intestine.

MSC have previously been shown to have anti-apoptotic effects in the lungs of mice with chronic obstructive pulmonary disease through a VEGF protective mechanism (Guan *et al.* 2013). However, when MSC were combined with SmPill® there was a significant loss in SmPill® mediated protection in systemic tissues (Liver and lung) but similar protection from apoptotic damage was evident. Following a similar trend to survival, SmPill® efficacy in preventing tissue damage and apoptosis in the target organs of aGvHD mice was maintained when it was combined with MSCγ. This shows that pre-activation of MSC is required for combination therapy with SmPill® and this correlates with findings from chapter 3. However, Sandimmune® IV was effective at reducing pathology and apoptotic damage within the tissues when combined with either resting MSC or MSCγ. These findings support the survival data and provided more evidence that pre-licensing of MSC was required for combined efficacy

with SmPill® but not Sandimmune® IV. Also, it highlights the difference in bioavailability between SmPill® and Sandimmune® IV as it suggests that sustained GI delivery of CsA coupled with systemic release via SmPill® provides an enhanced immunosuppression compared to systemic bursts of CsA from Sandimmune® IV. Ultimately, these pharmacological distinctions affect MSC activation differentially which, in turn, poses consequences for the efficacy of the drug. As mentioned earlier, CsA is a "critical dosage drug" and its impact on calcineurin suggests a benefit from consistent and persistent exposure to CsA (Morris 2003). Therefore, delivery of CsA via oral (targeted to GI tract) or intravenous routes (systemic) may have differential impacts on the inflammatory environment thus affecting MSC therapeutic efficacy.

Exploring the inflammatory environment by the establishment of cytokine profiles in aGvHD tissues, confirmed that activation status of MSC and relative bioavailability of CsA had varying effects on cytokine levels in systemic and GI tissues. Resting MSC were shown to weaken SmPill® efficacy of IL2 and TNFα reduction in the spleen. In the small intestine, there was further verification that MSC and CsA co-therapy efficacy was dependent on delivery of CsA, as Sandimmune® IV significantly enhanced MSC reduction of IFNγ whereas SmPill® significantly mitigated MSC reduction of TNFα. While a significant level of cytokine suppression was maintained by MSC and Sandimmune® IV co-therapy in the liver and colon, there was no significant enhancement of efficacy in comparison to single therapies. This data suggests that the delivery route and more likely the bioavailability of CsA can have differential effects on resting MSC and the potential for co-therapy efficacy reflects this. It is possible that benefits of a co-therapy in terms of proinflammatory cytokine reduction would be evident using a different dosing strategy.

An important limitation in the study to consider is the dependence of xenoreactivity and homeostatic expansion of human PBMC for activation of human MSC in this aGvHD model. Hill *et al.* have shown that 13 Gy total body irradiation was required to initiate a cytokine storm

in a murine model of allogeneic BMT (Hill *et al* 1997). Throughout this thesis 2.4 Gy was used as a preconditioning regimen and this would suggest that there was not a cytokine storm initiated in our model. NSG mice are more sensitive to irradiation and as they are immunocompromised (lacking T, B and NK cells), human PBMC can engraft readily (Pearson *et al.* 2008, Ali *et al.* 2012). Therefore, it was not necessary to use a higher dose of irradiation than 2.4 Gy for aGvHD development in our model. Cytokine analysis of GI tissue and serum at early timepoints post irradiation (6 h – 24 h) would determine the level of cytokines produced post irradiation and conclude if a cytokine storm is likely to be initiated in this model.

The pharmacological difference between Sandimmune® IV and SmPill® is that SmPill® provides a sustained release of CsA to the colon which was better at reducing IFNγ and TNFα in GI tissues. Thus, activation cues for MSC were reduced here. While cytokine reduction is similar in all co-treatment groups, it is important to note that this is a snapshot at day 13. Perhaps there were differences, as a result of sustained CsA release via SmPill® in comparison to Sandimmune® IV, in the IFNγ and TNFα levels at earlier timepoints such as day 4 or 5 before MSC administration on day 6. This would explain why we see differences in survival and histology but without significance in this case.

Throughout this thesis, the data has shown how CsA reduces the levels of IFNγ and TNFα producing CD3$^+$ T cells *in vitro* but also the efficacy of different CsA formulations in reducing the levels of CD4$^+$ and CD8$^+$ TNFα producing T cells in the tissues of aGvHD mice. Therefore, it was hypothesised that the requirement for MSC pre-licensing with IFNγ would be necessary for MSC efficacy. This lab has previously reported the reduction in total TNFα in the serum of aGvHD mice (Tobin *et al.* 2013), however the cellular source of this cytokine remained unclear. This thesis has shown that while there were differences in survival between resting MSC and licensed MSC, there was no difference in their capacity to decrease CD4$^+$ and CD8$^+$ TNFα producing T cells in the tissues of aGvHD mice.

However, while SmPill® enhanced the reduction of CD4+ and CD8+ TNFα producing T cells in the liver by both MSC therapies, the combination of SmPill® with resting MSC was less effective than SmPill® alone in reducing the number of TNFα producing CD4+ and CD8+ T cells in the liver. This provides further evidence of MSC activation status impacting CsA efficacy and supports our *in vitro* data where, at high PBMC densities, MSC hampered CsA suppression of TNFα producing CD3+ T cells. However, the efficacy of Sandimmune® IV in this regard was enhanced by either MSC or MSCγ in the spleen and lungs but reduced in the liver.

The different effects observed in the liver remain unclear but warrant further investigation. While it has largely been reported that following intravenous administration, MSC can get trapped in the lung (Barbash *et al.* 2003; Fischer *et al.* 2009; Assis *et al.* 2010), MSC cell debris has been detected in the liver (Eggenhofer *et al.* 2012). This may be a source for further APC activation and subsequent increase in number of TNFα producing T cells in the liver, therefore hampering CsA efficacy in the liver.

Tregs have already been shown to engraft in this humanised model of aGvHD and CsA treatment had no significant effect on the number of Tregs present in the tissues of aGvHD mice. It has been demonstrated that MSC increase the number of Treg in aGvHD mice (Joo *et al*. 2010). Also, previous unpublished data from this laboratory established that MSC increased the number of Treg in the liver and lung in this humanised aGvHD model (Healy 2015, Thesis). Interestingly, SmPill® spared MSC capacity to enhance Tregs *in vivo* while Sandimmune® IV significantly reduced MSC enhancement of Treg in the spleen. Importantly, the engraftment of Treg seem to be independent of SmPill® treatment and poses no impairment on MSC expansion of Treg. This finding is of great relevance as CsA is commonly used in the prevention and treatment of aGvHD, suggesting that CSA can co-operate with MSC expansion of Treg which would aid in regulating aGvHD development. However, it is important to note

that we are limited to the findings from a preliminary study (n=3 per group) which means that further experimentation is required to confirm this data.

This chapter is the first study to investigate the efficacy of a combination of MSC with clinically used and novel CsA treatments for aGvHD and adds significant knowledge to our understanding of these interactions. These findings present a framework from which suitable conditions for co-treatment of MSC and CsA can be adopted for aGvHD therapy. This study has provided evidence that a combinational therapy of MSC and CsA can be efficacious in prolonging survival and improving pathology in a human relevant pre-clinical model of aGvHD. This thesis has outlined the conditions by which this was facilitated by means of MSC activation or delivery method of CsA. The key findings from this study have shown that 1) CsA therapies did not impair MSC efficacy in aGvHD 2) Sandimmune® IV can be efficacious with both resting and licensed MSC therapy and 3) MSC but not licensed MSC hamper SmPill® efficacy. However, we have shown that if MSC are pre-activated before administration with SmPill®, these hampering effects are significantly reduced in terms of survival and histopathology.

There are a number of caveats to consider when using this model to assess the efficacy of aGvHD therapies. The rapid progression of aGvHD in mice following xenogeneic recognition and subsequent short therapeutic window make it difficult to accurately relate the efficacy of therapeutic intervention to the clinic. This aGvHD model requires human APC to process mouse antigens and present them in the presence of MHC class II. As human TCRs do not recognise mouse MHC (species restriction), this model of aGvHD is primarily dependent on CD4$^+$ T cells and limits its relativity to the clinic (Lucas *et al*. 1990). Therefore, drug interventions that specifically target CD8$^+$ T cells may not be useful to assess in this aGvHD model. In relation to the clinic, the primary antigenic targets of aGvHD are miHA rather than MHC molecules themselves. Moreover, investigating the role the microbiome

plays in altering the kinetics and severity of aGvHD is limited using this model given that the microbiome of a human is markedly different from that of a mouse housed in a pathogen-free facility (Cooke *et al.* 1998). In patients, haematopoietic reconstitution and achieving a GvL effect are the key objectives in HSCT. However, this model is GvHD development focused and therefore effects of potential therapies on GvL and haematopoietic reconstitution remain unclear. The separation of GvHD from GvL would provide the most clinically meaningful therapy for aGvHD but this is complicated as T cells mediate both GvHD and GvL.

Also, it is important to note that the recommended dosing strategy for CsA in the clinic is 3mg/kg/day (i.v) for prophylaxis and 12mg/kg/day (oral) following aGvHD development (Ruutu *et al.* 2014), however this study administered CsA at 25mg/kg/dose every second day as it was deemed effective for this model in pilot studies. Perhaps tapering the dose of CsA would increase the efficacy of SmPill® with MSC and provide a beneficial co-therapy. In parallel, the dose of MSC in these studies was 6.4×10^4 gram^{-1} which correlates to 1.6×10^6 total dose per 25g mouse. In the clinic, MSC has been administered in the range of 1×10^6 – 8×10^6 per kg (Katarina Le Blanc *et al.* 2004; Kebriaei *et al.* 2009). Thus, for a 25g mouse this dose correlates to a significantly higher dose of 64×10^6 kg^{-1} per infusion. Although this dose seems high, it is significantly lower than MSC doses reported in other studies (Sudres *et al.* 2006; Li *et al.* 2014). Therefore, to increase the clinical relevance of this study and its immunosuppressive effects in partnership with SmPill®, it is necessary to lower the dose of MSC therapy. This knowledge can be translated to inform better design of a combined cellular therapy and pharmacotherapy approach for aGvHD treatment.

Importantly, this thesis provides the proof of concept that targeted delivery of a novel CsA formulation, SmPill® to the GI, in addition to systemic, provides enhanced protection from aGvHD and that the activation of MSC is critical for its efficacy when co-administered with CsA. This supports the recommendations by the ISCT to carry out MSC potency assays prior

to clinical use (Krampera *et al.* 2013). The data provided here may highlight a potential reason for the variability in response between GvHD patients receiving the same donor MSC. It also suggests that the difference observed may be associated with reduced levels of cytokines (IFNγ) present in patients, which may negatively impact on MSC therapeutic efficacy. This thesis provides further support for the use of IFNγ licensed MSC for treatment of patients with GvHD. Therefore, this approach may tackle two problems, (1) the lack of activating cytokines present in patients and (2) possible negative impact of immunosuppressant drugs on MSC activation and subsequent efficacy.

Future studies to enhance its clinical relevance would comprise of using a lower dose of CsA within the bead (25mg/kg to 12mg/kg) to generate a dose response curve in conjunction with less MSC as *in vitro* data suggests that MSC in high PBMC densities have enhanced suppression in the presence of CsA. Pharmacokinetic studies would provide useful data in terms of CsA bioavailability and help to interpret this data in more detail. Moreover, the use of SmPill® as a prophylaxis therapy rather than a treatment remains to be investigated in this humanised mouse model of aGvHD. The partnership with MSC in this regard may prove even more efficacious.

Another interesting concept to explore would be the effect of this GI targeted drug (SmPill®) alone or in combination with MSC therapy on the microbiome. It has been shown that suppression of the gut microbiome can prevent aGvHD development (Vossen *et al*. 2014). This presents an interesting concept whereby the interplay between immune cells and the microbiome can be manipulated by these therapies. Overall, this thesis has furthered our knowledge of MSC interactions with CsA and presented translational pre-clinical results of a novel CsA formulation alone and in combination with MSC therapy for aGvHD.

CHAPTER 7
BIBLIOGRAPHY

Aggarwal, S. & Pittenger, M.F., 2005. Human mesenchymal stem cells modulate allogeneic immune cell responses. *Blood*, 105(4), pp.1815–1823.

Alfarano, C. et al., 2012. Intraparenchymal injection of bone marrow mesenchymal stem cells reduces kidney fibrosis after ischemia-reperfusion in cyclosporine-immunosuppressed rats. *Cell transplantation*, 21(9), pp.2009–2019.

Ali, N. et al., 2012. Xenogeneic graft-versus-host-disease in NOD-scid IL-2Rγnull mice display a T-effector memory phenotype. *PloS one*, 7(8), p.e44219.

Anderson, B.E. et al., 2003. Memory CD4+ T cells do not induce graft-versus-host disease. *The Journal of clinical investigation*, 112(1), pp.101–108.

Ankrum, J. & Karp, J.M., 2010. Mesenchymal stem cell therapy: Two steps forward, one step back. *Trends in molecular medicine*, 16(5), pp.203–9.

Ankrum, J. a et al., 2014. Performance-enhanced mesenchymal stem cells via intracellular delivery of steroids. *Scientific reports*, 4, p.4645.

Anthony, B.A. & Hadley, G.A., 2012. Induction of graft-versus-host disease and in vivo T cell monitoring using an MHC-matched murine model. *Journal of visualized experiments : JoVE*, (66), p.e3697.

Antin, J.H. & Ferrara, J.L., 1992. Cytokine dysregulation and acute graft-versus-host disease. *Blood*, 80(12), pp.2964–8.

Antin, J.H. et al., 2002. A phase I/II double-blind, placebo-controlled study of recombinant human interleukin-11 for mucositis and acute GVHD prevention in allogeneic stem cell transplantation. *Bone marrow transplantation*, 29(5), pp.373–377.

Akiyama, K. et al., 2012. Mesenchymal-stem-cell-induced immunoregulation involves FAS-ligand-/FAS-mediated T cell apoptosis. *Cell stem cell*, 10(5), pp.544–55.

Aldinucci, A. et al., 2010. Inhibition of immune synapse by altered dendritic cell actin distribution: a new pathway of mesenchymal stem cell immune regulation. *Journal of immunology (Baltimore, Md. : 1950)*, 185(9), pp.5102–5110.

Almeida, C.R. et al., 2012. Enhanced mesenchymal stromal cell recruitment via natural killer cells by incorporation of inflammatory signals in biomaterials. *Journal of the Royal Society, Interface / the Royal Society*, 9(67), pp.261–271.

Ankrum, J. a, Ong, J.F. & Karp, J.M., 2014. Mesenchymal stem cells: immune evasive, not immune privileged. *Nature biotechnology*, 32(3), pp.252–60.

Arora, M., 2008. Therapy of chronic graft-versus-host disease. *Best practice & research. Clinical haematology*, 21(2), pp.271–279.

Asari, S. et al., 2009. Mesenchymal stem cells suppress B cell terminal differentiation. *Experimental hematology*, 37(5), pp.604–615.

Ashton, B.A. et al., 1980. Formation of bone and cartilage by marrow stromal cells in diffusion chambers in vivo. *Clinical orthopaedics and related research*, (151), pp.294–307.

Assis, A.C.M. et al., 2010. Time-dependent migration of systemically delivered bone marrow mesenchymal stem cells to the infarcted heart. *Cell transplantation*, 19(2), pp.219–230.

Attur, M.G. et al., 2000. Differential anti-inflammatory effects of immunosuppressive drugs: cyclosporin, rapamycin and FK-506 on inducible nitric oxide synthase, nitric oxide, cyclooxygenase-2 and PGE2 production. *Inflammation research : official journal of the European Histamine Research Society ... [et al.]*, 49(1), pp.20–26.

Bacigalupo, A. et al., 2009. DEFINING THE INTENSITY OF CONDITIONING REGIMENS : working definitions. *Biology of blood and marrow transplantation : journal of the American Society for Blood and Marrow Transplantation*, 15(12), pp.1628–1633.

Badillo, A.T. et al., 2007. Murine bone marrow stromal progenitor cells elicit an in vivo cellular and humoral alloimmune response. *Biology of blood and marrow transplantation : journal of the American Society for Blood and Marrow Transplantation*, 13(4), pp.412–422.

von Bahr, L. et al., 2012. Long-term complications, immunologic effects, and role of passage for outcome in mesenchymal stromal cell therapy. *Biology of blood and marrow transplantation : journal of the American Society for Blood and Marrow Transplantation*, 18(4), pp.557–564.

Bai, L. et al., 2009. Human bone marrow-derived mesenchymal stem cells induce Th2-polarized immune response and promote endogenous repair in animal models of multiple sclerosis. *Glia*, 57(11), pp.1192–1203.

Balduzzi, A. et al., 1995. Unrelated donor marrow transplantation in children. *Blood*, 86(8),

pp.3247–3256.

Barbash, I.M. et al., 2003. Systemic delivery of bone marrow-derived mesenchymal stem cells to the infarcted myocardium: feasibility, cell migration, and body distribution. *Circulation*, 108(7), pp.863–868.

Barker, J.N. et al., 2005. Transplantation of 2 partially HLA-matched umbilical cord blood units to enhance engraftment in adults with hematologic malignancy. *Blood*, 105(3), pp.1343–1347.

Barry, F.P. et al., 2005. Immunogenicity of adult mesenchymal stem cells: lessons from the fetal allograft. *Stem cells and development*, 14(3), pp.252–265.

Bartholomew, A. et al., 2002. Mesenchymal stem cells suppress lymphocyte proliferation in vitro and prolong skin graft survival in vivo. *Experimental hematology*, 30(1), pp.42–48.

Batten, P. et al., 2006. Human mesenchymal stem cells induce T cell anergy and downregulate T cell allo-responses via the TH2 pathway: relevance to tissue engineering human heart valves. *Tissue engineering*, 12(8), pp.2263–2273.

Beauchesne, P.R., Chung, N.S.C. & Wasan, K.M., 2007. Cyclosporine A: a review of current oral and intravenous delivery systems. *Drug development and industrial pharmacy*, 33(3), pp.211–20.

Belperio, J.A. et al., 2003. Role of CXCL9/CXCR3 Chemokine Biology during Pathogenesis of Acute Lung Allograft Rejection. *The Journal of Immunology* , 171 (9), pp.4844–4852.

Bernardo, M.E. & Fibbe, W.E., 2013. Mesenchymal stromal cells: sensors and switchers of inflammation. *Cell stem cell*, 13(4), pp.392–402.

Beyth, S. et al., 2005. Human mesenchymal stem cells alter antigen-presenting cell maturation and induce T-cell unresponsiveness. *Blood*, 105(5), pp.2214–2219.

Bhatia, S. et al., 2005. Late mortality in survivors of autologous hematopoietic-cell transplantation: report from the Bone Marrow Transplant Survivor Study. *Blood*, 105(11), pp.4215–4222.

Billingham, R.E., 1966. The biology of graft-versus-host reactions. *Harvey lectures*, 62, pp.21–78.

Billingham, R.E., Brent, L. & Medawar, P.B., 1953. Actively acquired tolerance of foreign

cells. *Nature*, 172(4379), pp.603–606.

Biron, C.A., 1997. Activation and function of natural killer cell responses during viral infections. *Current opinion in immunology*, 9(1), pp.24–34.

Le Blanc, K. et al., 2003. Mesenchymal stem cells inhibit and stimulate mixed lymphocyte cultures and mitogenic responses independently of the major histocompatibility complex. *Scandinavian journal of immunology*, 57(1), pp.11–20.

Le Blanc, K. et al., 2004. Treatment of severe acute graft-versus-host disease with third party haploidentical mesenchymal stem cells. *Lancet (London, England)*, 363(9419), pp.1439–1441.

Le Blanc, K. et al., 2008. Mesenchymal stem cells for treatment of steroid-resistant, severe, acute graft-versus-host disease: a phase II study. *Lancet (London, England)*, 371(9624), pp.1579–1586.

Le Blanc, K. et al., 2004. Mesenchymal stem cells inhibit the expression of CD25 (interleukin-2 receptor) and CD38 on phytohaemagglutinin-activated lymphocytes. *Scandinavian journal of immunology*, 60(3), pp.307–15.

Blazar, B.R. et al., 1996. Infusion of anti-B7.1 (CD80) and anti-B7.2 (CD86) monoclonal antibodies inhibits murine graft-versus-host disease lethality in part via direct effects on CD4+ and CD8+ T cells. *The Journal of Immunology* , 157 (8), pp.3250–3259.

Blazar, B.R., Carroll, S.F. & Vallera, D.A., 1991. Prevention of murine graft-versus-host disease and bone marrow alloengraftment across the major histocompatibility barrier after donor graft preincubation with anti-LFA1 immunotoxin. *Blood*, 78(11), pp.3093–3102.

von Bonin, M. et al., 2009. Treatment of refractory acute GVHD with third-party MSC expanded in platelet lysate-containing medium. *Bone marrow transplantation*, 43(3), pp.245–251.

Borel, J.F., 1976. Comparative study of in vitro and in vivo drug effects on cell-mediated cytotoxicity. *Immunology*, 31(4), pp.631–641.

Borsotti, C. et al., 2007. Absence of donor T-cell–derived soluble TNF decreases graft-versus-host disease without impairing graft-versus-tumor activity. *Blood*, 110(2), pp.783–786.

Brown, G.R. et al., 1999. Tumor necrosis factor inhibitor ameliorates murine intestinal graft-

versus-host disease. *Gastroenterology*, 116(3), pp.593–601.

Buron, F. et al., 2009. Human mesenchymal stem cells and immunosuppressive drug interactions in allogeneic responses: an in vitro study using human cells. *Transplantation proceedings*, 41(8), pp.3347–52.

Cahill, E.F. et al., 2015. Jagged-1 is required for the expansion of CD4(+) CD25(+) FoxP3(+) regulatory T cells and tolerogenic dendritic cells by murine mesenchymal stromal cells. *Stem Cell Research & Therapy*, 6(1).

Cahn, J.-Y. et al., 2005. Prospective evaluation of 2 acute graft-versus-host (GVHD) grading systems: a joint Societe Francaise de Greffe de Moelle et Therapie Cellulaire (SFGM-TC), Dana Farber Cancer Institute (DFCI), and International Bone Marrow Transplant Registry (IBMTR) pros. *Blood*, 106(4), pp.1495–1500.

Cao, C., Dong, Y. & Dong, Y., 2005. [Study on culture and in vitro osteogenesis of blood-derived human mesenchymal stem cells]. *Chinese journal of reparative and reconstructive surgery*, 19(8), pp.642–647.

Caplan, A.I., 1991. Mesenchymal stem cells. *Journal of orthopaedic research : official publication of the Orthopaedic Research Society*, 9(5), pp.641–650.

Caplan, A.I. & Dennis, J.E., 2006. Mesenchymal stem cells as trophic mediators. *Journal of cellular biochemistry*, 98(5), pp.1076–1084.

Carpenter, P.A. et al., 2005. A phase II multicenter study of visilizumab, humanized anti-CD3 antibody, to treat steroid-refractory acute graft-versus-host disease. *Biology of blood and marrow transplantation : journal of the American Society for Blood and Marrow Transplantation*, 11(6), pp.465–71.

Casiraghi, F. et al., 2008. Pretransplant infusion of mesenchymal stem cells prolongs the survival of a semiallogeneic heart transplant through the generation of regulatory T cells. *Journal of immunology (Baltimore, Md. : 1950)*, 181(6), pp.3933–3946.

Che, N. et al., 2014. Impaired B Cell Inhibition by Lupus Bone Marrow Mesenchymal Stem Cells Is Caused by Reduced CCL2 Expression. *The Journal of Immunology,* 193(10):5306-14.

Chen, T. et al., 2004. Cyclosporin A impairs dendritic cell migration by regulating chemokine receptor expression and inhibiting cyclooxygenase-2 expression. *Blood*, 103(2), pp.413–

422.

Chen, X. et al., 2009. Blockade of interleukin-6 signaling augments regulatory T-cell reconstitution and attenuates the severity of graft-versus-host disease. *Blood*, 114(4), pp.891–900.

Chen, L. et al., 2007. Effects of human mesenchymal stem cells on the differentiation of dendritic cells from CD34+ cells. *Stem cells and development*, 16(5), pp.719–731.

Chen, X. et al., 2014. The interaction between mesenchymal stem cells and steroids during inflammation. *Cell death & disease*, 5, p.e1009.

Chen, Y. et al., 2016. Sca-1+mesenchymal stromal cells inhibit splenic marginal zone B lymphocytes commitment through Caspase-3. *Cell Biology International*, p.n/a–n/a.

Cheng, P. et al., 2003. Notch signaling is necessary but not sufficient for differentiation of dendritic cells. *Blood*, 102(12), pp.3980–3988.

Chiesa, S. et al., 2011. Mesenchymal stem cells impair in vivo T-cell priming by dendritic cells. *Proceedings of the National Academy of Sciences of the United States of America*, 108(42), pp.17384–17389.

Chinnadurai, R. et al., 2014. IDO-independent suppression of T cell effector function by IFN-γ-licensed human mesenchymal stromal cells. *Journal of immunology (Baltimore, Md. : 1950)*, 192(4), pp.1491–501.

Christianson, S.W. et al., 1997. Enhanced human CD4+ T cell engraftment in beta2-microglobulin-deficient NOD-scid mice. *Journal of immunology (Baltimore, Md. : 1950)*, 158(8), pp.3578–3586.

Chung, B.H. et al., 2013. Human adipose tissue derived mesenchymal stem cells aggravate chronic cyclosporin nephrotoxicity by the induction of oxidative stress. *PloS one*, 8(3), p.e59693.

Ciesek, S. et al., 2005. Effects of cyclosporine on human dendritic cell subsets. *Transplantation proceedings*, 37(1), pp.20–24.

Coenen, J.J. a et al., 2007. Rapamycin, not cyclosporine, permits thymic generation and peripheral preservation of CD4+ CD25+ FoxP3+ T cells. *Bone marrow transplantation*, 39(9), pp.537–45.

Cooke, K.R. et al., 1998. Tumor necrosis factor- alpha production to lipopolysaccharide stimulation by donor cells predicts the severity of experimental acute graft-versus-host disease. *J. Clin. Invest.* 102, 1882–1891.

Corcione, A. et al., 2006. Human mesenchymal stem cells modulate B-cell functions. *Blood*, 107(1), pp.367–372.

Cragg, L. et al., 2000. A randomized trial comparing prednisone with antithymocyte globulin/prednisone as an initial systemic therapy for moderately severe acute graft-versus-host disease. *Biology of blood and marrow transplantation : journal of the American Society for Blood and Marrow Transplantation*, 6(4A), pp.441–447.

Cuerquis, J. et al., 2014. Human mesenchymal stromal cells transiently increase cytokine production by activated T cells before suppressing T-cell proliferation: effect of interferon-γ and tumor necrosis factor-α stimulation. *Cytotherapy*, 16(2), pp.191–202.

Dahlke, M.H. et al., 2009. Toward MSC in solid organ transplantation: 2008 position paper of the MISOT study group. *Transplantation*, 88(5), pp.614–619.

Danby, R.D. et al., 2016. High proportions of regulatory T cells in PBSC grafts predict improved survival after allogeneic haematopoietic SCT. *Bone Marrow Transplant*, 51(1), pp.110–118.

Datta, A. et al., 2006. Differential Effects of Immunosuppressive Drugs on T-Cell Motility. *American Journal of Transplantation*, 6(12), pp.2871–2883.

Dausset, J., 1958. [Iso-leuko-antibodies]. *Acta haematologica*, 20(1-4), pp.156–166.

Dazzi, F., Lopes, L. & Weng, L., 2012. Mesenchymal stromal cells: A key player in "innate tolerance"? *Immunology*, 137(3), pp.206–213.

Deeg, H.J. et al., 1985. TREATMENT OF HUMAN ACUTE GRAFT-VERSUS-HOST DISEASE WITH ANTITHYMOCYTE GLOBULIN AND CYCLOSPORINE WITH OR WITHOUT METHYLPREDNISOLONE. *Transplantation*, 40(2).: 162-6.

Deeg, H.J., 2007. How I treat refractory acute GVHD. *Blood*, 109(10), pp.4119–4126.

Degos, L., 2009. Jean Dausset a scientific pioneer: intuition and creativity for the patients (1916–2009). *Haematologica*, 94(9), pp.1331–1332.

Djouad, F. et al., 2007. Mesenchymal stem cells inhibit the differentiation of dendritic cells

through an interleukin-6-dependent mechanism. *Stem cells (Dayton, Ohio)*, 25(8), pp.2025–2032.

Doherty, P.C. & Zinkernagel, R.M., 1975. A biological role for the major histocompatibility antigens. *Lancet (London, England)*, 1(7922), pp.1406–1409.

Dominici, M. et al., 2006. Minimal criteria for defining multipotent mesenchymal stromal cells. The International Society for Cellular Therapy position statement. *Cytotherapy*, 8(4), pp.315–7.

Drewe, J., Beglinger, C. & Kissel, T., 1992. The absorption site of cyclosporin in the human gastrointestinal tract. *British journal of clinical pharmacology*, 33(1), pp.39–43.

Du, M.R. et al., 2012. Cyclosporin A promotes crosstalk between human cytotrophoblast and decidual stromal cell through up-regulating CXCL12/CXCR4 interaction. *Human reproduction (Oxford, England)*, 27(7), pp.1955–1965.

Duijvestein, M. et al., 2010. Autologous bone marrow-derived mesenchymal stromal cell treatment for refractory luminal Crohn's disease: results of a phase I study. *Gut*, 59(12), pp.1662–1669.

Duperrier, K. et al., 2002. Cyclosporin A inhibits dendritic cell maturation promoted by TNF-α or LPS but not by double-stranded RNA or CD40L. *Journal of leukocyte biology,* 72(5), pp.953–961.

Dutt, S. et al., 2011. CD8+CD44(hi) but not CD4+CD44(hi) memory T cells mediate potent graft antilymphoma activity without GVHD. *Blood*, 117(11), pp.3230–3239.

Eapen, M. et al., 2011. Impact of donor-recipient HLA-matching at HLA-A, -B, -C and –DRB1 on outcomes after umbilical cord blood transplantation for leukemia and myelodysplastic syndrome: a retrospective analysis. *The lancet oncology*, 12(13), pp.1214–1221.

Edinger, M. et al., 2003. CD4+CD25+ regulatory T cells preserve graft-versus-tumor activity while inhibiting graft-versus-host disease after bone marrow transplantation. *Nature medicine*, 9(9), pp.1144–1150.

Eggenhofer, E. et al., 2011. Features of synergism between mesenchymal stem cells and immunosuppressive drugs in a murine heart transplantation model. *Transplant immunology*, 25(2-3), pp.141–147.

Eggenhofer, E. et al., 2012. Mesenchymal stem cells are short-lived and do not migrate beyond the lungs after intravenous infusion. *Frontiers in immunology*, 3, p.297.

Ehninger, A. & Trumpp, A., 2011. The bone marrow stem cell niche grows up: mesenchymal stem cells and macrophages move in. *The Journal of experimental medicine*, 208(3), pp.421–8.

Eibl, B. et al., 1996. Evidence for a graft-versus-tumor effect in a patient treated with marrow ablative chemotherapy and allogeneic bone marrow transplantation for breast cancer. *Blood*, 88(4), pp.1501–1508.

Eliopoulos, N. et al., 2005. Allogeneic marrow stromal cells are immune rejected by MHC class I– and class II–mismatched recipient mice. *Blood*, 106(13), pp.4057–4065.

English, K. et al., 2009. Cell contact, prostaglandin E(2) and transforming growth factor beta 1 play non-redundant roles in human mesenchymal stem cell induction of CD4(+)CD25(High)forkhead box P3(+) regulatory T cells. *Clinical and Experimental Immunology*, 156(1), pp.149–160.

English, K. et al., 2007. IFN-gamma and TNF-alpha differentially regulate immunomodulation by murine mesenchymal stem cells. *Immunology letters*, 110(2), pp.91–100.

English, K., Barry, F.P. & Mahon, B.P., 2008. Murine mesenchymal stem cells suppress dendritic cell migration, maturation and antigen presentation. *Immunology letters*, 115(1), pp.50–58.

European Multicentre Trial Group, 1983. CYCLOSPORIN IN CADAVERIC RENAL TRANSPLANTATION: ONE-YEAR FOLLOW-UP OF A MULTICENTRE TRIAL. *The Lancet*, 322(8357), pp.986–989.

Fang, B. et al., 2007. Favorable response to human adipose tissue-derived mesenchymal stem cells in steroid-refractory acute graft-versus-host disease. *Transplantation proceedings*, 39(10), pp.3358–3362.

Farge, D. et al., 2010. Autologous hematopoietic stem cell transplantation for autoimmune diseases: an observational study on 12 years' experience from the European Group for Blood and Marrow Transplantation Working Party on Autoimmune Diseases. *Haematologica*, 95(2), pp.284–292.

Feng, X. et al., 2008. Targeting minor histocompatibility antigens in graft versus tumor or graft versus leukemia responses. *Trends Immunol*, Dec:29(12):624-632.

Ferrara, J. et al., 2009. Graft-versus-host disease. *The Lancet*, 373(9674), pp.1550–1561.

Ferrara, J.L.M. et al., 2011. Regenerating islet-derived 3-alpha is a biomarker of gastrointestinal graft-versus-host disease. *Blood*, 118(25), pp.6702–6708.

Ferrara, J.L.M. & Deeg, H.J., 1991. Graft-versus-Host Disease. *New England Journal of Medicine*, 324(10), pp.667–674.

Ferrara, J.L.M. & Reddy, P., 2006. Pathophysiology of Graft-Versus-Host Disease. *Seminars in Hematology*, 43(1), pp.3–10.

Filipovich, A.H. et al., 2005. National Institutes of Health consensus development project on criteria for clinical trials in chronic graft-versus-host disease: I. Diagnosis and staging working group report. *Biology of blood and marrow transplantation : journal of the American Society for Blood and Marrow Transplantation*, 11(12), pp.945–956.

Finke, J. et al., 2009. Standard graft-versus-host disease prophylaxis with or without anti-T-cell globulin in haematopoietic cell transplantation from matched unrelated donors: a randomised, open-label, multicentre phase 3 trial. *The Lancet. Oncology*, 10(9), pp.855–864.

Fischer, U.M. et al., 2009. Pulmonary passage is a major obstacle for intravenous stem cell delivery: the pulmonary first-pass effect. *Stem cells and development*, 18(5), pp.683–692.

Flanagan, W.M. et al., 1991. Nuclear association of a T-cell transcription factor blocked by FK-506 and cyclosporin A. *Nature*, 352(6338), pp.803–807.

Flomenberg, N. et al., 2004. Impact of HLA class I and class II high-resolution matching on outcomes of unrelated donor bone marrow transplantation: HLA-C mismatching is associated with a strong adverse effect on transplantation outcome. *Blood*, 104(7), pp.1923–1930.

Francois, M. et al., 2012. Human MSC Suppression Correlates With Cytokine Induction of Indoleamine 2,3-Dioxygenase and Bystander M2 Macrophage Differentiation. *Mol Ther*, 20(1), pp.187–195.

Franquesa, M. et al., 2012. Immunomodulatory Effect of Mesenchymal Stem Cells on B Cells.

Frontiers in Immunology, 3.p.212

Franquesa, M. et al., 2015. Human adipose tissue-derived mesenchymal stem cells abrogate plasmablast formation and induce regulatory B cells independently of T helper cells. *Stem Cells*, 33(3), pp. 880-891.

Fraser, J.K. et al., 2006. Fat tissue: an underappreciated source of stem cells for biotechnology. *Trends in biotechnology*, 24(4), pp.150–154.

Friedenstein, A.J. et al., 1968. Heterotopic of bone marrow. Analysis of precursor cells for osteogenic and hematopoietic tissues. *Transplantation*, 6(2), pp.230–247.

Friedenstein, A.J. et al., 1974. Stromal cells responsible for transferring the microenvironment of the hemopoietic tissues. Cloning in vitro and retransplantation in vivo. *Transplantation*, 17(4), pp.331–340.

Friedenstein, A.J., Piatetzky-Shapiro, I.I. & Petrakova, K. V, 1966. Osteogenesis in transplants of bone marrow cells. *Journal of embryology and experimental morphology*, 16(3), pp.381–390.

Fujii, N. et al., 2001. Hepatic graft-versus-host disease presenting as an acute hepatitis after allogeneic peripheral blood stem cell transplantation. *Bone marrow transplantation*, 27(9), pp.1007–1010.

Fujii, N. et al., 2006. Serum cytokine concentrations and acute graft-versus-host disease after allogeneic peripheral blood stem cell transplantation: Concurrent measurement of ten cytokines and their respective ratios using cytometric bead array. *International Journal of Molecular Medicine*, 17(5), pp.881–885.

Fujioka, T. et al., 2013. Frequency of CD4+FOXP3+ regulatory T-cells at early stages after HLA-mismatched allogeneic hematopoietic SCT predicts the incidence of acute GVHD. *Bone Marrow Transplant*, 48(6), pp.859–864.

Galipeau, J., 2013. Concerns arising from MSC retrieval from cryostorage and effect on immune suppressive function and pharmaceutical usage in clinical trials. *ISBT Science Series*, 8(1), pp.100–101.

Galipeau, J. et al., 2016. International Society for Cellular Therapy perspective on immune functional assays for mesenchymal stromal cells as potency release criterion for advanced phase clinical trials. *Cytotherapy*, 18(2), pp.151–159.

Galipeau, J., 2013. The mesenchymal stromal cells dilemma-does a negative phase III trial of random donor mesenchymal stromal cells in steroid-resistant graft-versus-host disease represent a death knell or a bump in the road? *Cytotherapy*, 15(1), pp.2–8.

Gan, R. et al., 2003. Cyclosporine A effectively inhibits graft-versus-host disease during development of Epstein-Barr virus-infected human B cell lymphoma in SCID mouse. *Cancer science*, 94(9), pp.796–801.

García Cadenas, I. et al., 2014. Impact of Cyclosporine Levels on the Development of Acute Graft versus Host Disease after Reduced Intensity Conditioning Allogeneic Stem Cell Transplantation. *Mediators of Inflammation*, 2014, pp.1–7.

Ge, W. et al., 2009. Infusion of mesenchymal stem cells and rapamycin synergize to attenuate alloimmune responses and promote cardiac allograft tolerance. *American journal of transplantation : official journal of the American Society of Transplantation and the American Society of Transplant Surgeons*, 9(8), pp.1760–1772.

Ge, W. et al., 2010. Regulatory T-cell generation and kidney allograft tolerance induced by mesenchymal stem cells associated with indoleamine 2,3-dioxygenase expression. *Transplantation*, 90(12), pp.1312–1320.

Geng, L. et al., 2008. Cyclosporin a Up-regulates B7-DC expression on dendritic cells in an IL-4-dependent manner in vitro, which is associated with decreased allostimulatory capacity of dendritic cells. *Immunopharmacology and immunotoxicology*, 30(2), pp.399–409.

Gidlund, M. et al., 1978. Enhanced NK cell activity in mice injected with interferon and interferon inducers. *Nature*, 273(5665), pp.759–761.

Gieseke, F. et al., 2013. Proinflammatory stimuli induce galectin-9 in human mesenchymal stromal cells to suppress T-cell proliferation. *European Journal of Immunology*, 43(10), pp.2741–2749.

Girdlestone, J. et al., 2015. Enhancement of the immunoregulatory potency of mesenchymal stromal cells by treatment with immunosuppressive drugs. *Cytotherapy*, 17(9), pp.1188–1199.

Glennie, S. et al., 2004. Bone marrow mesenchymal stem cells induce division arrest anergy of activated T cells. *Blood*, 105(7), pp.2821–2827.

Gómez-Almaguer, D. et al., 2008. Alemtuzumab for the treatment of steroid-refractory acute graft-versus-host disease. *Biology of blood and marrow transplantation : journal of the American Society for Blood and Marrow Transplantation*, 14(1), pp.10–5.

Gorer, P.A., 1936. The Detection of Antigenic Differences in Mouse Erythrocytes by the Employment of Immune Sera. *British Journal of Experimental Pathology*, 17(1), pp.42–50.

Gorer, P.A., Lyman, S. & Snell, G.D., 1948. Studies on the Genetic and Antigenic Basis of Tumour Transplantation. Linkage between a Histocompatibility Gene and "Fused" in Mice. *Proceedings of the Royal Society of London B: Biological Sciences*, 135(881), pp.499–505.

Gotherstrom, C. et al., 2011. Fetal and adult multipotent mesenchymal stromal cells are killed by different pathways. *Cytotherapy*, 13(3), pp.269–278.

Graubert, T.A. et al., 1997. Perforin/granzyme-dependent and independent mechanisms are both important for the development of graft-versus-host disease after murine bone marrow transplantation. *The Journal of clinical investigation*, 100(4), pp.904–911.

Grinnemo, K.H. et al., 2004. Xenoreactivity and engraftment of human mesenchymal stem cells transplanted into infarcted rat myocardium. *The Journal of thoracic and cardiovascular surgery*, 127(5), pp.1293–1300.

Guan, X.-J. et al., 2013. Mesenchymal stem cells protect cigarette smoke-damaged lung and pulmonary function partly via VEGF-VEGF receptors. *Journal of cellular biochemistry*, 114(2), pp.323–335.

Gutiérrez-Aguirre, C.H. et al., 2012. Effectiveness of subcutaneous low-dose alemtuzumab and rituximab combination therapy for steroid-resistant chronic graft-versus-host disease. *Haematologica*, 97(5), pp.717–722.

Haider, A.S. et al., 2008. Identification of Cellular Pathways of "Type 1," TH17 T Cells, and TNF- and Inducible Nitric Oxide Synthase-Producing Dendritic Cells in Autoimmune Inflammation through Pharmacogenomic Study of Cyclosporine A in Psoriasis 1. *Journal of immunology (Baltimore, Md. : 1950)*, 180, pp.1930–1920.

Halloran, P.F. et al., 1999. The temporal profile of calcineurin inhibition by cyclosporine in vivo. *Transplantation*, 68(9), pp.1356–1361.

Hass, R. et al., 2011. Different populations and sources of human mesenchymal stem cells (MSC): A comparison of adult and neonatal tissue-derived MSC. *Cell Communication and Signaling : CCS*, 9, p.12.

Hattori, K. et al., 1998. Differential effects of anti-Fas ligand and anti-tumor necrosis factor alpha antibodies on acute graft-versus-host disease pathologies. *Blood*, 91(11), pp.4051–4055.

Healy, M.E., 2015. A Delineation of Mesenchymal Stromal Cell Therapeutic Action in New Models of Acute and Chronic Graft versus Host Disease. PhD thesis, National University of Ireland Maynooth.

Healy, M.E. et al., 2015. Mesenchymal stromal cells protect against caspase 3-mediated apoptosis of CD19(+) peripheral B cells through contact-dependent upregulation of VEGF. *Stem cells and development*, 24(20), pp.2391–2402.

Hequet, O., 2015. Hematopoietic stem and progenitor cell harvesting: technical advances and clinical utility. *Journal of Blood Medicine*, 6, pp.55–67.

Hermankova, B. et al., 2016. Suppression of IL-10 production by activated B cells via a cell contact-dependent cyclooxygenase-2 pathway upregulated in IFN-gamma-treated mesenchymal stem cells. *Immunobiology*, 221(2), pp.129–136.

Herrmann, R.P. & Sturm, M.J., 2014. Adult human mesenchymal stromal cells and the treatment of graft versus host disease. *Stem Cells and Cloning : Advances and Applications*, 7, pp.45–52.

Hess, A.D. & Tutschka, P.J., 1980. Effect of cyclosporin A on human lymphocyte responses in vitro. I. CsA allows for the expression of alloantigen-activated suppressor cells while preferentially inhibiting the induction of cytolytic effector lymphocytes in MLR. *The Journal of Immunology* , 124 (6), pp.2601–2608.

Hill, G.R. et al., 1997. Total body irradiation and acute graft-versus-host disease: the role of gastrointestinal damage and inflammatory cytokines. *Blood*, Oct 15;90(8):3204-13.

Hill, G.R. & Ferrara, J.L., 2000. The primacy of the gastrointestinal tract as a target organ of acute graft-versus-host disease: rationale for the use of cytokine shields in allogeneic bone marrow transplantation. *Blood*, 95(9), pp.2754–2759.

Hippen, K.L. et al., 2012. Blocking IL-21 signaling ameliorates xenogeneic GVHD induced by

human lymphocytes. *Blood*, 119(2), pp.619–628.

Le Hir, M. et al., 1995. In situ detection of cyclosporin A: evidence for nuclear localization of cyclosporine and cyclophilins. *Laboratory investigation; a journal of technical methods and pathology*, 73(5), pp.727–733.

Hoffmann-Fezer, G. et al., 1993. Immunohistology and immunocytology of human T-cell chimerism and graft-versus-host disease in SCID mice. *Blood*, 81(12), pp.3440–3448.

Hoffmann, P. et al., 2002. Donor-type CD4(+)CD25(+) regulatory T cells suppress lethal acute graft-versus-host disease after allogeneic bone marrow transplantation. *The Journal of experimental medicine*, 196(3), pp.389–399.

Holler, E. et al., 1990. Increased serum levels of tumor necrosis factor alpha precede major complications of bone marrow transplantation. *Blood*, 75(4), pp.1011–1016.

Hori, T. et al., 2008. CCL8 is a potential molecular candidate for the diagnosis of graft-versus-host disease. *Blood*, 111(8), pp.4403–12.

Horiuchi, T. et al., 2010. Transmembrane TNF-α: structure, function and interaction with anti-TNF agents. *Rheumatology (Oxford, England)*, 49(7), pp.1215–1228.

Horowitz, M.M. et al., 1990. Graft-versus-leukemia reactions after bone marrow transplantation. *Blood*, 75(3), pp.555–562.

Horwitz, E.M. et al., 2005. Clarification of the nomenclature for MSC: The International Society for Cellular Therapy position statement. *Cytotherapy*, 7(5), pp.393–5.

Hou, R.-Q. et al., 2010. [Transfusion of mesenchymal stem cells combined with haploidentical HSCT improves hematopoietic microenvironment]. *Journal of experimental hematology / Chinese Association of Pathophysiology*, 18(1), p.155—160.

Huang, W.-H. et al., 2014. Hypoxic mesenchymal stem cells engraft and ameliorate limb ischaemia in allogeneic recipients. *Cardiovascular research*, 101(2), pp.266–276.

Huang, Y. et al., 2010. Kidney-derived mesenchymal stromal cells modulate dendritic cell function to suppress alloimmune responses and delay allograft rejection. *Transplantation*, 90(12), pp.1307–1311.

Hughes, P.D. & Cohney, S.J., 2011. Modifiers of complement activation for prevention of antibody-mediated injury to allografts. *Current opinion in organ transplantation*, 16(4),

pp.425–433.

Inoue, S. et al., 2006. Immunomodulatory effects of mesenchymal stem cells in a rat organ transplant model. *Transplantation*, 81(11), pp.1589–1595.

Isakova, I.A. et al., 2014. Allo-Reactivity of Mesenchymal Stem Cells in Rhesus Macaques Is Dose and Haplotype Dependent and Limits Durable Cell Engraftment In Vivo. *PLoS ONE*, 9(1), p.e87238.

Jacobson, P.A. et al., 2003. Posttransplant day significantly influences pharmacokinetics of cyclosporine after hematopoietic stem cell transplantation. *Biology of blood and marrow transplantation : journal of the American Society for Blood and Marrow Transplantation*, 9(5), pp.304–311.

Jacobsohn, D. a & Vogelsang, G.B., 2007. Acute graft versus host disease. *Orphanet journal of rare diseases*, 2, p.35.

Janeway CA Jr, Travers P, Walport M, et al, 2001. Immunobiology: The Immune System in Health and Disease. 5th edition. New York: Garland Science. The complement system and innate immunity.Available from: http://www.ncbi.nlm.nih.gov/books/NBK27100/

Janeway CA Jr, Travers P, Walport M, et al, 2001. Immunobiology: The Immune System in Health and Disease. 5th edition. New York: Garland Science. Responses to alloantigens and transplant rejection.Available from: http://www.ncbi.nlm.nih.gov/books/NBK27163

Jenq, R.R. et al., 2012. Regulation of intestinal inflammation by microbiota following allogeneic bone marrow transplantation. *The Journal of experimental medicine*, 209(5), pp.903–11.

Ji, Y.R. et al., 2012. Mesenchymal stem cells support proliferation and terminal differentiation of B cells. *Cellular physiology and biochemistry : international journal of experimental cellular physiology, biochemistry, and pharmacology*, 30(6), pp.1526–1537.

Jia, Z. et al., 2012. Immunomodulatory effects of mesenchymal stem cells in a rat corneal allograft rejection model. *Experimental eye research*, 102, pp.44–9.

Joo, S.-Y. et al., 2010. Mesenchymal stromal cells inhibit graft-versus-host disease of mice in a dose-dependent manner. *Cytotherapy*, 12(3), pp.361–370.

Jorga, A., Holt, D.W. & Johnston, A., 2004. Therapeutic drug monitoring of cyclosporine.

Transplantation proceedings, 36(2 Suppl), p.396S–403S.

Ju, X.P. et al., 2005. Cytokine expression during acute graft-versus-host disease after allogeneic peripheral stem cell transplantation. *Bone marrow transplantation*, 35(12), pp.1179–86.

Jung, Y.-J. et al., 2007. MSC-DC interactions: MSC inhibit maturation and migration of BM-derived DC. *Cytotherapy*, 9(5), pp.451–458.

Kang, H.G. et al., 2007. Effects of cyclosporine on transplant tolerance: the role of IL-2. *American journal of transplantation : official journal of the American Society of Transplantation and the American Society of Transplant Surgeons*, 7(8), pp.1907–16.

Kaplan, D.H. et al., 2004. Target antigens determine graft-versus-host disease phenotype. *Journal of immunology (Baltimore, Md. : 1950)*, 173(9), pp.5467–5475.

Kappel, L.W. et al., 2009. IL-17 contributes to CD4-mediated graft-versus-host disease. *Blood*, 113(4), pp.945–52.

Kaufmann, Y. et al., 1984. Mechanism of action of Cyclosporin A: inhibition of lymphokine secretion studied with antigen-stimulated T cell hybridomas. *Journal of immunology (Baltimore, Md. : 1950)*, 133(6), pp.3107–3111.

Kavanagh, H. & Mahon, B.P., 2011. Allogeneic mesenchymal stem cells prevent allergic airway inflammation by inducing murine regulatory T cells. *Allergy*, 66(4), pp.523–531.

Ke, H. & Huai, Q., 2003. Structures of calcineurin and its complexes with immunophilins–immunosuppressants. *Biochemical and Biophysical Research Communications*, 311(4), pp.1095–1102.

Kebriaei, P. et al., 2009. Adult Human Mesenchymal Stem Cells Added to Corticosteroid Therapy for the Treatment of Acute Graft-versus-Host Disease. *Biology of Blood and Marrow Transplant*, 15(7), pp.804–811.

Kimura, S. et al., 2010. Pharmacokinetics of CsA during the switch from continuous intravenous infusion to oral administration after allogeneic hematopoietic stem cell transplantation. *Bone Marrow Transplantation*, 45(6), pp.1088–1094.

King, M.A. et al., 2009. Human peripheral blood leucocyte non-obese diabetic-severe combined immunodeficiency interleukin-2 receptor gamma chain gene mouse model of

xenogeneic graft-versus-host-like disease and the role of host major histocompatibility complex. *Clinical & Experimental Immunology*, 157(1), pp.104–118.

Kishi, Y. et al., 2005. Optimal initial dose of oral cyclosporine in relation to its toxicities for graft-versus-host disease prophylaxis following reduced-intensity stem cell transplantation in Japanese patients. *Bone marrow transplantation*, 35(11), pp.1079–82.

Korngold, R. et al., 2003. Role of Tumor Necrosis Factor-a in Graft-versus-Host Disease and Graft-versus-Leukemia Responses. *Biology of blood and marrow transplantation : journal of the American Society for Blood and Marrow Transplantation*, 9, pp.292–303.

Korngold, R. & Sprent, J., 1978. Lethal graft-versus-host disease after bone marrow transplantation across minor histocompatibility barriers in mice. Prevention by removing mature T cells from marrow. *The Journal of experimental medicine*, 148(6), pp.1687–1698.

Koyama, M. et al., 2012. Recipient nonhematopoietic antigen-presenting cells are sufficient to induce lethal acute graft-versus-host disease. *Nature medicine*, 18(1), pp.135–142.

Krampera, M. et al., 2003. Bone marrow mesenchymal stem cells inhibit the response of naive and memory antigen-specific T cells to their cognate peptide. *Blood*, 101(9), pp.3722–3729.

Krampera, M. et al., 2013. Immunological characterization of multipotent mesenchymal stromal cells--The International Society for Cellular Therapy (ISCT) working proposal. *Cytotherapy*, 15(9), pp.1054–61.

Krampera, M. et al., 2006. Role for interferon-gamma in the immunomodulatory activity of human bone marrow mesenchymal stem cells. *Stem cells (Dayton, Ohio)*, 24(2), pp.386–98.

Kroger, N. et al., 2002. In vivo T cell depletion with pretransplant anti-thymocyte globulin reduces graft-versus-host disease without increasing relapse in good risk myeloid leukemia patients after stem cell transplantation from matched related donors. *Bone marrow transplantation*, 29(8), pp.683–689.

Laemmli, U.K., 1970. Cleavage of Structural Proteins during the Assembly of the Head of Bacteriophage T4. *Nature*, 227(5259), pp.680–685.

Lanier, L.L., 1998. NK CELL RECEPTORS. *Annual Review of Immunology*, 16(1), pp.359–

393.

Lee, S.T. et al., 2002. Treatment of high-risk acute myelogenous leukaemia by myeloablative chemoradiotherapy followed by co-infusion of T cell-depleted haematopoietic stem cells and culture-expanded marrow mesenchymal stem cells from a related donor with one fully mismatched hu. *British journal of haematology*, 118(4), pp.1128–1131.

Lee, Y.-H. et al., 2007. Calcineurin inhibitors block MHC-restricted antigen presentation in vivo. *Journal of immunology (Baltimore, Md. : 1950)*, 179(9), pp.5711–5716.

Lee, R.H. et al., 2009. Intravenous hMSCs improve myocardial infarction in mice because cells embolized in lung are activated to secrete the anti-inflammatory protein TSG-6. *Cell stem cell*, 5(1), pp.54–63.

Levine, J.E. et al., 2008. Etanercept plus methylprednisolone as initial therapy for acute graft-versus-host disease. *Blood*, 111(4), pp.2470–2475.

Li, H. et al., 2012. Profound depletion of host conventional dendritic cells, plasmacytoid dendritic cells and B cells does not prevent GVHD induction. *Journal of Immunology (Baltimore, Md. : 1950)*, 188(8), pp.3804–3811.

Li, Y. & Lin, F., 2012. Mesenchymal stem cells are injured by complement after their contact with serum. *Blood*, 120(17), pp.3436–3443.

Li, W. et al., 2012. Mesenchymal stem cells: a double-edged sword in regulating immune responses. *Cell Death and Differentiation*, 19(9), pp.1505–1513.

Li, Y.-P. et al., 2008. Human mesenchymal stem cells license adult CD34+ hemopoietic progenitor cells to differentiate into regulatory dendritic cells through activation of the Notch pathway. *Journal of immunology (Baltimore, Md. : 1950)*, 180(3), pp.1598–1608.

Li, Z.Y. et al., 2014. Effects of bone marrow mesenchymal stem cells on hematopoietic recovery and acute graft-versus-host disease in murine allogeneic umbilical cord blood transplantation model. *Cell biochemistry and biophysics*, 70(1), pp.115–122.

Liang, J. et al., 2012. Allogeneic mesenchymal stem cells transplantation in patients with refractory RA. *Clinical rheumatology*, 31(1), pp.157–161.

Liang, Y. et al., 2014. IL-1β and TLR4 Signaling Are Involved in the Aggravated Murine Acute Graft-versus-Host Disease Caused by Delayed Bortezomib Administration. *Journal of*

immunology (Baltimore, Md. : 1950), 192, pp.1277–85.

Lin, R. & Liu, Q., 2013. Diagnosis and treatment of viral diseases in recipients of allogeneic hematopoietic stem cell transplantation. *Journal of Hematology & Oncology*, 6, p.94.

Van Lint, M.T. et al., 1998. Early treatment of acute graft-versus-host disease with high- or low-dose 6-methylprednisolone: a multicenter randomized trial from the Italian Group for Bone Marrow Transplantation. *Blood*, 92(7), pp.2288–2293.

Van Lint, M.T. et al., 2006. Treatment of acute graft-versus-host disease with prednisolone: significant survival advantage for day +5 responders and no advantage for nonresponders receiving anti-thymocyte globulin. *Blood*, 107(10), pp.4177–4181.

Liu, J. et al., 1991. Calcineurin is a common target of cyclophilin-cyclosporin A and FKBP-FK506 complexes. *Cell*, 66(4), pp.807–815.

Liu, W. et al., 2006. CD127 expression inversely correlates with FoxP3 and suppressive function of human CD4+ T reg cells. *The Journal of experimental medicine*, 203(7), pp.1701–11.

Liu, J., Ye, L. & Wang, X., 2011. Cyclosporin A inhibits hepatitis C virus replication and restores interferon-alpha expression in hepatocytes. *Transplant infectious ...*, 13(1), pp.24–32.

Liu, X. et al., 2012. Mesenchymal stem/stromal cells induce the generation of novel IL-10-dependent regulatory dendritic cells by SOCS3 activation. *Journal of immunology (Baltimore, Md. : 1950)*, 189(3), pp.1182–1192.

Liu, X. et al., 2015. Sca-1+Lin−CD117− Mesenchymal Stem/Stromal Cells Induce the Generation of Novel IRF8-Controlled Regulatory Dendritic Cells through Notch–RBP-J Signaling. *The Journal of Immunology* , 194 (9), pp.4298–4308.

Liu, Y. et al., 2014. MSCs inhibit bone marrow-derived DC maturation and function through the release of TSG-6. *Biochemical and biophysical research communications*, 450(4), pp.1409–1415.

Liu, K.A.I.S. et al., 2014. Effects of recombinant human interleukin-10 on Treg cells, IL-10 and TGF-β in transplantation of rabbit skin. *Molecular Medicine Reports*, 9(2), pp.639–644.

Ljunggren, H.G. & Karre, K., 1990. In search of the "missing self": MHC molecules and NK cell recognition. *Immunology today*, 11(7), pp.237–244.

Lu, Y. et al., 2015. TLR4 plays a crucial role in MSC-induced inhibition of NK cell function. *Biochemical and biophysical research communications*, 464(2), pp.541–547.

Lu, L. et al., 1993. Enrichment, characterization, and responsiveness of single primitive CD34 human umbilical cord blood hematopoietic progenitors with high proliferative and replating potential. *Blood*, 81(1), pp.41–48.

Lucas, P.J. et al., 1990. The human antimurine xenogeneic cytotoxic response. I. Dependence on responder antigen-presenting cells. *Journal of immunology (Baltimore, Md. : 1950)*, 144(12), pp.4548–4554.

Lucchini, G. et al., 2010. Platelet-lysate-expanded mesenchymal stromal cells as a salvage therapy for severe resistant graft-versus-host disease in a pediatric population. *Biology of blood and marrow transplantation : journal of the American Society for Blood and Marrow Transplantation*, 16(9), pp.1293–1301.

Luz-Crawford, P. et al., 2016. Mesenchymal Stem Cell-Derived Interleukin 1 Receptor Antagonist Promotes Macrophage Polarization and Inhibits B Cell Differentiation. *Stem cells (Dayton, Ohio)*, 34(2), pp.483–492.

Luz-Crawford, P. et al., 2013. Mesenchymal stem cells generate a CD4+CD25+Foxp3+ regulatory T cell population during the differentiation process of Th1 and Th17 cells. *Stem cell research & therapy*, 4(3), p.65.

Maccario, R. et al., 2005. Human mesenchymal stem cells and cyclosporin a exert a synergistic suppressive effect on in vitro activation of alloantigen-specific cytotoxic lymphocytes. *Biology of blood and marrow transplantation : journal of the American Society for Blood and Marrow Transplantation*, 11(12), pp.1031–2.

MacMillan, M.L., Weisdorf, D.J., Davies, S.M., et al., 2002. Early antithymocyte globulin therapy improves survival in patients with steroid-resistant acute graft-versus-host disease. *Biology of blood and marrow transplantation : journal of the American Society for Blood and Marrow Transplantation*, 8(1), pp.40–46.

MacMillan, M.L., Weisdorf, D.J., Wagner, J.E., et al., 2002. Response of 443 patients to steroids as primary therapy for acute graft-versus-host disease: comparison of grading

systems. *Biology of blood and marrow transplantation : journal of the American Society for Blood and Marrow Transplantation*, 8(7), pp.387–394.

Magenau, J.M. et al., 2010. Frequency of CD4(+)CD25(hi)FOXP3(+) regulatory T cells has diagnostic and prognostic value as a biomarker for acute graft-versus-host-disease. *Biology of blood and marrow transplantation : journal of the American Society for Blood and Marrow Transplantation*, 16(7), pp.907–914.

Mapara, M.Y. et al., 2006. Expression of chemokines in GVHD target organs is influenced by conditioning and genetic factors and amplified by GVHR. *Biology of blood and marrow transplantation : journal of the American Society for Blood and Marrow Transplantation*, 12(6), pp.623–34.

Marcen, R. et al., 2009. Evolution of rejection rates and kidney graft survival: a historical analysis. *Transplantation proceedings*, 41(6), pp.2357–2359.

Markey, K.A., MacDonald, K.P.A. & Hill, G.R., 2014. The biology of graft-versus-host disease: experimental systems instructing clinical practice. *Blood*, 124(3), pp.354–362.

Martin, P.J. et al., 1990. A retrospective analysis of therapy for acute graft-versus-host disease: initial treatment. *Blood*, 76(8), pp.1464–1472.

Martin, P.J. et al., 2012. First- and second-line systemic treatment of acute graft-versus-host disease: recommendations of the American Society of Blood and Marrow Transplantation. *Biology of blood and marrow transplantation : journal of the American Society for Blood and Marrow Transplantation*, 18(8), pp.1150–63.

Martin, P.J. et al., 2010. Prochymal Improves Response Rates In Patients With Steroid-Refractory Acute Graft Versus Host Disease (SR-GVHD) Involving The Liver And Gut: Results Of A Randomized, Placebo-Controlled, Multicenter Phase III Trial In GVHD. *Biology of Blood and Marrow Transplant*, 16(2), pp.S169–S170.

Matte, C.C. et al., 2004. Donor APCs are required for maximal GVHD but not for GVL. *Nature medicine*, 10(9), pp.987–992.

Matte-Martone, C. et al., 2008. CD8+ but not CD4+ T cells require cognate interactions with target tissues to mediate GVHD across only minor H antigens, whereas both CD4+ and CD8+ T cells require direct leukemic contact to mediate GVL. *Blood*, 111(7), pp.3884–3892.

McCredie, K.B., Hersh, E.M. & Freireich, E.J., 1971. Cells capable of colony formation in the peripheral blood of man. *Science (New York, N.Y.)*, 171(3968), pp.293–294.

Meisel, R. et al., 2004. Human bone marrow stromal cells inhibit allogeneic T-cell responses by indoleamine 2,3-dioxygenase-mediated tryptophan degradation. *Blood*, 103(12), pp.4619–21.

Melief, S.M. et al., 2013. Multipotent stromal cells induce human regulatory T cells through a novel pathway involving skewing of monocytes toward anti-inflammatory macrophages. *Stem cells (Dayton, Ohio)*, 31(9), pp.1980–1991.

Meng, Y.-H. et al., 2012. CsA improves the trophoblasts invasiveness through strengthening the cross-talk of trophoblasts and decidual stromal cells mediated by CXCL12 and CD82 in early pregnancy. *International Journal of Clinical and Experimental Pathology*, 5(4), pp.299–307.

Moll, G. et al., 2011. Mesenchymal stromal cells engage complement and complement receptor bearing innate effector cells to modulate immune responses. *PloS one*, 6(7), p.e21703.

Moll, G. et al., 2014. Do Cryopreserved Mesenchymal Stromal Cells Display Impaired Immunomodulatory and Therapeutic Properties? *STEM CELLS*, 32(9), pp.2430–2442.

Morris, R.G., 2003. Cyclosporin Therapeutic Drug Monitoring - an Established Service Revisited. *The Clinical Biochemist Reviews*, 24(2), pp.33–46.

Mosier, D.E. et al., 1988. Transfer of a functional human immune system to mice with severe combined immunodeficiency. *Nature*, 335(6187), pp.256–259.

Mounayar, M. et al., 2015. PI3kα and STAT1 Interplay Regulates Human Mesenchymal Stem Cell Immune Polarization. *STEM CELLS*, 33(6), pp.1892–1901

van Mourik, I.D., Thomson, M. & Kelly, D.A., 1999. Comparison of pharmacokinetics of Neoral and Sandimmune in stable pediatric liver transplant recipients. *Liver transplantation and surgery : official publication of the American Association for the Study of Liver Diseases and the International Liver Transplantation Society*, 5(2), pp.107–111.

Mowat, A.M., 1989. Antibodies to IFN-gamma prevent immunologically mediated intestinal damage in murine graft-versus-host reaction. *Immunology*, 68(1), pp.18–23.

Muller, S. et al., 1988. Lack of influence of cyclosporine on antigen presentation to lysozyme-specific T cell hybridomas. *Transplantation*, 46(2 Suppl), p.44S–48S.

Muller, I. et al., 2008. Application of multipotent mesenchymal stromal cells in pediatric patients following allogeneic stem cell transplantation. *Blood cells, molecules & diseases*, 40(1), pp.25–32.

Murphy, J.M. et al., 2002. Reduced chondrogenic and adipogenic activity of mesenchymal stem cells from patients with advanced osteoarthritis. *Arthritis & Rheumatism*, 46(3), pp.704–713.

Najar, M. et al., 2009. Mesenchymal stromal cells promote or suppress the proliferation of T lymphocytes from cord blood and peripheral blood: the importance of low cell ratio and role of interleukin-6. *Cytotherapy*, 11(5), pp.570–583.

Nakayama, T. et al., 2006. Prostaglandin E2 promotes degranulation-independent release of MCP-1 from mast cells. *Journal of leukocyte biology*, 79(1), pp.95–104.

Nauta, A.J. et al., 2006. Donor-derived mesenchymal stem cells are immunogenic in an allogeneic host and stimulate donor graft rejection in a nonmyeloablative setting. *Blood*, 108(6), pp.2114–2120.

Németh, K. et al., 2009. Bone marrow stromal cells attenuate sepsis via prostaglandin E(2)—dependent reprogramming of host macrophages to increase their interleukin-10 production. *Nature medicine*, 15(1), pp.42–49.

Nestel, F. et al., 1992. Macrophage priming and lipopolysaccharide-triggered release of tumor necrosis factor alpha during graft-versus-host disease. *The Journal of Experimental Medicine*, 175(2), pp.405–413.

Di Nicola, M. et al., 2002. Human bone marrow stromal cells suppress T-lymphocyte proliferation induced by cellular or nonspecific mitogenic stimuli. *Blood*, 99(10), pp.3838–3843.

Noone, C. et al., 2013. IFN-gamma stimulated human umbilical-tissue-derived cells potently suppress NK activation and resist NK-mediated cytotoxicity in vitro. *Stem cells and development*, 22(22), pp.3003–3014.

Orlic, D. et al., 2001. Bone marrow cells regenerate infarcted myocardium. *Nature*, 410(6829), pp.701–705.

Owen, M. & Friedenstein, A.J., 1988. Stromal stem cells: marrow-derived osteogenic precursors. *Ciba Foundation symposium*, 136, pp.42–60.

Panoskaltsis-Mortari, A. et al., 2004. In vivo imaging of graft-versus-host-disease in mice. *Blood*, 103(9), pp.3590–3598.

Panoskaltsis-Mortari, A. et al., 2000. Induction of monocyte- and T-cell-attracting chemokines in the lung during the generation of idiopathic pneumonia syndrome following allogeneic murine bone marrow transplantation. *Blood*, 96(3), pp.834–839.

Del Papa, B. et al., 2013. Notch1 modulates mesenchymal stem cells mediated regulatory T-cell induction. *European journal of immunology*, 43(1), pp.182–187.

Parekh, K., Trulock, E. & Patterson, G.A., 2004. Use of cyclosporine in lung transplantation. *Transplantation proceedings*, 36(2 Suppl), p.318S–322S.

Parekkadan, B. et al., 2011. Bone Marrow Stromal Cell Transplants Prevent Experimental Enterocolitis and Require Host CD11b+ Splenocytes. *Gastroenterology*, 140(3), pp.966–975.e4.

Park, S.H. et al., 2006. Current Trends of Infectious Complications following Hematopoietic Stem Cell Transplantation in a Single Center. *Journal of Korean Medical Science*, 21(2), pp.199–207.

Park, J.H. et al., 2014. Etanercept for steroid-refractory acute graft versus host disease following allogeneic hematopoietic stem cell transplantation. *The Korean Journal of Internal Medicine*, 29(5), pp.630–636.

Parquet, N. et al., 2000. New oral formulation of cyclosporin A (Neoral) pharmacokinetics in allogeneic bone marrow transplant recipients. *Bone marrow transplantation*, 25(9), pp.965–968.

Passweg, J.R. et al., 2015. Hematopoietic SCT in Europe 2013: recent trends in the use of alternative donors showing more haploidentical donors but fewer cord blood transplants. *Bone Marrow Transplant*, 50(4), pp.476–482.

Patel, S.A. et al., 2010. Mesenchymal Stem Cells Protect Breast Cancer Cells through Regulatory T Cells: Role of Mesenchymal Stem Cell-Derived TGF-. *The Journal of Immunology*, 184(10), pp.5885–5894.

Pearson, T., Greiner, D. & Shultz, L., 2008. Creation of "humanized" mice to study human immunity. *Current Protocols in immunology/ edited by John E Coligan…et al.,* chapter 15, p. Unit 15.21

Perez, J. et al., 2011. Accumulation of CD4+ T cells in the colon of CsA-treated mice following myeloablative conditioning and bone marrow transplantation. *American journal of physiology. Gastrointestinal and liver physiology*, 300(5), pp.G843–52.

Peter Gale, R. & Reisner, Y., 1986. GRAFT REJECTION AND GRAFT-VERSUS-HOST DISEASE: MIRROR IMAGES. *The Lancet*, 327(8496), pp.1468–1470.

Pidala, J. et al., 2009. Infliximab for Managing Steroid-Refractory Acute Graft-versus-Host Disease. *Biology of Blood and Marrow Transplant*, 15(9), pp.1116–1121.

Pino-Lagos, K. et al., 2010. Cyclosporin A-treated dendritic cells may affect the outcome of organ transplantation by decreasing CD4+CD25+ regulatory T cell proliferation. *Biological research*, 43(3), pp.333–337.

Pischiutta, F. et al., 2014. Immunosuppression does not affect human bone marrow mesenchymal stromal cell efficacy after transplantation in traumatized mice brain. *Neuropharmacology*, 79, pp.119–26.

Pittenger, M.F. et al., 1999. Multilineage potential of adult human mesenchymal stem cells. *Science (New York, N.Y.)*, 284(5411), pp.143–147.

Plumas, J. et al., 2005. Mesenchymal stem cells induce apoptosis of activated T cells. *Leukemia*, 19(9), pp.1597–1604.

Poggi, A. et al., 2005. Interaction between human NK cells and bone marrow stromal cells induces NK cell triggering: role of NKp30 and NKG2D receptors. *Journal of immunology (Baltimore, Md. : 1950)*, 175(10), pp.6352–6360.

Polchert, D. et al., 2008. IFN-gamma activation of mesenchymal stem cells for treatment and prevention of graft versus host disease. *European journal of immunology*, 38(6), pp.1745–1755.

Prasanna, S.J. et al., 2010. Pro-Inflammatory Cytokines, IFNγ and TNFα, Influence Immune Properties of Human Bone Marrow and Wharton Jelly Mesenchymal Stem Cells Differentially. *PLoS ONE*, 5(2), p.e9016.

Quarto, R. et al., 2001. Repair of Large Bone Defects with the Use of Autologous Bone Marrow Stromal Cells. *New England Journal of Medicine*, 344(5), pp.385–386.

Ramasamy, R. et al., 2007. Mesenchymal stem cells inhibit dendritic cell differentiation and function by preventing entry into the cell cycle. *Transplantation*, 83(1), pp.71–76.

Rasmusson, I. et al., 2007. Mesenchymal stem cells stimulate antibody secretion in human B cells. *Scandinavian journal of immunology*, 65(4), pp.336–343.

Rehermann, B. & Nascimbeni, M., 2005. Immunology of hepatitis B virus and hepatitis C virus infection. *Nat Rev Immunol*, 5(3), pp.215–229.

Ren, G. et al., 2010. Inflammatory cytokine-induced intercellular adhesion molecule-1 and vascular cell adhesion molecule-1 in mesenchymal stem cells are critical for immunosuppression. *Journal of immunology (Baltimore, Md. : 1950)*, 184(5), pp.2321–8.

Ren, G. et al., 2008. Mesenchymal stem cell-mediated immunosuppression occurs via concerted action of chemokines and nitric oxide. *Cell stem cell*, 2(2), pp.141–50.

Riddell, S. R., 2007. Engineering antitumor immunity by T cell adoptive immunotherapy. *Hematology*, 250-6.

van Rijn, R.S. et al., 2003. A new xenograft model for graft-versus-host disease by intravenous transfer of human peripheral blood mononuclear cells in RAG2-/- gammac-/- double-mutant mice. *Blood*, 102(7), pp.2522–2531.

Ringden, O. et al., 2006. Mesenchymal stem cells for treatment of therapy-resistant graft-versus-host disease. *Transplantation*, 81(10), pp.1390–1397.

Rodriguez-Otero, P. et al., 2012. Fecal calprotectin and alpha-1 antitrypsin predict severity and response to corticosteroids in gastrointestinal graft-versus-host disease. *Blood*, 119(24), pp.5909–5917.

Rosado, M.M. et al., 2014. Inhibition of B-Cell Proliferation and Antibody Production by Mesenchymal Stromal Cells Is Mediated by T Cells. *Stem Cells and Development*, 24(1), pp.93–103.

Rozemuller, H. et al., 2010. Prospective isolation of mesenchymal stem cells from multiple mammalian species using cross-reacting anti-human monoclonal antibodies. *Stem cells and development*, 19(12), pp.1911–1921.

Ruggeri, L. et al., 1999. Role of Natural Killer Cell Alloreactivity in HLA-Mismatched Hematopoietic Stem Cell Transplantation. *Blood*, 94(1), pp.333–339.

Ruutu, T. et al., 2014. Prophylaxis and treatment of GVHD: EBMT-ELN working group recommendations for a standardized practice. *Bone marrow transplantation*, 49(2), pp.168–73

Ryan, J.M. et al., 2005. Mesenchymal stem cells avoid allogeneic rejection. *Journal of Inflammation*, 2(1), pp.1–11. Available at: http://dx.doi.org/10.1186/1476-9255-2-8.

Ryan, J.M. et al., 2007. Interferon-gamma does not break, but promotes the immunosuppressive capacity of adult human mesenchymal stem cells. *Clinical and experimental immunology*, 149(2), pp.353–63.

Saito, K. et al., 1996. Effect of CD80 and CD86 blockade and anti-interleukin-12 treatment on mouse acute graft-versus-host disease. *European journal of immunology*, 26(12), pp.3098–3106.

Saito, H. et al., 2000. IFN regulatory factor-1-mediated transcriptional activation of mouse STAT-induced STAT inhibitor-1 gene promoter by IFN-gamma. *Journal of immunology (Baltimore, Md. : 1950)*, 164(11), pp.5833–5843.

Saito, T. et al., 2002. Xenotransplant cardiac chimera: immune tolerance of adult stem cells. *The Annals of Thoracic Surgery*, 74(1), pp.19–24.

Saland, E. et al., 2015. A robust and rapid xenograft model to assess efficacy of chemotherapeutic agents for human acute myeloid leukemia. *Blood Cancer Journal*, 5(3), p.e297.

Satake, A. et al., 2014. Inhibition of calcineurin abrogates while inhibition of mTOR promotes regulatory T cell expansion and graft-versus-host disease protection by IL-2 in allogeneic bone marrow transplantation. *PLoS ONE*, 9(3), pp.1–8.

Schmaltz, C. et al., 2002. Donor T cell–derived TNF is required for graft-versus-host disease and graft-versus-tumor activity after bone marrow transplantation. *Blood*, 101(6), pp.2440–2445.

Schmittgen, T.D. & Livak, K.J., 2008. Analyzing real-time PCR data by the comparative CT method. *Nat. Protocols*, 3(6), pp.1101–1108.

Schroecksnadel, S. et al., 2011. Influence of immunosuppressive agents on tryptophan degradation and neopterin production in human peripheral blood mononuclear cells. *Transplant immunology*, 25(2-3), pp.119–123.

Schroeder, M.A. & DiPersio, J.F., 2011. Mouse models of graft-versus-host disease: advances and limitations. *Disease models & mechanisms*, 4(3), pp.318–333.

Serody, J.S. et al., 2000. T-lymphocyte production of macrophage inflammatory protein-1alpha is critical to the recruitment of CD8(+) T cells to the liver, lung, and spleen during graft-versus-host disease. *Blood*, 96(9), pp.2973–2980.

Shen, Z. et al., 2013. Cyclosporin a inhibits rotavirus replication and restores interferon-beta signaling pathway in vitro and in vivo. *PloS one*, 8(8), p.e71815.

Sheng, H. et al., 2008. A critical role of IFNgamma in priming MSC-mediated suppression of T cell proliferation through up-regulation of B7-H1. *Cell research*, 18(8), pp.846–857.

Shi, D. et al., 2011. Human adipose tissue-derived mesenchymal stem cells facilitate the immunosuppressive effect of cyclosporin A on T lymphocytes through Jagged-1-mediated inhibition of NF-κB signaling. *Experimental hematology*, 39(2), pp.214–224.e1.

Shi, Y. et al., 2012. How mesenchymal stem cells interact with tissue immune responses. *Trends in immunology*, 33(3), pp.136–143.

Sotiropoulou, P.A. et al., 2006. Interactions between human mesenchymal stem cells and natural killer cells. *Stem cells (Dayton, Ohio)*, 24(1), pp.74–85.

Shlomchik, W.D. et al., 1999. Prevention of graft versus host disease by inactivation of host antigen-presenting cells. *Science (New York, N.Y.)*, 285(5426), pp.412–415.

Shultz, L.D. et al., 2005. Human Lymphoid and Myeloid Cell Development in NOD/LtSz-scid IL2Rγnull Mice Engrafted with Mobilized Human Hemopoietic Stem Cells . *The Journal of Immunology* , 174 (10), pp.6477–6489.

Shultz, L.D. et al., 1995. Multiple defects in innate and adaptive immunologic function in NOD/LtSz-scid mice. *Journal of immunology (Baltimore, Md. : 1950)*, 154(1), pp.180–191.

Sigmoid Pharma Ltd. 2009. ClinicalTrials.gov. [ONLINE] Available at:

https://clinicaltrials.gov/ct2/show/NCT01033305. [Accessed 25 February 16]

Snell, G.D., 1948. Methods for the study of histocompatibility genes. *Journal of genetics*, 49(2), pp.87–108.

Snell, G.D. & Higgins, G.F., 1951. Alleles at the histocompatibility-2 locus in the mouse as determined by tumor transplantation. *Genetics*, 36(3), pp.306–310.

Spaggiari, G.M. et al., 2006. Mesenchymal stem cell – natural killer cell interactions: evidence that activated NK cells are capable of killing MSCs, whereas MSCs can inhibit IL-2 – induced NK-cell proliferation. *Blood*, 107(4), pp.1484–1490.

Spaggiari, G.M. et al., 2008. Mesenchymal stem cells inhibit natural killer-cell proliferation, cytotoxicity, and cytokine production: role of indoleamine 2,3-dioxygenase and prostaglandin E2. *Blood*, 111(3), pp.1327–1333.

Spaggiari, G.M. et al., 2009. MSCs inhibit monocyte-derived DC maturation and function by selectively interfering with the generation of immature DCs: central role of MSC-derived prostaglandin E2. *Blood*, 113(26), pp.6576–6583.

Spranger, S., Frankenberger, B. & Schendel, D.J., 2012. NOD/scid IL-2Rgnull mice: a preclinical model system to evaluate human dendritic cell-based vaccine strategies in vivo. *Journal of Translational Medicine*, 10(1), pp.1–11.

Stamm, C. et al., 2003. Autologous bone-marrow stem-cell transplantation for myocardial regeneration. *Lancet (London, England)*, 361(9351), pp.45–6.

Stuber, E. et al., 1999. Intestinal crypt cell apoptosis in murine acute graft versus host disease is mediated by tumour necrosis factor alpha and not by the FasL-Fas interaction: effect of pentoxifylline on the development of mucosal atrophy. *Gut*, 45(2), pp.229–235.

Studier, F.W., 1973. Analysis of bacteriophage T7 early RNAs and proteins on slab gels. *Journal of molecular biology*, 79(2), pp.237–248.

Sudres, M. et al., 2006. Bone Marrow Mesenchymal Stem Cells Suppress Lymphocyte Proliferation In Vitro but Fail to Prevent Graft-versus-Host Disease in Mice. *The Journal of Immunology* , 176 (12), pp.7761–7767.

Tabera, S. et al., 2008. The effect of mesenchymal stem cells on the viability, proliferation and differentiation of B-lymphocytes. *Haematologica*, 93(9), pp.1301–1309.

Tang, R. et al., 2015. Mesenchymal stem cells-regulated Treg cells suppress colitis-associated colorectal cancer. *Stem Cell Research & Therapy*, 6(1):71.

Taur, Y. et al., 2014. The effects of intestinal tract bacterial diversity on mortality following allogeneic hematopoietic stem cell transplantation. *Blood*, 124(7), pp.1174–1182.

Tawara, I. et al., 2011. Interleukin-6 modulates graft-versus-host responses after experimental allogeneic bone marrow transplantation. *Clinical cancer research : an official journal of the American Association for Cancer Research*, 17(1), pp.77–88.

Taylor, P.A., Lees, C.J. & Blazar, B.R., 2002. The infusion of ex vivo activated and expanded CD4+CD25+ immune regulatory cells inhibits graft-versus-host disease lethality. *Blood*, 99(10), pp.3493–3499.

Tharayil John, G. et al., 2003. Epidemiology of systemic mycoses among renal-transplant recipients in India. *Transplantation*, 75(9), pp.1544–1551.

Tobin, L.M., 2012. Immune Mechanisms of Mesenchymal Stem Cell Therapy for Acute Graft versus Host Disease..PhD thesis, National University of Ireland Maynooth. Available at: http://eprints.maynoothuniversity.ie/4767/1/PhD Thesis Laura Tobin NUIM 2012.pdf [Accessed February 6, 2016].

Tobin, L.M. et al., 2013. Human mesenchymal stem cells suppress donor CD4(+) T cell proliferation and reduce pathology in a humanized mouse model of acute graft-versus-host disease. *Clinical and experimental immunology*, 172(2), pp.333–48.

Toma, C. et al., 2009. Fate of culture-expanded mesenchymal stem cells in the microvasculature: in vivo observations of cell kinetics. *Circulation research*, 104(3), pp.398–402.

Tomchuck, S.L. et al., 2012. Toll-Like Receptor 3 and Suppressor of Cytokine Signaling Proteins Regulate CXCR4 and CXCR7 Expression in Bone Marrow-Derived Human Multipotent Stromal Cells. *PLoS ONE*, 7(6), p.e39592.

Traggiai, E. et al., 2008. Bone marrow-derived mesenchymal stem cells induce both polyclonal expansion and differentiation of B cells isolated from healthy donors and systemic lupus erythematosus patients. *Stem cells (Dayton, Ohio)*, 26(2), pp.562–569.

Tramsen, L. et al., 2014. Immunosuppressive compounds exhibit particular effects on functional properties of human anti-Aspergillus TH1 cells. *Infection and Immunity*, 82(6), pp.2649–2656.

Trull, A.K. et al., 1995. Absorption of cyclosporin from conventional and new microemulsion

oral formulations in liver transplant recipients with external biliary diversion. *Br J Clin Pharmacol*, 39(6), pp.627–631.

Trzonkowski, P. et al., 2013. Treatment of Graft-versus-Host Disease with Naturally Occurring T Regulatory Cells. *Biodrugs*, 27(6), pp.605–614.

Tu, Z. et al., 2010. Mesenchymal Stem Cells Inhibit Complement Activation by Secreting Factor H. *Stem Cells and Development*, 19(11), pp.1803–1809.

Uhlin, M. et al., 2014. Risk factors for Epstein-Barr virus-related post-transplant lymphoproliferative disease after allogeneic hematopoietic stem cell transplantation. *Haematologica*, 99(2), pp.346–352.

Vaes, B. et al., 2012. Application of MultiStem((R)) Allogeneic Cells for Immunomodulatory Therapy: Clinical Progress and Pre-Clinical Challenges in Prophylaxis for Graft Versus Host Disease. *Frontiers in immunology*, 3, p.345.

Varey, A.M., Champion, B.R. & Cooke, A., 1986. Cyclosporine affects the function of antigen-presenting cells. *Immunology*, 57(1), pp.111–114.

Verburg, R.J. et al., 2001. High-dose chemotherapy and autologous hematopoietic stem cell transplantation in patients with rheumatoid arthritis: results of an open study to assess feasibility, safety, and efficacy. *Arthritis and rheumatism*, 44(4), pp.754–760.

Via, C.S. et al., 2001. In vivo neutralization of TNF-alpha promotes humoral autoimmunity by preventing the induction of CTL. *J Immunol*, 167(12), pp.6821–6826.

Vogelsang, G.B. et al., 1999. Immune modulation in autologous bone marrow transplantation : cyclosporine and gamma-interferon trial. *Bone Marrow Transplant*, 24(6), pp.637–640.

Vossen, J.M. et al., 2014. Complete Suppression of the Gut Microbiome Prevents Acute Graft-Versus-Host Disease following Allogeneic Bone Marrow Transplantation. *PLoS ONE*, 9(9), p.e105706.

Wang, R. et al., 2012. Natural killer cell-produced IFN-gamma and TNF-alpha induce target cell cytolysis through up-regulation of ICAM-1. *Journal of leukocyte biology*, 91(2), pp.299–309.

Wang Lei, Zhao Yinghua, Liu Yi, Akiyama Kentaro, Chen Chider, Qu Cunye, J.Y. and S.S., 2013. IFNg and TNFa Synergistically Induce Mesenchymal Stem Cell Impairment and

Tumorigenesis via NFkB Signaling. *Stem Cells*, 31(7), pp.1383–1395.

Wang, S.-C. et al., 2013. Cyclosporine A promotes in vitro migration of human first-trimester trophoblasts via MAPK/ERK1/2-mediated NF-kappaB and Ca2+/calcineurin/NFAT signaling. *Placenta*, 34(4), pp.374–380.

Wang, Y. et al., 2014. Plasticity of mesenchymal stem cells in immunomodulation: pathological and therapeutic implications. *Nat Immunol*, 15(11), pp.1009–1016.

Washington, K. & Jagasia, M., 2009. Pathology of graft-versus-host disease in the gastrointestinal tract. *Human Pathology*, 40(7), pp.909–917.

Watashi, K. et al., 2014. Cyclosporin A and its analogs inhibit hepatitis B virus entry into cultured hepatocytes through targeting a membrane transporter, sodium taurocholate cotransporting polypeptide (NTCP). *Hepatology (Baltimore, Md.)*, 59(5), pp.1726–37.

Webber, I., Peters, W. & Back, D., 1992. Cyclosporin metabolism by human gastrointestinal mucosal microsomes. *British Journal of Clinical Pharmacology*, 33, pp.661–664.

Weisdorf, D.J. et al., 1990. Acute upper gastrointestinal graft-versus-host disease: clinical significance and response to immunosuppressive therapy. *Blood*, 76(3), pp.624–9.

Welniak L. A. et al. 2007. Immunobiology of allogeneic hematopoietic stem cell transplantation. *Annual Rev Immunol,* vol 25:139-170.

Wu, T. et al., 2015. miR-21 Modulates the Immunoregulatory Function of Bone Marrow Mesenchymal Stem Cells Through the PTEN/Akt/TGF-beta1 Pathway. *Stem cells (Dayton, Ohio)*, 33(11), pp.3281–3290.

Xu, G. et al., 2007. The role of IL-6 in inhibition of lymphocyte apoptosis by mesenchymal stem cells. *Biochemical and biophysical research communications*, 361(3), pp.745–50.

Xu, L. et al., 2013. Histologic findings in lung biopsies in patients with suspected graft-versus-host disease. *Human pathology*, 44(7), pp.1233–1240.

Yang, Y.-G. et al., 2005. Role of Interferon-gamma in GVHD and GVL. *Cellular & molecular immunology*, 2(5), pp.323–329.

Yang, S.-H. et al., 2009. Soluble mediators from mesenchymal stem cells suppress T cell proliferation by inducing IL-10. *Exp Mol Med*, 41, pp.315–324.

Yao, H. & Yu, J., 2009. [Dynamic changes of serum MCP-1 and MIP-2 chemokines after renal

transplantation in rats]. *Journal of Southern Medical University*, 29(12), pp.2512—3, 2516.

Yates, J. et al., 2007. The maintenance of human CD4+CD25+ regulatory T cell function: IL-2, IL-4, IL-7 and IL-15 preserve optimal suppressive potency in vitro. *International Immunology*, 19(6), pp.785–799.

Yocum, D.E. et al., 2000. Microemulsion formulation of cyclosporin (Sandimmun Neoral) vs Sandimmun: comparative safety, tolerability and efficacy in severe active rheumatoid arthritis. On behalf of the OLR 302 Study Group. *Rheumatology (Oxford, England)*, 39(2), pp.156–64.

Zappia, E. et al., 2005. Mesenchymal stem cells ameliorate experimental autoimmune encephalomyelitis inducing T-cell anergy. *Blood*, 106(5), pp.1755–1761.

Zeiser, R. et al., 2006. Inhibition of CD4(+)CD25(+) regulatory T-cell function by calcineurin-dependent interleukin-2 production. *Blood*, 108(1), pp.390–399.

Zhang, W., Qin, C. & Zhou, Z.M., 2007. Mesenchymal stem cells modulate immune responses combined with cyclosporine in a rat renal transplantation model. *Transplantation proceedings*, 39(10), pp.3404–8.

Zhang, B. et al., 2009. Mesenchymal stem cells induce mature dendritic cells into a novel Jagged-2-dependent regulatory dendritic cell population. *Blood*, 113(1), pp.46–57.

Zhang, L. et al., 2014. SOCS1 Regulates the Immune Modulatory Properties of Mesenchymal Stem Cells by Inhibiting Nitric Oxide Production. *PloS one*, 9(5), p.e97256.

Zhao, W. et al., 2008. TGF-beta expression by allogeneic bone marrow stromal cells ameliorates diabetes in NOD mice through modulating the distribution of CD4+ T cell subsets. *Cellular immunology*, 253(1-2), pp.23–30.

Zhao, H.-B. et al., 2012. CXCL12/CXCR4 axis triggers the activation of EGF receptor and ERK signaling pathway in CsA-induced proliferation of human trophoblast cells. *PloS one*, 7(7), p.e38375.

Zhou, Y. et al., 2011. Prevention of acute graft-versus-host disease by magnetic nanoparticles of Fe 3 O 4 combined with cyclosporin A in murine models. *Int J Nanomedicine*, 6, pp.2183–2189.